Master Thesis report

The future cruise terminal in the Port of Rotterdam

by

Lodovico de Vito

in partial fulfillment of the requirements for the degree of

Master of Science

in Civil Engineering

at the Delft University of Technology

Thesis committee

Chairman:	Prof. dr. ir. S. N. Jonkman	TU Delft
Supervisors:	Dr. ir. J.G. de Gijt	TU Delft
	Dr. ing. M.Z. Voorendt	TU Delft
	Ir. P. Quist	TU Delft/Witteveen+Bos
	Ir. J.J. de Nooijer	Port of Rotterdam

Preface

This master thesis is the final product of the Master of Science degree in Hydraulic Engineering at the Faculty of Civil Engineering and Geosciences of the Delft University of Technology. The research is performed under the guidance of the Delft University of Technology in cooperation with Witteveen+Bos and Havenbedrijf Rotterdam.

First of all, I would like to express my gratitude towards my graduation committee. Many thanks to Ir. P. Quist and Ir. J.J. de Nooijer for introducing me this interesting topic and for their valuable advice regarding during the study. Many thanks to Dr. ir. J.G. de Gijt and Dr. ing. M.Z. Voorendt for their constructive feedback and meetings during the graduation period. I would like to extend my gratitude to Prof. dr. ir. S.N. Jonkman for his expertise and feedback, adding to the overall level of the report.

Second, I would like to thank Witteveen+Bos for allowing me to work amongst passionate and skillful civil engineers, helping me with required literature, advice and feedback.

Furthermore, I would like to thank all my friends, especially to Adele, Francesca, Belisa, Giovanni and Matteo for making the journey towards this Master and the stay in Delft very enjoyable and an unforgettable experience. Special gratitude and appreciation to my girlfriend, Marina, for her continuous support, patience and help throughout the last year and the thesis.

Last but not least, special gratitude goes to my family, especially to my parents and my brother, on whom I could always count and who made all this possible.

Lodovico de Vito

Delft, April 2018

Summary

The city of Rotterdam and its port have been constantly growing over the last decades. As the port is ensuring a place in the top ten ports in the world, the city of Rotterdam is changing as well, growing and becoming a more international town. The municipality of Rotterdam is planning to build a 3rd bridge that will cross the *Nieuwe waterweg* and will connect the eastern or western part of the city center to improve the economic growth, welfare and attainability of the city. Although the exact location of the bridge is still under investigation, the construction of the bridge will obstruct the passage of cruise ships and consequently, they will not be able to reach Kop van Zuid where the current cruise terminal is located.

Moreover, new buildings will be constructed in the coming years at Kop van Zuid. The construction of these buildings will lead to more logistics problems at the current terminal that will influence the viability of the entire area. Currently, the port of Rotterdam is facing an increase of entrance demand of cruise ships. The number of double mooring calls and the dimensions of the cruise ships are expected to grow in the coming years. The current cruise terminal cannot, without technical improvements, guarantee enough berthing space for two cruise ships at the same time.

For these reasons, in 2015 the Port of Rotterdam Authority started the project “Zeecruise lange termijn visie”. One of the conclusions of the “Zeecruise lange termijn visie” project in case that the Port of Rotterdam Authority and the municipality of Rotterdam decide to change the location of the cruise terminal, was that the most suitable location for the future cruise terminal is Pier 1 of the Merwehaven. The Merwehaven is composed of four piers that were constructed between 1923 and 1931 using caissons as quay walls as shown in the figure below.

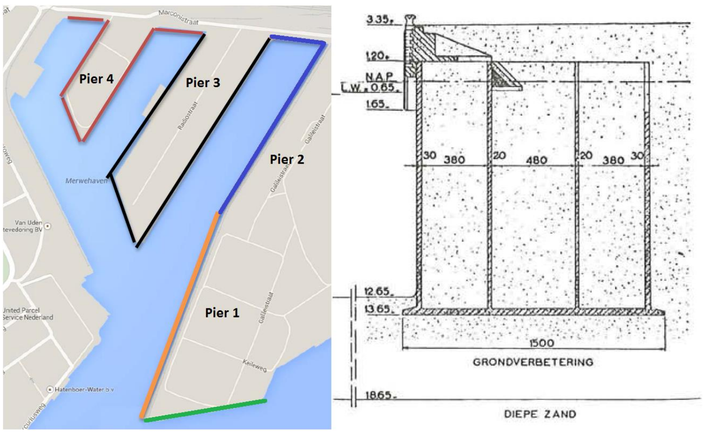

Top view of the Merwehaven (left) and a cross-section of the caisson used as quay wall in the Merwehaven (right)

Due to the age of the construction of the caissons and the requirements imposed by the new cruise terminal, a full feasibility study of the Merrwehaven had to be performed. The feasibility study is described in this report and mainly concerns the adaptation of the existing quay wall of Pier 1. The aim of this study was to maintain the existing caissons, avoiding the demolition of the structure and the need for constructing a completely new quay wall.

The approach used to achieve this objective follows the principles of the basic design cycle of Roozenburg and Eekels. Different design phases distinguish this method and the structure of this report follows these phases.

In the first phase, the functions, operational aspects, boundary conditions and assumptions of the Merwehaven and cruise market were analyzed. Based on this analysis the quay walls of Pier 1 were assessed. The main scope of the assessment was to establish whether the quay walls meet the requirements for the new cruise terminal and to identify the main issues that hinder the mooring of the cruise ships. The assessment proved that the quay walls do not meet the requirements of the

new cruise terminal. Therefore, the conclusion was that to maintain the existing caissons of Pier 1 and ensure their stability a technical design solution must be provided.

Different design concepts were proposed to solve the issues that hinder the mooring of the cruise ships along the caissons. Through a first design loop, the design concepts that did not have sufficient feasibility to become the final solution were excluded. From the remaining design variants the best design variant was selected, by means of an evaluation based on a Multi Criteria Analysis (MCA) and a cost estimation. From this evaluation, it turned out that the best technical design solution is to drive an underwater sheet pile wall in front of the caissons of Pier 1 as shown in the next figure.

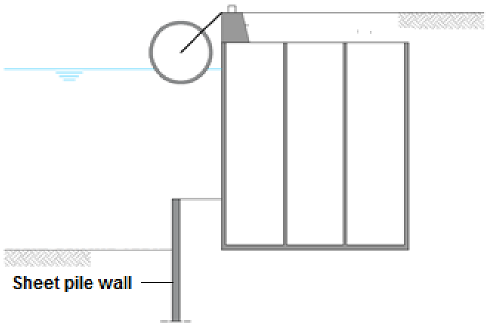

Design variant with underwater sheet pile wall

Then, before performing the detailed design of the best design variant, special attention was given to the design bollard capacity of the cruise terminal. The bollard force is an important load in the design of quay walls. Hence, an extended study concerning the loads acting on the design cruise ship was carried out to define the required bollard capacity of the new cruise terminal. From this study, it turned out that the wind force is the dominant load acting on the design cruise ship and that the effect of passing vessels can be neglected. Based on this conclusion a static mooring analysis was performed to determine the load on the mooring lines of the design cruise ship and consequently the required bollard capacity. On the basis of the results of this analysis, the conclusion was that the existing bollards located on top of the caissons cannot withstand the mooring force and therefore new bollards with a capacity of 1700 kN have to be provided.

In the last phase, the design variant with underwater sheet pile wall was elaborated in more detail. This detailed design was performed by analyzing the overall stability of the caisson and the deformation of the underwater sheet pile wall using the PLAXIS software. Based on these analyses the conclusion was that the design variant with the underwater sheet pile wall can adapt the existing caisson, used as quay wall at Pier 1 in the Merwehaven for the future cruise terminal of Rotterdam.

Table of contents

1. Introduction

The topic of this MSc thesis report is the future cruise terminal in the port of Rotterdam. This chapter starts with a brief introduction to the area of study. Then it introduces the motivation and the objective of this study. Finally, it presents the adopted approach and the structure of this MSc report.

1.1 History of the port of Rotterdam

The port of Rotterdam, located in the city of Rotterdam, Netherlands, is the largest port in Europe and is ranked in the top ten largest in the world (Port of Rotterdam Authority, 2017). The port of Rotterdam has served as a central hub for shipping for centuries. The harbor was first established during the Middle Ages in the center of the present city. However, it became important for The Netherlands only after the second half of the nineteenth century. During Industrial Revolution, several developments occurred (IsGeschiedenis, 2014). The most relevant was the realization, during the second half of the nineteenth century, of the *Nieuwe Waterweg* ("New Waterway") serving to connect industry along the Rhine and Meuse rivers to the North Sea. During the Second World War, approximately half of the harbor was destroyed during aerial bombardments. After the war, the port saw an immense growth. The *Nieuwe Waterweg* was deepened to allow the entrance of larger vessels. The *Europoort* ("Gate to Europe"), a massive complex on the mouth of the *Nieuwe Waterweg* was developed. After the realization of this project, the port of Rotterdam became the primary fossil fuel center of Europe (IsGeschiedenis, 2014). The most recent developments are the realization of the *Maasvlakte* (1970-2008) and the *Maasvlakte 2* (2008-2013). An overview of the history of the port of Rotterdam is presented in the figure below.

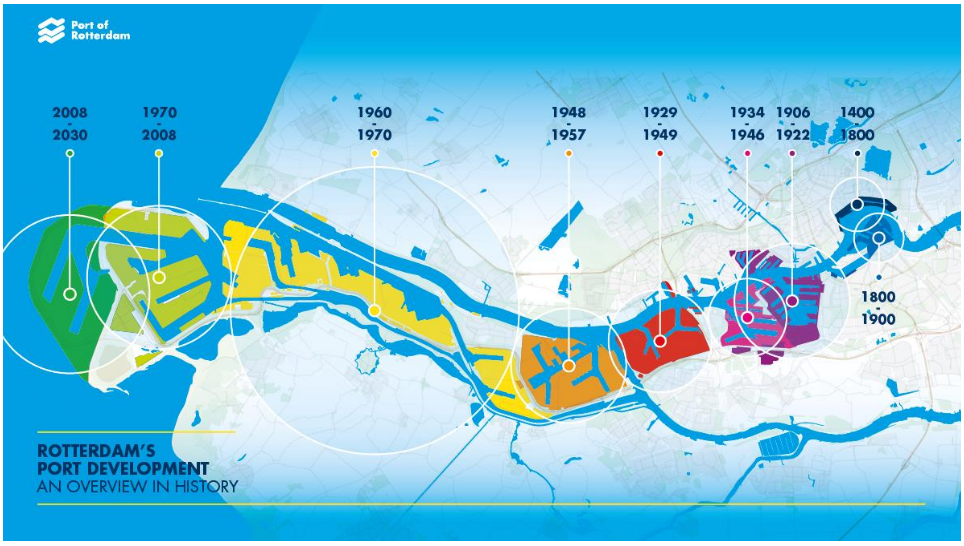

Figure 1: Rotterdam's port development in time (Port of Rotterdam)

Nowadays, the port of Rotterdam has a total area of 12.643 ha and stretches over a total distance of 42 km (Port of Rotterdam Authority, 2015). The port hosts the largest container port in Europe (Port of Rotterdam Authority, 2017). Even the largest vessels can always enter the port due to the significant navigation depth and because of the absence of restriction from tides or navigation locks. Approximately 135000 vessels per year sail in and out the port (Port of Rotterdam Authority, 2017) The throughput in 2016 was 461.2 million tonnes (Port of Rotterdam Authority, 2017). The port of Rotterdam connects Western Europe to the world at large, and development shows no sign of slowing down.

1.2 Motivation of the study

Cruise ships in the Port of Rotterdam are also a growing phenomenon. In 2017 cruise ships entered the port of Rotterdam sixty-two times and the next year the number of entrances are expected to increase to eighty-three (Havenkrant, 2017). Cruise tourism has been one of the fastest growing sectors of the tourist industry for the past 25 years. Since 1980, the industry has had an average annual passenger growth rate of some 8 % per year (PIANC, Guidelines for cruise terminal, 2016). In Europe, the number of cruise passengers increased with a 3,4% reaching 6.7 million passengers in 2016 (Maritiem Nederland, 2017). This growth is expected to continue in the future.

The current cruise terminal, used by passenger vessels that visit Rotterdam, is located in the city center along *Wilhelminapier* at *Kop van Zuid* (see Figure 2). The terminal is called Holland America quay because it served as arrival and departure of the Holland America Line that was founded 143 years ago.

Figure 2: The location of the cruise terminal in the port of Rotterdam (Google Earth)

Like its port also the city of Rotterdam has been constantly growing over the last decade. The expansion of the city of Rotterdam and its ports will most likely continue far into the future. As the port is ensuring a place in the top ten ports in the world, the city of Rotterdam as well, is becoming an international city. To be able to adapt to the changing demands of the future and not to restrain the economic growth, welfare and mobility a good infrastructure planning for the city is one of the key factors. Therefore, the municipality of Rotterdam (Gemeente Rotterdam) is planning to build a 3rd bridge in the city center. The bridge will cross the *Nieuwe waterweg* and will connect the eastern or western part of the city center. Although the exact location of the bridge is still under investigation, in case of the selection of the western option, the construction of the bridge will obstruct the passage of cruise ships and consequently, they will not be able to reach the current cruise terminal.

Moreover, new buildings will be constructed in the coming years at Kop van Zuid. The construction of these buildings will reduce the space for the embarkments and disembarkations of the cruise ships passengers. Hence, this will lead to even more logistics problems (already present) at the current terminal that will influence the viability of the entire area.

Lastly, the port of Rotterdam is facing an increase of entrance demand of cruise ships. Due to the increment the number of double mooring calls is expected to grow in the coming years. The current cruise terminal is not able to guarantee enough berthing space for two cruise ships at the same time without technical improvements.

For the reasons mentioned above, in 2015 the Port of Rotterdam Authority (Havenbedrijf Rotterdam) together with the municipality of Rotterdam started the project “Zeecruise lange termijn visie” (Cruise long term vision). This project studies the best location for future cruise terminals, taking into account the development, the environment and the surrounding of the port of Rotterdam and its city.

1.3 Aim

One of the conclusions of the “Zeecruise lange termijn visie” project in case that the Port of Rotterdam Authority and the municipality of Rotterdam decide to change the location of the cruise terminal, was that the most suitable location for the future cruise terminal is Pier 1 of the Merwehaven. The Merwehaven is located on the north bank of the *Nieuwe Maas* (New-Meuse), approximately 5 km more downstream from the current location of the cruise terminal at the Wilhelminapier (see Figure 3).

Figure 3: The location of the Merwehaven in the port of Rotterdam (Google Earth)

Nowadays, the port is still in use for the transhipment of goods and several warehouses are present on the different piers. The Merwehaven is composed of four piers (see left Figure 4). The piers were constructed between 1923 and 1931 using caissons as quay walls. A typical cross-section of the caissons of Pier 1 in the Merwehaven is presented below (right Figure 4).

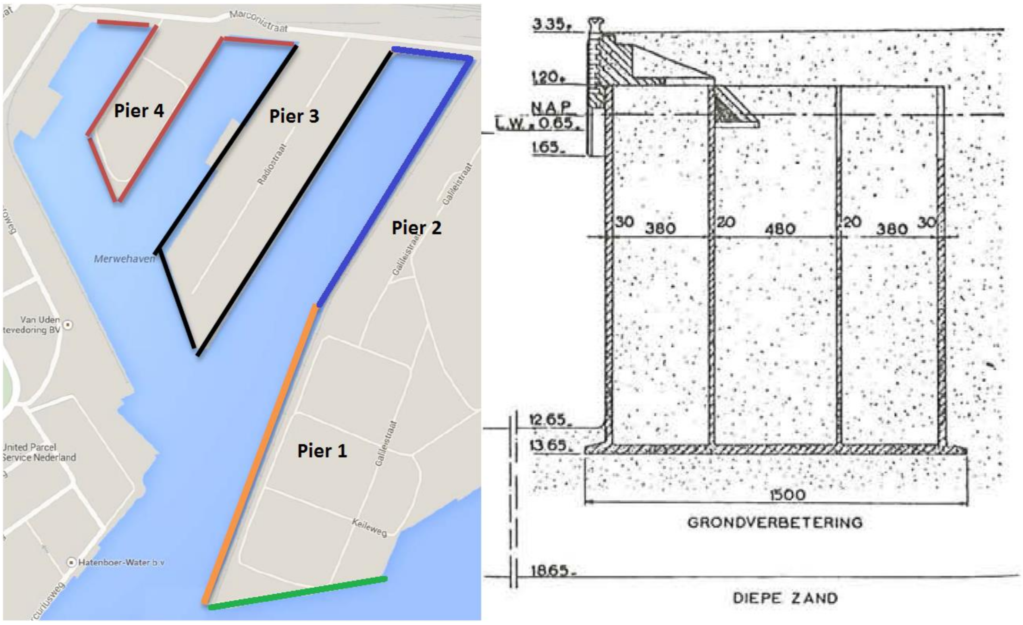

Figure 4: Top view of the Merwehaven (Google Maps) and a cross-section of the caisson used as quay wall in the Merwehaven (HBG, 1977)

Due to the age of the construction of the existing quay walls and the new requirements imposed by the new cruise terminal, a full feasibility study of the Merrwehaven has to be performed. The feasibility study focuses on the adaptation of the existing quay walls of Pier 1, to avoid the demolition of the existing structure and the complete construction of new quay walls. Therefore, the objective of this MSc thesis can be formulated as follows:

Study the feasibility of adapting the existing quay walls in the Merwehaven to its future use for the cruise terminal of the port of Rotterdam.

1.4 Approach

This section presents the approach that is used to achieve the objective of this MSc thesis. The approach follows the principles of the basic design cycle of Roozenburg and Eekels (Roozenburg & Eekels, 1995). This method applies an iterative and cyclic process and is distinguished by different design phases as shown in Figure 5.

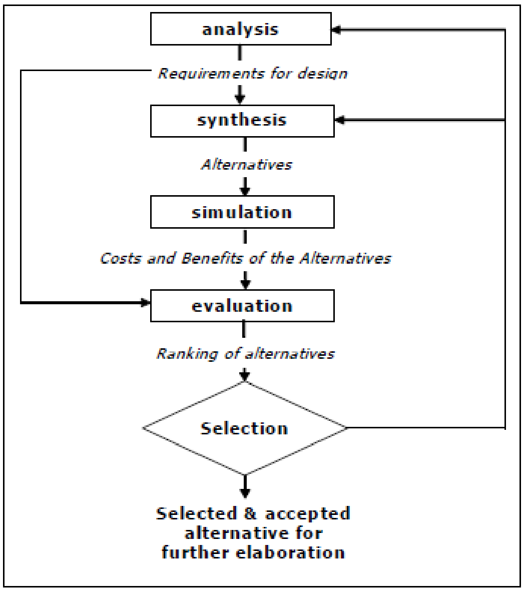

Figure 5: The basic design cycle of Roozenburg and Eekels (Roozenburg & Eekels, 1995)

The first phase is the *Analysis*. In this phase, the functions, operational aspects, boundary conditions and assumptions of the structure are analyzed. Usually, the analysis phase results in a "List of Requirements" (Bezuyen, et al., 2009). Based on these requirements different design concepts are elaborated during the *Synthesis*. In the *Simulation* phase, the different concepts are developed further, verified and brought into a more detailed level through design loops. During the *Evaluation* phase the feasibility of the concepts, which were developed, are evaluated by a suitable type or level of evaluation (Voorendt, 2017). The evaluation can involve, for example, a Cost-benefit analysis or Multi Criteria Analysis. Finally, the design should converge towards one final variant during the *Selection* phase.

The phases mentioned above are pursued during the entire design process. During each design phase, several activities are performed. The design can, therefore, be divided into different steps. These steps are presented are below together with a short description of the activities associated with each step.

1) Start

The first step consists of collecting and reviewing available data and literature to explore the background and the problem outline. This phase finishes with the definition of the aim of the study.

2) Analysis

From the literature study and the collected data, the current situation of the project area is described, and the project requirements and the boundary conditions are formulated.

3) Assessment of the present situation

Before the development of different design concepts, based on the program of requirements and the boundary conditions an assessment of the existing situation of Pier 1 is carried out. Two different parts compose this assessment. The first part concerns about the functional-spatial assessment of the current situation. The second part regards the structural assessment of the existing quay walls.

The scope of these assessments is to define whether the existing quay walls do not meet the program of requirements. Moreover, the assessments detect the main issues that can hinder the mooring of the cruise ships and compromise the stability of the existing caissons.

4) Design concepts

This step starts with the development of different design concepts. These concepts are developed based on the conclusions of the assessments. Then the different design concepts are elaborated and verified by means of a design loop through the use of hand calculations and technical reasoning for a tentative design. The scope of this verification is to identify those design concepts that have a certain level of feasibility and value which make them design variant and a candidate for the final solution. The remaining design variants are then evaluated and rated based on a Multi Criteria Analysis (MCA) and a cost estimation.

5) In-depth design

Once the best design variant is selected, based on the evaluation, the best variant is further elaborated by means of a more detailed design loop. First, special attention is given to the calculation of the forces, due to the wind and passing ships, acting on the design cruise ships that are transferred to the bollards of the quay walls. Then, a detailed design of the best design variant is carried out by investigating and calculating in depth the main aspects. The elaborated design should be able to ensure the stability of the existing caissons, avoiding the demolition and the complete construction of new quay wall.

In the figure below the activities pursued, during the design process, are presented in correspondence to each phase of the adopted approach.

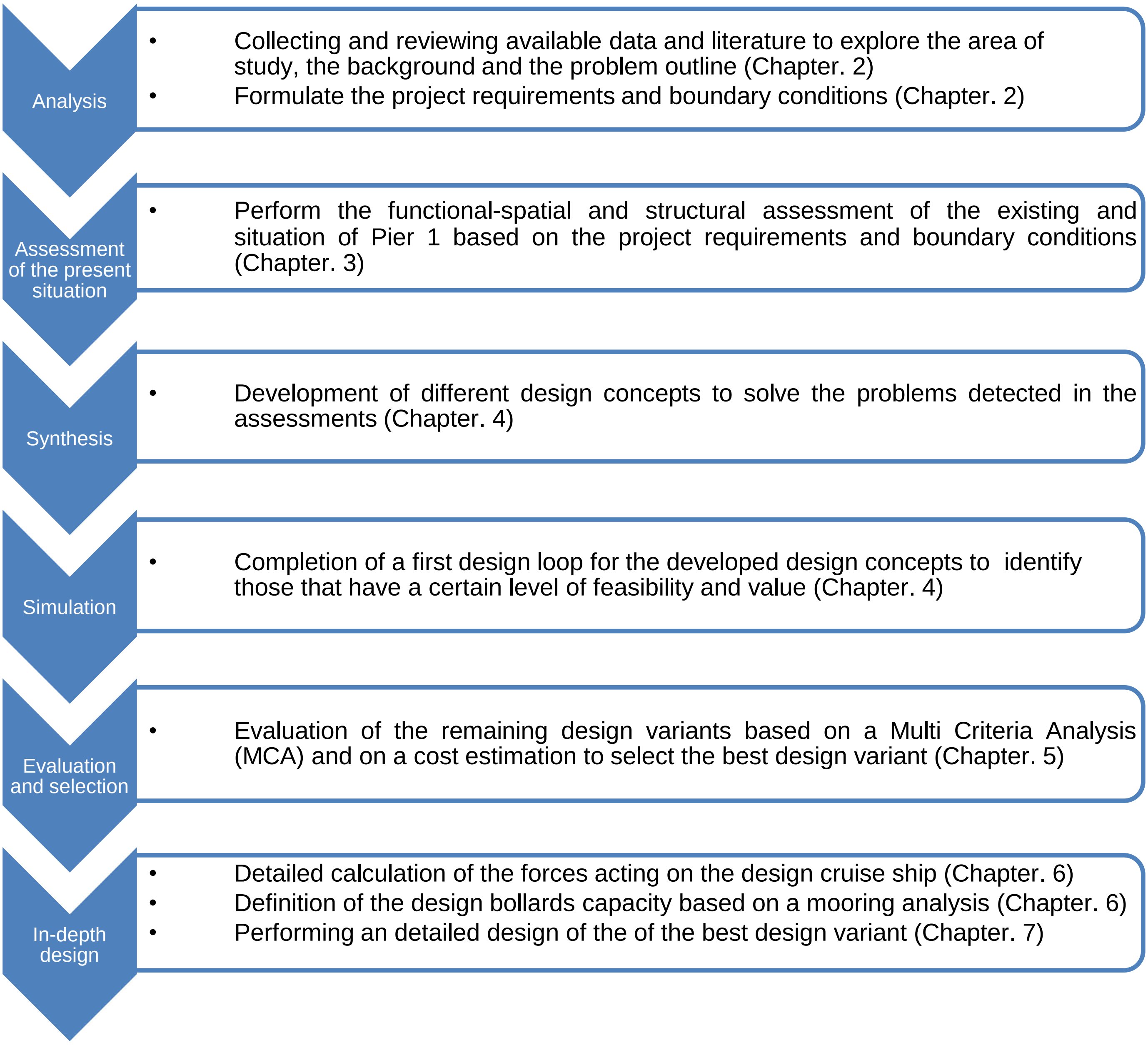

Figure 6: Activities pursued during the design process

1.5 Report structure

The structure of the report follows the approach described in the previous section (see Figure 6). In Chapter 2 first, an orientation on the problem and its environment is presented. Then, the program of requirements and the boundary condition are described. The suitability for the selected location of the new cruise terminal is assessed in Chapter 3. The assessments define what are the technical issues that obstruct the mooring of the cruise ship. In Chapter 4 different design concepts, to solve the main technical issues, are first proposed and then further elaborated and verified. The remaining design variants are evaluated through a Multi Criteria Analysis (MCA) and a cost estimation in Chapter 5. The in-depth design starts in Chapter 6. In this chapter the calculations of the forces, due to the wind and passing ships, acting on the design cruise ship and the definition of the required bollard capacity of the new cruise terminal are presented. The best design solution is developed in detail and further evaluated in Chapter 7. The conclusions, recommendations and some general consideration regarding the adaptation of the existing quay walls are given in Chapter 8.

2. Analysis

2.1 Introduction

This chapter concerns the first phase of the design cycle of Roozenburg and Eekels. The analysis phase consists of an orientation on the problem and its surrounding. In Section 2.2 a detailed description of the current situation of the Merwehaven and its quay walls is presented. Then the general aspects of cruise terminals and cruise ships are described (Section 2.3). This is done to define the program of requirements that the new cruise terminal must fulfill. The program of requirements for the new cruise terminal is presented in Section 2.4. Finally, the boundary conditions and the assumptions related to the project area and needed for the design are described in Section 2.5.

2.2 The Merwehaven

As mentioned in the previous chapter the Merwehaven is the selected location for the new cruise terminal of the port of Rotterdam. The Merwehaven, also known as the *Fruitport* when in 1971 fruit warehouses were opened for the storage of fruit and vegetables,

Nowadays, the port is in use for the transhipment of goods and different warehouse are present. The Merwehaven has a total area of 46 ha and a total quay wall length of 4228 m (HBG, 1977). The construction of the port started in 1923 and was completed in 1931.The harbor is composed of four piers (see left Figure 7). The quay walls of the piers were constructed using caissons. The caissons have different forms, varying in dimensions and slightly in shape due to the difference in depth inside the port.

The exact location for the new cruise terminal in the Merwehaven is Pier 1. Along Pier 1 two different berthing areas are available for the mooring of cruise ships (see right Figure 7). The first location is along the quay wall at the port side (see left Figure 7 orange line) the other is along the quay wall at the Nieuwe Maas side (see left Figure 7 green line). In the figure below (right) an example of a mooring configuration at Pier 1 with two cruise ships is presented.

Figure 7: Top view of the Merwehaven (Google Maps) and mooring configuration at Pier 1 (Zeecruise lange termijn visie)

2.2.1 Pier 1

In this section, a detailed description of Pier 1 is presented. The description concerns the most relevant dimensions and structural aspects of the existing quay walls. The quay walls, at the portside and riverside, have different structural characteristics and dimensions.

Characteristics, dimensions and cross-sectional properties of quay wall at the portside

The current required nautical depth (NGD) of the berth area and its approach channel along the quay wall at the portside is equal NAP -10 m. The available berth length is approximately 580 m and the minimum width of the port channel is 150 m (see Figure 8).

Figure 8: Main dimensions of Pier 1 in the Merwehaven (Globespotter)

The quay wall at the portside is constructed using caissons. The foundation level of the caisson is located at a depth of NAP -13.65 m (see Figure 9). The structural details of the caisson are shown in the table below.

Dimensions caissons at the port side of Pier 1	
Total height of the quay wall	17 m
Height of the superstructure	2.15 m
Height of the caisson	14.85 m
Total length of the caisson	43.65 m
Total width of the caisson	15.0 m
Width of the caisson (excluding toe and heel)	13.4 m
Thickness of the outer walls (x2)	0.3 m
Thickness of the inner walls (x2)	0.2 m
Thickness of the floor	0.35 m

Table 1: Cross-section dimensions of the caisson used as quay wall at the port side of Pier 1

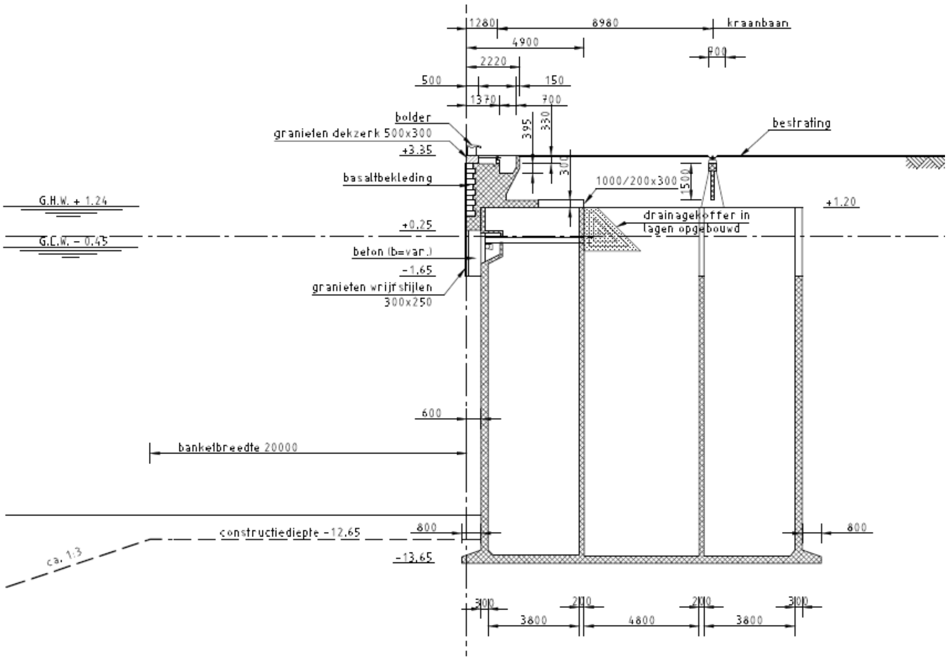

Figure 9: Detailed cross-section of the caisson used as quay wall at the portside of Pier 1 (Port of Rotterdam)

The top of the structure of the quay wall is located at NAP +3.35 m (see Figure 9). On top of it heavy cranes are located, that move on rails and allow the transhipment of goods. Bollards are placed on top of the quay wall, with a center to center distance (c.t.c) of approximately 20 m. The bollards are provided with “breaking bolts” so that the maximum allowed and possible mooring force is 750 kN (HBG, 1977). The frontage of the quay wall is made of basalt revetment. Energy absorbing fender systems are not present along the berth length. Vertical granite beams provide sufficient distance between the quay wall and the moored vessels. As shown in Figure 10.

Figure 10: Bollards and granite columns along the quay wall at the portside of Pier 1 (Port of Rotterdam)

Characteristics, dimensions and cross-sectional properties of quay wall at the riverside
The quay wall at the riverside of Pier 1 is located along the *Nieuwe Maas* and is currently not used as a berthing area. Consequently, along this side mooring systems and energy absorbing fenders system are not present. Moreover, the riverside consists of two distinct parts that are characterized by different structures. The first part, close to the access of the port, is constructed using a bank protected by a basalt revetment with a slope in 1:3 (see Figure 11). The second part of the edge of the pier continues with a quay wall constructed using an anchored sheet pile wall. The connection between the two different parts is presented in Figure 12. The toe of the sheet pile is located at NAP -9.0 m and the superstructure is at NAP +3.45 m (see Figure 13). Consequently, the sheet pile has a total height a total height of 12.45 m. The bottom level in front of the structure is at NAP -0.7 m and continues with a slope 1:3 made of rubble stone. The available berth length along the riverside of Pier 1 is approximately 310 m (see Figure 8).

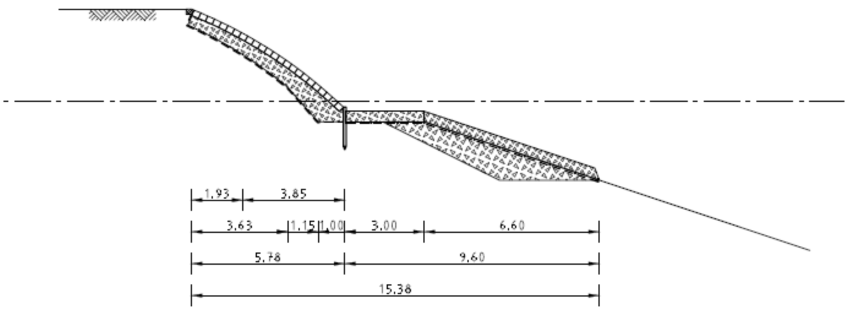

Figure 11: Cross-section of the slope revetment at the riverside of Pier 1 (Port of Rotterdam)

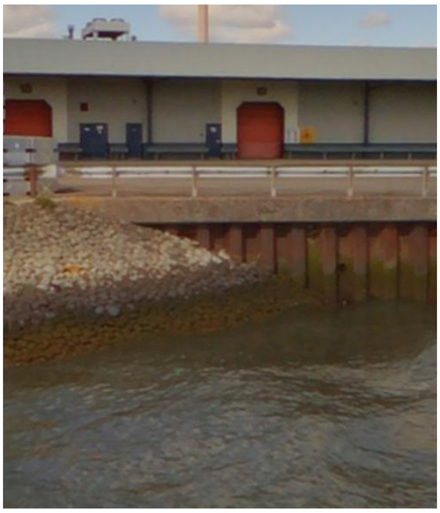

Figure 12: Connection between the protected slope and the sheet pile at the riverside of Pier 1

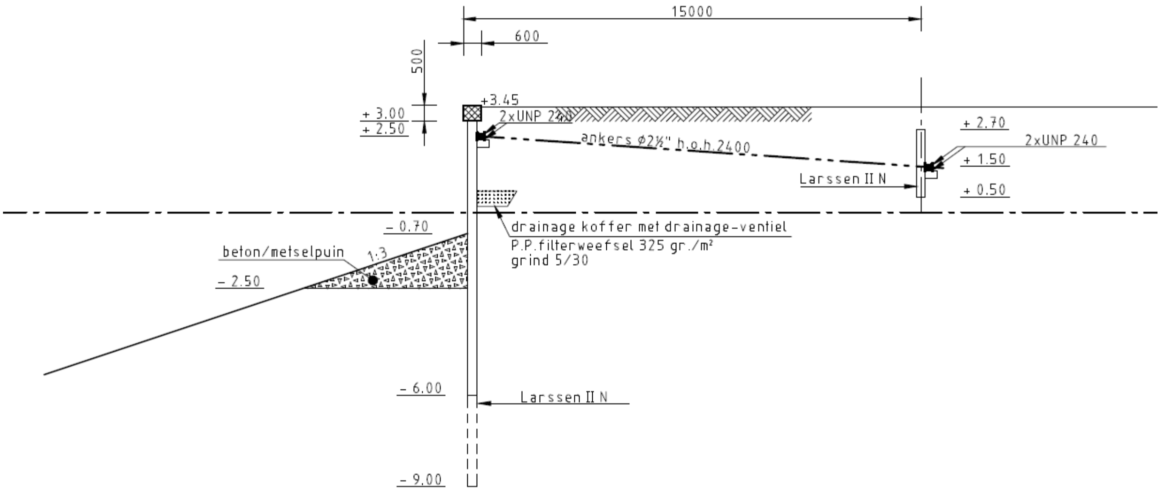

Figure 13: Cross-section of the sheet pile wall at the riverside of Pier 1 (Port of Rotterdam)

2.3 Cruise ships general aspects

The cruise market makes an essential contribution to port economies. It creates jobs and wealth for ports and their region. Therefore, more ports have developed an interest in expanding their cruise activities.

2.3.1 Cruise terminal

The location of the terminal should be in line with the master plan of the port, so that, in the long term, it is fully integrated with transport and urban planning strategies. To guarantee good accessibility, cruise terminals should be located close to the city, highways, road traffic and public transport facilities. From a maritime point of view, cruise terminal should provide minimal draught, berthing facilities and navigation channels for the cruise ships.

Cruise terminals are composed of different areas and structures (see Figure 14): apron area, terminal building, ground transportation area, city connectivity and waterside.

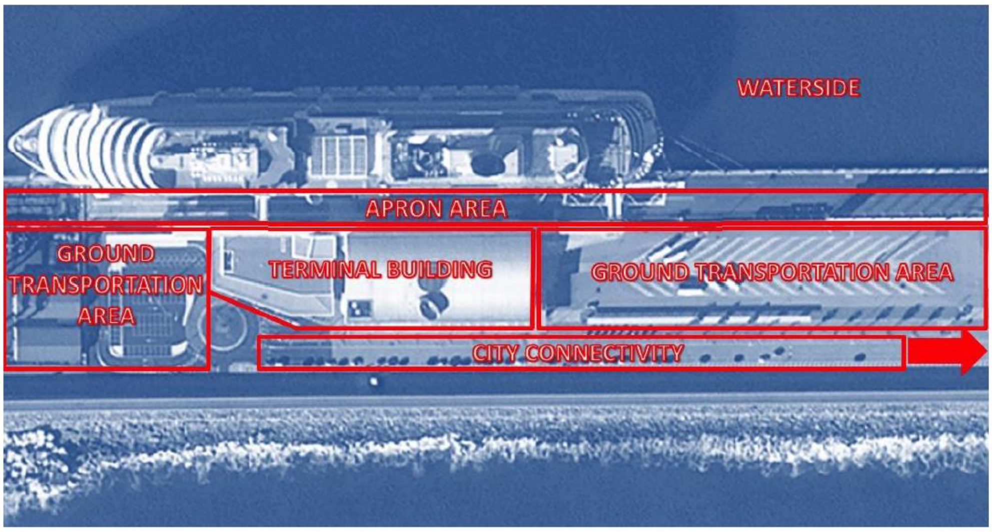

Figure 14: Layout of a cruise terminal (PIANC, Guidelines for cruise terminal, 2016)

Apron area
The apron is located on top of the quay wall. It is the area included between the edge of the berth and the terminal building. Usually, its width varies between 6 m to 30 m. The apron is a secure area with access control at all entry (PIANC, Guidelines for cruise terminal, 2016). This area provides space for the embarkation/disembarkation of the passengers, loading/unloading of utilities, supplies and waste. Besides, it provides a connection for electrical power and access for the gangways, cranes and fuel trucks.

Terminal building
The terminal building is located immediately adjacent to the apron area. The primary function of the building is to address the passengers, baggage and provisions of cruise ships during both embarkation and disembarkation. At times, these buildings have secondary uses such as event space for shopping areas, cafeterias, restaurants and warehouse.

Ground transportation area (GTA)
The GTA of a cruise terminal is the area next to the terminal building and the apron area where passengers arrive to embark on the cruise and where they disembark to travel inland. This area must be located close to the terminal building and must be connected to the public road system or public transports facilities.

Waterside
The waterside is the area where the maneuvers and mooring operation of the cruise ships take place. The dimensions and its equipment depend mainly on the number and size of the vessels that may use the facility. The main elements that characterized the waterside are the approach channel, berth length, nautical depth, mooring system and fendering systems.

2.3.2 Dimensions of cruise ships

As mentioned before the cruise market is constantly growing and to follow this mark request, the cruise ships have continued to grow in all dimensions over the past 40 years (PIANC, Guidelines for cruise terminal, 2016). This trend shows no sign of abating. Therefore, cruise terminals have to be able to guarantee sufficient mooring space for the future cruise ships.

In the figures below the trend of the average evolution of gross tonnage (GRT), passengers and cruise length overall (LOA) are presented over a period of 15 years from 1999 to 2014.

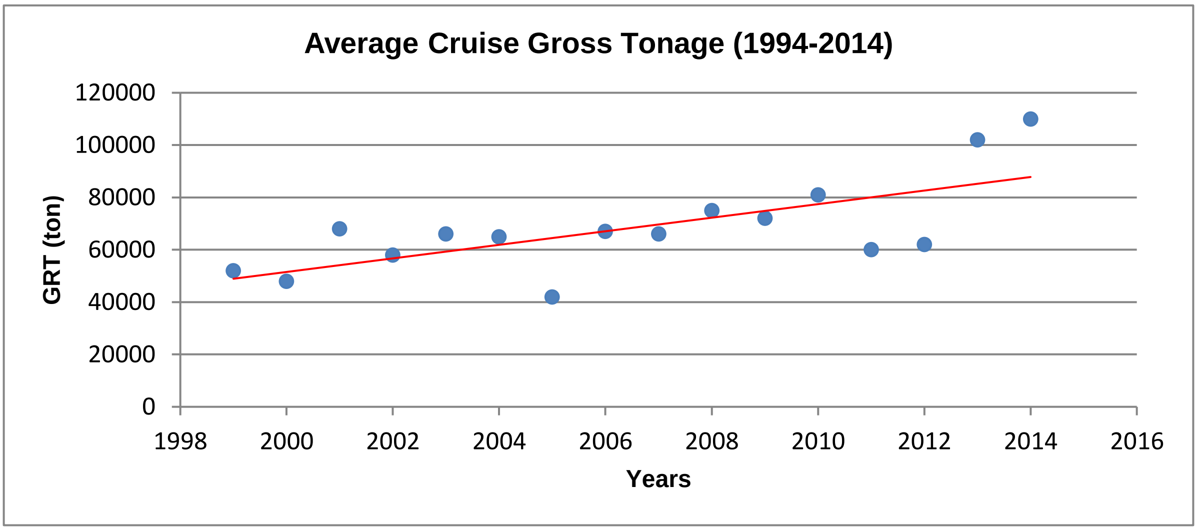

Figure 15: Evolution of the cruise average gross tonnage (GRT) between 1999 and 2014

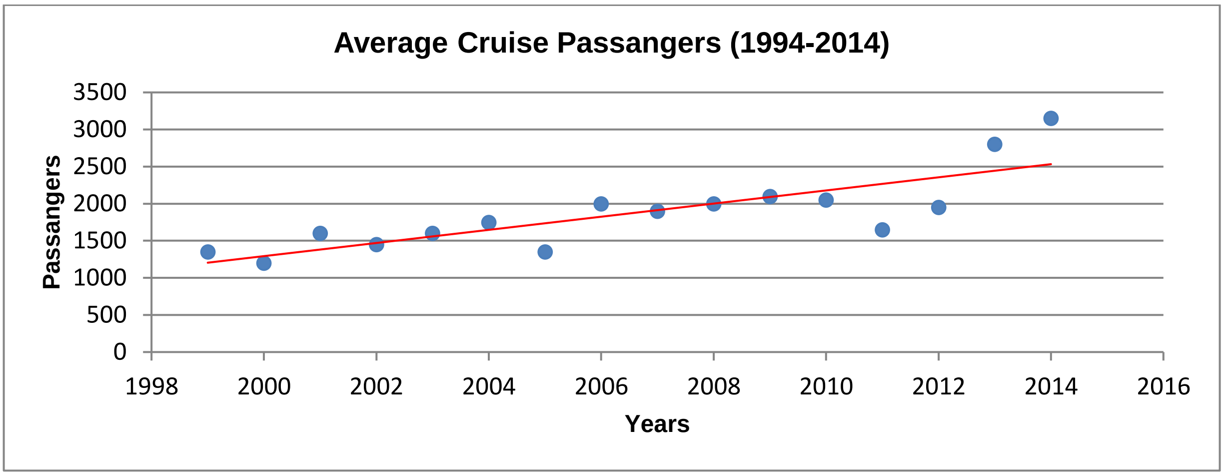

Figure 16: Evolution of the cruise passengers per cruise ship between 1999 and 2014

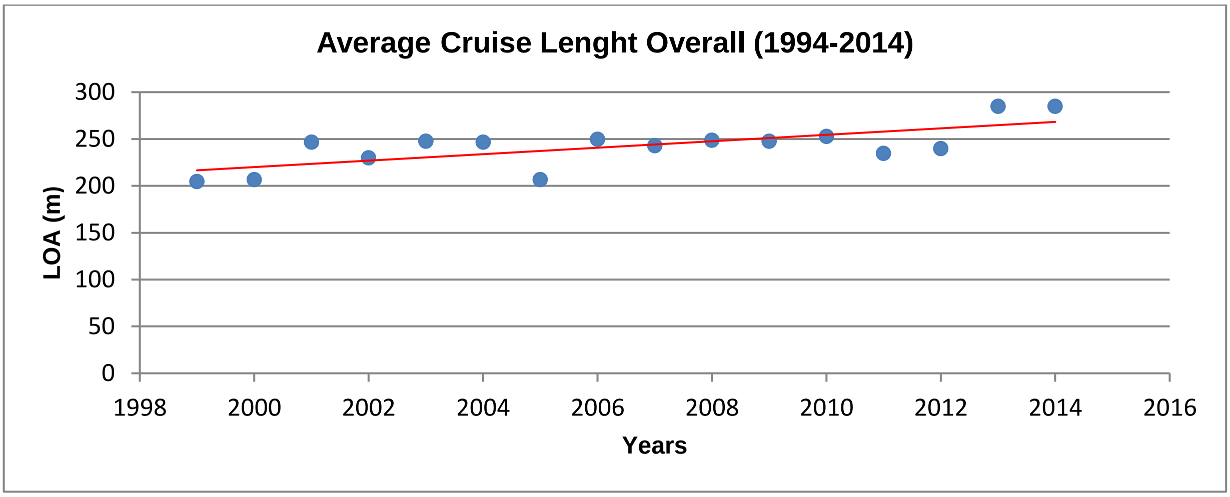

Figure 17: Evolution of the average cruise length overall (LOA) between 1999 and 2014

Form the above graphs it is clear the cruise ships are constantly growing and most likely this trend will also continue in the future. The size of the cruise ships is not the only change experienced in the last year. Cruise ships are increasing their maneuverability due to powerful propellers and thruster jets allowing them to perform the difficult maneuver and consequently approaching berthing facilities with less risk (PIANC, Guidelines for cruise terminal, 2016).

2.4 Program of requirements

The program of requirements of a project is essential for the design and constructions process. Therefore, it is necessary that these requirements are defined. Within the project requirements, a distinction can be made between functional and technical requirements.

2.4.1 Functional requirements

The main functional requirement for the new cruise terminal is that it needs to be able to accommodate, at any time, two different cruise ships. However, as stated before, different areas compose the cruise terminals. These areas have various functions and consequently, need different considerations. A distinction can be made between the functional requirements of the landside and waterside of the cruise terminal. The functional requirements of each part are listed below.

The landside of the cruise terminal must provide:

- embarkation/disembarkation and transportation of passengers
- loading/unloading and storage of supplies
- deposit of sewage and waste

- connection for electrical power and refuelling
- access to heavy trucks

The waterside must provide:

- mooring facilities
- berthing and mooring ships
- manoeuvring of the cruise ships
- passage of other vessels

In the figure below the functional requirements of the cruise terminal are presented in a function tree.

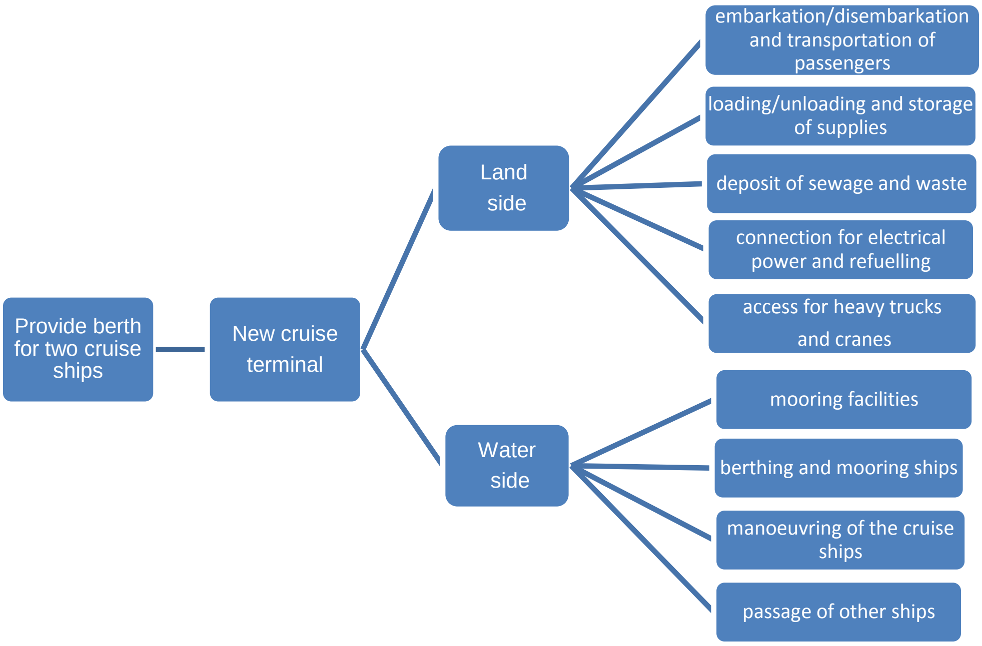

Figure 18: Primary functions of the new cruise terminal

In order to meet these requirements, the quay walls of the cruise terminal, in this case, the existing caissons, need to fulfill their functions. The functional requirements of the quay walls of the cruise terminal are presented and described below.

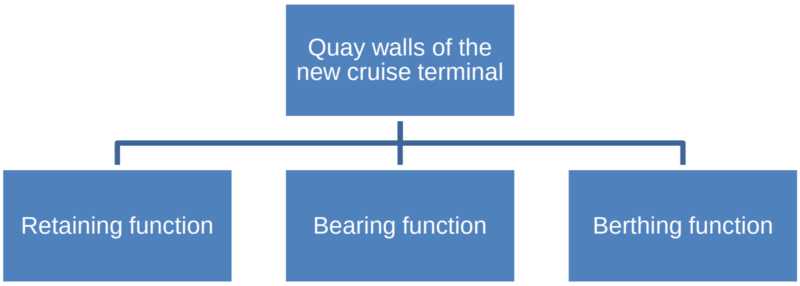

Figure 19: Functional requirements of the quay-walls

The retaining function

The quay wall must be able to retain soil and water. The height in between the top and bottom level of the quay wall determines the retaining height.

Bearing function

The quay wall must be able to bear the loads imposed by cranes, vehicles and equipment used for the loading/unloading operations of the vessels or the terminal buildings present on top. The loads depend on the function and type of vessels and the required equipment.

Berthing function
The quay wall must ensure that the vessels can berth quickly and safely and perform the loading/unloading operations without damaging the ships or the structure itself. Moreover, the quay wall must be able to withstand the loads imposed by the berthing operations. Depending on the type of ships, mooring equipment and bottom protection are placed on the top and at the toe of the quay wall respectively.

2.4.2 Technical requirements
From the functional requirements, it is possible to define the technical requirements. The most important requirements are presented and discussed below.

Design lifetime of the structure
Like most of the civil engineering projects, the design lifetime of the structure should be 50 years. During its entire design lifetime, the structure must be stable and provide enough strength to bear the imposed acting loads.

Design cruise ships
Berth areas, mooring equipment and facilities are designed based on the range of vessel types, sizes, and conditions requested by vessel operators. Therefore, it is crucial for the design to define which kind of cruise ships will moor at the cruise terminal.
At the Holland America quay, the current cruise terminal of Rotterdam, different cruise ships can moor: the Norwegian Gateway and the Aida Prima. However, as stated in the previous section, cruise ships are getting bigger. Hence, the Port of Rotterdam authority (PoR) requires that the new cruise terminal must be able to accommodate a cruise ship that is not designed yet. The dimensions of this future vessel are the maximum expected during the design lifetime of the structure (50 years). The dimensions of the design cruise ships that the new cruise terminal must be able to accommodate are presented in the following table.

Design cruise ships			
Name	Future cruise ship	Norwegian Getaway	Aida Prima
Length overall (m)	380	300	326
Beam (m)	55	37.6	40
Draft (m)	10	8.1	8.8
Passengers	Ca. 6000	3250	3963
Required nautical depth (NAP +m)	-11.75	-9.8	-10.5
Required construction depth (NAP +m)	Ca. -14	Ca. -13	Ca. -12
Required berth length (m)	460	360	390
Approach channel width (m)	110	75.2	80

Table 2: Characteristic of the design cruise ships with the related dimensions

Required nautical depth
A minimum water depth at the berth area and the approach channel has always be guaranteed. The design depth incorporates the draught of the design ship and the desired keel clearance typically identified by the port authorities and by the vessel owner/operator. According to the Port and waterways Guidelines of the Port of Rotterdam Authority (Havenbedrijf Rotterdam NV, 2014) the required nautical depth (Nautisch Gegarandeerde Diepte NGD) relative to NAP (New Amsterdam Level) is the minimum depth that must always be guaranteed inside the port or at the quay wall. According to the Port of Rotterdam Authority (PoR) the required nautical depth can be computed using the following equation:

$$NGD_{NAP} = ALAT - T_{max} - FWA - UKC - HMT$$

Where:

NDG_{NAP} is the nautical required depth [m]

ALAT is the Approximately Lowest Astronomical Tide, its value varies along the Port of Rotterdam, for the Merwehaven is equal to NAP -0.7 m

T_{max} is the maximum draught of the cruise ship in seawater [m]

FWA is the increase of the draught of the cruise ship due to changes of water density. It is estimated to be 2.5% of the draught [m]

UKC is the minimum required keel clearance and is equal to 0.5 m

HMT is the meteorological effects allowance, this factor takes into consideration atmospheric effects and low river discharges and its value is equal to 0.3 m

Construction depth

The construction depth (relative to NAP) is the reference level used for the stability calculation of the structure. It corresponds to the foundation depth of the structure. The required construction depth is given by adding to the above mentioned required nautical depth (NGD) an additional distance. This distance, always required by PoR, accounts for: a maintenance margin, the thickness of scour protection (if needed) and the tolerance margin for dredging and construction operations. The value of the maintenance margin depends on the project location and the presence of bottom protection. For the Merwehaven, PoR sets maintenance margin equal to 1 m. The thickness of the scour protection depends on the bed velocity currents generated by the thruster jets of the design ship. The accuracy margin of dredging and construction operations are in the order of 10-20 cm.

If the foundation of an existing structure is located at a smaller depth than the required construction depth, countermeasures have to be provided to guarantee the stability of the structure.

Berth length

To guarantee a safe departure and arrival of the cruise ship a minimal berth length is required. According to the Port and waterways Guidelines of the PoR (Havenbedrijf Rotterdam NV, 2014), the required minimum berth length that the quay wall should have can be calculated by the following equation:

$$L_{quaywall} = L_{ship} + 2 \cdot 0.1 \cdot L_{ship}$$

Where:

$L_{quaywall}$ is the minimum length of the quay wall [m]

L_{ship} is the overall length (LOA) of the cruise ship [m]

Approach channel width

To provide enough maneuver space so that cruise ships can reach the berthing area safely, the approach channel should have a minimum width. According to the PIANC guidelines the minimum required approach channel width for cruise ships can be obtained using the equation below:

$$W_{channel} = 2 \cdot B_{ship}$$

Where:

$W_{channel}$ is the width of the approach channel [m]

B_{ship} is the beam of the cruise ship [m]

Passage space and turning basin for passing ships

When a cruise ship is moored along quay, a minimum distance is required to ensure the safe passage and maneuver of other vessels (see Figure 20). Therefore, a minimum channel width and turning basin area are needed behind the moored cruise ship so that other vessels can reach the other piers of the Merwehaven. According to the Port and waterways Guidelines (Havenbedrijf

Rotterdam NV, 2014) the minimum channel width for inland vessels can be computed using the following formula:

$$W_{channel} = 2 \cdot B_{ship}$$

Where:
$X_{channel}$ is the minimum required width of the navigation channel behind the moored cruise ship [m]
B_{ship} is the maximum beam of the passing ship [m]

The minimum required diameter of the turning basin for inland ships can be obtained using the following equation:

$$D_{basin} = 1.2 \cdot L_{ship}$$

Where:
D_{basin} is the minimum diameter of the turning basin [m]
L_{ship} is the overall length of the passing ship [m]

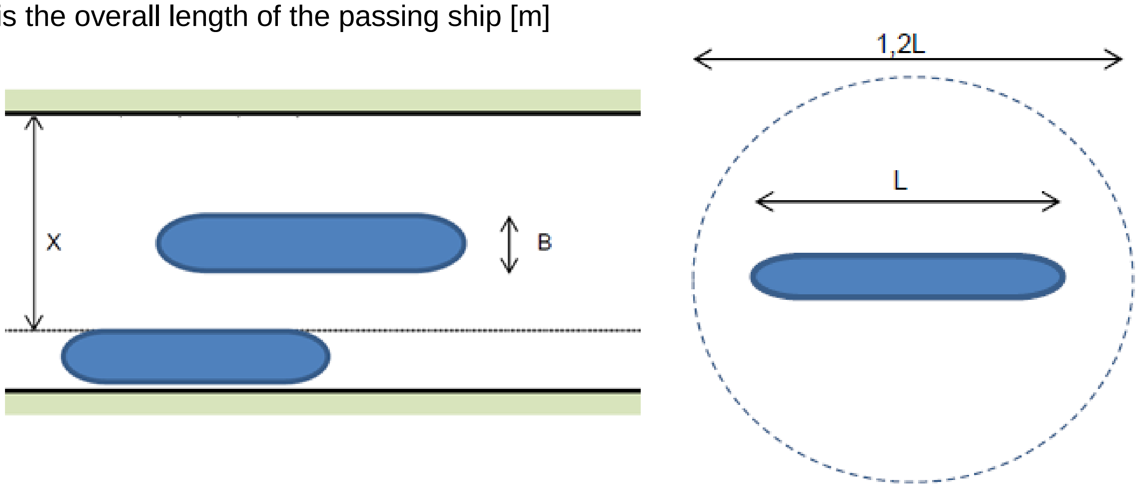

Figure 20: Width of the navigation channel and turning basin (Havenbedrijf Rotterdam NV, 2014)

Retaining height
The retaining height of the quay wall is the maximum height along which they quay walls must retain the water and the soil pressure. This height is between the level of the superstructure and the level of the construction depth (Broeken & Gijt, 2014).

Width of the quay wall (Apron area)
A minimum width of the Apron area is required to perform the operations that have to take place safely. Hence, the distance between the bollards line and the terminal building should be at least equal to 20-25 m. Besides, this area should be flat.

Vertical design loads on top of the quay wall
The vertical load acting on the superstructure that the quay wall has to bear is given by weight of the heavy vehicles such as the LNG tanker truck and cranes that have access to the apron area. These are used for the different the operations that take place in the apron area.

Scour protection
To avoid erosion along the berth area and consequently ensure the stability of the quay wall, a scour protection is required. The design of the bottom protection depends on the velocity of the bed currents generated by the propeller and traverse thrusters jets of the design cruise ships.

Mooring and fendering systems
The design of an efficient mooring system is essential for the safety of the ship, her crew, the terminal and the environment (OCIMF, 2008). The mooring system is composed of bollards or mooring dolphin where the lines of the vessels are tied and fenders or breasting dolphin that absorb the impact of the ships.

The bollards, together with the lines and the winches, form the system that restrains the vessel movements and avoids that the ship turns away. The bollards located at the quay wall of the current cruise terminal (Wilhelminapier) have a capacity of 800 kN. Also, two storm bollards are present in correspondence of the bow and stern of the ship with a capacity of 1200 kN (Port of Rotterdam Authority). The design of the bollard capacity has to be studied in detail by calculating the loads acting on the design cruise ship.

Fendering systems absorb the berthing energy of the vessel and provide a soft buffer between the quay wall and ship while moored (PIANC, Guidelines for cruise terminal, 2016). To berth the cruise ships along the quay wall, a fendering system has to be designed. Along the quay wall of the current cruise terminal floating fenders are adopted. The fenders are supported by huge panels that spread the impact load over a bigger surface of the quay wall. This fendering type may also be adopted for the new cruise terminal.

2.5 Boundary conditions and assumptions

In this section, the boundary condition and the assumptions required for the design of the cruise terminal are described.

Hydraulic properties
The tide influences the water levels of the port of Rotterdam. For this reason, several measuring stations that measure the water level are located inside the harbor. The location of the stations is presented in Figure 21.

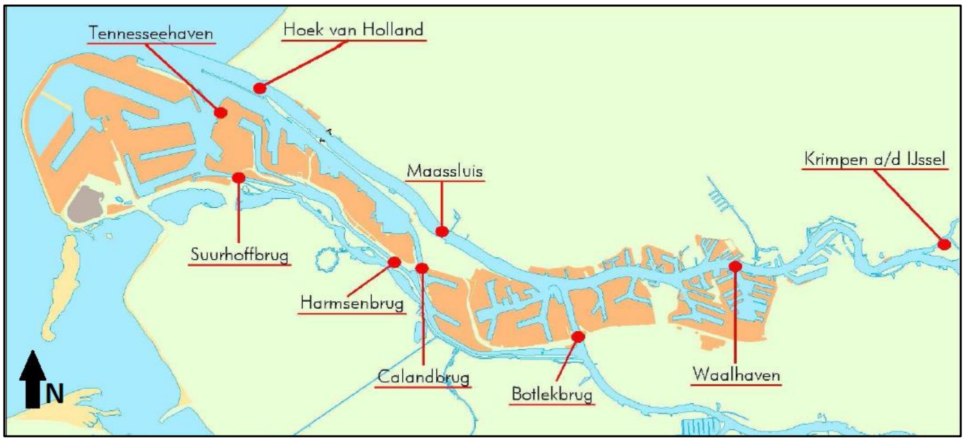

Figure 21: Measuring stations of water levels in the port of Rotterdam (Port of Rotterdam, HydroMeteoBundel, 2012)

The design water levels are taken according to the HydroMeteo Bundel nr 4, 2012. The water levels changes, due to the tide, are calculated during extreme discharges with a return period of one every ten years. The closest measuring station to the project area is at the Waalhaven (see Figure 22). The water level changes (in cm respect to NAP) at the Waalhaven during springtide, neap tide and mean tide with extreme discharges are presented in the figure below.

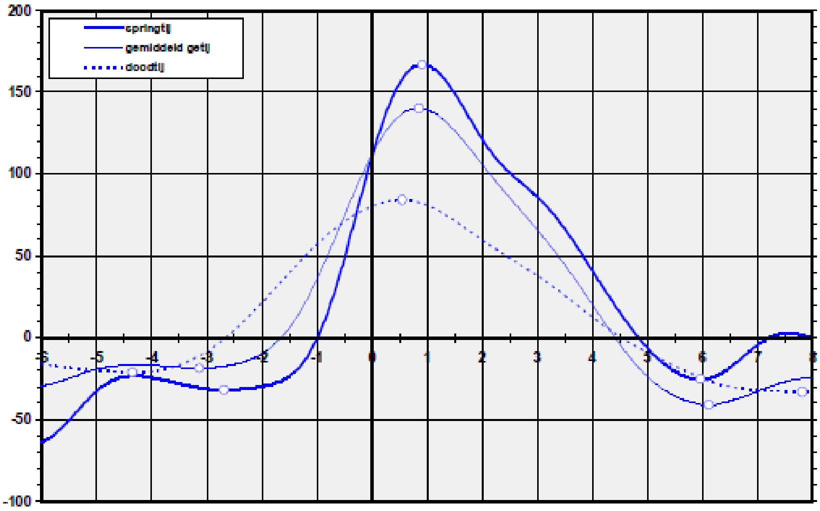

Figure 22: Water level relative to NAP in time at the Waalhaven due to tide during extreme discharges with a return period of 1 per 10 years (Port of Rotterdam, HydroMeteoBundel, 2012)

The maximum and minimum water levels are NAP +1.7 m and NAP -0.7 m respectively. The minimum water level coincides with the Lowest astronomical tide (LAT). Note that Figure 22 shows only the effect of the tide on the water levels. During the design phase also the impact of wind, meteorological and sea level rise should be included.

The importance of seiches like short-term atmospheric depressions has become much less relevant due to the presence of the Hartelkering and the Maeslantkering (Voorendt & Molenaar, Manual Hydraulic Structures, 2017). Hence, these meteorological effects are not considered in the design.

In literature, flow velocities due to the tidal currents are found just above 1.5 m/s (Port of Rotterdam, HydroMeteoBundel, 2012). Thus, a maximum current velocity of 1.5 m/s is assumed for the design. However, in the vicinity of the berthing structures, the action of propeller and traverse thruster jets cause higher flow velocities. These currents are essential for the design of the bottom protection and thus for the stability of the structure.

Waves

In a sheltered environment, like a port, waves are not a critical factor for structures. However, they influence the mooring operations. Therefore, the design of the berthing facility should take into consideration the impact of waves generated by wind and passing vessels.

Wind properties

Wind velocity and direction are crucial aspects for the calculation of the mooring loads. In the Port of Rotterdam, several measurement stations are present. In Figure 23 the location of the measurement stations is shown.

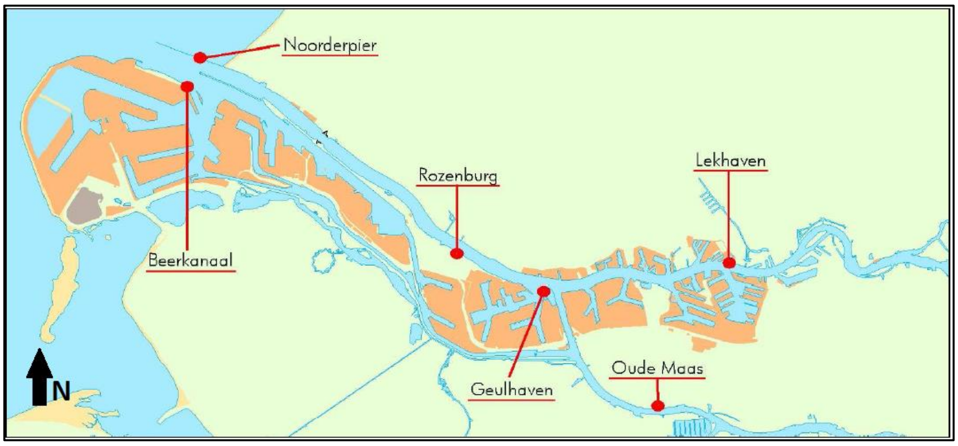

Figure 23: Measuring station of the wind in the port of Rotterdam (Port of Rotterdam, HydroMeteoBundel, 2012)

The Lekhaven station is the nearest to the project area (see Figure 23). The figure below shows the measured wind rose of the Lekhaven station.

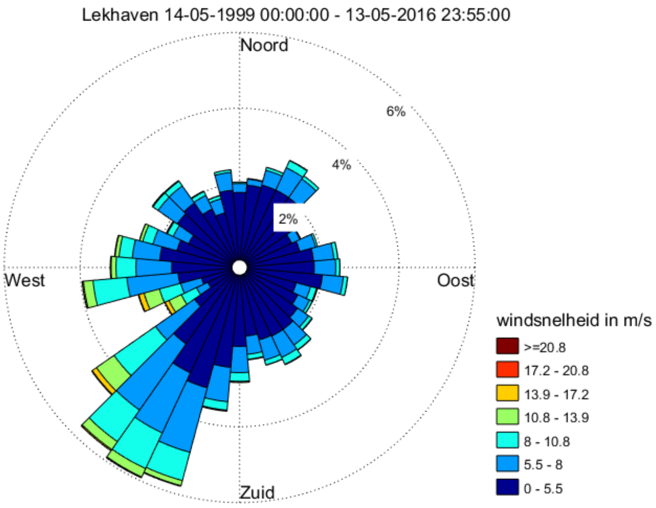

Figure 24: Wind rose Lekhaven measured based on mean values of 5 minutes intervals (Port of Rotterdam, Windstatistiek Lekhaven, 2016)

The presented wind rose covers 17 years, between 14 may 1999 and 13 may 2016. The measuring point is located at 35 m above quay wall height and data is presented as mean values of 5 minutes intervals (Port of Rotterdam, Windstatistiek Lekhaven, 2016). This data can be used to define which are the most critical wind direction for the calculation wind load acting on the cruise ships. However, to determine the design wind load, wind speed with a higher return period (50 or 100 years) and with a lower average interval are needed. To obtain these wind speeds a probabilistic extrapolation may be required.

Geotechnical properties

The soil properties of the Merwehaven are typical for the western part of Holland and are characterized by the following aspects:

- At the surface a layer of sand is present.
- Below this, many different layers of weak, cohesive soil types are found.
- Around NAP - 15/20 m strong layers of sand are present.

A cone penetration test (CPT) results at Pier 1 and behind de caisson are presented in Appendix A.

The foundation level of the caisson is at NAP -13.65 m (see Section 2.2.1). Before placing the caissons, the soft cohesive layer, present at this depth above the strong layers of sand, was removed, and a foundation sand layer was placed. Because foundations are never situated directly on cohesive materials but always on sand or gravel (Voorendt & Molenaar, Manual Hydraulic Structures, 2017). This is done to avoid consolidation settlement issues that could lead to instability problem of the structure. Note that this assumption is verified in detail in this report. The foundation layer was most likely placed on a slope (see Figure 25).

According to the result of the CPT (see Appendix A) the soil behind the caissons was backfilled and the deep sand layer starts at NAP -17.65 m. In the figure below the caisson and the different soil layers are presented.

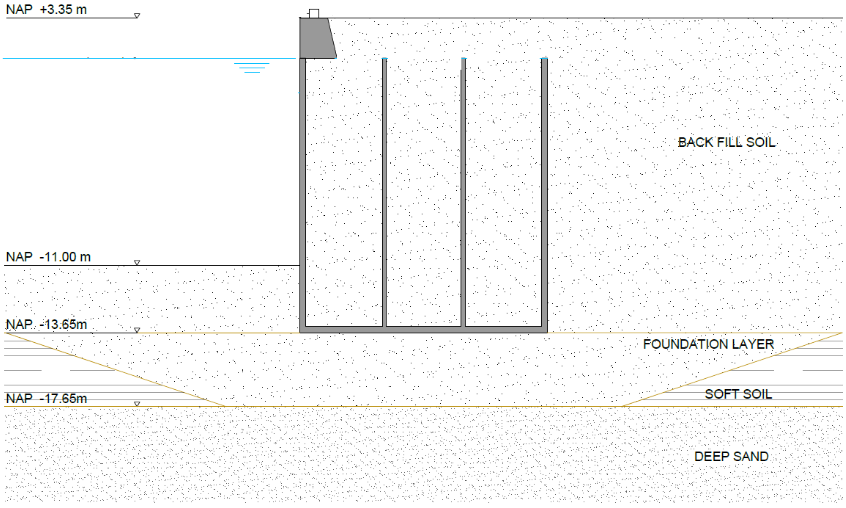

Figure 25: Caissons placed on a sloped foundation layer and different present soil layer

It is assumed that the backfill soil is comparable to the soil that was removed and would, therefore, be silty sand.

The foundation layer and the backfill soil are assumed to have the same mechanical properties with the following characteristics.

Mechanical properties backfill soil	
Dry weight	18 kN/m^3
Submerged weight	20 kN/m^3
Angle of internal friction	30 deg

Table 3: Characteristics backfill soil

The mechanical properties of the deep sand layer are presented in the table below:

Mechanical properties deep sand	
Dry weight	19 kN/m^3
Submerged weight	21 kN/m^3
Angle of internal friction	32 deg

Table 4: Characteristics deep sand layer

According to the soil investigations available on *Dinoloket* the bed material inside the Merwehaven is clay (see Appendix A). It is assumed that the clay is slightly sandy. The properties of the clay layer are taken according to Eurocode 7 NEN-EN9997 and have the following mechanical properties.

Mechanical properties of the bed	
Submerged weight	18 kN/m^3
Angle of internal friction	22.5 deg
Cohesion	5 kN/m^2

Table 5: Characteristics bed soil inside the Merwehaven

The soil investigations and their location regarding Pier 1 of the Merwehaven are all presented in Appendix A.

Water level inside Pier 1

Water levels behind the quay wall at Pier 1 are available on *Funderingsloket* of the municipality of Rotterdam. The maximum and minimum water levels behind the caisson are obtained by the closest water pressure sensor and are equal to NAP +1.21 m and NAP +0.46 m respectively. The water pressure sensor measured over a period of 34 years between 1951 and 1985. The position of the water pressure sensor is presented in Appendix A.

According to the Quay Wall Second edition, 2014, the design water pressure difference over a quay wall with permeable soil conditions is given by the following equation:

$$\Delta H = LLWS + 0.5 \cdot h_{tide;spring} = 1.2 \text{ m}$$

Where:

LLWS is the Low LowWater Spring Tide [m]

$h_{tide,spring}$ is the water level difference between high and low water during spring tide, equal to 2.4 m (see Figure 22)

Vertical loads on top of the quay wall
The type and order of magnitude of the vertical loads present on top of the quay wall are not specified. Therefore, to calculate the bearing capacity of the foundation and the earth pressure acting on the retaining structure an average surface load, for cargo handling and container areas of 30 to 50 kN/m^2 can be assumed (de Gijt, 2004).

Material properties
The type of concrete and steel reinforcement used for the realization of the caissons is not specified in any drawings or other documents. Therefore, it is assumed that a concrete type C28/35 and a steel S 235 type were used for the construction of the caissons. According to Eurocode 2, the compressive strength of the concrete increases with time. The current compressive strength increase can be computed by multiplying the initial mean compressive strength by a specific factor β_{cc}. This factor depends on the age of the concrete and the type of cement. However, in another study (Danad, 2015) regarding the old caissons in the port of Rotterdam (among which the Merwehaven), it is found that after 55 years the compressive strength of the concrete is a factor 3.84 times higher than the initial design strength. However, the steel reinforcement may not have the same strength properties as the initial one due to corrosion.

Design cruise ship
The design cruise ship is a vessel that does not exist yet. The main dimensions (length, width and draught) are given by PoR and are presented in the project requirements (see Section 2.4.2). The remaining characteristics of the design cruise ship are estimated based on the literature study. These characteristics are the maximum expected during the design lifetime of the structure (50 years). In Table 6 the characteristics and dimensions of the design cruise ship are presented.

Dimensions of the design "future" cruise ship							
Gross register tonnage GRT (t)	Dead weight DWT (t)	Water displacement (t)	Length overall LOA (m)	Length between pp LPP (m)	Beam B (m)	Draught T (m)	Air draught (m)
240000	25000	120000	380	350	55	10	75

Table 6: Dimension design cruise ship

According to the British Standard, the normal berthing velocity and the berthing angle of the design cruise ship can be assumed to be equal to 0.08 m/s and 6° respectively (see Appendix B). The maximum roll angle is assumed to be equal to 5° (Havenbedrijf Rotterdam NV, 2014).

Design passing vessels
Different types of vessels have to reach the other piers present in the Merwehaven. According to the Dutch waterways (Rijkswaterstaat, 2017) the Merwehaven is currently used by vessels CEMT-class IV. The dimensions of this type of vessel are presented below:

Dimension passing vessel				
CEMT-class	Length (m)	Beam (m)	Draught (m)	Air draught (m)
IV	105	9.5	3	6.7

Table 7: Dimensions passing ship in the Merwehaven

Given the above dimensions of the passing ship and the technical requirements (see Section 2.4.2) the minimal required passage space and the diameter of the of the turning basin are equal to 19 m and 126 m respectively.

3. Suitability of the existing Pier 1

3.1 Introduction

Now that the program of requirements, boundary conditions and assumptions are defined the current situation of Pier 1 can be assessed. This chapter first presents a functional-spatial assessment of the existing quay walls (Section 3.2 and 3.3). The scope of this assessment is to establish if the quay walls meet the requirements for the new cruise terminal. If the requirements are not met, the assessment identifies the main issues that can hinder the mooring of the cruise ships. Then the chapter presents a structural assessment that is focused on the caissons used as quay walls at the port side of Pier 1 (see Section 3.4). The aim of this assessment is mainly to establish the failure mechanism that may compromise the stability of the caissons. Besides, this section includes a geotechnical assessment and a sensitivity analysis of the parameters that influence the stability of the caissons. The conclusions of the assessments are presented in Section 3.5.

3.2 Functional-spatial assessment of the quay wall at the portside

As mentioned in the description of Pier 1 (see Section 2.2.1), the quay wall at the port side has a length of approximately 580 m and the approach channel has a minimum width of 150 m. The required berth length and width of the approach channel for the design cruise ship are 460 m and 110 m respectively (see Section 2.4.2). Therefore, the quay wall at the port side of Pier 1 can provide mooring for the design cruise ships. Furthermore, when the design cruise ship is moored, the approach channel has a remaining width approximately 95 m. This value is obtained by subtracting from the total width of the approach channel the beam of the design cruise (see Table 6) and an additional distance present between the cruise ship and the quay wall equal to 10 m (conservative assumption) due to the presence of the fenders. The minimum required passage space needed for the vessels that have to reach the other piers of the Merwehaven is 19 m (see Section 2.5). Hence, when the design cruise ship is moored the approach channel is wide enough to ensure the passage of other vessels. However, when the design cruise ship is moored along the berth area, the turning basin area is over crossed as shown in the figure below. The negative impact on the maneuvers for the passing vessels due to this space reduction should be investigated.

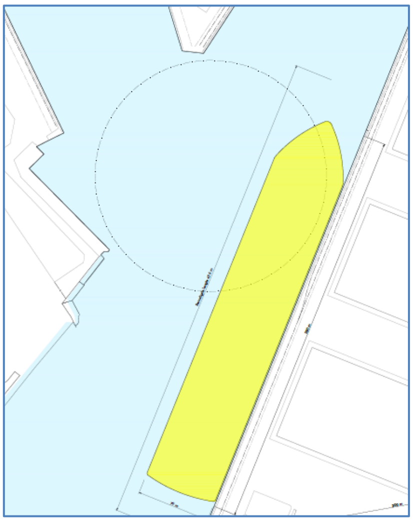

Figure 26: Turning basin for passing vessels over crossed in the Merwehaven

Furthermore, to allow the mooring of the design cruise ship, the existing quay wall at the port side of Pier 1 would require several adaptations. The most challenging problems concern the required nautical depth (NGD) and the construction depth. Due to the bigger draught, of the design cruise ship, the NGD and the construction depth values increase. According to technical requirements (see

Section 2.4.2), the new required design values of the NGD and the construction depth are equal to NAP-11.75 m and NAP-14 m respectively (see Table 2).

The required construction depth is obtained by adding to the required nautical depth the given maintenance margin equal to 1 m (see Section 2.4.2), the thickness of the scour protections equal to 1 m (assumption) and a tolerance margin of the dredging and construction operations both equal to 0.15 m (assumption).

The current required nautical depth level is equal to NAP -10 m and the foundation depth of the caisson is at a depth of NAP- 13.65 m (see Section 2.2.1). Hence, it is clear that the current NGD and the construction depth do not meet the new requirements and consequently deepening of the berth area and approach channel is required. Although the difference between the current foundation depth of the caisson and the new required construction depth may seem relatively small (approx. 0.35 m), this may lead to instability problems. Therefore, a technical solution must be provided to ensure the stability of the caissons.

To summarize what has been described so far, the following table compares the current dimensions of the quay wall at the port side of Pier 1 with the required dimensions of the future cruise terminal.

Current dimensions of the quay wall at the portside of Pier 1 vs. Required dimensions of the future cruise terminal			
Component	**Current**	**Required**	**Satisfied**
Berth length (m)	580	460	Yes
Minimum width of the approach channel (m)	150	110	Yes
Minimum width of the channel for other vessels (m)	95	20	Yes
Required nautical depth (NAP+ m)	-10	-11.75	No
Required construction depth (NAP+ m)	-13.65	-14	No

Table 8: Current dimensions of the quay wall at portside of Pier 1 vs. required dimensions of the future cruise terminal

Another important aspect that has to be considered is the bollards capacity. Bollards are placed every 20 m along the full length of the quay wall. The design capacity of the existing bollards is equal to 750 kN (HBG, 1977) which is much lower than the imposed load according to the MBL criteria (see Appendix G). Furthermore, cruise ships are characterized by huge areas exposed to wind and hence substantial air draught that consequently may cause considerable wind loads. However, the favorable orientation of the Pier 1 may lead to relatively low wind loads. The critical wind direction, which would cause the highest loading for the bollards, Easterly. In the port of the Rotterdam, this wind direction is not frequent and is characterized by relatively low wind speeds (see Figure 24). For this reason, a detailed study of the wind load must be performed to determine the design bollard capacity.

Moreover, the quay wall requires a fendering system to provide mooring for the design cruise ships. Along the existing structure, fenders are not present. For this reason, a new fender system has to be provided. The floating fender system that is currently used at the Holland America quay could be adopted, or an alternative system could be designed. In both cases, the loads imposed by the berthing energy impact and by the own weight of the fenders should be withstood by the basalt revetment and by the underlying caisson. Therefore, the resistance of the basalt revetment and the concrete strength of the caissons should be assessed and verified.

Lastly, a new scour protection has to be designed to avoid erosion of the bottom due to high current flow velocities caused by the powerful cruise ship propellers and thruster jets of the design cruise ship.

3.3 Functional-spatial assessment of the quay wall at the riverside

As stated earlier the quay wall at the riverside of Pier 1 is not used as a berth area (see Section 2.2.1). The quay is constructed with a sheet pile wall and a protected bank. The bed level in front of the sheet pile is NAP -0.7 m and the toe of the wall is located at NAP -9.0 m. Therefore, to achieve the required design values of the NGD (NAP -11.75 m) a completely new quay wall is required. The design of the new quay wall should also include the design of the mooring equipment and the fendering system.

Moreover, the quay wall has a length of approximately 310 m. This length is not sufficient to provide mooring for any of the design cruise ships (see Table 6). To solve this problem, a mooring dolphin can be placed beyond the end of berth area or the new quay wall can be extended. However, to avoid obstruction for the vessels that need to reach the Keilehaven, the port located more upstream, attention should be given to the extension of the quay wall or the position of the mooring dolphin (see Figure 27).

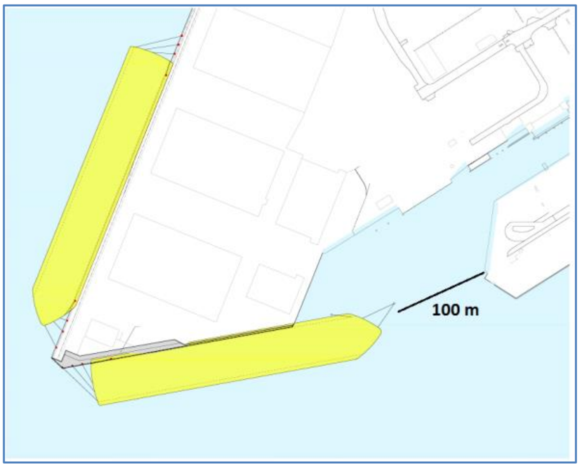

Figure 27: New quay wall with mooring dolphin at the riverside Pier 1

The quay wall of the riverside of Pier 1 is located along the *Nieuwe Maas*. Therefore, along the quay wall, there are no restrictions regarding the minimum approach channel width for the design cruise ship.

To summarize the following table presents the current dimensions of the quay wall at the port side of Pier 1 and the required dimensions of the future cruise terminal.

Current dimensions of the quay wall at the riverside of Pier 1 vs. Required dimensions of the future cruise terminal			
Component	**Existing**	**Required**	**Satisfied**
Berth length (m)	310	456	No
Minimum width of the approach channel (m)	No restrictions	-	Yes
Minimum width of the channel for other vessels (m)	100	28.5	Yes
Required nautical depth (NAP + m)	-10	-11.75	No
Required construction depth (NAP + m)	-13.65	-14	No

Table 9: Current dimensions of the quay wall at riverside of Pier 1 vs. required dimensions of the future cruise terminal

3.4 Structural assessment of the quay wall at the port side

In this section, the stability checks for the existing caisson at the portside of Pier 1 are performed. The stability checks aim to define what are the main mechanisms that may compromise the stability of the quay wall in the current situation and due to the deepening of the port.

3.4.1 General aspects of caissons

As mentioned in the previous chapter the quay walls in the Merwehaven were constructed using caissons. For this reason, it is essential to describe the most relevant aspects of this type of structure.

In civil engineering, caissons are gravity structures that are usually used as a temporary or permanent watertight retaining structures. Caissons are large hollow cellular concrete elements. They are prefabricated in the dry or floating docks or cofferdam. Then they are usually floated and transported to their final location and where they are sunk into their final position. Caissons are usually designed so that, after sinking the top is just above the water level. The cells are ballasted with sand or sometimes with gravel or concrete. Also during transportation, the caissons need to be ballasted to guarantee the stability in floating condition. The effect of waves, especially long waves might be critical for the stability during transport and hence must be considered in the design phase (BS 6349-4 Part 4, 2014). The top of the structure and the joints between the caissons are finally cast in-situ after that the initial settlement of the subsoil has taken place. In case that caissons are used as quay wall the top of the structure is equipped with berthing facilities such as bollards and fenders. The presence of these facilities causes concentrated horizontal forces that should be considered in the design of the structure. Caissons are usually placed on a granular foundation layer to minimize the settlement and guarantee sufficient bearing capacity. The foundation layer is placed by means of dredging or excavation, followed by filling the trench by coarse sand or stone filter layers. It is also necessary to protect the bottom in front of the caisson against erosion.

The caissons should be designed so that the overall stability is guaranteed at every stage of the construction and service time. Lastly, the reinforced concrete structure has to withstand the load acting on the caisson walls and therefore, the reinforced concrete must ensure the required strength of the structure.

3.4.2 General stability of caissons

The stability of the caisson is carried out using the stability checks for a gravity structure. These checks are based on static analysis. Gravity structures retain the acing loads by transferring the loads to the foundation by means of a compression force and a friction force. These forces act on the foundation surface and both are the results of the dead weight of the structure. Hence, it requires that the foundation layer, located beneath the structure has sufficient bearing capacity.

The caissons used as a quay wall have to retain horizontal pressure, caused by the vertical surcharge of the quay wall, the soil and the water head difference present behind the structure. In addition, they have also to withstand the horizontal mooring forces caused by the presence of the bollards. The figure below presents the different loads that the caisson used as a quay wall has to withstand.

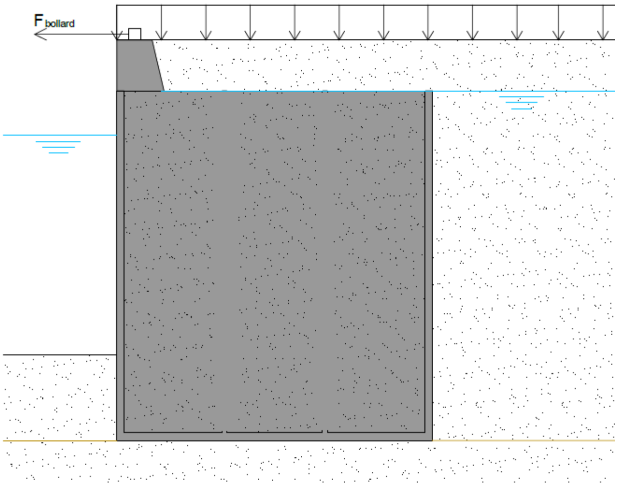

Figure 28: Loads acting on the caisson used as quay wall

Therefore, the structure is defined stable if the horizontal, vertical and rotational stability are satisfied (Manual Hydraulic Structures, 2017). This implies that:

$$\Sigma H_{total} = 0$$

$$\Sigma M_{total} = 0,$$

$$\Sigma V_{total} = 0$$

Where:

ΣH_{total} is the total of the horizontal components of the acting and resisting forces

ΣM_{total} is the total of the moment caused by the acting and resisting forces

ΣV_{total} is the total of the vertical components of the acting and resisting forces

The caisson is horizontally stable if the friction force of the foundation soil resists the resulting total acting horizontal force. This friction force is determined by the total of the forces acting on the structure in vertical direction multiplied by a dimensionless friction coefficient (f). The friction force should not be less than the total acting horizontal forces to prevent the structure from sliding aside. Thus, the structure is horizontal equilibrium is stable if the following equation is verified:

$$\Sigma H < f \cdot \Sigma V$$

Where:

ΣH is the total of acting horizontal forces

f is the friction coefficient equal to tan(2/3*φ) where φ is the friction angle of the foundation soil

ΣV is the total of acting vertical forces

The caisson is rotationally stable if the sum of the resisting moments is not smaller than sum of the overturning moments. However, the evaluation of the wall stability against overturning mode of failure is usually not required if the resultant vertical force is within the core of the structure that is defined as the middle third of the wall base of the structure (de Gijt, 2004). This can be verified by the following equation:

$$e_R = \frac{\Sigma M}{\Sigma V} \leq \frac{1}{6} b$$

Where:

e_R is the distance from the middle of the caisson to the intersection point of the resulting force and the bottom line of the caisson

ΣV is the total of acting vertical forces

ΣM is the sum of the acting moments, around halfway the width of the foundation of the caisson

b is the width of the caisson

The caisson is vertically stable if the vertical effective soil stress, required to resist the acting loads does not exceed the maximum bearing capacity of the soil otherwise the soil will collapse. Thus, the structure is horizontal equilibrium is stable if the following equation is verified:

$$\sigma_{k,max} < p'_{max}$$

The maximum load ($\sigma_{k.max}$) acting on the foundation soil can be computed with:

$$\sigma_{k,max} = \frac{F}{A} + \frac{M}{W} = \frac{\sum V}{b \cdot \ell} + \frac{\sum M}{\frac{1}{6}\ell b^2}$$

The minimum load ($\sigma_{k.min}$) acting on the foundation soil has always to be greater than zero and can be computed according to the flowing equation:

$$\sigma_{k,max} = \frac{F}{A} - \frac{M}{W} = \frac{\sum V}{b \cdot \ell} - \frac{\sum M}{\frac{1}{6}\ell b^2} > 0$$

where:

ΣV is the total of acting vertical forces

A is the area of the foundation

W is the section modulus of the contact area of the foundation

b is the width of the caisson

ℓ is the length of the caisson

ΣM is the sum of the acting moments, around halfway the width of the foundation of the caisson

The bearing capacity (p'_{max}) of the foundation soil can be computed according to the Brinch Hansen method. As shown in the following equation:

$$p'_{max} = c'N_c s_c i_c + \sigma'_q N_q s_q i_q + 0{,}5\gamma' b N_\gamma s_\gamma i_\gamma$$

Which consists of contributions from cohesion (index c), surcharge including soil coverage (q), the specific weight of the soil below the foundation (γ). All the three contributions are multiplied by the bearing capacity factors (N), shape factors of the foundation (i) and load factors (s).

Safety factors representing the horizontal, rotational and vertical are introduced to have a quick assessment of the stability of the structure. The safety factors are defined as the ratio between the resisting and the driving load. A structure can be determined stable if the safety factors are bigger than one. The safety factors are presented below:

$$F_{s,Horizontal} = \frac{f \cdot \Sigma H}{\Delta V}$$

$$F_{s,Vertical} = \frac{\sigma_{k,max}}{p'_{max}}$$

Where:

$F_{s,Horizonatal}$ is the safety factor for the horizontal stability

$F_{s,Vertical}$ is the safety factor for the vertical stability

Regarding the rotational stability as mentioned before, if the resultant vertical force is within the core of the structure the stability against overturning mode is usually not required, therefore the safety factor is given by the ratio between the middle third of the wall base of the structure and the eccentricity of the resulting load. The safety factor is shown below:

$$F_{s,Rotational} = \frac{b/6}{e_R}$$

Where:

$F_{s,Rotational}$ is the safety factor for the rotational stability

3.4.3 Geotechnical assessment

Before performing the stability checks of the caisson a geotechnical assessment is necessary. This, assessment proves that before placing the caisson the soft soil package was removed entirely. In case that the soft soil layer was not removed, due to the weight of the caisson, the soft soil layer would consolidate and consequently settle. Consequently, this settlement may lead to instability problems of the caisson.

According to the CUR2003-7, in case of the realization of structures with shallow foundation, soils present below the foundation characterized by a cone resistance (q_c) lower than 2 MPa should be replaced by a sand layer with a thickness of 2-3 m. The foundation level of the caisson is at the NAP -13.65 m (see Section 2.2.1), the deep sand layer starts at NAP -17.65 m (see Section 2.5). Hence, it seems reasonable to assume that the entire soft soil layer was removed. However, to prove this assumption a calculation of the consolidation settlement of the soft layer is carried out.

Since the length of the caisson is large compared to its height, the assessment is performed using 1D compression analysis. Hence, three components have to be considered to evaluate the change in thickness of the soft layer; the generated strains due to the virgin loading, the reloading and the secondary compression (creep). The consolidation settlement is given by multiplying the height of the soft soil layer times the consolidation strain. The strain can be computed with the equation below.

$$\varepsilon = \frac{C_r}{1+e_0}\log\left(\frac{\sigma'_2}{\sigma'_{vc}}\right) + \frac{C_c}{1+e_0}\log\left(\frac{\sigma'_{vc}}{\sigma'_1}\right) + C_{ae}\log\left(\frac{t}{t_{ref}}\right)$$

Where e_0 is the initial void ratio, σ'_{vc} is the pre-consolidation stress, σ'_1 and σ'_2 are respectively the initial and final effective stress and C_r, C_c and C_{ae} are respectively the recompression, primary compression and secondary compression indices. Lastly, t is the duration of the application of the load and t_{ref} is the reference duration (usually equal to one day).

Notice that the above formula is a combination between the primary compression from Karl von Terzaghi and the equation for creep from prof. Keverling Buisman.

The initial effective stress and the pre-consolidation stress depend on the soil conditions, the stratigraphy and the load history of the area. Unfortunately, not many information is found regarding the conditions of the area before the construction of the Merwehaven. Most likely, the Merwehaven was constructed by land reclamation as shown in the figure below.

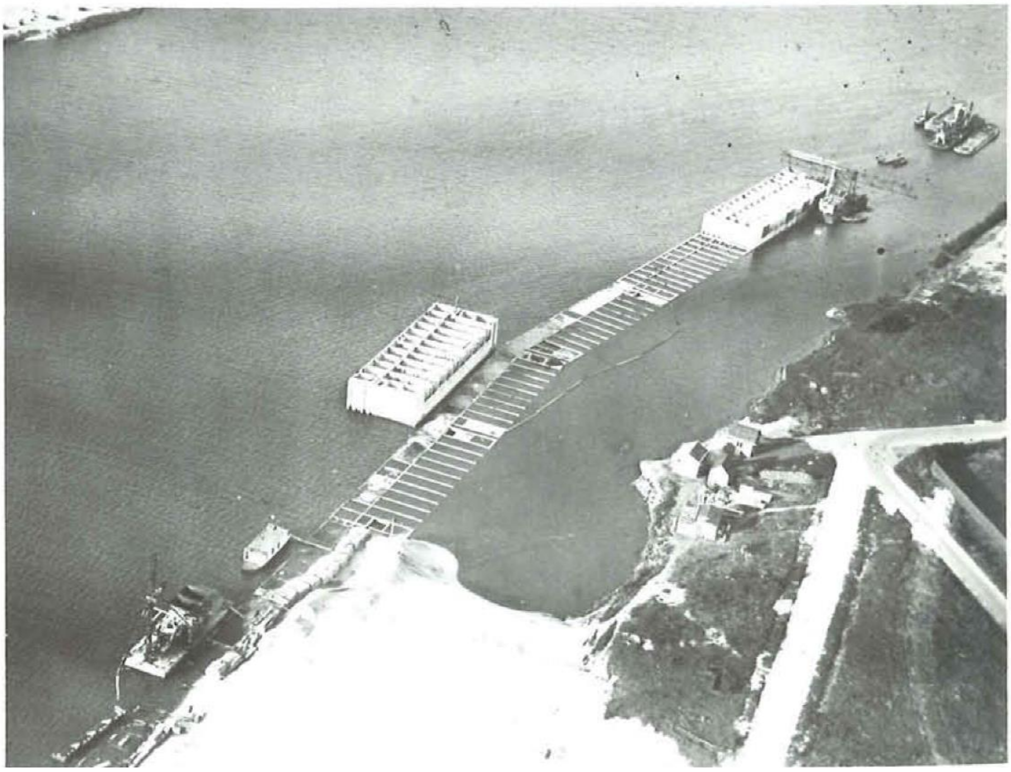

Figure 29: Aerial photo of the construction of the Merwehaven (HBG, 1977)

For the assessment, it is assumed that the reclaimed land had a typical soil stratigraphy of the western part of Holland (see Section 2.5 and Appendix A) with a bed level at the height of NAP -5.5 m. The bed stratigraphy was characterized by a top layer of sand with a thickness of approximately 1 m due to the river deposition and a soft soil layer till the deep sand layer beneath. The soft soil package is usually composed of different soil layers (clay and peat) that are characterized by different mechanical properties. For the sake of simplicity, the soft soil package is assumed to be characterized by a homogeneous layer of slightly sandy clay. The mechanical properties of the slightly sandy clay are taken according to Eurocode 7 NEN-EN9997 and are presented in the following table:

Mechanical properties of the soft soil package	
Submerged weight	18 kN/m^3
Cohesion	5 kN/m^2
Primary compression coefficient	0.24
Reloading coefficient	0.08
Secondary compression coefficient	0.009
Coefficient of consolidation	1*10^{-7} m^2/s

Table 10: Mechanical properties of the soft soil package

Assuming that a 2 m thick sand layer was placed under the caisson, the remaining soft soil layer package could have a height of approximately 2 m. Considering this scenario, the settlement is computed at mid-height of the soft soil package, at a depth of NAP -16.65 m. Therefore, the initial effective stress, at this depth, is given by the weight of the soil above and is approximately equal 90 kN/m^2. The final effective stress after the construction of the quay wall is given by the quay wall surcharge, the weight the caisson and by the soil below the caisson that is equal to 245 kN/m^2. The calculations are described is Appendix C.

However, the consolidation process should be considered to obtain a clear picture of the settlements during and after construction. The consolidation process itself has an attenuating character with time. It starts when the load is applied (positioning of the caisson) which leads to an immediate increase of the water pressure in the soft soil layers. The process ends when the excess water pressure has been dissipated. To simplify the calculations, it can be assumed that secondary compression (creep) starts when the primary compression (consolidation) has been finished. The hydrodynamic period is the time needed to reach the end of the consolidation process and can be computed to estimate the order of magnitude of the effects of the consolidation rate.

According to Terzaghi (1943), the duration of one-dimensional consolidation until the end of the hydrodynamic duration can be computed with:

$$t_h = \frac{d_c^2 \cdot T_v}{c_v}$$

Where:

d_c is the consolidation seepage length, equal to 1 m that is the half of the thickness of the soft soil

T_v dimensionless time factor, at the end of the consolidation it is equal to 2

c_v is the coefficient of consolidation (see Table 10)

Inserting the values into the above formula, the hydrodynamic period for the soft soil layer is approximately 80 days.

Finally, assuming a virgin loading condition (OCR=1) and that the end of the consolidation is reached ($t = t_h$) the settlement is calculated as shown in the equation below:

$$\Delta H = H_o \cdot \varepsilon = H_o \cdot \left(\frac{C_c}{1+e_0} \log\left(\frac{\sigma_2'}{\sigma_1'}\right) + C_{ae} \log\left(\frac{t}{t_{ref}}\right) \right) = 0.24 \text{ m}$$

Where:

ΔH is the consolidation settlement of the soft soil

H_o is the initial height of the soft soil package, equal to 2 m

ε is the consolidation strain

From the above results, it is clear that the consolidation settlement is considerable, therefore, to avoid instability problems of the caisson, the entire soft soil package was most likely removed and replaced by a sand layer before placing the caissons. Moreover, due to the overturning moment of the caisson, the effective stresses under the toe of the caisson are higher than the one at foundation level and consequently, the settlement under the toe of the caisson would be even more significative leading to a differential settlement and thus a higher probability of instability.

3.4.4 Stability checks for the current situation

The stability checks are first performed for the caisson in the current situation to understand the accuracy and the sensitivity of the stability check results. For the stability calculation, a cross-section in the middle of a caisson (length direction) is considered. The influence of the headwalls, transversal walls, toe and heels of the caisson are neglected, which works out as conservative considerations.

The dimensions of the caisson are given in Section 2.2.1. It is assumed that the caisson is filled with the same soil as the backfill sand. Furthermore, it is assumed that the soil in front, behind and below the caisson has the mechanical properties of the backfill soil (see Table 3). According to the CPT, the deep sand layer starts at NAP -17.65m (see Appendix A).

The water levels behind (landside) and in front (waterside) of the caisson are taken so that the maximum unbalanced hydrostatic pressure is developed. Therefore, the considered water levels are:

- At the landside the water level is taken from the water pressure measurement present at Pier 1 that is equal to NAP +1.2 m (see Section 2.5)
- At the waterside the water level is taken equal to NAP -0.7 m that is the lowest low astronomical tide level (ALAT) (see Section 2.5)

The current bed level in front of the caisson is obtained by subtracting from the current NGD level (NAP -10 m) the maintenance margin (see Section 2.4.2) so it equal to NAP -11 m.

The ground level behind the caisson is equal to NAP +3.35 (see Section 2.2.1). The vertical load acting on the on top of the quay wall is taken equal to 30 kN/m^2 (see Section 2.5).

For this assessment, the bollard force per running meter is obtained by considering the maximum capacity of the existing bollard multiplied by the number of bollards present on one caisson and divided by the length of the caisson. Two bollards are present on each caisson with a maximum capacity of 750 kN (see Section 3.2), the length of the caissons is approximately 45 m (see Section 2.2.1). Thus, the bollards force is obtained as shown in the following equation.

$$F_{bollard} = \frac{2 \cdot 750}{45} = 33.3 \text{ kN/m}$$

The bollard force is assumed to be applied at the ground level on top of the quay wall as shown in Figure 30.

The variables required for the stability calculation are presented in the table below. Notice that the water levels and soil level are taken with respect to the foundation level of the caisson that in equal to NAP -13.65 m (see Section 2.2.1).

Value of the variables for the stability calculation			
Variable	**Symbol**	**Value**	**Unit**
Water level in front of the caisson	h_{w_1}	12.95	m
Water level behind the caisson	h_{w_2}	14.85	m
Density of the water	γ_w	10.25	kN/m^3
Soil height in front of the caisson	h_{s_1}	2.65	m
Soil height behind the caisson	h_{s_2}	17	m
Surcharge on top of the quay wall	q	30	kN/m^2
Bollard force	$F_{bollard}$	33.3	kN/m
Dry volumetric weight of the backfill soil	γ_{dry_1}	18	kN/m^3
Saturated volumetric weight of the backfill soil	γ_{sat_1}	20	kN/m^3
Friction angle of the backfill soil	φ_{s_1}	30	deg

Table 11: Values of the variable for the stability checks in the current situation

To perform the stability checks of the caisson in the current situation the following load configuration is considered. The stability checks are performed per running meter without the use of partial factors.

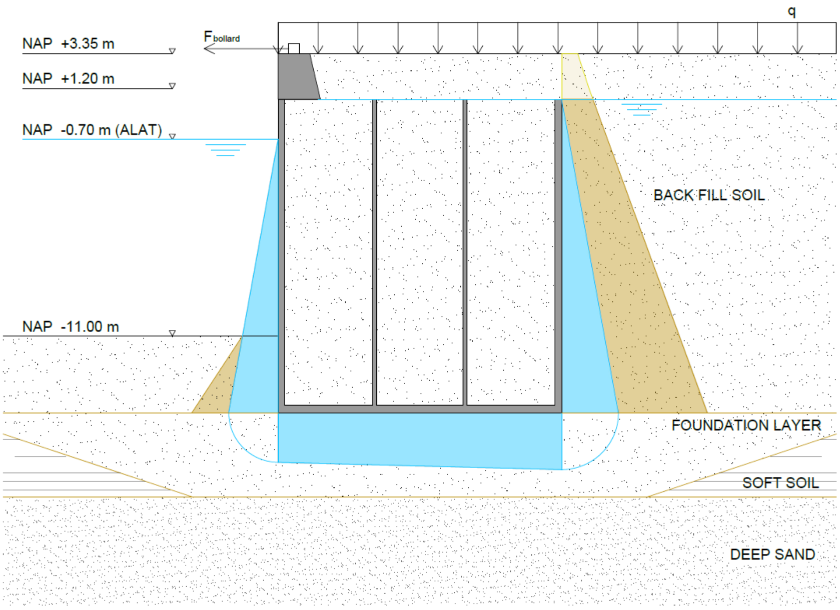

Figure 30: Load configuration on the caisson in the current situation

Given the above schematization and the values of the variables (see Table 11), the stability checks for the current situation are performed and described below. Only the final results of the checks are presented. The detailed calculations are described in Appendix D.

Horizontal stability

The total horizontal force (ΣH) is obtained by subtracting from the horizontal forces, exercised by active soil pressure and water pressure at the landside, the horizontal forces exercised by the passive soil pressure and water pressure at the waterside. The total vertical force (ΣH) is given by the dead weight of the caisson and the loads present on top of the quay wall minus the uplift buoyance force. The result of the horizontal equilibrium with the related safety factor are shown below:

$$\Sigma H < f \cdot \Sigma V \rightarrow 877.2\ \text{kN} < 1125.2\ \text{kN}$$

$$F_{s,Horizontal} = \frac{f \cdot \Sigma H}{\Delta V} = 1.27$$

From the result of the equilibrium, the caisson is horizontally stable.

Rotational stability

For the rotational stability, the eccentricity of the resulting acting force is calculated by dividing the sum of the acting moments (ΣM*)* calculated around halfway the width of the foundation of the caisson, by the total vertical force (ΣV). The result of the rotational equilibrium is presented below:

$$e_R = \frac{\Sigma M}{\Sigma V} \leq \frac{1}{6} b \rightarrow 2.22\ \text{m} \leq 2.23\ \text{m}$$

$$F_{s,Rotational} = \frac{b/6}{e_R} = 1.01$$

From the result of the above equation, the caisson is rotationally stable. However, the resulting action force is just inside the core of the structure. This small difference may be due to the conservative assumption of the caisson, due to the significative water head difference over the structure or due to uncertainties in the mechanical properties of the soils.

Vertical stability

The maximum vertical effective soil stress acting below the foundation of the caisson is obtained by adding the two soliciting components. The first is the total vertical force (ΣV) divided by the area of the foundation the second is the sum of the acting moments (ΣM*)* calculated around halfway of the foundation divided by the section modulus of the foundation. The bearing capacity of the foundation layer is computed using Brinch Hansen method in drained condition. The bearing capacity is given by the contribution of the soil coverage at the waterside and the specific weight of the soil below the foundation component. The result of the vertical equilibrium is presented below:

$$\sigma_{k,max} < p'_{max} \rightarrow 460.2\ \text{kN/m}^2 < 538\ \text{kN/m}^2$$

$$\sigma_{k,min} = 2.13\ \text{kN/m}^2$$

$$F_{s,Vertical} = \frac{\sigma_{k,max}}{p'_{max}} = 1.30$$

As it is shown in the above equations the bearing capacity of the foundation is higher than the maximum load and no tensile stress are developed at the foundation level of the caisson, therefore the caisson is vertically stable.

To summarize the results of the stability checks of the caisson in the current situation, the safety factors are presented in the following table.

Safety factors	
Horizontal safety factor	1.27
Rotational safety factor	1.01
Vertical safety factor	1.30

Table 12: Safety factors of the stability checks of the caisson in the current situation

Results of the "old design" stability calculations

Before performing the stability checks for the deepened situation, the results of the old stability calculation of the caisson are presented. These calculations were carried out by the contractor that built the different piers of the Merwehaven. The figure below shows the stress diagram at the foundation level of the caissons.

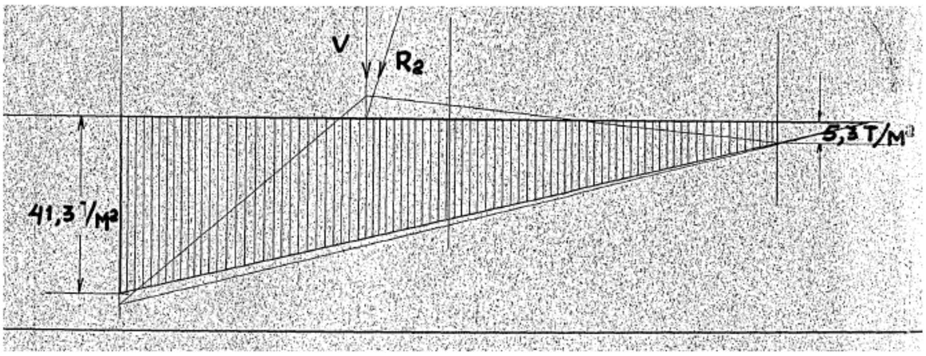

Figure 31: Stress diagram from the old stability calculations (Port of Rotterdam Authority)

According to the above figure, the maximum and minimum soil pressures at the foundation level of the caissons are 413 kN/m^2 and 53 kN/m^2 respectively. From these results, it is clear that the order of magnitude of the maximum soil pressure between the performed stability checks and the old calculations is the same. The results of the two calculation (approximately 50 kN/m^2) may differ due to the conservative assumptions, due to the different design value of the surcharge on top of the quay wall and the water head difference over the caisson.

3.4.5 Sensitivity analysis

A sensitivity analysis is carried out to define which of the loads and mechanical properties of the soils have the most influence on the results of the stability checks of the caisson in the current situation. The analysis is performed by changing the value of each variable one at a time and by recalculating the safety factors of the stability checks. The effect on the stability checks of each variable is defined depending on how the value of the safety factors change. The results of the sensitivity analysis are summarized in the next table, the detailed results for each variable are presented in Appendix E.

Variable	Value	Horizontal Safety factor	Rotational Safety factor	Vertical Safety factor
Current situation	-	1.27	1.01	1.3
Dry and saturated volumetric weight of the backfill soil	17 and 19 kN/m^3	1.23	0.98	1.26
	19 and 21 kN/m^3	1.30	1.04	1.33
Friction angle of the backfill soil	27°	1.14	0.93	1.11
	33°	1.42	1.09	1.49
Saturated volumetric weight of the foundation soil	19 kN/m^3	1.27	1.01	1.24
	21 kN/m^3	1.27	1.01	1.36
Friction angle of the foundation soil	27°	1.13	1.01	0.85
	33°	1.41	1.01	2.01
Surcharge on top of the quay wall	20 kN/m	1.28	1.02	1.38
	40 kN/m	1.25	1.00	1.22
Bollard force	20 kN/m	1.29	1.04	1.34
	45 kN/m	1.25	0.98	1.26
Water head difference over the caisson	1.0 m	1.43	1.16	1.53
	1.5 m	1.34	1.07	1.4

Table 13: Results of the sensitivity analysis for the stability check of the caisson in the current situation

According to the results of the sensitivity analysis, the friction angle of the backfill soil and the foundation layer are the mechanical properties that have the most influence on the stability of the caisson. Between the acting loads, the water head difference over the caisson is the one that has the most impact on the stability results. The surcharge on top of the quay wall, on the other hand, has a limited impact. This may due to the fact that the loads behind the structure are mainly supported by the soil and partly by the structure, which is the result of friction between the soil and the structure (Bezuyen, et al., 2009). Although the bollard force has not the most significant impact on the stability results, it has a considerable influence on the stability of the caisson.

In more detail, the friction angle of the backfill sand and the water head difference influence the results of all three the stability mechanisms, while the friction angle of the of the foundation layer affects only the horizontal and vertical stability. While the acting loads influence all three the stability mechanisms.

3.4.6 Piping

Piping is the groundwater flow, caused by water head difference over a structure that causes erosion. This groundwater flow can occur at the plane separating the impermeable structure and a loose grain layer (Manual Hydraulic Structures, 2017). The groundwater flow created by erosion under the foundation of the structure may lead to instability. Therefore, it is important to verify if piping may occur below the caisson.

To estimate whether piping may occur under retaining structures Lane's method is adopted (Manual Hydraulic Structures, 2017). According to this method, there is a limit state with a critical ratio between the water head difference and the seepage distance (i_{max}). The limit state is a function of the type of soil and is presented in the table below.

Piping method:	Lane	
criterion	$L \geq \gamma \cdot C_L \cdot \Delta H$	
used seepage length	$L = \sum L_{vert} + \sum \frac{1}{3} L_{hor}$	
	C_L	i_{max}
Soil type:		
Very fine sand / silt /sludge	8,5	11,8 %
Fine sand	7,0	14,3 %
Middle fine sand	6,0	16,7 %
Coarse sand	5,0	20,0 %
(fine) gravel (+sand)	4,0	25,0 %

Table 14: Piping limit state for different types of soils (Manual Hydraulic Structures, 2017)

The foundation layer is assumed to be composed of middle fine sand (see Section 2.5) hence, according to the above table, the critical ratio between the water head difference and the seepage distance is equal to 16.7%. The following equation gives the ratio between the water head difference and the seepage distance of the caisson:

$$i = \frac{\Delta \mathrm{H}}{\mathrm{L}} = 0.142 = 14.2\ \%$$

Where;

i is the ratio of the water head difference and the seepage distance of the caisson

ΔH is the water head difference over the caisson, equal to 1.9 m (see Section 3.4.4)

L is the seepage length, equal to the width of the caisson (see Section 2.2.1)

According to the above equation, piping may not occur. Moreover, the duration of the water level difference has to be sufficiently long to start this mechanism (Manual Hydraulic Structures, 2017). The water levels inside the port of Rotterdam highly depend on tidal fluctuations (see Section 2.5) therefore, piping is not a problem for the stability of the caissons.

3.4.7 Stability checks for the future situation with deepening

The following load configuration is considered to perform the stability checks of the situation with deepening in front of the quay wall.

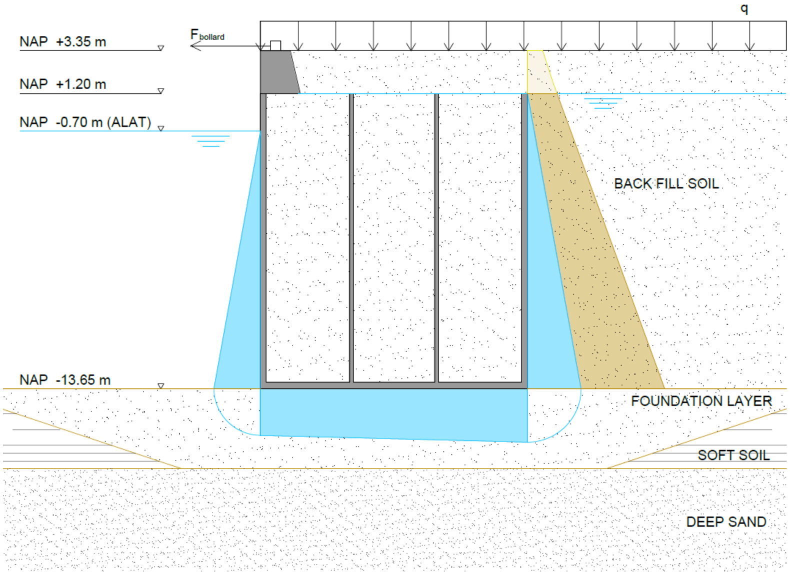

Figure 32: Load configuration on the caisson in the scenario with deepening

The only difference from the previous situation (see Section 3.4.4) is that the soil in front of the quay wall is removed so that the new NGD is guaranteed. Consequently, the new required bed level is equal to the foundation level of the caisson (see Figure 32). Due to the removal of the bed material, the passive force acting on the caisson is removed. Given the above schematization, the stability checks are carried out again for the new situation. Also for this case, only the final results of the stability checks are presented. The full calculations are described in Appendix D.

Horizontal stability

The total horizontal force (ΣH) is obtained by subtracting from the horizontal forces, exercised by active soil pressure and water pressure at the land side, the horizontal forces exerted by the water pressure at the waterside. The total vertical force (ΣV) is given by the dead weight of the caisson and the loads present on top of the quay wall minus the uplift buoyance force. The result of the horizontal equilibrium is shown below:

$$\Sigma H < f \cdot \Sigma V \rightarrow 991\,\text{kN} < 1125.2\,\text{kN}$$

$$F_{s,Horizontal} = \frac{f \cdot \Sigma H}{\Delta V} = 1.14$$

From the result of the equilibrium, the caisson is still horizontally stable. However, the difference between the resisting and acting forces is reduced due to the removal of the soil in front of the caisson.

Rotational stability

For the rotational stability, the eccentricity of the resulting acting force is calculated by dividing the sum of the acting moments (ΣM*)* calculated around halfway the width of the foundation of the caisson, by the total vertical force (ΣV). The result of the rotational equilibrium is presented below:

$$e_R = \frac{\Sigma M}{\Sigma V} \leq \frac{1}{6} b \rightarrow 2.244\,\text{m} \leq 2.233\,\text{m}$$

$$F_{s,Rotational} = \frac{b/6}{e_R} = 0.99$$

Form the above equation it turns out that the caisson is not rotationally stable because the action line of the resulting force is located outside the core of the structure (b/6). This means that tensions stresses develop at the foundation of the caisson ($\sigma_{k.min}$<0), that is not allowed and thus only part of the soil below the caisson contributes to the bearing.

Vertical stability

The maximum vertical effective soil stress acting below the foundation of the caisson is obtained by adding the two soliciting components. The first is the total vertical force (ΣV) divided by the area of the foundation the second is the sum of the acting moments (ΣM*)* calculated around halfway of the foundation divided by the section modulus of the foundation. The bearing capacity of the foundation layer is computed using Brinch Hansen method in drained condition. In this situation, the bearing capacity is only given by the specific weight of the soil below the foundation component. The result of the vertical equilibrium is presented below:

$$\sigma_{k,max} < p'_{max} \rightarrow 462.5 \text{ kN/m}^2 < 267.8 \text{ kN/m}^2$$

$$F_{s,Vertical} = \frac{\sigma_{k,max}}{p'_{max}} = 0.59$$

As shown in the above equation the maximum acting load is considerably higher than the bearing capacity of the foundation layer and consequently, the caisson is not vertically stable.

To summarize the results of the stability checks of the caisson in the future situation, the safety factors are presented in the following table.

Safety factors	
Horizontal safety factor	1.14
Rotational safety factor	0.99
Vertical safety factor	0.59

Table 15: Safety factors of the stability checks of the caisson in the current situation

3.5 Conclusions

From the results of the functional-spatial assessment (see Section 3.2 and 3.3), it turns out that both quay walls (portside and riverside) of Pier 1 do not meet the requirements of the new cruise terminal. Hence, technical solutions are required. In more detail, this assessment argues that:

- The quay wall at the portside requires a technical solution to ensure the stability of the caissons.
- The quay wall at the riverside requires an entirely new quay wall and mooring systems.

The structural assessment (see Section 3.4) focusses only on the caissons used as a quay wall at the portside. The assessment proves that:

- The soft soil packaged was removed and a foundation layer was placed before placing the caissons to avoid instability problems due to the consolidation settlement.
- In the current situation the rotational stability of the caisson has the lowest safety factors and hence it is the most critical failure mechanism.
- The friction angles of the backfill sand and foundation layer are the mechanical properties of the soils that have the biggest impact on the stability of the caissons.
- The water head difference over the caisson is the load that has the most effect on the stability checks results.
- The bollard force has a considerable influence on the stability of the caisson.
- Piping is not a problem for the stability of the caissons.
- Deepening of the bed level in front of the caissons reduce the safety factors of the rotational and vertical stability checks and hence it leads to instability of the caisson.
- The soil coverage in front of the caissons, at the waterside, has a crucial role in the stability of the existing quay wall consequently, only deepening of the berth area is not a feasible design solution.
- A technical design solution must be provided to maintain the existing caissons, guarantee the new required nautical depth, ensure the stability of the caissons and provide adequate mooring for the design cruise ship.

4. Development and assessment of design concepts

4.1 Introduction

This chapter focuses on the caisson used as a quay wall at the portside of Pier 1, as concluded in the previous chapter, technical solutions are required, to adapt the existing quay to the new cruise terminal of the port of Rotterdam. In this chapter, different design concepts are developed to solve the issues that obstruct the mooring of the cruise ships. The design concepts developed to provide the necessary stability to the existing caissons and to allow the berthing of the design cruise ships are described in Section 4.2. Then the different design concepts are assessed through a first design loop (Section 4.3). In detail, the design loops consist of hand calculations and technical reasoning. The scope of this assessment is to identify those design concepts that have a certain level of feasibility and value, which make them design variant and a candidate for the final solution. The conclusions of this chapter are presented in Section 4.4.

4.2 Technical design concepts

The technical design concepts are adaptations of the existing quay wall. The design concepts have to address and solve the technical issues mentioned in Section 3.2 and 3.4 to fulfill the project requirements. Several structural elements compose the technical design concepts. However, as specified in the previous section, it is crucial for the stability of the existing quay wall that the technical solutions maintain the soil coverage in front of the caisson or increase its weight. In the figure below the structural elements that each design concept should include are presented.

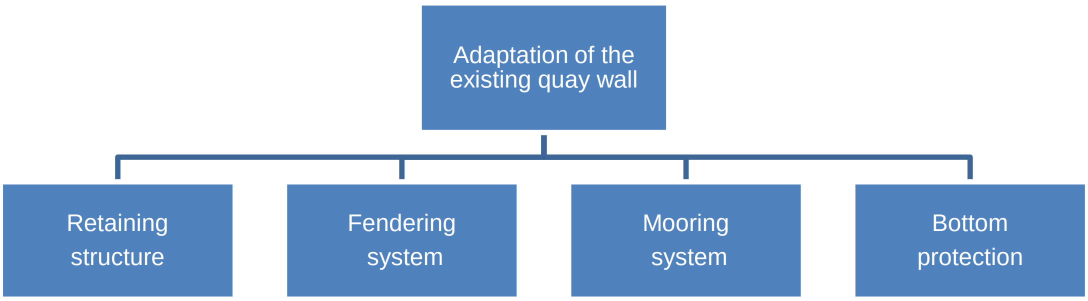

Figure 33: Structural components required for the adaptation of the existing quay wall

In the following text, the developed design concepts are described.

4.2.1 Concept A; Grout injections

The first design concept uses the grouting injection technique. Grout is injected in front of the caisson to ensure the stability of the quay wall and guarantee the new required nautical depth. The grout injections increase the mechanical properties of the soil coverage in front of the caisson. In this way, the passive acting force of the soil is increased. This grouting technique was already used at the Waalhaven in the port of Rotterdam (Quay Wall Second edition, 2014). The grout body also prevents bottom erosion at the toe of the caisson. Therefore, the scour protection is not required and consequently, the construction depth can be reduced and the bed level increased. The fendering system is placed along the frontage of the caisson and has to ensure sufficient distance between the cruise ship and the quay wall. Big floating fenders can be adapted to increment this distance so that the depth in front of the caissons can be reduced even more and the stability improved (see

Figure 34). These fenders are hanged from the superstructure of the caisson and serve to absorb the impact energy of the design cruise ship and also guarantee sufficient distance from the quay wall. Moreover, these fenders spread the load imposed by the impact energy of the vessel over a bigger area leading to lower pressure on the basalt revetment.

To increase the capacity of the bollards an anchor, connected to the foundation of the bollards is placed. The anchor is constructed through the existing superstructure and is anchored to an anchor wall or a driven pile located behind the caisson. Alternatively, new bollards can be placed on the superstructure of the quay wall. In Figure 34 the design concept is shown.

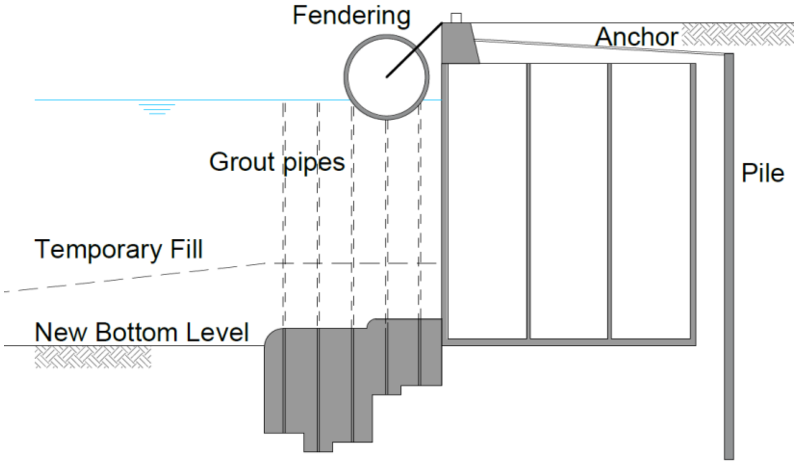

Figure 34: Design concept with grout injections (Concept A)

4.2.2 Concept B; Concrete floor

The second design concept concerns the use of a concrete floor. The floor is placed in front of the existing quay wall. This solution can bear a significant force that is useful to ensure the stability of the caisson and increases the considerably the weight of the soil in front of structure improving the vertical stability. Piles may be required to support the concrete floor if the bearing capacity of the subsoil is overtaken. Another advantage of this concept is that there is no need for scour protection and consequently, the construction depth is reduced, leading to a higher bed level that increases the stability. Also for this design concept floating fenders and the anchored bollards may be included. In the figure below this design concept is presented.

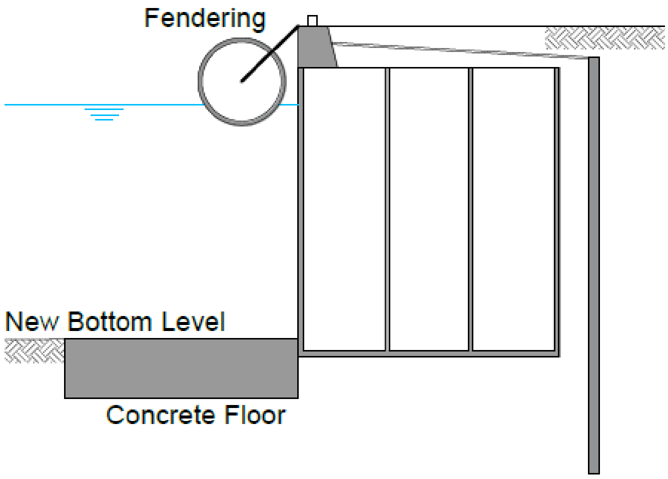

Figure 35: Design concept with concrete floor (Concept B)

4.2.3 Concept C; Anchored sheet pile wall

This design concept involves the use of a sheet pile wall. The sheet pile is driven in front of the existing caissons and ensures that along berth length the new required nautical depth is reached without compromising the stability of the caisson. An anchor system, passing through the existing superstructure, may be necessary to provide the stability of the sheet pile wall. The space between the sheet pile and the caisson is backfilled with soil. At the upper side of the sheet pile, a new concrete element is cast where new bollards are placed and the fendering system is connected. Scour protection is required to avoid erosion of the new bed level and provide stability to the new structure. In the figure below the design concept is shown.

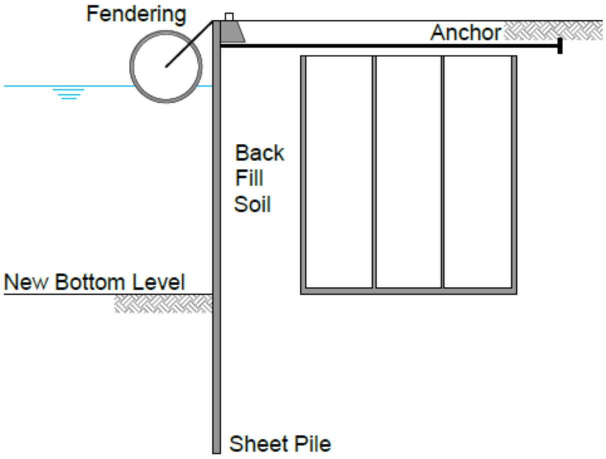

Figure 36: Design concept with sheet pile (Concept C)

4.2.4 Concept D; Underwater sheet pile wall

The following design concept involves the use of an underwater sheet pile wall placed in front of the caisson. The sheet pile wall is driven close to the toe of the caisson to reach the new required nautical depth along the berth length. The sheet pile must retain the soil at the toe of the caisson so that the rotational and vertical stability are satisfied. Besides, the sheet pile has to provide enough strength to guarantee the overall stability of the quay wall preventing the development of slide circles. Also for this design concept, big floating fenders are necessary to ensure sufficient distance between the keel of the moored cruise ship and the underwater sheet pile wall. To increase the capacity of the bollards an anchor or new bollards are placed on the top of the structure of the quay wall. Scour protection is required on top of both bottom levels to prevent erosion. The design concept is presented in the figure below.

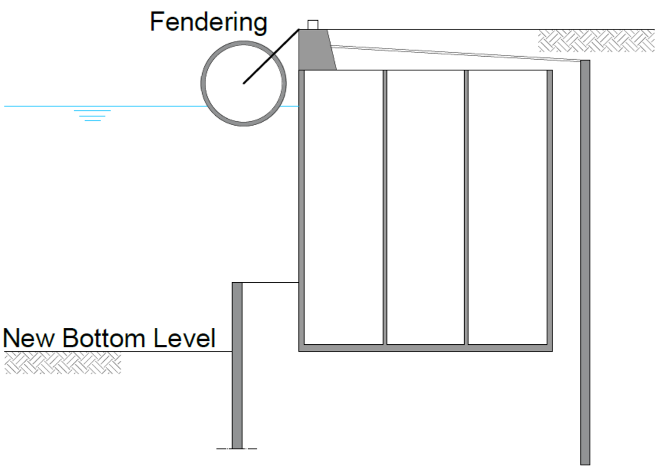

Figure 37: Design concept with underwater sheet pile (Concept D)

4.2.5 Concept E; Guiding structures

This design variant consists of the use of guiding structures, also called berthing and mooring dolphins. These structures are designed by using one or more piles that can be flexible or rigid. A combination of flexible and rigid dolphins is placed in front of the berth length. The flexible structures have to absorb the impact of the vessel and ensure the distance from the existing quay wall. Therefore, the berthing dolphins should be placed over the full berth length. The mooring dolphins, have to resist the uplift forces caused by vessel lines. Hence, they should be placed in front of the quay wall in correspondence of the bow and the stern of the design cruise ship. With this pile arrangement, sloping bed with revetment can be placed starting from caisson. However, for this design concept, at the terminal, bigger and longer gangways are required to board the passengers, crew and supplies. In the next figure, the design concept with breasting dolphins is presented.

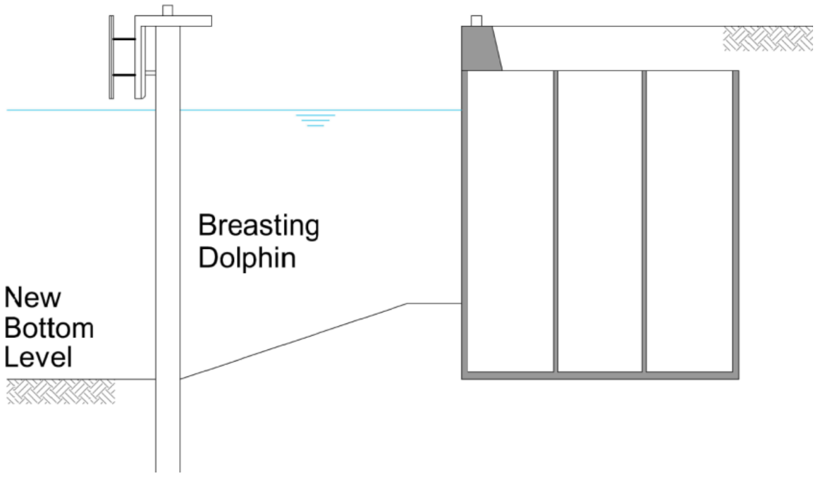

Figure 38: Design concept with guiding structures (Concept F)

4.2.6 Concept F; Piled structure

This design concept involves the construction of piled structure along the full length of the existing quay wall. The structure consists of a horizontal deck supported by steel piles. The structure has to reinforce the front of the quay by absorbing, through the use of fenders, the impact energy of the cruise ship. The bollards are placed on the deck of the structure. However, this may lead to high uplift and horizontal forces caused by the vessel lines. Therefore, the design of the structure should be checked carefully because the stability of piled structures depends mainly on the lateral load-carrying capacity of the piles (de Gijt, 2004). A short sheet pile wall is driven close to the piles to provide the new required nautical depth. In this way, a sloping bed is avoided and consequently, the length of the piled structure is reduced (see Figure 39). Besides, the sheet pile retains the soil at the toe of the caisson and provides the stability of the quay wall. Scour protection is required on top of both bottom levels to prevent scour. In Figure 39 this design concept is described.

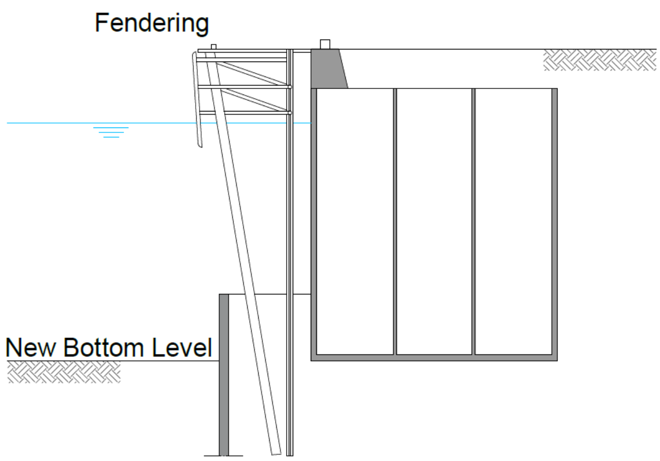

Figure 39: Design concept with flexible piled structure (Concept F)

4.3 Assessment of the design concepts

In order to identify which of the above-presented design concepts have a certain level of feasibility and value, the design concepts are assessed as part of a first design loop. The assessment consists of hand calculations and technical reasoning.

4.3.1 Concept A; Grout injections

The technical concept with the grout injection is a feasible solution. This technique is increasingly being used in the last decades. However, the mechanical properties (γ_{sat}, φ and c) of the strengthened soil due to the injected grout are challenging to estimate. These parameters depend mainly on the soil where the injections are performed, and on the mixing technique that is used to mix the grout. Usually, in civil engineering projects, before the implementation of this technique laboratory tests are carried out to define the mechanical properties.

However, for this study laboratory tests are not available. Therefore to define the required specific weight and the dimensions of the grout injected soil, the stability checks are used. They are obtained by performing the rotational and vertical stability checks iteratively till the caisson become stable. The other involved parameters, used for the calculations are the same as in Table 11.

In the next table, the required specific weight and the dimensions of the injected soil layer obtained from the iteration process are presented:

Grout injected soil	
Submerged weight	21 kN/m^3
Height of the soil above foundation level	1.4 m
Height of the soil below foundation level	2.0 m
Total height of the grout	3.4 m
Width of the grout	5.0 m

Table 16: Characteristics and dimensions of the grout injected soil

In the next figure, the main dimensions of the grout injected coverage soil are presented in detail.

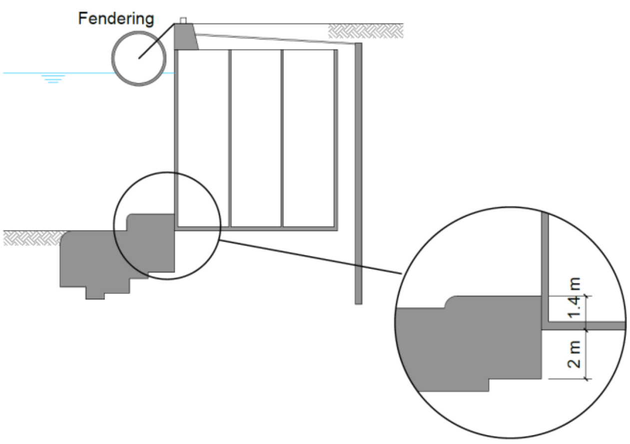

Figure 40: Grout soil coverage dimensions

An accurate grout injection plan is required to avoid erosion problems of the subsoil that may lead to instability of the caissons. Lastly, to maintain enough distance between the moored cruise ship and the soil coverage in front of the caisson, big floating fenders are placed along the full frontage of the quay wall.

4.3.2 Concept B; Concrete floor

The technical concept with an underwater concrete floor is not a feasible solution. Although, the floor provides the required stability, the reason because it is not possible, is related to the construction of the concrete floor. To place the floor, at the required depth, dredging of the bottom level in front of the caisson is first necessary and consequently, this excavation may lead to instability problems of the caisson during the construction.

4.3.3 Concept C; Anchored sheet pile wall

The technical design concept with the sheet pile wall supported by an anchor is a suitable solution. A simplified schematization is adopted and several consideration and assumptions are made to perform a first design of the sheet pile wall.

According to the Manual of Hydraulic Structures, the anchored sheet pile wall the structure is schematized as a beam on two free supports and assumed to be driven at a certain distance from the caisson. The space in between is backfilled. The new backfill soil is considered to have the same mechanical properties as the backfill soil present behind and in front of the caisson (see Table 3). For simplicity the mechanical properties of the deep sand layer are assumed to be equal to the backfill soil. With these assumptions, the influence of the caisson on the horizontal stresses acting on the sheet pile can be neglected, because the difference in the effective vertical stress on the foundation level due to the weight of the caisson and due to the backfill soil is relatively small. This is demonstrated below.

The effective vertical stress at the foundation level of the caisson is given by the dead weight of the structure ($Q_{concrete}$ and $Q_{ballast}$) and by loads present on top ($Q_{superstructure}$) minus the water pressure, while the effective stress, at the same level, under the backfill is given by the weight of the soil and the surcharge minus the water pressure. Therefore, it can be calculated that the values of these two effective stresses are close and consequently the influence of the caisson can be neglected as shown below:

$$\sigma'_{v,caisson} = \frac{Q_{concrete} + Q_{ballast} + Q_{superstrutcture}}{b} - u = 236.6 \text{ kN/m}^2$$

$$\sigma'_{v,backfill} = q + \gamma_{dry} d_{dry} + \gamma_{sat} d_{wet} - u = 229.2 \text{ kN/m}^2$$

$$\frac{\sigma'_{v,backfill}}{\sigma'_{v,caisson}} = \frac{229.2}{236.6} = 0.97 \simeq 1$$

Where:

$\sigma'_{v,caisson}$ is the effective stress under the caisson

$\sigma'_{v,backfill}$ is the effective stress of the backfill soil at the caisson foundation level

u is the water pressure at the foundation level during low water

According to the schematization and assumptions mentioned above, the anchored sheet pile wall and its acting load can be schematized as shown in Figure 41. All the other parameters used for the calculations are the same as presented in Table 11, except for the water head difference over the sheet pile that is calculated according to equation provided by Quay Wall Second edition (see Section 2.5).

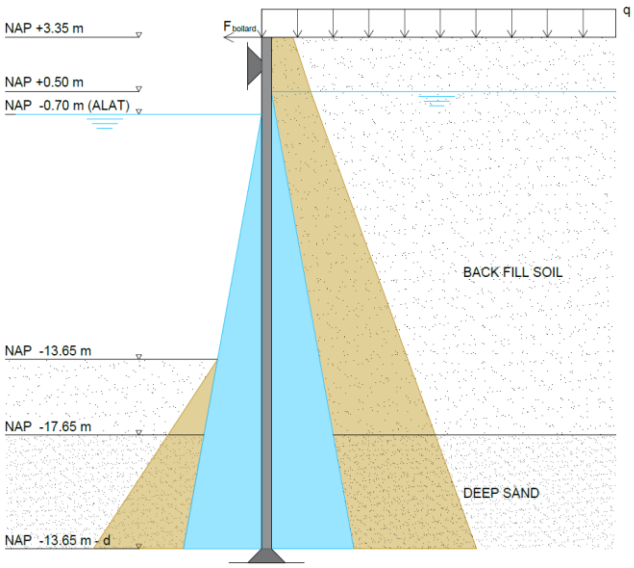

Figure 41: Horizontal load configuration acting on the sheet pile wall

Notice that according to the above schematization the active soil pressure is entirely acting on the sheet pile wall, while in reality due to the presence of the caisson the active slide surface may not be entirely developed. Hence, this schematization is on the conservative side.

The embedded depth (d) and the anchor force (support reaction F_{anchor}) of the sheet pile wall are the only unknown and are computed analytically. The first unknown is obtained by the calculating the equilibrium of moments around the anchor point, the anchor force is calculated from the horizontal equilibrium. Their value is presented in the next table.

Structural characteristics	
Embedded depth	8.8 m
Anchor force	690 kN/m

Table 17: Structural characteristics of sheet pile wall

To compute the displacement of the wall and select an appropriate sheet pile profile, the software *D-Sheet Piling* is used. The figure below presents the moments, shear and displacement diagrams as a function of the depth of the anchored sheet pile wall with an Anchelor profile AZ 50 with steel quality of S 430.

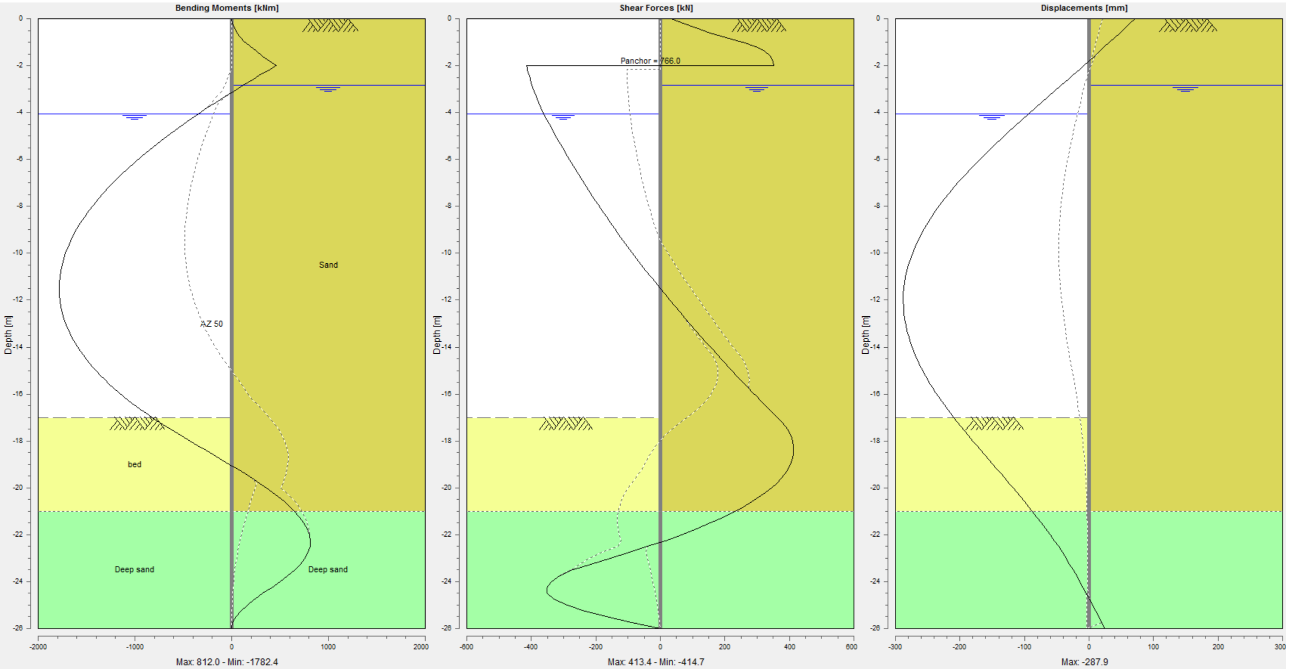

Figure 42: Moment, shear and displacement diagrams in function of the depth of the anchored sheet pile wall

From the displacement diagram (see right Figure 42) it is clear that the deformation of the chosen profile is too high (δ_{max}= 288 mm) and thus a profile with a higher flexural stiffness is required. To increase the flexural stiffness and consequently to minimize the deformation a combi-wall is the best solution. In addition, to reduce the final deformation particular attention should be given to the construction stages of the combi-wall.

4.3.4 Concept D; Underwater sheet pile wall

The design concept with the underwater sheet pile wall placed in front of the caisson is a feasible solution. To perform a preliminary design, according to Blum method, the underwater sheet pile can be schematized as a cantilever sheet pile wall. Besides, consideration and assumptions are made.

The sheet pile is assumed to be driven at 2.5 m distance from the toe of the caisson and the space in between is assumed to be the backfill sand. The sheet pile has to retain a height of 2.65 m. This is given by the difference between the current and the new required bed level (see Section 3.2). In this scenario, the presence of the caisson leads to an additional horizontal stress acting on the sheet pile and therefore must be accounted in the design. According to the Manual of Hydraulic Structures, the influence of the caisson and the backfill behind, acting on the underwater sheet pile the can be considered using the following schematization.

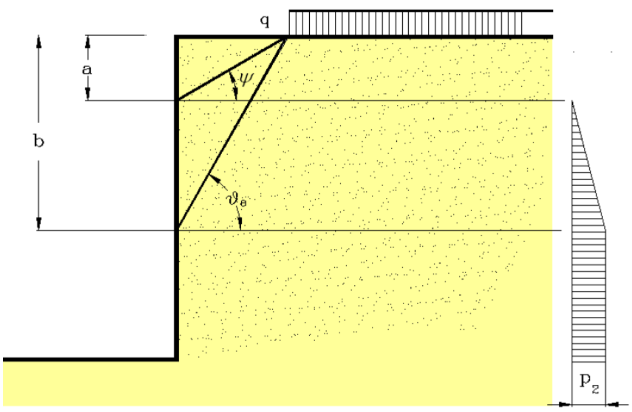

Figure 43: Infinite surface load at a distance of a wall (Manual of Hydraulic Structures, 2017)

In this case, the maximum horizontal soil pressure (P_2) is given by the vertical load multiplied by the coefficient of active soil pressure (K_a) and the angles could be assumed equal to: ψ = 45° and ϑa = 45° + ½φ = 60°, with φ friction angle of the soil.

For the preliminary design, a uniform vertical load (q_{mean}) is chosen. This load is assumed to be equal to an average value between the maximum pressure exerted by the caisson at the foundation level ($\sigma_{k.max}$) in the current situation (see Section 3.4.4) and the load exerted by the backfill soil and the present behind the caisson (see Appendix D). This mean load value is obtained as shown below:

$$\sigma_{k,max} = 460.2 \text{ kN/m}^2$$

$$\sigma'_{v,backfill} = q + \gamma_{dry} d_{dry} + \gamma_{sat} d_{wet} - u = 229.2 \text{ kN/m}^2$$

$$q_{mean} = \frac{\sigma_{k,max} + \sigma'_{v,backfill}}{2} = 344.7 \text{ kN/m}^2$$

Where:

$\sigma_{k,max}$ is the maximum vertical effective pressure exerted by the caisson on the foundation level in the current situation

$\sigma'_{v,backfill}$ is the vertical effective pressure just behind the caisson at foundation level due to the backfill soil

q_{mean} is the average between the two vertical effective pressures

Now that the vertical load and its acting points are defined, the horizontal stresses acting on the underwater sheet pile are obtained as presented in the figure below:

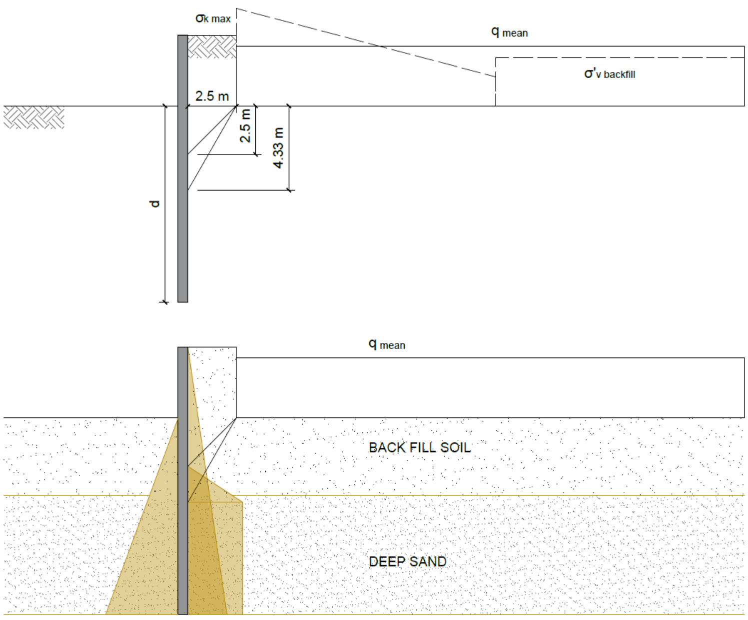

Figure 44: Loads schematization (above) and the horizontal stresses (under) acting and on the sheet pile

The embedded depth (d) of the sheet pile wall is the only unknown and is computed analytically by calculating the equilibrium of moments around the toe of the sheet pile (see lower Figure 44). The obtained embedded depth is equal to approximately 4 m.

Also for this design concept, the software *D-Sheet Piling* is used to compute the displacement of the underwater sheet pile wall and select an appropriate sheet pile profile. However, this software is not able to describe this scenario accurately due to the interaction between the two structures. Hence, the results are only considered qualitatively.

The figure below presents the moments, shear displacement diagrams as a function of the depth of the underwater sheet pile wall with an Anchelor profile AZ 18 with steel quality of S 320. Notice that the embedded is increased to 7 m to avoid the development of sliding circles that may compromise the overall stability of the quay wall.

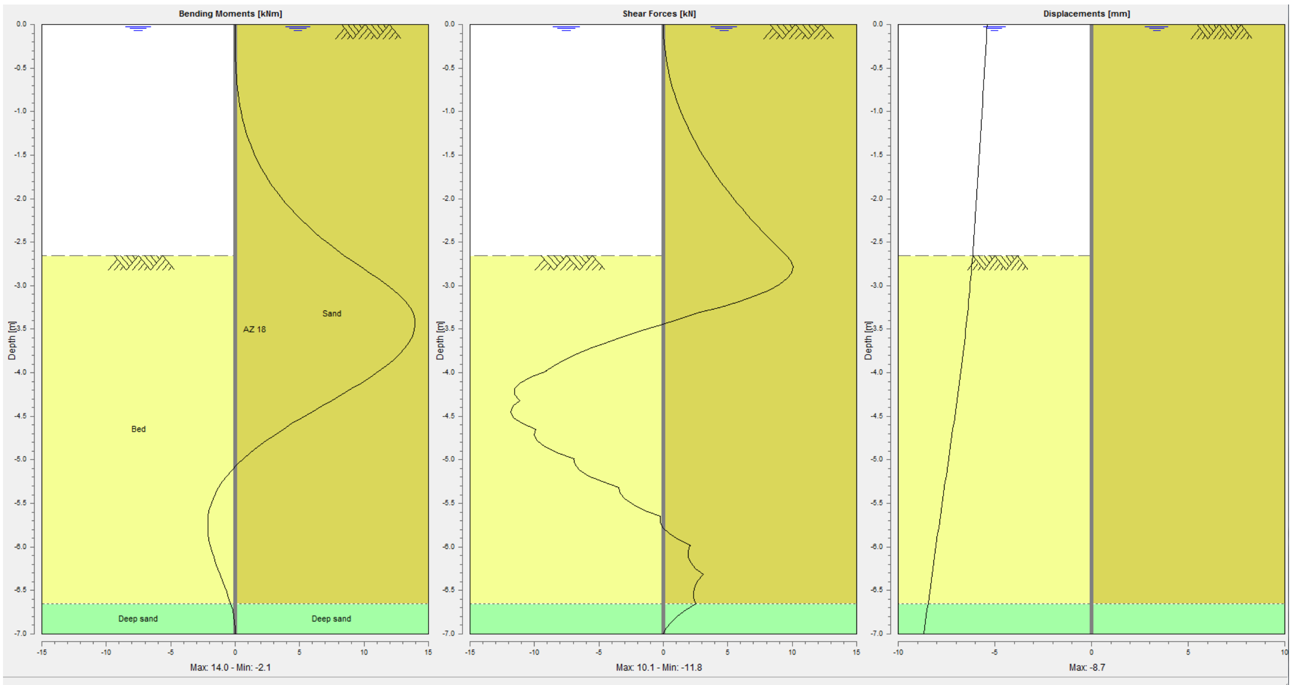

Figure 45: Moment, shear and displacement diagrams in function of the depth of the underwater sheet pile wall

Although the displacement is limited (δ_{max}= 10 mm) it is clear that due to the presence of the caisson, the sheet pile wall will move towards the water side (see right Figure 45). This mechanism may lead to settlements of the of the caisson or even too big instability problems. Therefore, to describe the influence of this displacement on the caisson stability more precisely, this design concept should be modeled with more advanced software.

Lastly, to avoid the collision of the cruise ship with the underwater sheet pile wall, big floating fenders are placed along the full frontage of the berth length. Fenders primary functions are to absorb the berthing energy of the vessel and provide a soft buffer between the quay wall and the ship while moored. Furthermore, fenders spread the load across a wider section of the quay and may also be used to keep vessels at a certain distance from berth structure.

Two different scenarios may lead to the collision between the cruise ship with the underwater sheet pile wall and hence must be considered: during berthing operation and while the cruise ship is moored. In the first scenario, during berthing of the design cruise ship, the fender absorbs the kinetic energy of the berthing ship through elastic deformation. Therefore, the fenders should be dimensioned in such a way that the minimum distance between the keel of the vessel and the sheet pile wall is guaranteed when the maximum compression of the fender is reached.

The selected floating fender (type "*ISO standard*") has a diameter and a length of 4.5 m and 9 m respectively, as shown in the figure below. The detailed technical characteristics of the selected type of fender are presented in Appendix F.

Figure 46: Floating fender dimension

This type of floating fenders can absorb the berthing energy of the cruise that is equal to 516 kNm (see Appendix F) and maintain enough distance between the cruise ship and the sheet pile. As mentioned before, the sheet pile wall is placed at a distance of 2.5 m from the frontage of the caisson. The maximum deflection of the fender, due to the vessel impact is equal to 1.44 m (32% of the diameter). Hence, the fender ensures sufficient distance between the cruise ship and the sheet pile wall. The maximum deflection of the floating fender is computed by multiplying the percentage of defection by the diameter of the fender. The percentage of defection is obtained using the performance curve of the fender as shown below.

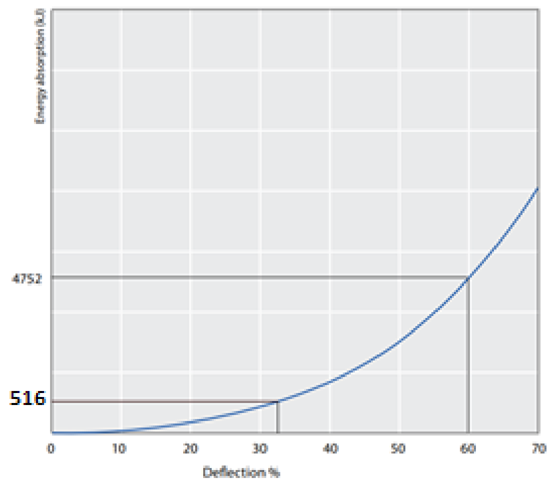

Figure 47: Performance curve of the floating fender (ISO Standard Brochure)

The second scenario that must be considered, is when the cruise ship is moored at the berth. Due to the wind load, the vessel may roll around its vertical axis and consequently, the keel may hit the underwater sheet pile. The maximum roll angle and the draught of the cruise ship are equal to 5° and 10 m respectively (see Section 2.5). Therefore, the keel vessel may move towards the quay wall with a maximum value of approximately 0.9 m as shown in the figure below. Consequently, the floating fenders guarantee the required distance also when the cruise ship is moored (see Figure 48).

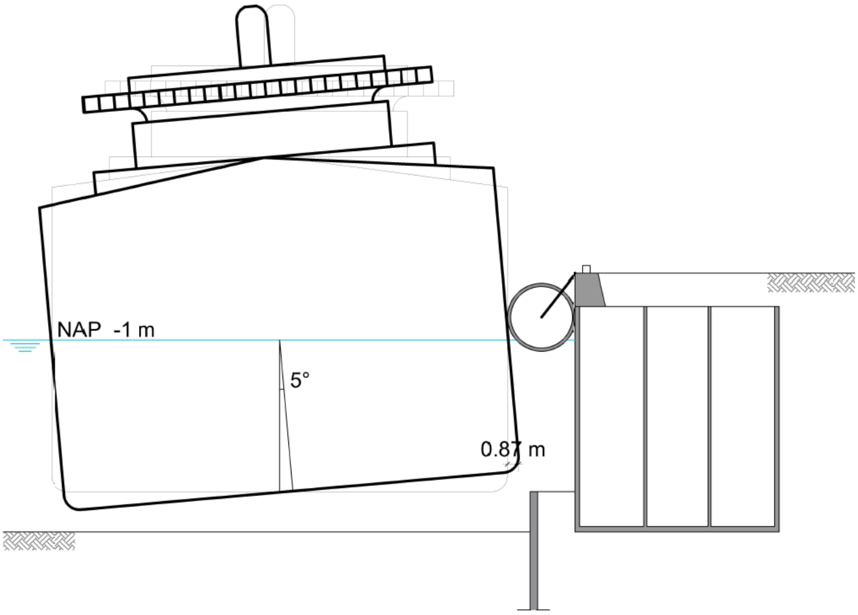

Figure 48: Rolling cruise ship along the berth

4.3.5 Concept E; Guiding structures

The design concept with guiding structures is a feasible solution. To perform a preliminary design of these structures Blum's method for laterally loaded piles is used. However, Blum's schematization results in a reasonable approximation of the maximum absorbable lateral load on a foundation pile as long as the soil can be schematized as one layer (Manual Hydraulic Structures, 2017). Therefore, the soil is assumed as one fictitious layer, the mechanical properties of this layer are taken equal to a mean value of the clay and the deep sand layers (see Section 2.5). The mechanical properties of the fictitious layer are presented below.

Mechanical properties of the fictitious soil layer	
Submerged weight	19 kN/m^3
Angle of internal friction	26.5 deg

Table 18: Mechanical properties of the fictitious soil layer

The breasting dolphin has to absorb the berthing energy of the cruise ship that is equal to 516 kNm (see Appendix F). The breasting dolphins are flexible structures, hence displacement is allowed. The berthing energy of the cruise ship is divided by the maximum allowable displacement of the dolphin to obtain the impact force that the pile has to withstand. For a preliminary design, the maximum displacement of the structure is assumed to be equal to 1 m. Thus, the force acting on the pile can be computed according to following equation:

$$F = \frac{E_d}{\delta} = \frac{516}{1} = 516 \text{ kN}$$

Where:

F is the acting force on the pile due to the ship impact

E_d is the design berthing energy

δ maximum allowable displacement of the pile

The maximum load that the soil wedge behind the pile can withstand is computed with the following expression:

$$F_{max} = \gamma' \cdot K_p \cdot \frac{d^3}{24} \cdot \frac{d^3 + 4 \cdot b}{d + h}$$

Where:

F_{max} is the maximum force that the pile can withstand

b is the width of the pile perpendicular to the load (outer diameter)

h is the height of the unsupported part of the pile

d is the embedded depth of the pile

K_p is the passive soil pressure coefficient

However, to compute the maximum force that the pile can withstand few assumptions regarding the pile are made. The pile has the following characteristics:

Characteristics of the breasting dolphins	
Outer diameter	1.10 m
Inner diameter	1.04 m
Thickness	0.03 m
Area	0.101 m^2
Moment of inertia	0.014 m^4
Young modulus (steel)	$2x10^8$ kN/m^2

Table 19: Characteristics and dimension of the breasting dolphins

Assuming that the cruise ship hits the breasting dolphin during high water (worst scenario) at a height of 3 m above the high-water mark that is equal to NAP +1.7 m (see Section 2.5) the length of the unsupported part of the pile is equal to 18.35 m (see Figure 49).

The embedded depth of the pile is the only unknown. The minimum embedded depth can be obtained can be computed by substituting the acting force in the equation above equation and solving for d.

The minimum embedded depth of the pile required to withstand the acting force is approximately 11.5 m. Now that embedded depth is known the maximum displacement of the pile is verified. According to Blum’s method, the pile can be modeled pile as a cantilever beam with concentrated horizontal load, hence the displacement can be computed by the following equation:

$$\delta = \frac{F \cdot L_i^3}{3EI} = \frac{F \cdot (h + 0.65d)^3}{3EI} = 1.03 \text{ m}$$

where:

δ is the maximum displacement

F is the horizontal force

L_i is the not-supported part of the pile

EI is bending stiffness of the pile

From the results of the above equation, it turns out that the assumed displacement is approximately equal to the computed maximum displacement. Thus, the designed breasting dolphin is able to absorb the berthing energy of the design cruise ship cruise.

The breasting dolphins should be placed at a distance of approximately 13 m from the quay wall. This distance is obtained by adding the length that the coverage soil, located in front of the caisson, so that the passive pressure is developed (approximately 5 m), the length of the bed, placed with a protected natural slope of 1:3, that runs from the caisson to the new required depth (see Figure 49).

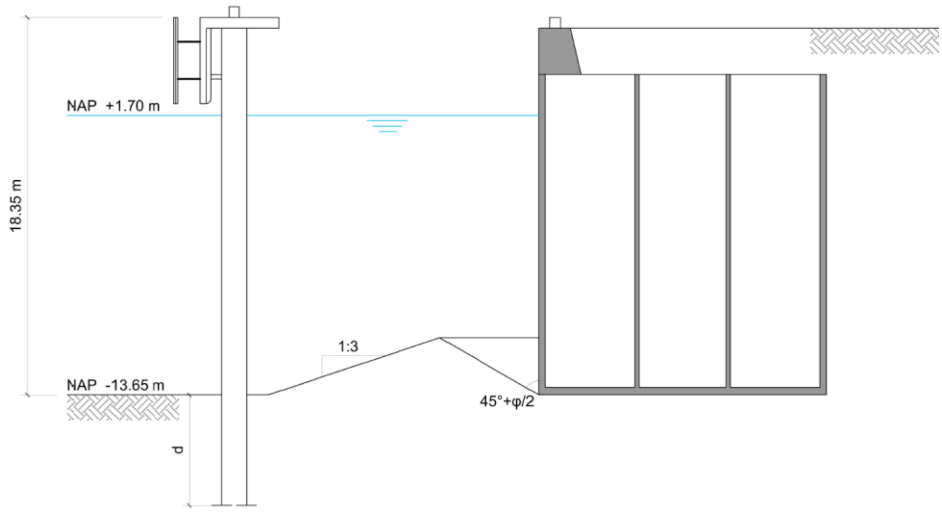

Figure 49: Dimensions design concept with guiding structures (concept F)

4.3.6 Concept F; Piled structure

The design concept with piled structure is not a suitable solution, mainly for two reasons. The first reason is related to the installation of the piles. The driving of the piles, close to the existing quay wall, may cause settlement of the caissons, liquefaction or erosion of the foundation soil that may lead to a high possibility of the instability of the quay wall. The second reason concerns the loads acting on underwater sheet pile driving in front of the piled structure (see Figure 39). The mooring lines loads and the impact loads acting on the upper part of the structure lead to high uplift and horizontal forces that are transferred to the subsoil. Consequently, the underwater sheet pile will need to bear considerable soil horizontal pressures that may cause failure of the structure.

4.4 Conclusion

From the results of the assessment (see Section 4.3), it turns out that:

- Not all the proposed design concepts, developed to solve the technical issues that obstruct the mooring of the design cruise ships along the quay wall of the portside, are suitable.
- The remaining design variant that have a certain level of feasibility and value, which may make them into a candidate for the final variant are: design concept with grout injections, the design concept with the anchored sheet pile wall, the design concept with the underwater sheet pile wall and the design concept with the guiding structures.

5. Evaluation of the verified design variants

5.1 Introduction

In this chapter, the remaining verified design variants are evaluated and rated based on a Multi Criteria Analysis (MCA) and cost estimation. The MCA is described in Section 5.2 with its main aspects and criteria. The cost estimation of the design variants is presented in Section 5.3. The best design concept is selected based on the results of the evaluation (Section 5.4).

5.2 The Multi Criteria analysis

Multi Criteria Analysis (MCA) is a valuable method to arrive at a reliable and traceable choice between competing variants (Van der Toorn, 2015). The MCA supports the comparison of different variants based on a set of aspects or criteria. The different competing variants are evaluated using the set of criteria. For each criterion a score is given to each competing variant. Various methods of rating are possible. Besides, to the criteria itself, a relative weight factor may be assigned by means of a subjective relative ranking of importance (Van der Toorn, 2015).

An MCA is applied to select the most suitable design variant for the adaptation of the existing quay wall at the portside of Pier 1 in the Merwehaven. The rating system of the different design solutions for each criterion is based on a point score. The worst variant is rated with 1 point the second worst with 2 points up to the best variant (see Table 21). However, to obtain a reliable comparison, it is essential to ensure a balance between the criteria. To do so, the criteria are first clustered to determine the importance of the criteria with respect to the design function. The balance is made by clustering the criteria in a matrix so that it is possible to compare the criteria one by one with respect to all the other criteria. The most important is rated with 1 and the less important with 0, in this manner it is possible to establish which of the two criteria is more important. In the end, a weight factor for each criterion is obtained (see Table 20).

5.2.1 MCA criteria and weight factors

The criteria selected for the comparison of the different design variant are presented and described briefly in the following paragraph:

Criterion 1; Use of the existing caissons
As mentioned before the aim of this study is to avoid the demolition of the existing quay wall. Therefore, the first criterion concerns the use that the design variants make of the existing caissons. The design variants are rated according to how the caissons are used. In more detail, if in the design of the variants the existing caissons still perform their functions such as berthing facility and retaining structure (see Section 2.4.1).

Criterion 2; Adaptability of the design for different vessels
This criterion regards the adaptability of the design concepts. The adaptability of a structure can be seen as the ability to adapt to changing circumstances, because these may change during the lifetime of the structure. For a quay wall, the circumstances are type and vessel dimensions. The design variants are rated based on the capability, of their design, to accommodate ships with different functions, dimensions or more vessels at the same time.

Criterion 3; Reuse of the materials
This criterion concerns the possibility of reuse of the material used for the design of the variants. Reuse of the material may happen during the removal of the structure at the end of the lifetime or in case of earlier than planned adaptation or deviation of the design. The design variants are rated based on the possibility of reusing or selling the material adopted in the design.

Criterion 4; Impact on the navigation
This criterion depends on the available width of the approach channel of the berthing facility. The extension of the quay wall reduces the width of the approach channel and consequently increases the difficulty of the approach manoeuvres, which the cruise ships have to perform before reaching the quay wall. Besides, the extension of the quay wall reduces the available navigation space behind the moored cruise, hindering the passage of other vessels that need to reach the other piers of the Merwehaven. The design variants are graded in function of their extension towards the water side.

Criterion 5; Impact on the surrounding
The last criterion concerns the surrounding impact of the different design variants. The variants score depend on their impact on the local surrounding that depends mainly on how easy the design variant can be removed or demolished.

5.2.2 The weight factors

Now that the criteria are defined it is possible to establish which of the criteria is more important as it is explained in Section 5.2. By inserting the criteria in a matrix, the weight factors for each criterion are obtained by dividing their score by the total points as shown in the table below.

	Use of the existing caissons	Adaptability of the design for different vessels	Reuse of the materials	Impact on the navigation	Impact on the surrounding	Score	Weight factor
Use of the existing caissons		1	1	1	1	4	0.40
Adaptability of the design for different vessels	0		1	0	1	1	0.20
Reuse of the materials	0	0		0	1	2	0.10
Impact on the navigation	0	1	1		1	3	0.30
Impact on the surrounding	0	0	0	0		0	0.00
Total points						10	1.00

Table 20: Matrix for the determination of the criteria weight factors

According to the above table, the most important criterion is the *Use of the existing caissons* because the adaptation and reuse of the existing structure is the main objective of this study. The difficulty of the approach manoeuvres for the cruise ships play an important role in the safety of the cruise terminal. Moreover, the hindering for the passage of other vessels leads to an economical lost for the port. Therefore, the *Impact on the navigation* is the second most important criterion. The *Adaptability of the design for different vessels* and *Reuse of the materials* criteria are respectively the third and fourth most important criteria. The impact on the surrounding is the criterion that scores the lowest and hence its weight factor is equal to zero. Although this criterion should be removed from the evaluation to include this criterion, it is chosen to assign to its weight factor a value of 0.05.

5.2.3 MCA scores

To obtain the best design solution, the variants are first rated based on the criteria and then multiplied by the weight factors corresponding to the criteria (see Section 5.2). By multiplying the scores by the weight factors, a balanced total score per variant is obtained. The MCA results are presented in the next table.

Criteria	Weight factor	Grout injections	Anchored sheet pile wall	Underwater sheet pile wall	Guiding structures
Use of the existing caissons	0.40	4	1	4	2
Adaptability of the design for different vessels	0.20	3	4	3	1
Reuse of the materials	0.10	1	4	4	2
Impact on the navigation	0.30	4	2	4	1
Impact on the surrounding	0.05	1	3	2	4
Score excl. factor		13	14	17	10
Score incl. factor		3.55	2.35	3.90	1.70

Table 21: Results of the Multi Criteria Analysis

5.2.4 Motivation of the MCA scores

In this section, the motivations of the MCA scores for each criterion (see Table 21) are described.

Criterion 1; Use of the existing caissons

The design variant with grout injections and underwater sheet pile wall score the best on this criterion because in their design the cruise design cruise ship can moor along the existing caissons and consequently the caissons keep the berthing and the retaining function. The variants with guiding structures is second because in its design the cruise ship is moored along the breasting dolphins, therefore, the caissons perform only the retaining function. The design variant with the anchored sheet pile wall scores the least on this criterion because the caisson is entirely buried in the soil and therefore lose all its functions.

Criterion 2; Adaptability of the design for different vessels

The design of the anchored sheet pile wall scores the best because if during the lifetime of the structure the design circumstances may change, this solution has no restrictions regarding depth or minimal distance from the quay. The design variants with grout injections and with the underwater sheet pile wall require floating fenders to ensure the distance between the keel of the vessels and the underwater elements present in front of the quay wall. Moreover, the significant dimensions of the floating fenders may obstruct the mooring of smaller vessels. Hence, these two variants score the same. The variants with guiding structures scores the least because the dolphin structures will be designed according to the dimensions and characteristics of the design cruise ship and therefore they may be not suitable for vessels with smaller dimensions. Besides, the mooring dolphins will be placed more towards the water side and hence they may create navigational problems for the vessels that need to reach the quay wall.

Criterion 3; Reuse of the materials

For this criterion, the design variants that make use of a sheet pile wall score the best due to the fact that usually sheet pile walls can be reused or melt to make new steel. While the design variant with dolphin structures, the reuse of the adopted piles is more limited and therefore its score is lower. Thus, this variant has the second highest score. The design variant with the grout injections has the lowest rating due to the fact the injected grout is a permanent solution that requires much more effort to be demolished and removed. Moreover, the grout material has limited possibility of reuse.

Criterion 4; Impact on the navigation

The motivation of the score for this criterion is straightforward. The variants are rated based on their extension of the quay wall to the water side. Therefore, the design variant with the underwater sheet pile wall and the grout injection score the most. The second-best variant is the anchored sheet pile wall and the last one is the design that makes use of the guiding structures.

Criterion 5; Impact on the surrounding
For this criterion, the design variant with the guiding structures scores the highest. Because the piles can be easily removed from the subsoil. The design variants that make use of a sheet pile walls can also be easily removed, however they score less due to the fact that more material is driven in the subsoil. The variant with underwater sheet pile wall scores less because it is completely located under the waterline and hence is more difficult to remove it. The variant with grout injection scores the least because it is a permanent solution that is has a significative impact of the surrounding and is challenging to remove.

5.3 Costs estimation

Costs have to be included in the evaluation to define the best design variant. Therefore, a cost estimation of each design concept is performed. The cost of each design variant is estimated based on the amount of the used materials, the price of the materials and the construction costs. Notice that the total costs include only the costs of the main components and elements that characterize the different design variants. The cost estimation of the various design variant is based on literature study.

Variant A; Grout injection
According to literature study, grout injections costs approximately 500 €/m^3. The total volume of grout required for the design variant is given by the dimension (height and width) of the grout injection (see Table 16) multiplied by the length of the quay wall that is equal to 580 m (see Section 2.2.1). Hence, the volume of grout is equal to 10150 m^3 and consequently, the material costs are equal to € 5.075.000. The grout injection technique requires difficult construction planning and advanced construction method. Hence, the construction costs are estimated around 15% of the material costs. The total costs for this design variant are approximately € 6,800,000.

Variant C; Anchored sheet pile wall
As mentioned in the preliminary design of the sheet pile wall design variant, to increase the flexural stiffness and consequently to minimize the deformation a combi-wall should be constructed (see Section 4.3.3). Based on the literature study and expert judgment the price of the material and construction of an anchored combi-wall is around 1000 €/m^2. The retaining height of the wall and the embedded depth are equal to 17 m and 9 m respectively (see Section 4.3.3). Hence, the total height of combi-wall is approximately 26 m. The total area of the retaining height of the combi-wall is given by the total height of the combi-wal multiplied by the length of the quay wall (see Section 2.2.1) and is equal to 15080 m^2. Hence, the cost of the retaining structure is approximately equal to € 15,000,000.

Variant D; Underwater sheet pile wall
The price of the material and construction of a sheet pile wall without anchor is around 600 €/m^2. The retaining height of the wall is equal to approximately 3 m (see Section 4.3.4). The total area of the underwater sheet pile wall is equal to 4640 m^2 that is given by the total height of the wall, equal to 8 m, multiplied the length of the quay wall. Therefore, the total costs for this design variant are approximately € 2,800,000. However, the cost of this variant may be higher due to the fact that the sheet pile should be placed entirely underwater.

Figure 50 presents the relationship between the total costs of a quay wall as a function of the retaining height (de Gijt, 2011). From the figure the costs of the design variants with the sheet pile walls are estimated as shown below.

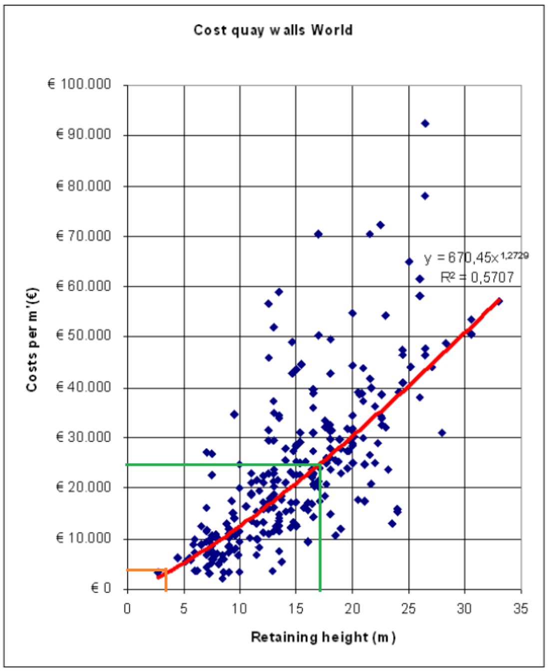

Figure 50: Costs of quay walls as a function of the retaining height (de Gijt, 2011)

The orange and the green lines represent the design variant with the underwater sheet pile wall and the anchored sheet pile wall respectively. The cost per running meter approximately 3500 € and 24000 € respectively. The length of the quay wall is 580 m (see Section 2.2.1). Hence, the total cost of the variant with the underwater sheet pile wall is 2,030,000 € while the total costs of the variant with the anchored sheet pile wall is 13,920,000 €. Therefore, it can be concluded that the estimated total costs of the design variants with the sheet pile walls are in line with the one presented in the above graph.

Variant E; Guiding structures

The total costs of this design variant are based on the amount and the price of steel used for the construction of the guiding structures. According to the preliminary design of the breasting dolphin (see Section 4.3.5) the amount of steel required is equal to 3 m^3. The density of steel and its price is 7.8 t/m^3 and 1000 €/t respectively. Thus, each dolphin cost approximately 25.000 €, assuming that eight breasting and four mooring dolphins are required to ensure the mooring of the design cruise vessel the costs of the breasting dolphins including 10% of the total costs for the construction cost is equal to € 300,000. However, due to the distance between the moored cruise ship and the quay wall, at the terminal, bigger and longer gangways are required to board the passengers, crew and supplies. Hence, this leads to a more expensive gangway. This increase in the price of the gangway with respect to the other design variants is estimated equal € 2,500,000. Therefore, adding the costs of the guiding structures the total cost for this design variant is approximately € 2,800,000.

5.3.1 Costs estimation parameters

A non-dimensional cost parameter for each variant is defined to include cost in the evaluation. The cost parameter is obtained by dividing the cost of each variant by the cost of the most expensive variant. The total costs with the respective cost parameter of each design variant are presented in the table below.

Cost estimation and cost parameter		
Design variant	**Total cost (€)**	**Cost parameter**
Grout injections	6,800,000	0.45
Anchored sheet pile wall	15,000,000	1.0
Underwater sheet pile wall	2,800,000	0.19
Guiding structures	2,800,000	0.19

Table 22: Total cost and cost parameter of the different design variants

5.4 Result of the evaluation

Now that the MCA scores and the cost of each design are defined, the best design variant can be identified. The best design variant is obtained by dividing the MCA scores of each variant (see Table 21) by the corresponding cost parameter (see Table 22). The variant that has the highest score is the best design variant. The results of the evaluation are presented in Table 23. The table presents the MCA score, the cost parameter, and the final score of each design variant.

Final scores of the evaluation			
Design variant	**MCA score**	**Cost parameter**	**Final score**
Grout injections	3.55	0.45	7.89
Anchored sheet pile wall	2.35	1.0	2.35
Underwater sheet pile wall	3.90	0.19	20.53
Guiding structures	1.70	0.19	8.95

Table 23: Final scores of the evaluation with MCA score and cost parameter of the different design variants

Based on the evaluation, the design variant with the underwater sheet pile wall is the best design variant to solve the technical issues that obstruct the mooring of the design cruise ships along the quay wall of the port side of Pier 1 and adapt the existing caisson, in the Merwehaven for the future cruise terminal of Rotterdam.

6. In depth design for the determination of design mooring forces

6.1 Introduction

This chapter is the first part of the in-depth design. As mentioned before, quay walls are equipped with mooring systems such as bollards and fenders. Bollards cause concentrated horizontal forces that must be considered in the design of the quay wall because they have an important impact on the stability of the structure. Therefore, it is crucial to first define the required bollard capacity of the new cruise terminal before performing the detailed design of the best design variant.

In this chapter, special attention is given to the calculation of forces, due to the wind and passing ships acting on the moored design cruise ship, which are transferred to the bollards of the quay wall. The chapter starts with a description of the bollards and with an indication of the mooring capacity, that the bollards of the cruise terminal should have, according to the most common guidelines and standards (Section 6.2). A short description of the background information regarding the movements of a moored ship is given in Section 6.3. The calculation of the mooring forces due to the wind and the due to the passing ships are presented in Section 6.4 and 6.5 respectively. In Section 6.6 an analysis of the expected line forces is carried out to define the design bollard capacity required for the cruise terminal. Based on the obtained design bollard capacity it is concluded if the existing bollards, can withstand the mooring loads. The conclusions of this chapter are presented in Section 6.7.

6.2 Bollards and minimum bollard capacity

Bollards are posts, placed along the berthing facilities where the lines of vessels are tied. The bollards, together with the lines and the winches, form the system that restrains the vessel movements and avoids that the ship turns away. The required capacity of bollards depends on the following factors:

- Size of the ship
- Wind force
- The layout of berth and quay
- Wave action and currents

For a preliminary design, most of the most common guidelines and standards provide tables for the minimum mooring capacity of the bollards in function of the type and water displacement of the vessel. Some of these tables are presented below:

TABLE 3.4.2.3.5.15 MINIMUM HORIZONTAL MOORING LOADS FOR SHIPS WITH DISPLACEMENT GREATER THAN 20,000 t

DISPLACEMENT (t)	MOORING LOADS (t)
20,000 ~ 50,000	80
50,000 ~ 100,000	100
100,000 ~ 200,000	150
> 200,000	200

Table 24: Minimum mooring loads for vessels with water displacement greater than 20000 t (Spanish ROM)

Loaded displacement in ton (DWT)	Hawser force in kN representative values
<10,000	300
<20,000	600
<50,000	800
<100,000	1,000
<200,000	1,500
<250,000	2,500
>250,000	>2,500

Table 25: Mooring loads for vessels with different deadweight tonnage (DWT) (Quay Wall Second edition)

Seagoing vessels	
water displacement of ship [ton]	mooring force [kN]
< 2 000	0 - 100
2 000 ~ 10 000	100 - 300
10 000 ~ 20 000	300 - 600
20 000 ~ 50 000	600 - 800
50 000 ~ 100 000	800 - 1000
100 000 ~ 200 000	1000 - 1500
> 200 000	1500 - 2000

Table 26: Mooring loads for seagoing vessels with different water displacement (Manual Hydraulic Structures 2017)

The mass of the design cruise ship is equal to 120000 t (see Section 2.5), according to Table 24 and Table 25, the capacity that the bollards of the cruise terminal should have is equal to 1500 kN. While using Table 26, the minimum capacity of the bollards is obtained by interpolation as shown below:

$$F_{min} = 1000 + \frac{500 \cdot (120 - 100)}{(200 - 100)} = 1100 \text{ kN}$$

The Port of Rotterdam Authority provides a guideline called "*Bolderbelasting Standardisatie Rotterdam*" that suggests the required bollard capacity for quay wall in the port of Rotterdam. In this standard, the bollard capacity is based on the Minimal Breaking Load (MBL) of the lines equipped by the vessel. Usually, cruise ships are equipped with lines with an MBL equal to 1300 kN and maximum two lines are tied at on one bollard (Port of Rotterdam Authority, 2015). Consequently, according to this standard, the required design capacity of the bollards is 2340 kN (see table Appendix G). In the port of Rotterdam bollards with a maximum capacity of 2400 kN are used for quay walls used by large container ships (Port of Rotterdam Authority, 2015).

The existing bollards placed on top of the quay wall of Pier 1 have a capacity of 750 kN (see Section 3.2), hence, according to the above-mentioned guidelines and standards, the bollard capacity is not sufficient. At the current cruise terminal location (Wilhelminapier), the existing bollards have a capacity of 800 kN. But besides, two storm bollards are placed in correspondence of the bow and stern of the vessels, with a capacity of 1200 kN (Port of Rotterdam Authority). However, the cruise ships that currently moor along the Wilhelminapier are much smaller than the design cruise ship. Thus, due to the presence of the storm bollards, the capacity is in the order of the values provided by guidelines and standards. Moreover, in case of heavy storms, tugboats are used to keep the moored vessel along the berth and consequently reduce the loads on the bollards

Form the above values, it is clear that the provided values for the bollard capacity have a significative difference. Therefore, an extensive study regarding the loads acting on the moored cruise ship and the expected line forces is carried out to define and to optimize the required bollard capacity of the future cruise terminal.

.

6.3 Motion of a moored ship

This section provides a theoretical background on the main physical aspects that are exerted on a moored ship. A vessel that is moored against fenders and is secured with mooring lines has a dynamic behavior due to wind, waves and currents. This dynamic behavior generates forces that the mooring lines and fendering have to withstand. In more detail, a moored ship has six degrees of freedom, each mode of motion has a different name:

- Surge is the translation of the ship along its transverse axis
- Sway is the translation of the ship along its longitudinal axis
- Heave is the translation of the ship along its vertical axis
- Roll is the rotation of the ship around its longitudinal axis
- Pitch is the rotation of the ship around its transverse axis
- Yaw is the rotation of the ship around its vertical axis

The six motion modes are presented in the figure below.

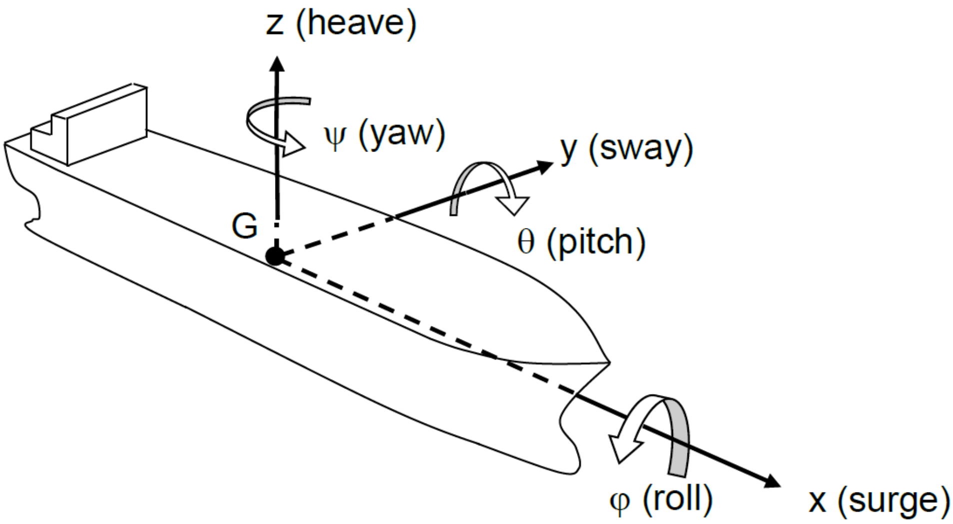

Figure 51: Definition of ship motion (Ship-Moorings Manual)

Notice that, in the above figure the arrows indicate the positive signs of forces and moments. The motions of the moored ship that have to be considered in the design of the mooring systems are *surge, sway* and *yaw* because these motions cause the highest forces in the mooring lines.

6.4 Wind load

Wind is a critical load for port infrastructures. The wind load does not only work directly on the port structure but also on the moored vessels. The wind load, acting on a moored ship, depends mainly on the wind velocity and on the exposed area of the vessel. Cruise ships are characterized by substantial air draught and hence huge areas exposed to wind that consequently may lead to considerable wind loads. Therefore, for the bollards design, it is crucial to define the wind force acting on the design cruise ship.

For simplicity, the wind load on a ship can be broken down into two components: a longitudinal force acting parallel to the longitudinal axis (surge) of the ship and a transverse force acting perpendicular to the longitudinal axis (sway). According to the British Standard (BS), the overall wind force can be described by two transverse forces, one at each perpendicular, combined with a longitudinal force as shown in the figure below.

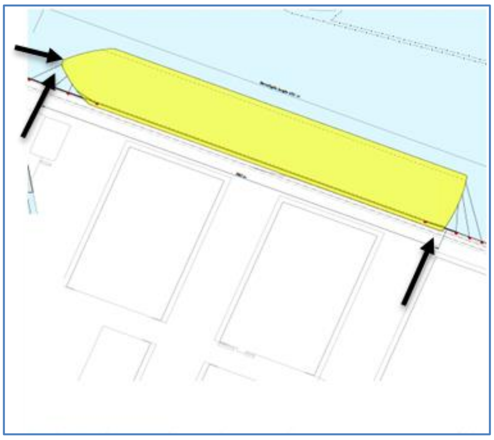

Figure 52: Wind load schematization according to the British Standard

The sum of the forward and aft force components give the total sway wind force. The longitudinal force component provides the surge force.

The force components, acting on the moored ship, are a function of the wind speed, the direction of the wind relative to the ship and the exposed area of the vessel. According to the BS, the wind force components can be computed using the following equations:

$$F_{TW} = C_{TW} \cdot \rho_A \cdot A \cdot V_W{}^2 \cdot 10^{-4}$$

$$F_{LW} = C_{LW} \cdot \rho_A \cdot A \cdot V_W{}^2 \cdot 10^{-4}$$

Where:

F_{TW} is the transverse wind force (sway), in kilonewtons (kN)

F_{LW} is the longitudinal wind force (surge), in kilonewtons (kN)

C_{TW} is the transverse wind coefficient, forward or aft (-)

C_{LW} is the longitudinal wind coefficient (-)

ρ_A is the density of the air that is assumed to be equal to 1.25 kg/m^3

A is exposed area of the vessel above the water line, in square meters (m^2)

V_w is the wind speed at a height of 10 m above water level, in meter per second (m/s)

The wind velocity, the exposed area of the ship and the wind coefficient are the most influential variables in the calculations of the wind force. The exposed area is the longitudinal projected area of the cruise ship that varies according to the wind direction. In the longitudinal direction it is given by the air draught of the cruise ship multiplied by its beam (see Section 2.5), while for the transverse direction the air draught is multiplied by the length between the two perpendiculars (L_{pp}), hence, these areas are equal to 4400 m^2 and 26250 m^2 respectively. Although the exposed areas are easily obtained, the other two variables, wind coefficient and wind speed, need to be discussed in more detail.

6.4.1 Wind coefficients

The wind force coefficients depend on the angle of wind attack, type and geometry of vessel and the extent of loading by cargo (fully loaded or only ballasted). The wind coefficients (C) apply to a horizontal wind flow on the ship, with a uniform wind speed both along the entire ship height and the ship length and are valid for unsheltered vessels in open water (BS 6349-4 Part 4, 2014).

To define the values for the wind coefficients, the British Standard provides several graphs for different types of vessels based on the approach angle of the wind and on the loading conditions of the ship. Unfortunately, no graphs are available for cruise ships. Therefore, to estimate the wind force coefficients for the design cruise ship, the envelope for container ship is adopted, because these type of vessels, when they are fully loaded, are the most similar to a cruise ship, due to the potential high exposed area over the full length of the ship. The envelope for container ship is presented in the figure below.

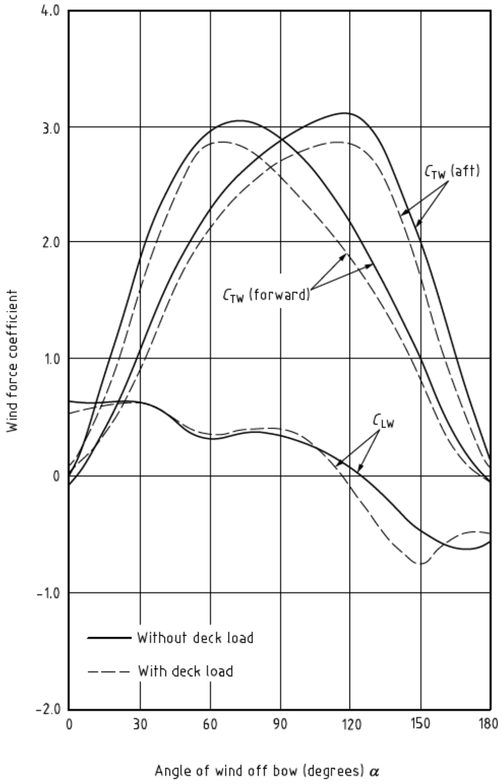

Figure 53: Envelop of the wind force coefficients for typical container ship (BS 6349-4 Part 4)

The selected wind coefficient envelope for the calculation of the wind load is the one described by the curve *"With deck load"* (see Figure 53). Notice that the forward and transverse aft coefficients are described by different curves consequently the forward and transverse aft force have different values. In this manner, the effect of the yaw moment acting on the cruise ship due to the wind is included.

The values of the wind coefficient used for the calculations obtained from Figure 53 are given in the table below, as a function of the wind angle in respect of the bow.

Value of the wind force coefficients			
Angle of attack off the bow	**C_{TW} forward**	**C_{TW} aft**	**C_{LW}**
0°	0	0	0.65
30°	1.55	0.9	0.65
60°	2.8	2.1	0.55
90°	2.55	2.65	0.55
120°	1.9	2.8	- 0.1
150°	0.9	1.75	- 0.8
180°	0	0	- 0.55

Table 27: Value of the wind force coefficients per wind angle in respect of the bow (BS 6349-4 Part 4)

According to the above values, the range of wind angle off the vessel's bow, that lead to the highest transverse force component is between 60° and 120°. While 150° is the wind angle that leads to the highest longitudinal force component.

6.4.2 Design wind speed

As stated previously, the wind speed has a crucial role in the order of magnitude of the wind load acting on a moored ship. Hence, to define a proper design value of the wind speed, a detailed study is performed. The study first describes the indication of the design wind velocity according to the most common guidelines and standards. Then, the available measured wind speed data is analyzed and compared to the value of the different guidelines. Finally, based on this study the design wind speed is defined.

The design wind speed is obtained by applying several steps. These steps are presented below:

- Definition of the wind directions that lead to loading of the mooring lines and consequently of the bollards (see Measured wind velocities).
- Computing the design wind speed with a return period of 50 years for the critical directions using the GEV probability distribution (see Basisstocasten WBI-2017).
- Multiplying the obtained design wind speed with the factors that take into consideration the wind interval (gust) capable of overcoming the inertia of the moored ship (see Spanish ROM) and the effect of roughness of the project area (see Eurocode).

Eurocode

According to the Dutch national annex of the Eurocode 1, for the design of civil engineering projects, a characteristic average wind speed of 27 m/s over a period of 10 minutes must be used for the Rotterdam area (see Figure 54, wind area II).

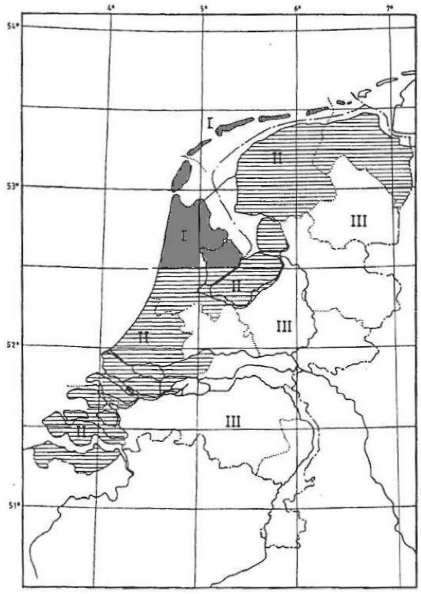

Figure 54: Wind pressure zone in the Netherlands (Eurocode 1, Dutch national annex)

This average wind speed is applied at a height of 10 meters above the ground level in an open area. The Eurocode also offers the possibility to take into consideration the roughness of the terrain that is related to the environment of the project area (open or built-on area). When there is a built environment, the characteristic 10-minute average wind speed can be adapted.

Basisstochasten WBI-2017
The *Basisstochasten WBI-2017* presents the boundary conditions for the design of flood defenses in the Netherlands based on statistical analysis of the stochastic variables like seawater levels, wind speeds and river discharges. According to this report, the wind speed annual maximum can be described with the Generalized Extreme Value (GEV) distribution. Thus, the wind speed for a given return period can be obtained using the following equation:

$$u_m = u + \sigma \cdot \ln(\lambda \cdot m)$$

Where:
u_m is the wind speed for a given return period (m/s)
u is the threshold value (m/s)
σ is the scale parameter of the exponential probability distribution (m/s)
λ is the location parameter of the exponential probability distribution (1/years)
m is the return period (years)

The *Basisstochasten WBI-2017* provides the parameters for several locations in the Netherlands obtained through Peaks over Threshold (POT) series with an average speed wind of 1 hour at 10 m height above an open area. These parameters are available for omnidirectional and the directional wind sectors of 30 degrees (see Appendix H).

The Zestienhoven station (Rotterdam The Hague Airport) is the nearest to the Merwehaven. In the following table, the parameters of the GEV distribution for the directional wind sectors of the Zestienhoven station are presented.

Parameters of the exponential distribution			
Wind direction	**Threshold value u (m/s)**	**Scale parameter σ**	**Location parameter λ**
0°N	9.2	4.34	1.59
30°N	8.2	5.67	1.45
60°N	9.4	1.86	0.89
90°N	8.1	3.59	1.10
120°N	7.4	4.92	1.02
150°N	8.4	4.60	1.22
180°N	11.1	4.79	1.30
210°N	13.7	3.22	1.39
240°N	13.5	6.20	1.96
270°N	13.1	4.12	2.14
300°N	13.1	2.55	2.15
330°N	10.2	4.95	2.00

Table 28: Exponential distribution parameters of the wind speed per each direction of the Zestienhoven station

Using the above parameters the wind speed with an average of 1 hour can be computed, for each wind direction and for a given return period.

Spanish ROM
The Spanish ROM provides a method for determining the loads on a moored vessels based on the environmental conditions (wind and current) of the project area. According to this guideline, the wind load is based on the average wind velocity determined in the shortest interval (gust) capable of overcoming the ship's inertia. An average velocity corresponding to the following gust values should be adopted:

- 1 minute for ships of length equal to or greater than 25 m
- 5 seconds for ships of length less than 25 m

According to the above values the wind force, for the design cruise ships, should be computed using the 1-minute average wind speed. However, most of the wind velocity measurements are carried out based on a 10-minutes average. Therefore, the Spanish ROM provides conversion factors for determining the wind speed for different time average intervals from the 10-minutes average at a height of 10 meters, both for open or built-on area. These factors are presented in the following table.

Conversion factors		
Gust duration	**Open area at a height of 10 m**	**Built-on area at a height of 10 m**
3 seconds	1.44	1.96
5 seconds	1.42	1.91
15 seconds	1.38	1.82
1 minute	1.31	1.67

Table 29: Conversion factors for different gust duration from 10-minutes average wind speed at a height of 10 meters (Spanish ROM)

Note that, due to the presence of high buildings the turbulence phenomena may enhance the wind speed and therefore, the conversion factors for built-on areas are higher than the conversion factors for open area.

British Standard

The British Standard recommends a method for determining the loads on moored vessels based on the environmental conditions of the project area. This guideline also advises using the 1-minute average wind speed to compute the wind load acting on a moored ship.

Oil Company International Marine Forum (OCIMF)

The OCIMF provides a calculation method for the determination of the loads acting on the moored vessel based on wind and current. This calculation method is comparable with the methodologies from the British Standard and Spanish ROM, but is explicitly adopted to tankers and gas carriers. However, for the calculation of the wind load, it advises using an average wind speed over a period of 30 seconds. The 30-second period applies to all ship dimensions.

Measured wind velocities

As has been already mentioned, the favorable orientation of Pier 1 (see Figure 55) may lead to relatively low wind loads acting on the design cruise ship. However, to prove if this is the case and to define the design wind speed, an analysis of the wind measurements is performed.

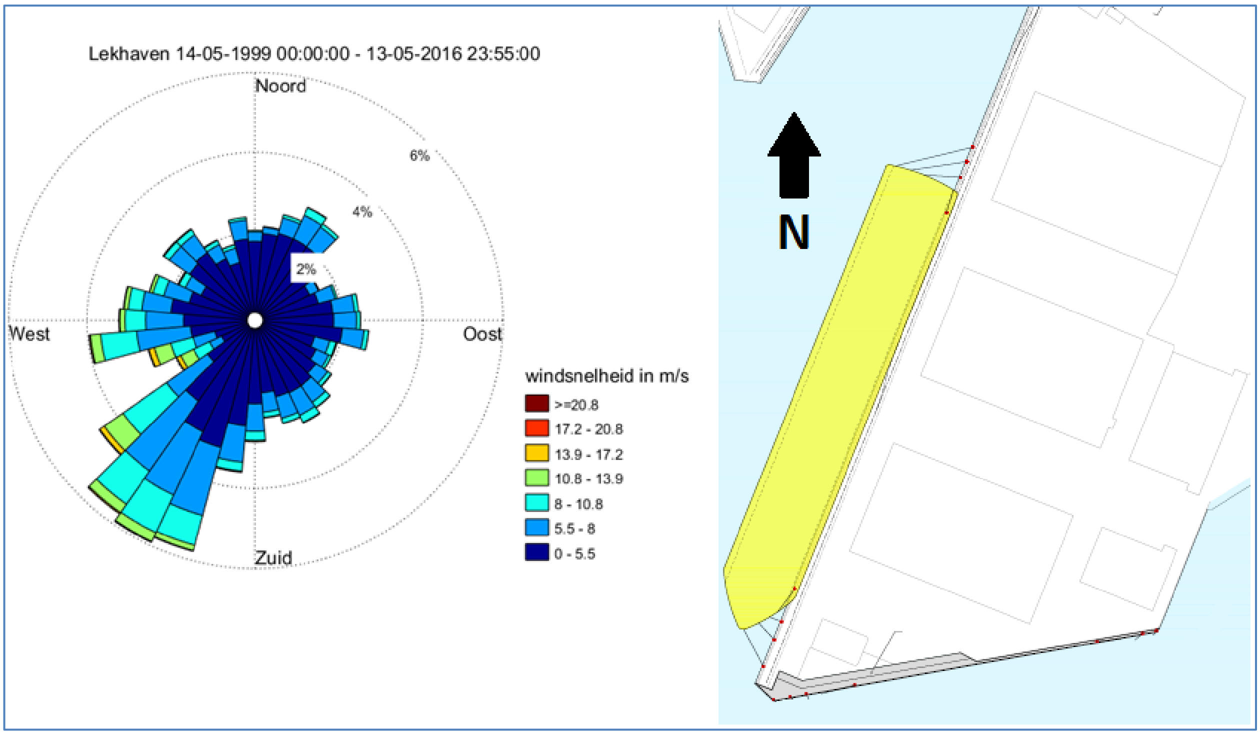

Figure 55: Wind rose Lekahaven (left) and orientation of Pier 1 (right)

From the above figure, it can be noticed that Pier 1 is oriented, with respect to the Nord (N) of approximately 25-30° (see right Figure 55). When the design cruise ship is moored, the wind directions that lead to loading of the mooring lines and consequently of the bollards, are between 30°N and 210°N. The wind directions 30°N, 180°N and 210°N are mainly of interest for the longitudinal wind force component (surge) while the directions in between generate mainly the transverse force component (sway). According to the wind coefficient envelope (see Figure 53), the wind angle, in respect of the bow, which causes the highest sway force on the cruise ship are between 60° and 120°. Hence, taking into consideration the orientation of Pier 1 these angles are related to the wind direction between 90°N and 150°N.
From the data measured by the Lekhaven wind station (see Section 2.5), the following graph is obtained.

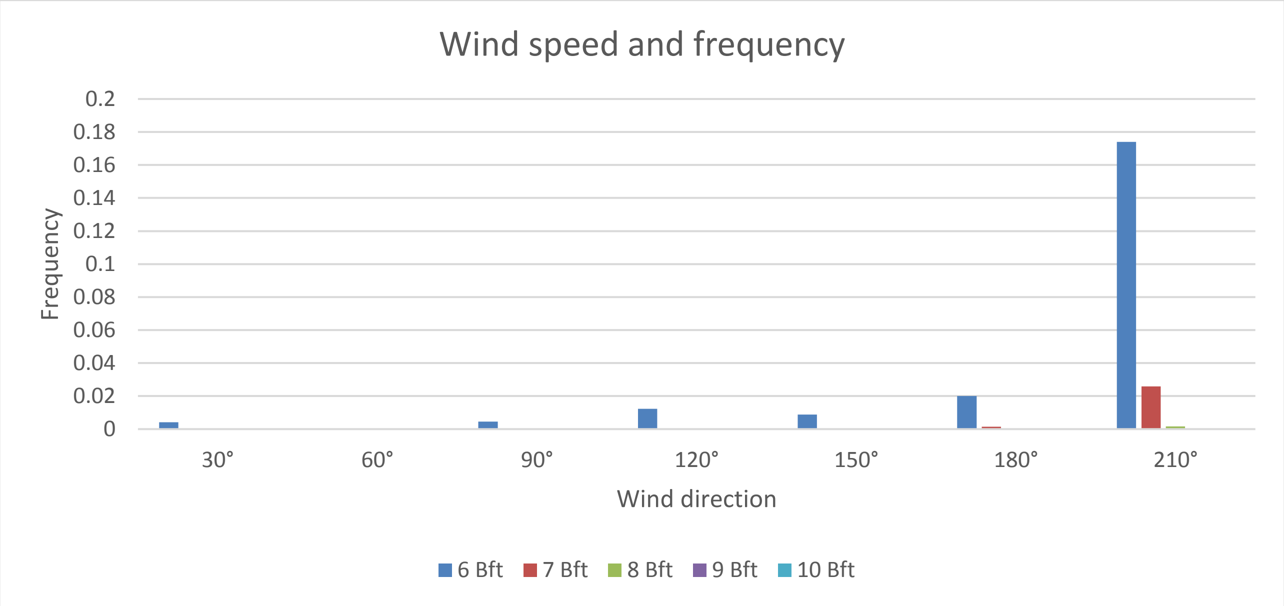

Figure 56: Wind frequency and wind speed of the win direction obtained that lead to loading of the bollards

The figure presents the frequency only of the interested wind directions (30°N- 210°N) characterized by wind speeds higher than five on the Beaufort scale, during the measured period (17 years). The frequency, for each direction, is obtained by dividing the number of times that the wind blew with speed higher than five on the Beaufort scale, by the total number of times that the blew with a speed higher than five on the Beaufort scale in all the directions. The Beaufort scale with the corresponding wind speed is presented in Table 30.

Beaufort scale		
Wind force	**Lower bound of the wind speed at 10 m height (m/s)**	**Upper bound of the wind speed at 10 m height (m/s)**
4	5.5	7.9
5	8.0	10.7
6	10.8	13.8
7	13.9	17.1
8	17.2	20.7
9	20.8	24.4
10	24.5	28.4

Table 30: Beaufort scale with the corresponding lower and upper velocity bound at 10 m height

From Figure 56, it is evident, that the wind directions that generate mainly transverse wind force (between 90°N and 150°N) are not frequent. In more detail, from these directions, the wind blew with a speed higher than six on the Beaufort scale only 0.2% of the covered interval (17 years). Moreover, for the wind directions in between 90°N and 150°N, that lead to the highest sway force, the maximum measured wind velocity was seven on the Beaufort scale. For the 180°N and 210°N directions, that cause mainly surge force, the wind reached a wind speed of ten on the Beaufort scale. Hence, it can be concluded that for the calculation of the wind load acting on the design cruise ship a distinction should be made between the wind velocity for each direction.

Based on what has been discussed so far, the design wind speed for each direction is computed according to the *Basisstochasten WBI*-2017. The required return period for port infrastructure, according to the British Standard, is 50 years. Hence, using the parameters of the GEV distribution for the Zestienhoven station, the wind speeds for the interested wind directions (30°N- 210°N), with a return period equal to 50 years, are computed and presented in the table below. Wind speeds with different return periods for each wind direction of the Zestienhoven station are presented in the Appendix H.

Wind direction	Wind velocity (m/s)
30°N	16.4
60°N	13.4
90°N	13.8
120°N	13.0
150°N	15.0
180°N	18.2
210°N	20.8

Table 31: Wind speed per direction with a return period of 50 years

The values given in Table 31 are related to 1-hour average and for open area. However, these wind speeds have to be multiplied by factors to take into consideration the wind interval (gust) capable of overcoming the inertia of the ship and to include the effect of roughness of the project area.

To convert the wind speed, from a 1-hour average to 1-minutes average the velocity has to be multiplied by a conversion factor. The Spanish ROM provides conversion factors only from 10-minutes average. Therefore, first, the wind speed is multiplied by a conversion factor to convert the wind speed from a 1-hour average to 10 minutes average. The factors are function of the exposure of the project area and are presented below.

Exposure at +10 m		Reference Period	Gust Factor G_{τ,T_o}				
			Gust Duration τ *(s)*				
Class	Description	T_o (s)	*3*	*60*	*120*	*180*	*600*
In-Land	Roughly open terrain	3600	1.75	1.28	1.19	1.15	1.08
		600	1.66	1.21	1.12	1.09	1.00
		180	1.58	1.15	1.07	1.00	
		120	1.55	1.13	1.00		
		60	1.49	1.00			
Off-Land	Offshore winds at a coastline	3600	1.60	1.22	1.15	1.12	1.06
		600	1.52	1.16	1.09	1.06	1.00
		180	1.44	1.10	1.04	1.00	
		120	1.42	1.08	1.00		
		60	1.36	1.00			

Table 32: Recommended wind speed conversion factors (Harper, Kepert, & Ginger, 2008)

Then, to covert, the wind speed from 10-minutes average to 1-minute, the conversion factor provided by the Spanish ROM (see Table 29) is adopted. Furthermore, the velocity is multiplied by the roughness factor to include the effect of roughness of the project area. The design wind velocities for each direction is obtained as shown in the following equation:

$$V_d = V_{50} \cdot \gamma_{Tab} \cdot \gamma_{ROM} \cdot c_r(z)$$

Where:

$$k_r = 0.19 \cdot \left(\frac{z_0}{0.05}\right)^{0.07} = 0.22$$

$$c_r(z) = k_r \cdot \ln\left(\frac{z}{z_0}\right) = 0.67$$

Z_o is the roughness height of the area, for built-on areas it can be taken equal to 0.5 m (Eurocode)

k_r area factor

z is the height at which the velocity is measured, equal to 10 m

c_r roughness factor

γ_{Tab} is the conversion factor from 1-hour average to 10-minutes average for roughly open terrain, equal to 1.08 (see Table 32)

γ_{ROM} is the conversion factor from 10-minutes average to 1-minute for built-on areas, equal to 1.67 (see Table 29)

v_{50} is the wind velocity at 10 m height with a return period of 50 years for the different wind directions (see Table 31)

Finally, the design wind velocities for the interested wind directions (30°N-210°N), with a return period equal to 50 years, are presented in the following table.

Wind direction	Design wind velocity (m/s)
30°N	19.8
60°N	16.2
90°N	16.7
120°N	15.7
150°N	18.2
180°N	22.0
210°N	25.1

Table 33: Design wind velocity at 10 m height of the interested wind directions with a return period of 50 years

6.4.3 Results

Now that all the variables are defined, the wind forces acting on the design cruise ship are computed according to the equations described in Section 6.4, assuming that the cruise ship is moored with its bow towards the *Nieuwe Maas* (see right Figure 55) (this is usually done because in case of emergency the vessel can immediately leave the berth) the value of the longitudinal, the forward and aft transverse force components for the different wind direction are given in the following table.

Wind force						
Wind direction	**Angle of attack off the bow**	**Design wind velocity (m/s)**	**$F_{Longitudinal}$ (kN)**	**$F_{Transverse\ forward}$ (kN)**	**$F_{Transverse\ aft}$ (kN)**	**$F_{Transverse\ total}$ (kN)**
30°N	180°	19.8	-118	0.0	0	0.0
60°N	150°	16.2	-116	778	1513	2291
90°N	120°	16.7	-15	1736	2558	4294
120°N	90°	15.7	75	2070	2151	4221
150°N	60°	18.2	100	3032	2274	5307
180°N	30°	22.0	173	2466	1432	3898
210°N	0°	25.1	208	0	0	0

Table 34: Wind force components acting on the design cruise ship per wind direction

Notice that, although the design wind velocities that lead mainly to transverse force component are lower than those that lead mainly to longitudinal force component, the transverse wind force component is still considerably bigger the longitudinal component. This is because from these directions the wind acts on a greater exposed area (see Section 6.4) and the wind coefficients have a higher value (see Section 6.4.1).

From the table, it is clear that most critical wind directions that lead to the highest wind forces are 150°N and 180°N. The first direction causes the highest total transverse wind force, while the latter, generates a high longitudinal wind force component in combination with a significant transverse forward force component. Hence, these two load combination of the wind directions are considered for the calculation of the design bollard capacity.

6.5 Load due to passing ships

The passage of ship close to moored vessels involves complex three-dimensional hydrodynamic effects that consequently lead to forces and moments acting on the moored ship that vary in time. To define the loads acting on the design cruise ship due to the passing ships, that need to reach the other pier of the Merwehaven, two approaches are used. First, the loads are established through hand calculation according to Wangs's method. Then, the loads are obtained using the software Ropes. Finally, the results obtained from the adopted methods are compared.

6.5.1 Wangs's method

For the design of the mooring systems, only the peak value of the forces and moments acting on the ship are of interest (Wang, 1975). For this purpose, Wang, proposed non-dimensional graphs, obtained from numerical methods, to estimate the peak surge, sway force and the yaw moment due to the passage of a ship parallel to a moored vessel. These graphs are a function of two ratios. The first ratio is given by the separation distance between the moored and the passing ship, divided by the length of the moored vessel. The second is the ratio between the length of the passing vessel and the length of the moored ship. Therefore, to use these graphs, it is necessary to define the value of these ratios.

Assuming that the passing ship sails in the middle of the channel behind the moored design cruise ship, the first ratio is obtained using the following equations:

$$\eta = \frac{B_{cruise}}{2} + \left(\frac{W_{channel} - B_{cruise} - D_{fender}}{2}\right) = 72.5\ \text{m}$$

$$\frac{\eta}{L_{cruise}} = 0.2$$

Where:

η is the separation distance between the moored design cruise ship and the passing vessel

B_{cruise} is the beam of the design cruise ship (see Section 2.5)

$W_{channel}$ is the minimum width of the passage channel (see Section 2.2.1)

D_{fender} is the diameter of the adopted fender (see Section 2.2.14.3.4)

L_{cruise} is the length between perpendiculars (L_{pp}) of the design cruise ship (see Section 2.5)

The ratio between the length of the design cruise ship and the length of the passing ship is equal to:

$$\frac{L_{ship}}{L_{cruise}} = 0.3$$

Where:

L_{cruise} is the length between perpendiculars (L_{pp}) of the design cruise ship (see Section 2.5)

L_{ship} is the length of the passing vessels (see Section 2.5)

Now that these two ratios are defined, the peak surge, sway force and of the yaw moment, acting on the cruise ship, can be estimated.

Unfortunately, the non-dimensional graphs have a limitation. The peak values are only available till a ratio, between the length of the ships, equal to 0.5. The ratio between the length of the passing vessel and the length of the moored design cruise ship is equal to 0.3. For this reason, to define the peak values for this ratio a graphical interpolation is used as shown below:

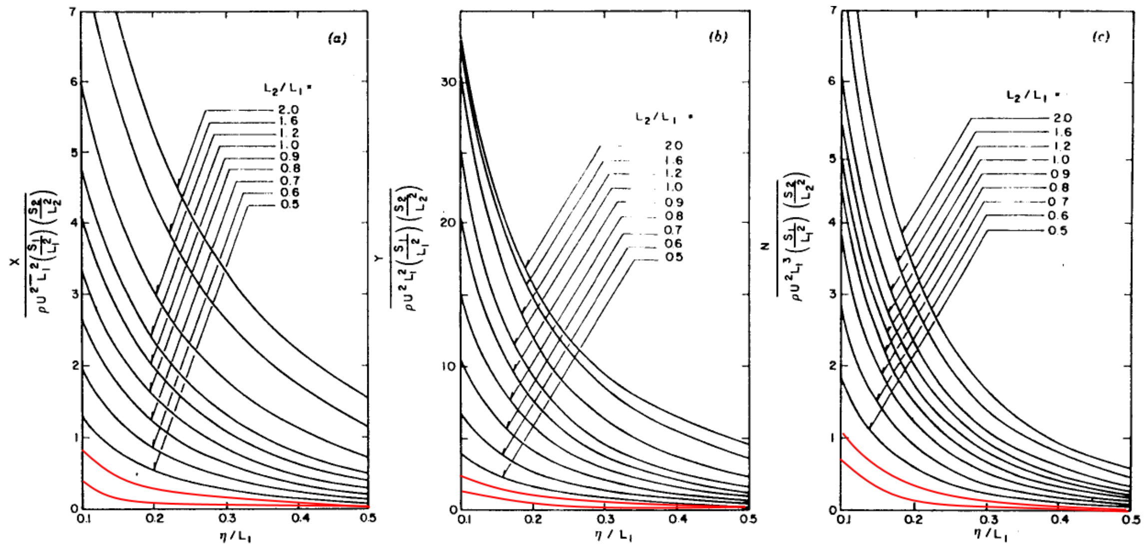

Figure 57: Non-dimensional peak surge, sway force and for the yaw moment on the moored cruise ship as a function of its lateral separation from the passing ship and ships length (Wang, 1975)

The red curves represent the non-dimensional peak surge, sway force and for the yaw moment for ratios between the length of the two ships equal to 0.4 and 0.3. Notice that these curves are based on graphical interpolation and therefore their validation is not verified.

Given the ratio between the separation distance and the length of the moored cruise ship and using the lowest red curve the following values of peak surge, sway force and for the yaw moment acting on the moored cruise ship are obtained:

$$\frac{X}{\rho \cdot U^2 \cdot L_{cruise}^2 \cdot \left(\frac{S_{cruise}}{L_{cruise}^2}\right) \cdot \left(\frac{S_{ship}}{L_{ship}^2}\right)} = 0.1$$

$$\frac{Y}{\rho \cdot U^2 \cdot L_{cruise}^2 \cdot \left(\frac{S_{cruise}}{L_{cruise}^2}\right) \cdot \left(\frac{S_{ship}}{L_{ship}^2}\right)} = 0.5$$

$$\frac{N}{\rho \cdot U^2 \cdot L_{cruise}^3 \cdot \left(\frac{S_{cruise}}{L_{cruise}^2}\right) \cdot \left(\frac{S_{ship}}{L_{ship}^2}\right)} = 0.1$$

Where:

X is the peak surge force due to the effect of the passing ship

Y is the peak sway force due to the effect of the passing ship

N is the is the peak yaw moment due to the effect of the passing ship

ρ is the water density

L_{cruise} is the length between perpendiculars (L_{pp}) of the design cruise ship (see Section 2.5)

L_{ship} is the length of the passing vessels (see Section 2.5)

S_{cruise} is the midship area of the design cruise ship

S_{ship} is the midship area of the passing vessels

Assuming that the passing ship sails with a constant velocity of 1.0 m/s and by substituting the geometric dimensions of the cruise ship and of the passing vessel (see Section 2.5) in the above equations the following values are obtained:

Peak values	
Longitudinal force (surge)	16 kN
Transversal force (sway)	79 kN
Yaw moment	5526 kNm

Table 35: Peak values of surge, sway force and for the yaw moment

However, the above graphs are valid for infinite water depth. To include the effects of water depth, Wang introduces other non-dimensional charts. The charts present the ratios of the peak force and moment to their values in infinite water depth, computed above. The charts that include the effects of water depth for the peak surge, sway force and for the yaw moment are presented below.

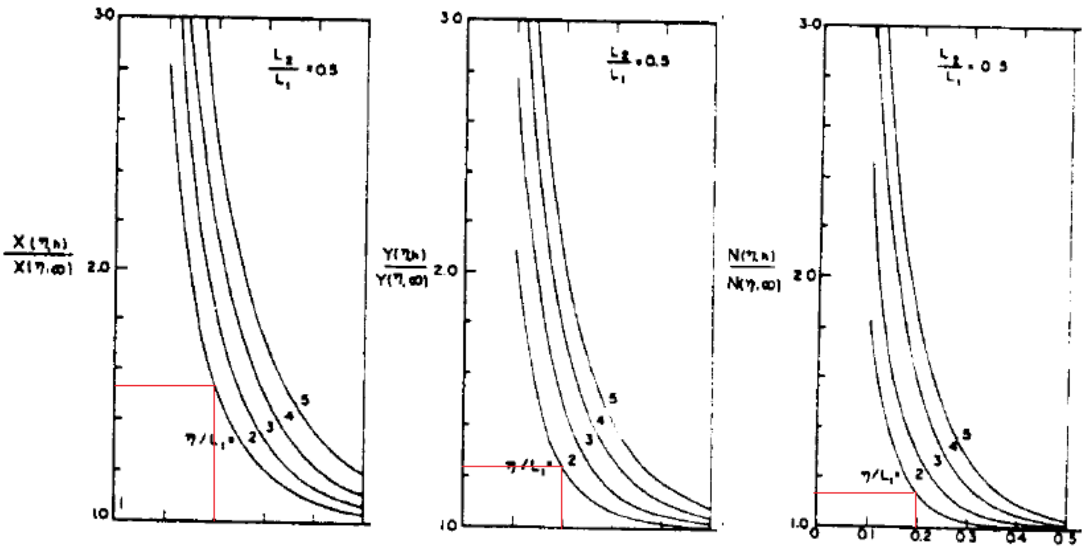

Figure 58: Effects of water depth on the peak surge, sway force and for the yaw moment on the moored cruise ship as a function of its lateral separation from the passing ship and ratio between the length of the ships (Wang, 1975)

Notice that also for these graphs the lowest value of the length ratio is equal to 0.5. Hence, the obtained peak values are again on the conservative side. From the above graphs the following ratios are obtained:

$$\frac{X(\eta,h)}{X(\eta,\infty)} = 1.5$$

$$\frac{Y(\eta,h)}{Y(\eta,\infty)} = 1.2$$

$$\frac{N(\eta,h)}{N(\eta,\infty)} = 1.1$$

Where:

$X(\eta, \infty)$ is the is the peak surge force with infinite water depth

$X(\eta, h)$ is the is the peak surge force with finite water depth

$Y(\eta, \infty)$ is the is the peak sway force with infinite water depth

$Y(\eta, h)$ is the is the peak sway force with finite water depth

N (η,∞) is the is the peak yaw moment with infinite water depth

N (η,h) is the is the peak yaw moment with finite water depth

Substituting the peak values with infinite water depth in the above equation the peak surge, sway force and for the yaw moment with the effect of finite water depth are obtained. These values are presented in the following table:

Peak values	
Longitudinal force (surge)	24 kN
Transversal force (sway)	95 kN
Yaw moment	6079 kNm

Table 36: Peak values of surge, sway force and for the yaw moment with the effect of water depth

Notice that the above results are obtained by graphical interpolation of the non-dimensional peak with infinite depth (see Figure 57) and therefore their validation is not verified. However, they may give insight about the order of magnitude of the peak surge, sway force and for the yaw moment acting on the moored design cruise ship due the passage of vessels.

6.5.2 ROPES

To obtain, a quantitative data for the evaluation of mooring loads acting on moored design cruise ship due to the effect of passing ships the computer program ROPES is used. ROPES is based on three-dimensional flow calculations for real hull forms and the flow calculations are based on the so-called "Double-body flow" method (Pinkster Marine Hydrodynamics, 2011). The software is used to compute the effect of ship-ship interaction forces for a given port geometry and an arbitrary depth.

The program is supplied with four standard ship's hull forms: a tanker, a container vessel, an LNG carrier and a typical inland barge. Hence, to model the design cruise ship a container vessel hull form is selected, with the dimension of the cruise ship. While for the passing vessels an inland barge with the dimension of a CEMT IV is adopted. The quay wall is located at a distance of 5 m from the moored cruise ship due to the presence of the fendering system. The considered water depth is during the Lowest astronomical tide that is equal 12.65 m so that the mooring loads are maximized. The sailing velocity of the passing ship is assumed to be equal to 1.0 m/s. The perpendicular distance between the moored cruise ship and the passing vessels is equal to 72.5 m (see Section 6.5.1). The initial and final longitudinal distance between the two is assumed to be approximately 100 m.

The above mentioned design conditions (input parameters of the software) are described in the figure below. The figure presents the hull of the moored design cruise ship and the hull of the passing vessel.

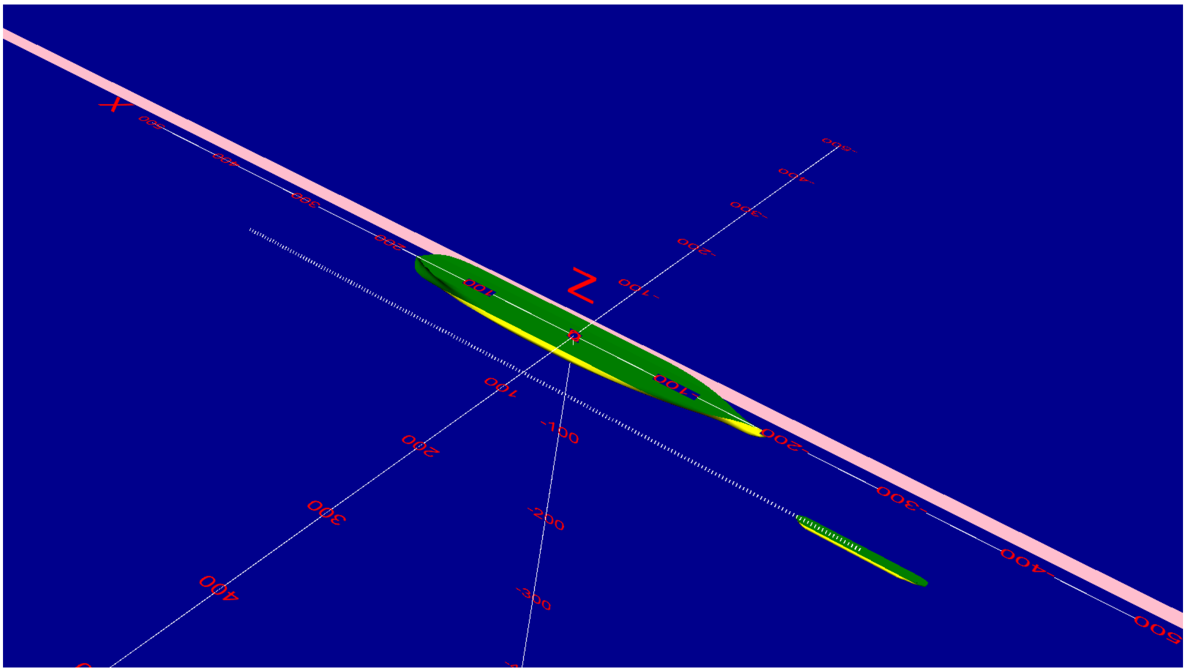

Figure 59: Design cruise ship moored along the quay wall with passing CEMT IV ship (preview from ROPES)

Now that the input parameters are defined the calculation using ROPES are carried out. The forces and moments acting on the design cruise ship are described in the form of time-domain records. The figure below presents the output of the calculation of the surge force acting on the moored design cruise ship in time during the passage of the CEMT IV vessel.

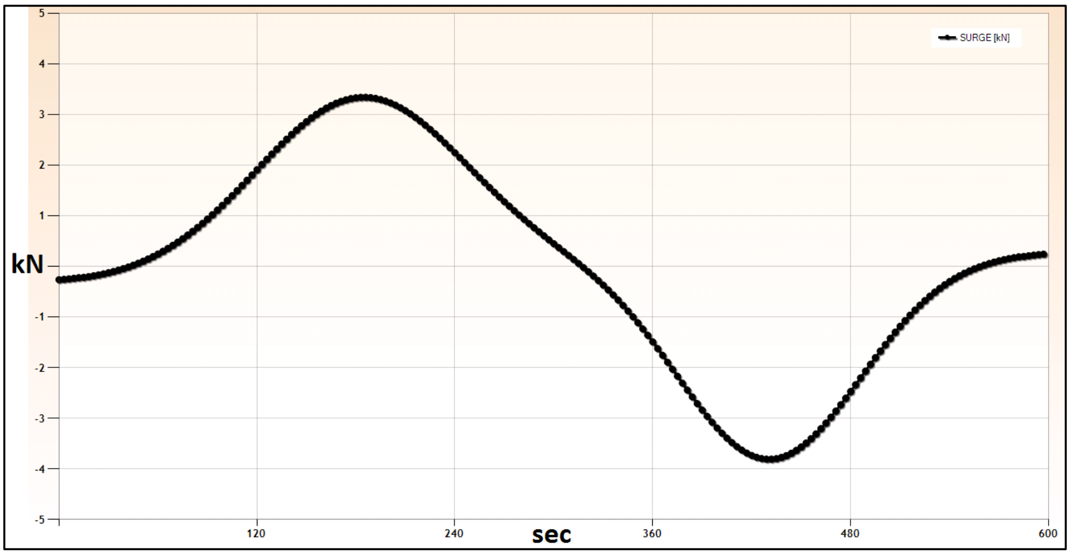

Figure 60: Surge force (kN) acting on the moored design cruise ship in time (sec) during the passage of the CEMT IV vessel with a sailing speed of 1 m/s

From the above figure it is visible that in the initial stages of the passing maneuver, the surge force on the moored cruise ship shows that the vessel is pushed gently away from the overtaking vessel. As the passing vessel comes closer, the positive peak in the surge force is reached equal to approximately 3.5 kN. When the passing vessel is abreast of the moored cruise ship, the surge force passes through zero. As the moving vessel passes closer, the negative peak is reached approximately equal to 4 kN and the moored vessel is pushed back. As the vessel proceeds past the moored ship, the surge force changes sign so that the moored vessel is again sucked into the direction of the passing vessel.

The next figure describes the output of the calculation of the surge force acting on the moored design cruise ship in time during the passage of the CEMT IV vessel.

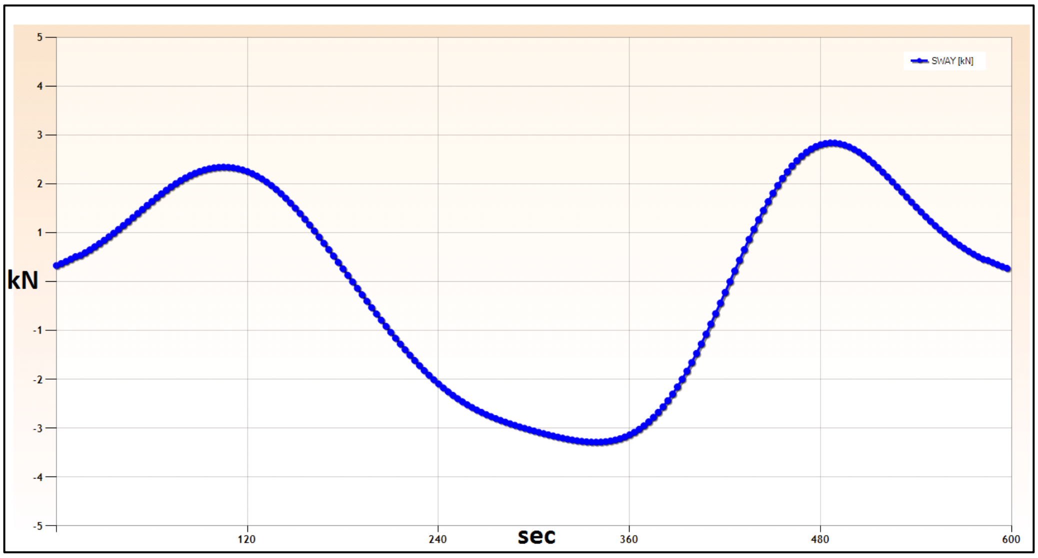

Figure 61: Sway force (kN) acting on the moored design cruise ship in time (sec) during the passage of the CEMT IV vessel with a sailing speed of 1 m/s

As the passing vessel approaches, the sway force on the moored vessel is dominated by a positive peak equal to 2 kN. This means that the moored cruise ship is pushed away from the passing vessel. When the passing vessel is almost abreast of the moored vessel, the sway force reaches its negative peak approximately equal to 3 kN, leading to a suction-type force towards the passing vessel. As the vessel passes the sway force changes sign again, pushing the moored vessel away from the passing vessel.

The last figure presents the output of the calculation of the yaw moment acting on the moored design cruise ship in time during the passage of the CEMT IV vessel.

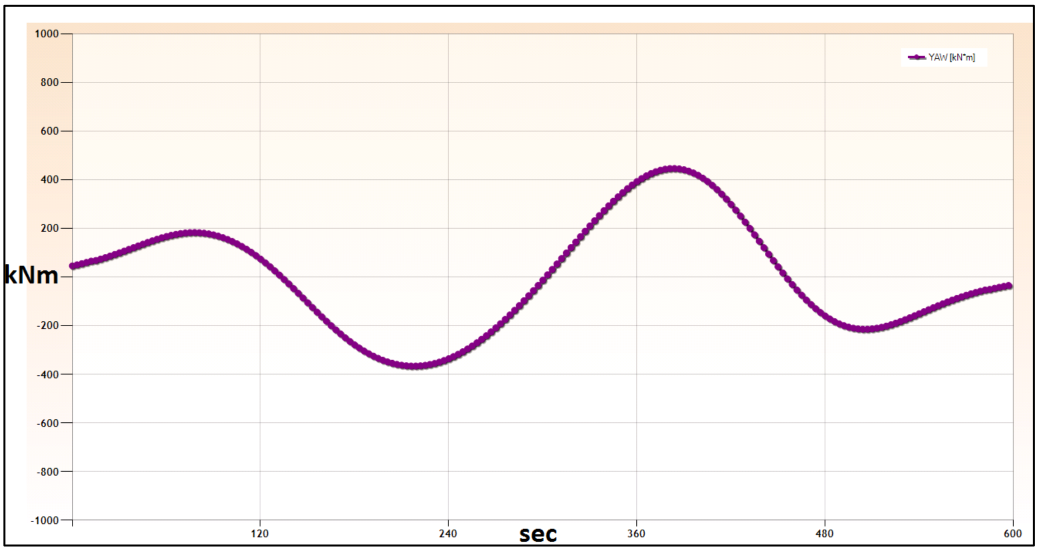

Figure 62: Yaw moment (kNm) acting on the moored design cruise ship in time (sec) during the passage of the CEMT IV vessel with a sailing speed of 1 m/s

The yaw moment is strongly related to the sway force and the moment arm of the sway force as the vessel approaches and passes. In the initial stages, the effective point of application of the sway force is at the forward end of the moored vessel. A positive sway force results in a positive yaw moment and a negative sway force in a negative yaw moment. When the mid-ships of the vessel have passed each other a positive sway force yields a negative yaw moment and a negative sway force a positive yaw moment. The maximum yaw moment is approximately equal to 450 kNm.

To sum up, the results of the computed of the peak surge, sway force and the yaw moment, due to the passage of the vessel parallel to the moored design cruise ship obtained using ROPES are presented in the next table.

Peak values	
Longitudinal force (surge)	4 kN
Transversal force (sway)	3 kN
Yaw moment	450 kNm

Table 37: Peak values of surge, sway force and for the yaw moment acting on the moored cruise ship obtained using ROPES

6.5.3 Results and comparison between the two approaches

Table 36 and Table 37 present the results of the computed of the peak surge, sway force and the yaw moment, obtained with the Wangs's method and ROPES respectively. From the tables, it is clear that the results obtained with the Wangs's method are one order of magnitude higher than the results obtained with ROPES. This may due to the fact that the Wangs's method has some limitation regarding the ratio of the length of the ships. To describe the design scenario, the Wangs's non-dimensional graphs are adapted through graphical interpolation (see Section 6.5.1), that is not validated. Hence, the results obtained with Wangs's method are most likely overestimated. Moreover, the values of the obtained forces due to the passing ship, with both methods, are much lower than the wind forces acting on the cruise ship (see Table 34, Table 36 and Table 37). Therefore, for the calculation of the design bollard capacity, the effect of passing ships is neglected.

6.6 Expected line forces

Now that the loads acting on the design cruise ship are defined, the maximum line force and consequently the required bollard capacity can be obtained. To do so, first, the mooring pattern is described then, based on the mooring pattern the maximum force that the bollards have to withstand is obtained by performing a static mooring analysis using MatrixFrame.

6.6.1 Mooring pattern

The mooring pattern is an essential aspect of an efficient and secure mooring system. It is the arrangement of the mooring lines between the vessel and the berth. The mooring pattern must be able to cope with all the acting forces. To do so, some lines are placed in the longitudinal direction (spring lines) and some lines in the transverse direction (breast lines). A typical mooring pattern is presented below.

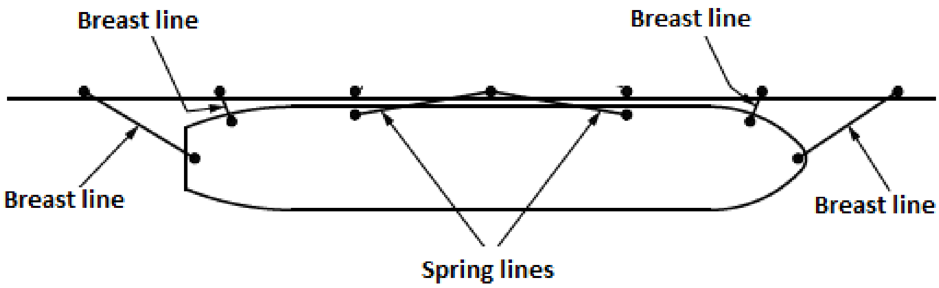

Figure 63: Typical mooring pattern (British standard)

The two types of lines have different functions. The spring lines restrain the vessel in the longitudinal direction (forwards and afterward). While the breast lines restrain the transverse direction, only in the direction off the berth, restraint in on-berth direction is provided by the fendering system. Because the spring lines are placed parallel to the ship, these lines are always less loaded than the breast lines. Indeed a vessel always turns away from the bow or stern (Port of Rotterdam, Bolderbelasting Standardisatie Rotterdam, 2015).

The effectiveness of a mooring line is influenced by the elasticity of the lines and by the vertical and longitudinal angles that the lines form with the deck of the berth structure. The vertical angle is between the line and the quay wall deck and the horizontal angle is between the line and the parallel side of the ship. The larger these angles, the less effective the lines are in resisting the loads. The elasticity depends mainly on the material, length and diameter of the line. For this reason, the following guidelines (Scherpenzeel, 2011) should be followed for the design of mooring systems:

- Mooring lines should be placed as symmetrical as possible respect the midpoint of the vessel.
- Lines with the same function should have the same length.
- The vertical angle should not be larger than 20-30 degrees.
- Spring lines should be oriented as parallel as possible to the longitudinal side of the ship.
- Breast line should be oriented as perpendicular as possible to the longitudinal line of the ship.

Usually, cruise ships are moored with several breast lines tied at three or four different bollards in correspondence of the bow and at the stern and two or four spring lines tied at bollards placed along the ship length. A typical mooring pattern adopted at the current cruise terminal of the port of Rotterdam is presented in the next figure.

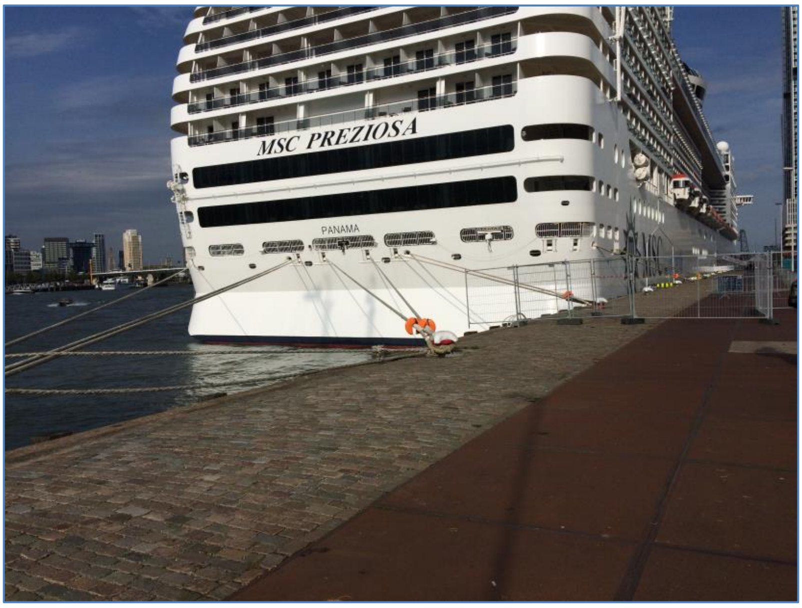

Figure 64: Mooring pattern of the MSC Preziosa at the Holland America cruise terminal (photo 20/09/2017)

The mooring pattern along the quay wall of the portside of Pier 1 for the design cruise ship is assumed to be composed by three breast lines each for the bow and the stern and two springs lines along the side of the cruise ship. The bollards are placed along the quay wall with a center to center distance (c.t.c) of 20 m (see Section 2.2.1).

6.6.2 Static mooring analysis

As it has been already mentioned a vessel that is moored along a berth is characterized mainly by a dynamic behavior. However, to define the maximum force that the bollards of the quay wall have to withstand, a static mooring analysis is performed. The static mooring analysis is carried out using the software MatrixFrame.

As mentioned in Section 6.4.3 two wind loading are considered. These wind loading conditions are presented in the table below.

Loading conditions				
Wind direction	**$F_{Longitudinal}$ (kN)**	**$F_{Transverse\ forward}$ (kN)**	**$F_{Transverse\ aft}$ (kN)**	**$F_{Transverse\ total}$ (kN)**
150°N	99.8	3032	2274	5307
180°N	173	2466	1432	3898

Table 38: Loading conditions for the bollard capacity calculation

For the static mooring analysis, the design cruise ship is schematized as a rigid body using truss structure, the lines are schematized as beams that can be stressed only by tension stresses and the bollards are simplified as spring supports. Along the quay wall, the bollards are placed at a distance c.t.c of 20 m. Although, usually two lines are tied at one bollard and the lines start from different winches placed at different location of the vessel (see Appendix G), to schematize the mooring pattern the breast lines are assumed to be tied at the middle of the bow and stern of the cruise ship while the spring lines are tied at the corners close to the quay wall. The schematization used for the static mooring analysis carried out in MatrixFrame is presented below.

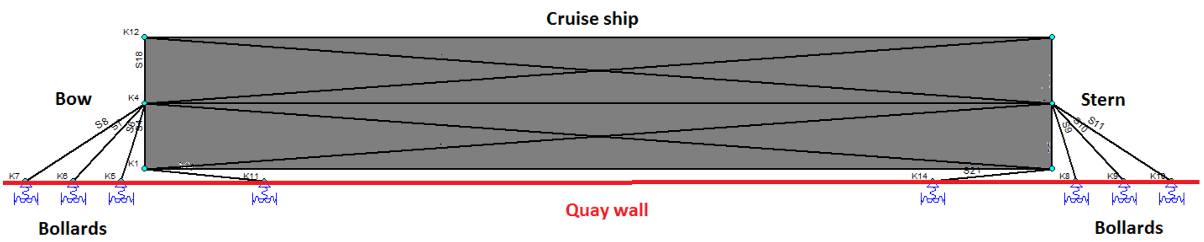

Figure 65: Schematization for the static mooring analysis (MatrixFrame)

Due to the orientation of the moored cruise ship (see Section 6.4.3), the transverse forward force and the longitudinal force components are applied at the bow, while the transverse aft force is applied at the stern of the design cruise ship. The considered wind loading conditions are described in Appendix I.

The unbalance between the forward and transverse aft forces, for both loading conditions (see Table 38), provides the rotation (yaw) of the cruise ship, that tries to turn away around the stern. However, in the schematization, due to this rotation, the spring line tied at the stern of the vessel experiences compression stresses (see Appendix I) that in reality is not possible. Therefore, the schematization is modified and the spring line tied at the corner at the stern is removed as shown in the figure below.

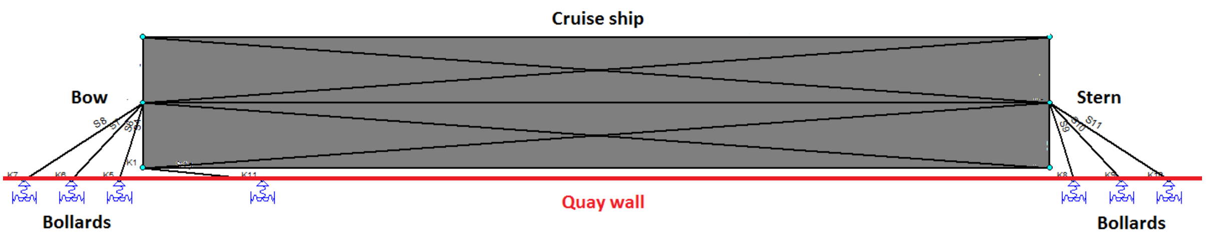

Figure 66: Modified schematization for the static mooring analysis without spring line at the stern (MatrixFrame)

The results of the of the static mooring analysis calculation for the two loading conditions are presented in the following table:

Results of the of the static mooring analysis			
Loading condition wind direction	**Line**	**Length of the line (m)**	**Maximum tension stress (kN)**
150°N	Bow breast	34	1666
	Bow breast	44	1235
	Bow breast	60	881
	Stern breast	34	1218
	Stern breast	44	979
	Stern breast	60	758
	Bow spring	50	310
180°N	Bow breast	34	1377
	Bow breast	44	981
	Bow breast	60	671
	Stern breast	34	733
	Stern breast	44	639
	Stern breast	59	529
	Bow spring	50	369

Table 39: Results of the static mooring analysis for the two loading conditions (MatrixFrame)

From the results of the static analysis, it can be concluded that the loading condition characterized by the wind direction 150°N leads to a maximum lines load equal to 1666 kN. This means that the breast lines exert a force on the bollards that is higher than the current bollard capacity (750 kN). The spring lines on the other hand, because they are placed parallel to the cruise ship are subjected by a much lower force. Therefore, storm bollards with a capacity of at least 1700 kN should be placed in correspondence of the bow and stern of the ship to ensure the design cruise ship along the berth.

Notice that in the static analysis the effect of the elasticity of the lines in not considered. The elasticity of a mooring line is a measure of its ability to stretch under a certain load (OCIMF, 2008). Elasticity plays an important role in the absorption of the dynamics loads.

6.7 Conclusions

According to the different guidelines, the required bollard capacity that the quay wall of the cruise terminal should provide, to withstand the mooring forces acting on the design cruise ship, varies between 1100 kN and 1500 kN. According to the guideline of the Port of Rotterdam Authority, the bollards of the cruise terminal should have a capacity of 2340 kN (see Section 6.2). Because of the significative difference between these values, a mooring analysis is performed to define and to optimize the design of the bollard capacity of the future cruise terminal.

Based on the calculation of the forces, with a return period of 50 years, acting on the moored design cruise ship and the results of the static mooring analysis presented in this chapter, it is concluded that the required bollard capacity of the cruise terminal is equal to 1700 kN. Hence, the quay wall has to withstand a much higher bollard force.

In more detail, from the calculation of the mooring forces (see Section 6.4 and 6.5) and static mooring analysis (see Section 6.6) it turns out that:

- The wind load has the most crucial role in the design of the bollard capacity of the new cruise terminal.
- The wind directions that lead to the highest loading on the lines of the cruise ship and hence on the bollards of the cruise terminal are 150°N and 180°N.
- The effect of passing ships, behind the moored cruise ship is much lower than the wind loading and therefore is negligible.
- The current bollards located on top the quay wall are not able to withstand the mooring forces consequently it is advised to place storm bollards with a capacity of 1700 kN in correspondence of the bow and stern of the cruise ship.

7. In depth design of the best design variant

7.1 Introduction

Now that the best design variant is selected and that the required bollard capacity is defined, the design variant with the underwater sheet pile is elaborated in detail. The in depth design mainly focusses on the geotechnical aspects of the design variant. In more detail, a deformation and a stability analysis are carried out to argue that the design variant with the underwater sheet pile wall can adapt the existing caissons to future cruise terminal of the port of Rotterdam. These analyzes are performed through the modeling of the design variant with the software PLAXIS 2D. A short description regarding the software and the related background information are presented in Section 7.2. A geotechnical assessment is performed using PLAXIS 2D and is discussed in Section 7.3. The design variant with the underwater sheet pile wall is elaborated and analyzed in detail in Section 7.4. The conclusions of this chapter are given in Section 7.5.

7.2 PLAXIS 2D

PLAXIS 2D is a two-dimensional finite element program used to perform deformation, stability and flow analysis for various types of geotechnical applications (PLAXIS 2D, Reference Manual, 2017). This program can model the mechanical behavior of soils at various degree of accuracy. The mechanical behavior of soils depends on the stress-strain relationship that is called constitutive model or material model. Hence, the models form the theoretical framework and the qualitative mechanical behavior of the soils (Brinkgreve, Lecture notes CIE4361 Behavior of Soils and Roks). In literature, to represent the stress-strain behavior of soils and rocks, different constitutive models are available. The different constitutive models involve different input parameters to quantify the soil behavior. The main aspects and characteristics of these models are explained in this section.

7.2.1 Constitutive models

In PLAXIS 2D different constitutive models are available. This section presents the main aspects of the various models and the input parameters that are relevant for the scope of analysis.

Linear Elastic model

The Linear Elastic model is based on Hooke's law of isotropic elasticity (PLAXIS 2D, Material Models, 2017). The theory of Elasticity deals with reversible deformations. This means that when defined stress is applied, a strain increment will occur, and when the stress increment is removed, the strain increment will disappear. As long as it follows this definition, elasticity may even involve a non-linear stress-strain relationship.

The figure below presents the linear-elastic stress-strain behavior, that is related by a straight line (see left Figure 67) and the non-linear elastic behavior, that is characterized by a curved the stress and strain relationship (see right Figure 67).

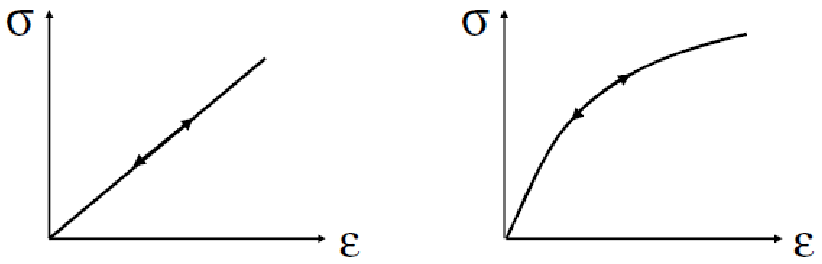

Figure 67: The linear-elastic (left) and non-linear (right) stress-strain behavior (lecture notes CIE4361)

This model only involves two elastic parameters: Young's modulus (E) and Poisson's ratio (v). The Linear Elastic model may be used to model stiff volumes in the soil like concrete elements (PLAXIS 2D, Material Models, 2017).

Mohr-Coulomb model

The linear elastic perfectly-plastic Mohr-Coulomb model is based on the theory of Plasticity that deals with irreversible or plastic deformations. This means that after elastic loading, the behavior becomes perfectly plastic, but during unloading and reloading, the behavior becomes elastic again, leaving some residual strain. Consequently, in this model, the stress increment is not only a function of the strain increment but also of the stress level itself. The theoretical formulation of a plasticity model involves a yield function and plastic potential. The following diagram shows the linear elastic perfectly plastic stress-strain behavior.

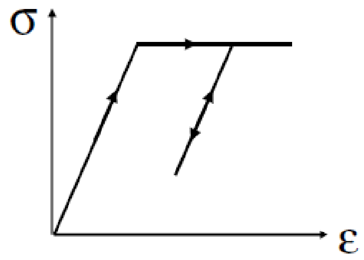

Figure 68: The linear elastic perfectly plastic stress-strain behavior (lecture notes CIE4361)

This model involves five parameters:

- Two elastic parameters; Young's modulus (E) and Poisson's ratio (*v*)
- Three plastic and strength paraments; cohesion (c), friction angle (φ), dilatancy angle (ψ)

The Mohr-Coulomb model may be used for a first analysis of the problem because the parameter values are not unique for a particular type of soil or soil layer (lecture notes CIE4361). In reality, soil stiffness is not a constant, but it depends on the stress level, the stress path and the strain level. This means that the stiffness generally increases with depth. Therefore, the parameters have to be considered by taking into consideration the applicable stress and strain conditions. (PLAXIS 2D, Reference Manual, 2017)

Hardening Soil model

The Hardening Soil model is also based on the theory of Plasticity. However, this model differs from the Mohr-Coulomb because the stress increment also depends on a hardening parameter. This means that the Hardening Soil model also accounts for stress-dependency and thus the stiffness increases with pressure (PLAXIS 2D, Material Models, 2017). In case of elastoplastic strain-hardening, the non-linearity comes from an increase of plastic strain. During unloading and reloading, the behavior is stiffer and may involve hysteresis as shown in the figure below.

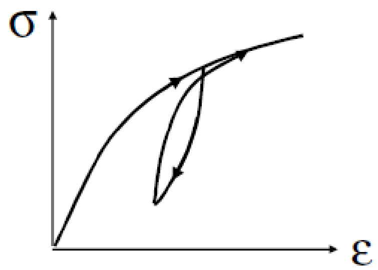

Figure 69: The elastoplastic strain-hardening stress-strain behavior (lecture notes CIE4361)

This model involves several input parameters:

- Four stiffness parameters; the triaxial loading stiffness (E_{50}), the triaxial unloading stiffness (E_{ur}), the oedometer loading stiffness (E_{oed}) and the rate of stress-dependency (m)
- One elastic parameter; the Poisson's ratio (*v*)
- Three strength paraments; cohesion (c), friction angle (φ), dilatancy angle (ψ)

The Hardening Soil model requires many input parameters that are mainly obtained by triaxial tests and therefore it is more advanced and accurate model for the simulation of soil behavior.

7.2.2 Parameter determination

The determination of parameters should preferably be based on a geotechnical site investigation (SI) report. This report usually contains soil data from field tests and good quality lab tests with similar stress level, stress path and strain level as in the practical application (lecture notes CIE4361). The data may be obtained by performing the following activities:

- Borehole data, providing an overview of the different soil layers with depth
- Field test data, such as direct measurements from cone penetration tests (CPT), standard penetration tests (SPT)
- Laboratory test data, such as results from compression tests, triaxial tests, shear tests or other lab test results.

The input parameters are estimated by interpretation of the data and properties of the soil layers. Table 40 and Table 41 present an overview of the input parameter, which can be obtained from different field and laboratory test.

Test	Measured quantities	Correlates to
CPT(u)	q_c , f_s , R_f , p_w	S_u , E_{50} , D_r , φ , k
SPT	N , N_{60}	S_u , E_{50}
PMT	(p,ε) for different depths	S_u, G_{50} , G_{ur} , OCR , K_0
DMT	p , I_D , S_u , K_D , E_D	γ , OCR , K_0 , D_r , E_{oed}
VST	M	S_u
Seismic	v_s , v_p	G_0 , $E_{oed,0}$

Table 40: Overview of the input parameters that can be obtained from the different filed test (lecture notes CIE4361)

Test	Measured quantities	Correlates to
Index tests	LL , PL , I_p , e_0 , D_r , d_{50}	S_u , φ', E_{oed} , k
Compression (Oedometer, CRS)	(σ_1, ε_1(t)) , (σ_1, e(t)) , p_c	C_c ,C_s ,C_α ,m_v ,c_v ,$E_{oed}(\sigma)$, $E_{oed,ur}$ m ,OCR , K_0 , k
Triaxial (CID,CIU, UU)	($\lvert\sigma_1$-$\sigma_3\rvert$, ε_1) , (ε_v, ε_1) or (p_w, ε_1)	S_u , c', φ', ψ, E_{50}, E_{ur} , ν, m
DSS	τ, γ	S_u , c', φ', ψ, G_{50} ,G_0
Bender elem., Resonant col.	V_s , v_p , G(γ)	G_0 , $E_{oed,0}$, $\gamma_{0.7}$

Table 41: Overview of the input parameters that can be obtained from the different laboratory test (lecture notes CIE4361)

In case of not sufficient geotechnical site investigation reports, the input parameters can be estimated using empirical formulations present in literature.

7.3 Geotechnical assessment

Before performing the analysis of the design variant with the underwater sheet pile wall a geotechnical assessment is performed using PLAXIS 2D. This assessment has two objectives. The first objective is to prove that before placing the caissons, the soft soil package was removed entirely and thus, that a ground improvement was performed. The second objective is to define the effect of the loads acting on the caisson and to get a better estimate of the geotechnical parameters. This is done through a sensitivity analysis based on the occurred settlement of the caisson in the current situation.

Caissons are built on dense granular soils so that they undergo most of the expected settlement by the time its positioning and backfilling are completed. Doing so, the long-term settlement is negligible, because settlement immediate due to the rapid dissipation of pore pressures (de Gijt, 2004). However, in case that a soft soil layer, under the structure, is present this is not valid because the excess pore pressure in the soft soil layer generated due to the positioning of the caisson dissipates very slowly. For this reason, in case that a soft soil layer is present, both the immediate and long-term settlement analysis are required.

For caissons, a certain amount of settlement is expected. The geotechnical assessment analyses whether the immediate, long-term, and differential displacements are within tolerable limits for the overall satisfactory performance of the structure. Two different scenarios are considered. In the first scenario, the soft soil package is still present under the caisson (see left Figure 70). In the second is scenario the soft soil layer is completely removed and replaced by sand foundation layer (see right Figure 70).

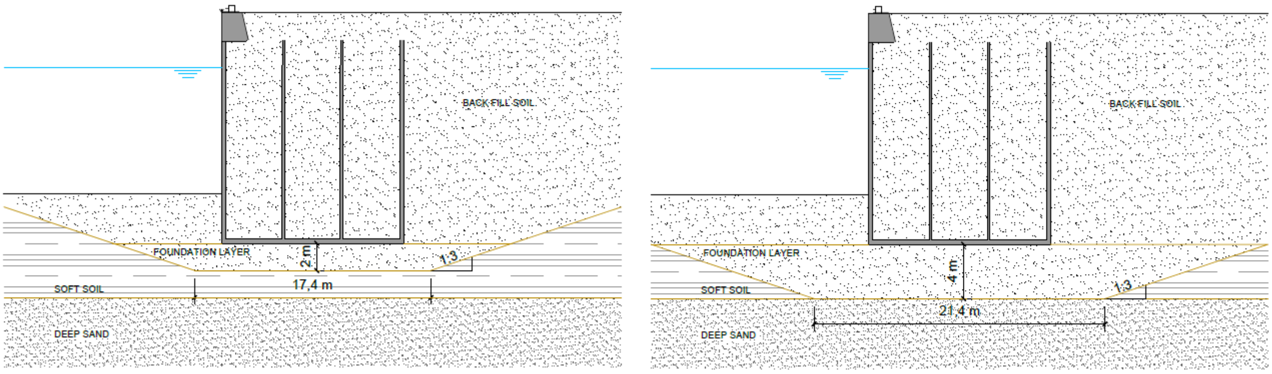

Figure 70: Scenario with the soft soil package still present under the caisson (left) scenario without the soft soil package under the caisson (right)

The assessment first computes the immediate settlement (short-term) that occur during the construction of the caisson. The long-term settlement analysis is carried out whether the immediate settlements are within the tolerable limits. The tolerable limits are established according to the following table.

	Mode of Displacement (cm)					
	Uniform Settlement (cm)		Tilt (radian)		Horizontal (cm)	
Type of Wall	Gurevich	Brum et. al.	Gurevich	Brum et. al.	Gurevich	Brum et. al.
Blockwork	-	10 15	-	0,01	-	-
Floating-in caisson	12 - 15	15 - 20	0,005 - 0,008	0,015	5 - 8	-
L-shaped with internal anchorage	10 - 12	-	0,005 - 0,008	-	4 - 6	-
L-shaped with external anchorage	10 - 12	-	0,005	-	4 - 6	-

Table 42: Allowable displacements for gravity quay walls (de Gijt, 2004)

The rotational stability is the most critical failure mechanism according to the performed stability checks of the caisson (see Section 3.4.4). Therefore, using the tilt angle given in Table 42 and by considering the retaining height of the structure (see Section 2.2.1) the maximum allowable rotational displacement of the top caisson is obtained and is approximately equal to 10 cm.

7.3.1 Adopted constitutive models and input parameters

To perform the geotechnical assessment of the different scenarios first the constitutive models and the required input parameters have to be defined. Moreover, also some simplifications have to be made. This section presents the assumptions, the constitutive models and the input parameters selected for the different soil layer and materials.

As it already been mentioned, the determination of the input parameters should preferably be based on a geotechnical site investigation report (see Section 7.2.2). Unfortunately, only one CPT test carried out behind the caissons is available. In this CPT, only the test cone resistance (q_c) is measured (see Appendix A). According to Table 40, only one stiffness parameter (E_{50}) of the soil layer can be estimated from a CPT test. For this reason, the soil layers are assumed to behave according to the Mohr-Coulomb model, because this model requires only one stiffness input parameter (see Section 7.2.1).

The input parameters of the soil layers are estimated based on the measured cone resistance of the CPT according to the Manual Hydraulic Structures and CUR2003-7. The equations and the calculation performed for the estimation of the parameters are presented in Appendix J. The input parameters for the different soil layers are given in the table below together with the constitutive models and the cone resistance.

Soil	Constitutive model	Cone resistance	Unit weight dry-saturated	Young Modulus	Poisson ratio	Friction angle	Dilatancy angle	Cohesion
Backfill sand	Mohr Coulomb	10 MPa	18-20 kN/m^3	25 MPa	0.3	30°	0°	-
Soft material	Mohr Coulomb	0.7 MPa	18 kN/m^3	3.5 MPa	0.33	22.5°	0°	5 kN/m^2
Deep sand	Mohr Coulomb	20 MPa	21 kN/m^3	42 MPa	0.3	32°	2°	-

Table 43: Constitutive models, cone resistance and input parameters for the different soil layers

For the computations, a cross-section in the middle of a caisson (length direction) is considered. The caisson is schematized as a rectangular box with its dimensions. The influence of the headwalls, toe and heels of the caisson are neglected (see Section 3.4.4). The unit weight of the caisson is an average value between the concrete structure part and the backfill part (see Appendix D). To ensure that the caisson behaves as a rigid body and avoid its deformation a high stiffness is assumed (see Table 44). Moreover, it is schematized that the bollards are placed in a concrete element. The concrete element is assumed to be fixed to the top part of the caisson. The caisson and the concrete element are described according to the Linear Elastic model (see Section 7.2.1). The required input parameters and the constitutive models of these materials are presented in the following table.

Material	Constitutive model	Unit weight	Young Modulus	Poisson ratio
Concrete	Linear elastic	25 kN/m^3	35000 MPa	0.2
Caisson	Linear elastic	20.3 kN/m^3	30000 MPa	0.2

Table 44: Constitutive models and input parameters for the different materials

7.3.2 Short-term settlement of the caisson with the soft soil layer

Now that the constitutive models and the input parameters of the different soils are defined the geotechnical assessment is carried out. The first considered scenario concerns the short-term settlement during the positioning of the caisson and the backfilling with the soft soil layer still present under the structure.

The foundation sand layer between the caisson and the soft soil layer is assumed to be 2 m thick, 17.4 m wide and placed on a slope of 1:3 (see left Figure 70) and assumed to have the same mechanical properties of the backfill soil. The water level is taken equal to NAP level. It is essential to specify that the soft soil has an undrained behavior because in a short-term analysis the excess of water pressure has no time to dissipate (see Section 7.4). Notice that in this scenario the quay wall surcharge, bollards force and water head difference over the caisson are not applied yet.

The output of the total deformations computed with PLAXIS for this scenario is presented in the figure below. The total deformations are given by the sum of the vertical and horizontal deformation components.

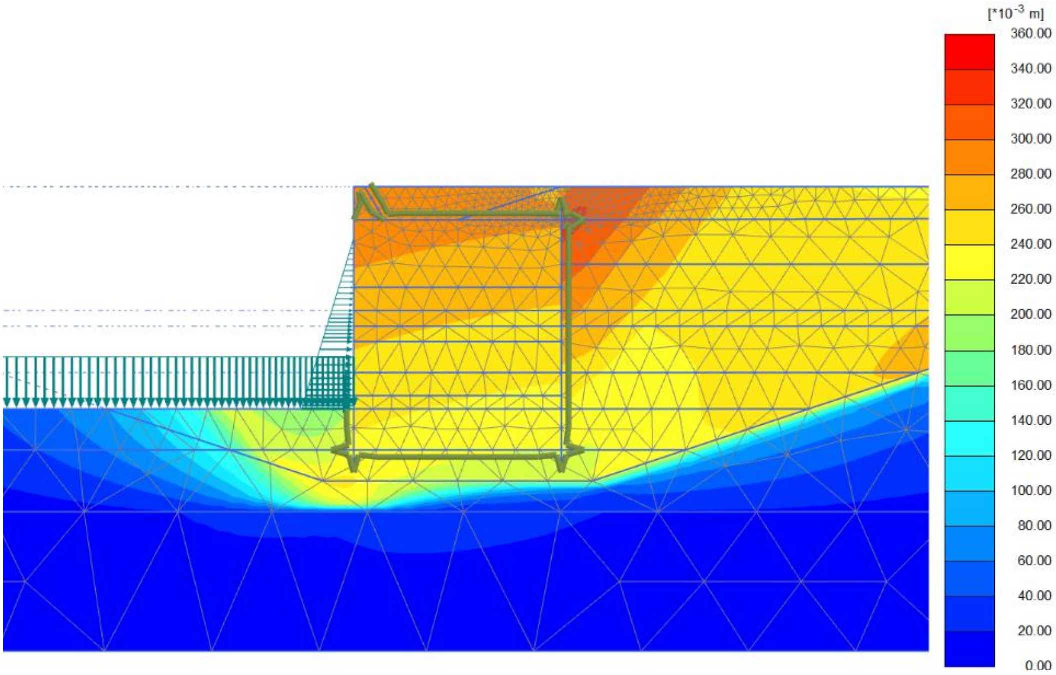

Figure 71: Short-term's total displacements of the caisson with the soft soil layer still present (PLAXIS)

From the figure, it is clear that the settlement under the toe of the caisson is more significant than the overall settlement of the foundation and thus the total displacement of the top of the quay wall is considerable bigger (approximately 35 cm see Figure 71) than the maximum allowed rotational displacement (approximately 10 cm). Besides, it can be noticed that the entire structure slides over the soft soil layer soil towards the water side. This sliding could lead to a high possibility of instability during construction.

From these results, it can be concluded that the soft soil layer was entirely removed before placing the caissons and consequently a long-term settlement analysis for this scenario is not necessary.

7.3.3 Short-term settlement of the caisson without the soft soil layer

The second considered scenario concerns the caisson with the soft soil layer under the structure entirely removed and replaced by a sand foundation layer. The only difference from the previous scenario is that the foundation layer starts immediately above the deep sand level. Consequently, the foundation layer is 4 m thick, 21.4 m wide and is placed on a slope of 1:3 (see right Figure 70). All the other variables are the same. Figure 72 presents the total deformations for this scenario obtained with PLAXIS.

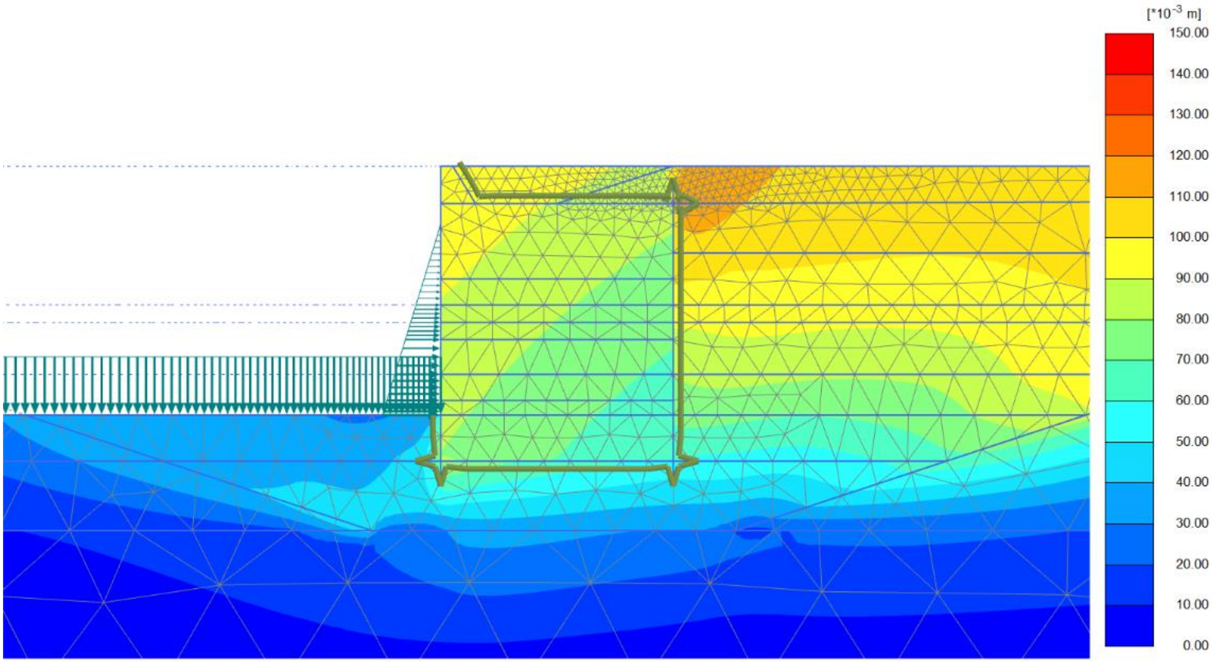

Figure 72: Short-term's total displacements of the caisson without the soft soil layer (PLAXIS)

As it can be noticed, due to the replacement of the soft soil layer with the foundation layer the total displacements of the caisson are considerably reduced. In addition, the settlement of the foundation is more uniform leading to a limited total displacement of the top of the quay wall of approximately 10 cm (see Figure 72). Hence, the displacement of the top of the quay wall is the is within the maximum allowed.

However, in this scenario, the quay wall surcharge, bollards force and water head difference over the caisson are not considered. The application of the loads leads to an increase of the total deformation and consequently an increase in the displacement of the top of the quay wall that may compromise the performance of the structure.

7.3.4 Long-term settlement of the caisson without the soft soil layer

As mentioned above, the application of the loads acting on the caisson leads to an increase of the displacement of the top of the quay wall that may compromise the performance of the structure. Therefore, a long-term settlement analysis for this scenario is required. A long-term settlement analysis implies that all the acting loads are applied and that the excess pore pressure is entirely dissipated (see Section 7.3). Hence, the analysis concerns the expected settlement of the caisson in the current situation (see Section 3.4.4).

However, before performing the long-term analysis, the effect of the individual loads on the total displacement is defined. The loads acting on the caisson are the quay wall surcharge, the bollard force and the water head difference over the caisson as shown in the figure below.

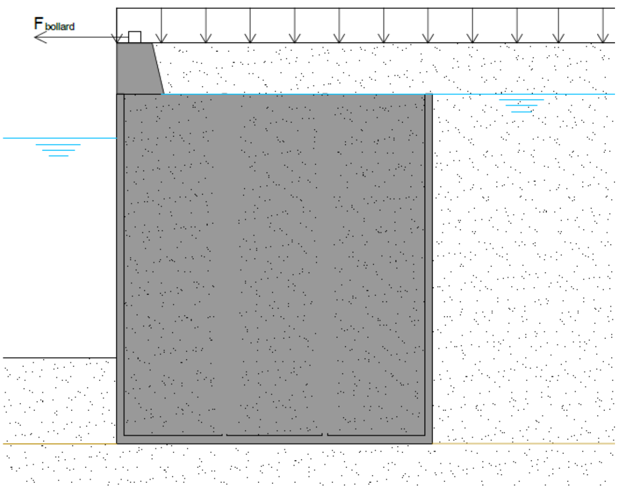

Figure 73: Loads acting on the caisson used as a quay wall

The effect of the individual loads on the total displacement is obtained by applying one load at a time to the previous scenario (see Section 7.3.3) and by calculating the total displacement of the top of the quay wall. The effect of each load is estimated depending on how the value of the total displacement increases. The results of these calculations for different load values are summarized in the table below.

Effect of the loads on the total caisson displacements			
Load	**Value**	**Displacement top of the quay wall (cm)**	**Displacement increase (%)**
Caisson without soft soil layer	-	10	-
Quay wall surcharge	20 kN/m	11.7	17
	30 kN/m	12.8	28
	40 kN/m	13.9	39
Bollard force	20 kN/m	10.5	5
	33.3 kN/m	10.9	9
	45 kN/m	12	12
Water head difference	0.5 m	11.1	11
	1.2 m	12.5	25
	1.9 m	14.6	46

Table 45: Effect of the different acting loads on the total caisson displacements

From the above results, it is clear that the water head difference is the load that has the most impact on the total displacement of the caisson. This result is in line with the results of the sensitivity analysis of the stability check (see Section 3.4.5). However, in this analysis, the quay wall surcharge has a more considerable effect on the total displacement than its effect in the stability checks (see Section 3.4.5).

Moreover, from these results, it can be concluded that due to the application of the loads the caisson exceeds the maximum allowable displacement. This proves that the long-term settlement analysis is strictly necessary.

The long-term analysis computes the total displacement of the caisson in the current situation. The load configuration is the same as in Section 3.4.4. The only difference is the design value of the water head difference over the caisson. The design value of the water head difference is taken according to the Quay Wall Second edition, 2014 (see Section 2.5). The output of the effective principal stresses and the total deformations of the caisson in the current scenario computed with PLAXIS are presented in the following figures.

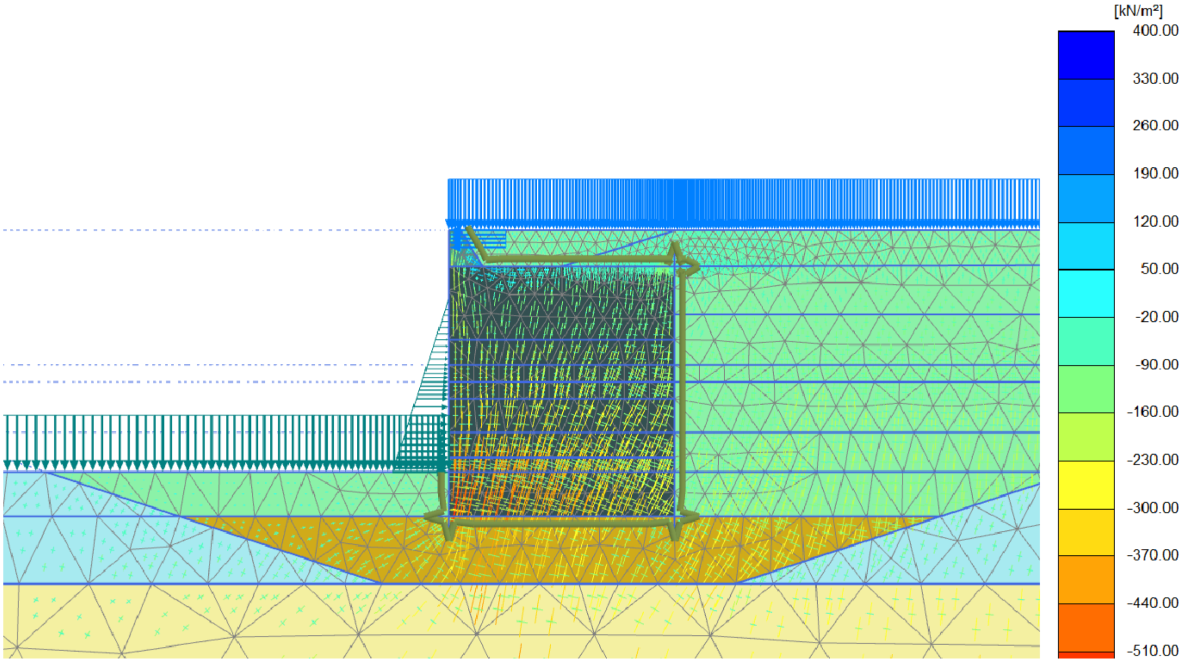

Figure 74: Long-term's principal effective stresses of the caisson in the current situation (PLAXIS)

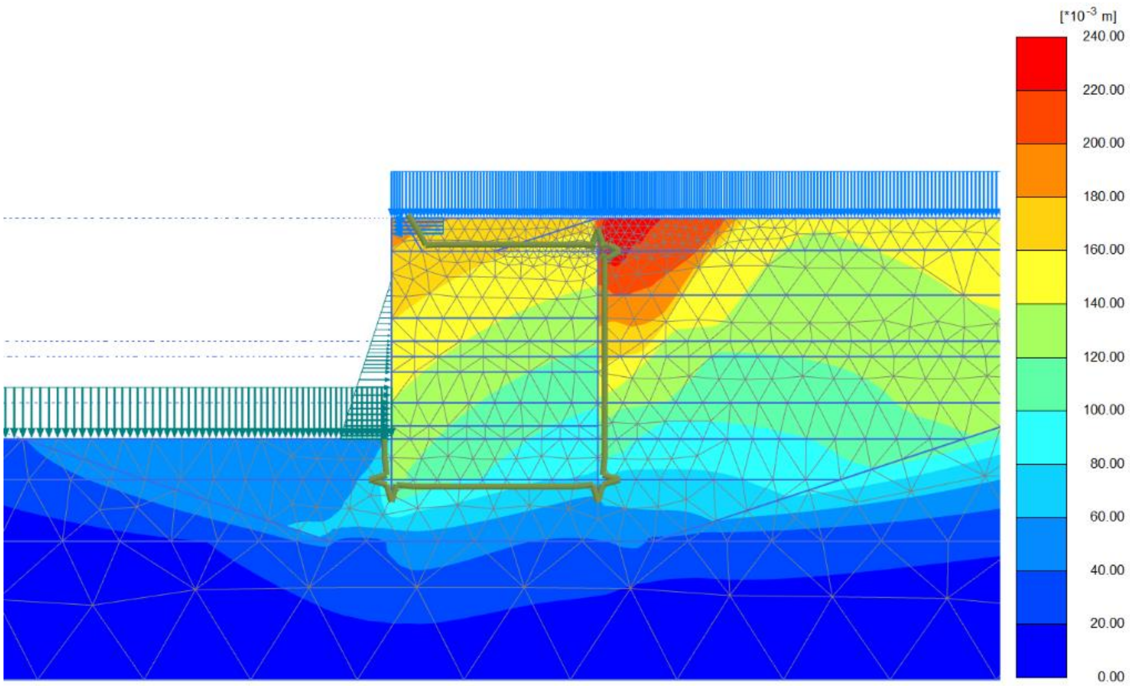

Figure 75: Long-term's total displacements of the caisson in the current situation (PLAXIS)

From Figure 74 it is clear that the highest principal effective stresses occur near the toe of the caisson. The maximum and minimum soil compression stresses at the foundation level of the caissons are -403 kN/m^2 and -9.7 kN/m^2 respectively (see also Appendix K). Notice that PLAXIS presents the compressions stresses with a negative sign. The maximum compression stress is in the same order of magnitude of the maximum soil pressures ($\sigma_{k,max}$) computed in the stability checks (see Section 3.4.4). The difference between the two results (approximately 60 kN/m^2) may differ due to the different value in the water head difference over the caisson.

From the Figure 75, it can be concluded that due to the application of the different loads the total deformation increases considerably. The most significant deformation occurs immediately behind the caisson where the active sliding surface develops. The active sliding surface is clearly visible in Figure 75. The total displacement of the top of the quay wall is approximately equal to 20 cm (see Figure 75). Hence, as expected, the caisson in the current situation exceeds the maximum allowable rotational displacement (approximately 10 cm).

Although the magnitude of displacement could have compromised the performance and the stability of the caissons, the quay walls of the Merwehaven are still in use. Moreover, no reports regarding stability problems or required intervention or displacement measurements have been found.

From these argumentations, it is possible to argue that the model seems to overestimate the total displacement of the caisson in the current situation. This may occur due to the conservative assumptions in the geotechnical input parameters (see Appendix J) and due to the limited features of the soil behavior in the Mohr-Coulomb model (see Section 7.2.1).

7.3.5 Sensitivity analysis

A better estimation of the geotechnical input parameters is required to reduce the computed deformation of the caisson in the current situation and consequently avoid the overestimation of the total deformation also in the design variant with the underwater sheet pile wall. The better estimation of the geotechnical input parameters is obtained through a sensitivity analysis.

The analysis is carried out by changing the value of the geotechnical variables (see Table 43) one at a time of the caisson in the current situation (see Section 7.3.4) and by calculating by calculating the total deformation. Depending on how the total displacement of the top of the quay wall changes with respect to the previous value the impact of each input parameter is established. The values of the geotechnical input parameters used in the analysis are chosen based on a literature study. The most significative results of the sensitivity analysis are summarized in the next table. The full results of the sensitivity analysis for each geotechnical parameter are described in Appendix K.

Geotechnical input parameter	Value	Displacement top of the quay wall (cm)	Variation in the Displacement (%)
Caisson in the current situation	-	19	-
Friction angle of the backfill soil	27°	22	+15.8
	33°	15	-21.1
Friction angle of the foundation soil	27°	21	+10.5
	33°	16	-15.8
Young's modulus of the foundation soil	32.5 MPa	16	-15.8
	40 MPa	15	-21.1
Young's modulus of the soft soil layer	2 MPa	20	+5.3
	5 MPa	18	-5.3

Table 46: Results of the sensitivity analysis of the geotechnical input parameters

From the results of the sensitivity analysis it can be concluded that the geotechnical input parameters that have the most impact on the total deformation of the quay wall are the friction angle of the backfill soil and of the foundation soil and the Young's modulus of the foundation soil. In more detail, the friction angle of the backfill has a significative impact on the order of magnitude of the horizontal soil pressure acting on the caisson. While Young's modulus and friction angle of the foundation soil, influence the displacement of the quay wall. Because these parameters determine the strength and consequently the deformation of the foundation soil. Moreover, it can be noticed that the geotechnical properties of soft soil layer, however it is limited, has still an effect on the results of the total deformation. This means that also the dimensions of the foundation layer have an impact on the settlement of the caisson.

7.3.6 Long-term settlement with improved geotechnical parameters

Based on the results of the sensitivity analysis it is possible to conclude that to reduce the total settlement of the caisson in the current situation, the foundation layer is composed by dense granular soils with higher mechanical properties than the backfill soil. This layer also increases the sliding resistance of the caissons (see Section 3.4.5). To meet the maximum allowable displacement of the caisson the following geotechnical input parameters are selected.

Soil	Young's modulus	Friction angle	Dilatancy angle
Backfill	30 MPa	31.5°	1.5°
Foundation layer	40 MPa	32°	2°
Deep sand	50 MPa	34°	4°

Table 47: Improved geotechnical input parameters

The values of the improved geotechnical input parameters of the backfill soil and deep sand are in line with the values computed according to the Manual of Hydraulic Structures (see Appendix J). While the foundation soil is assumed to be composed by sand with a moderate consistency and its geotechnical parameters are taken according to the Eurocode 7 NEN-EN9997.

The total deformation of the caisson in the current scenario with the above input parameters is computed again and the output is shown in the following figure.

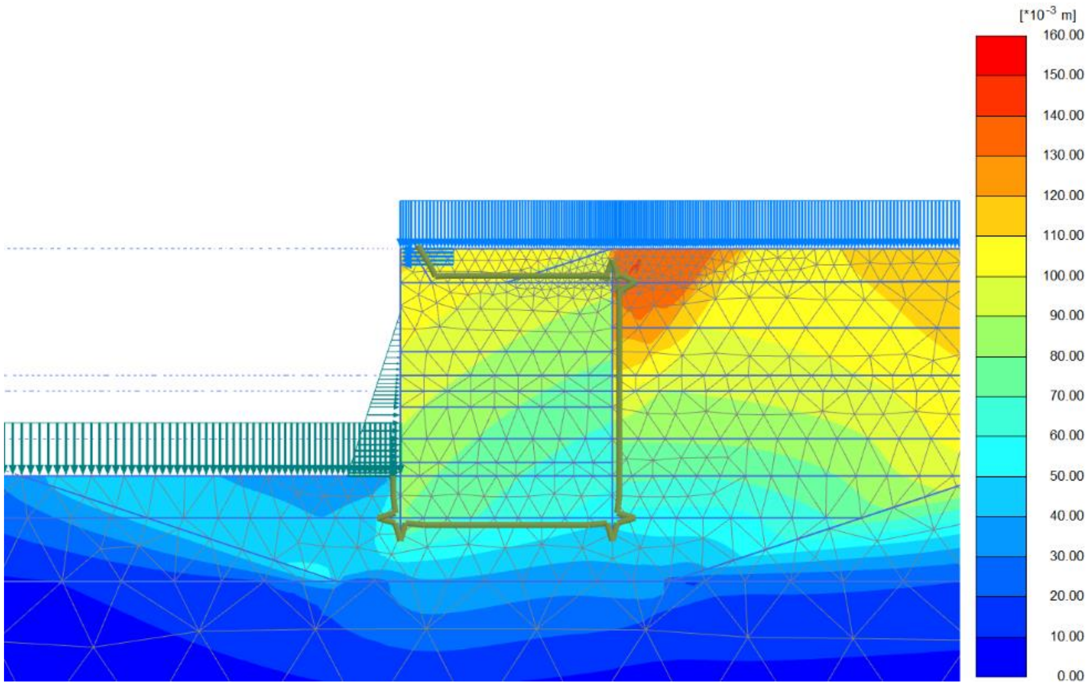

Figure 76: Long-term's total displacements of the caisson in the current situation with improved geotechnical parameters (PLAXIS)

From the figure it is clear that the total displacements are considerably reduced due to the improved foundation layer. The most significant deformation occurs still occurs immediately behind the caisson where the active sliding surface develops. The total displacement of the top of the quay wall is now approximately 11 cm (see Figure 76). Hence, this value of the displacement is now in the order of the tolerable limits of the maximum allowable rotational displacement (approximately 10 cm).

7.4 Variant D; Underwater sheet pile wall

Now that the geometry and the mechanical properties of the soil layers are defined the design variant with the underwater sheet pile is elaborated in detail. The scope of this detailed study is to establish if the design variant can adapt the existing caissons to future cruise terminal of the port of Rotterdam. The detailed design mainly focusses on the overall stability of the quay wall and the deformation of the underwater sheet pile wall.

7.4.1 Characteristics of the sheet pile wall

The underwater sheet pile wall is assumed to be driven at a distance of 3 m in front the caisson. The sheet pile wall has to retain a height of 2.65 m. This height is given by the difference between the current and the new required bed level (see Section 3.2). As a rule of thumb, an unanchored sheet pile should have an embedded depth equal to three times the retaining height and the maximum deformation should not exceed 1/100 of the retaining height. Hence, the toe of the sheet pile is at a depth of NAP -21.65 m and the maximum allowable deformation is approximately 3 cm. The chosen profile of the sheet pile is an Anchelor profile AZ 50-700 with steel quality S240 and an elastic bending moment resistance of 1189 kNm/m. The detailed dimensions and characteristics of the sheet pile profile are described below.

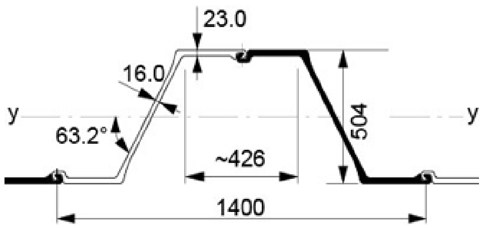

	Sectional area	Mass per m	Moment of inertia	Elastic section modulus	Radius of gyration	Coating area*
	cm^2	kg/m	cm^4	cm^3	cm	m^2/m
Per m of wall	302.6	237.5	124890	4955	20.32	1.46

Figure 77: Dimensions and characteristics of the sheet pile wall Anchelor profile AZ 50-700 (ArcelorMittal)

7.4.2 Adopted constitutive models input parameters and design loads

The constitutive models and the required input parameters of the different soil layer required for stability and deformation analysis of the design variant with underwater sheet pile wall are presented in the tables below. The constitutive models and input parameters for the concrete and caisson are the same as in the geotechnical assessment (see Table 44).

Soil /Material	Constitutive model	Unit weight dry-saturated	Young Modulus	Poisson ratio	Friction angle	Dilatancy angle	Cohesion
Backfill sand	Mohr Coulomb	18-20 kN/m3	25 MPa	0.3	31.5°	1.5°	-
Foundation sand	Mohr Coulomb	20 kN/m3	40 MPa	0.3	32°	2°	
Soft material	Mohr Coulomb	18 kN/m3	3.5 MPa	0.33	22.5°	0°	5 kN/m^2
Deep sand	Mohr Coulomb	21 kN/m3	50 MPa	0.3	34°	4°	-

Table 48: Constitutive models and input parameters for the different soil layers and materials

The design bollard force per running meter is obtained by considering the required capacity of the new bollards obtained from the mooring analysis (see Section 6.6) multiplied by the number of bollards present on one caisson and divided by the length of the caisson. The maximum capacity of the current bollards is 1700 kN the length of the caissons is approximately 45 m (see Section 2.2.1). Thus, the design bollards force is defined as shown in the following equation.

$$F_{bollard} = \frac{2 \cdot 1700}{45} = 75.5 \text{ kN/m}$$

The design loads acting on the caisson are given in the following table.

Load	Value
Quay wall surcharge	30 kN/m^2
Bollard force	75.5 kN/m
Water head difference	1.2 m

Table 49: Design loads acting on the quay wall

7.4.3 Overall stability and settlement

Now that the constitutive models, the required input parameters and the design loads are defined, the principal effective stress and total deformation of the quay wall with the underwater sheet pile wall are computed using PLAXIS and presented below.

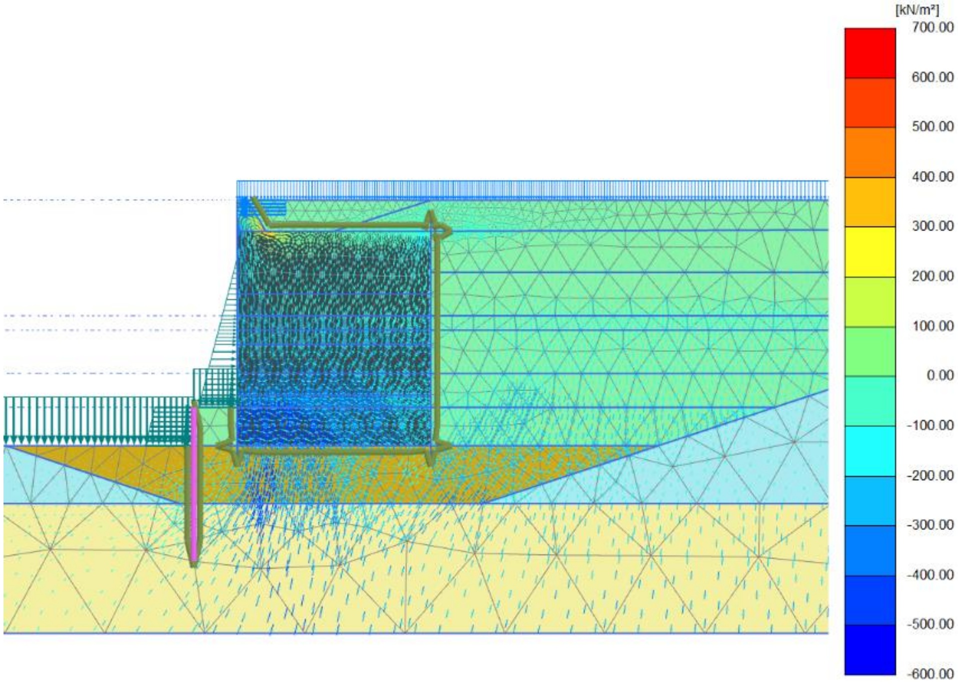

Figure 78: Principal effective stresses of the caisson with underwater sheet pile wall (PLAXIS)

From Figure 78 it can be noticed that due to the significative increase in the design bollard force the compression stresses below the toe are higher than the compression stresses in correspondence of the hill of the caisson. Moreover, the higher bollard force causes high tension stresses in the concrete element, where the bollards are placed, and at the connection between with the caisson.

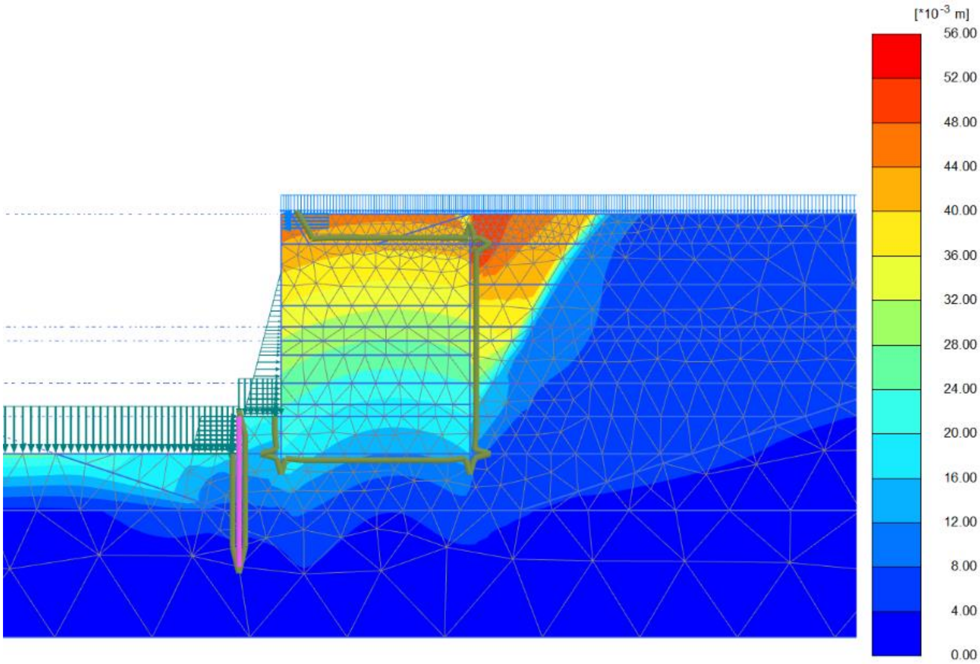

Figure 79: Total displacements of the caisson with underwater sheet pile wall (PLAXIS) the scale of the displacement differs from the previous figures

The above figure represents the total displacement of the caisson with underwater sheet pile wall in the final design stage. The displacement occurred before the placing the sheet pile wall are neglected so that only the effect of design variant on the overall stability of the quay wall is described. From Figure 79, it is visible that the most significative displacement still occurs in the active sliding surface. Although the higher design bollard force leads to a differential settlement of the foundation with a bigger settlement under the toe of the caisson, the total displacement of the top of the quay wall is limited. The total displacement of the top of the quay wall is approximately equal to 5 cm and therefore it is within the allowable displacement of 10 cm (see Section 7.3). A figure representing the overall (scaled) displacement of the quay wall is given in Appendix K.

7.4.4 Stability and deformation of the underwater sheet pile wall

This section focuses on the stability and deformation of the underwater sheet pile wall. In the following figures, the moment diagrams (see Figure 80) and the total deformation (see Figure 81) of the underwater sheet pile wall at its final design stage are presented.

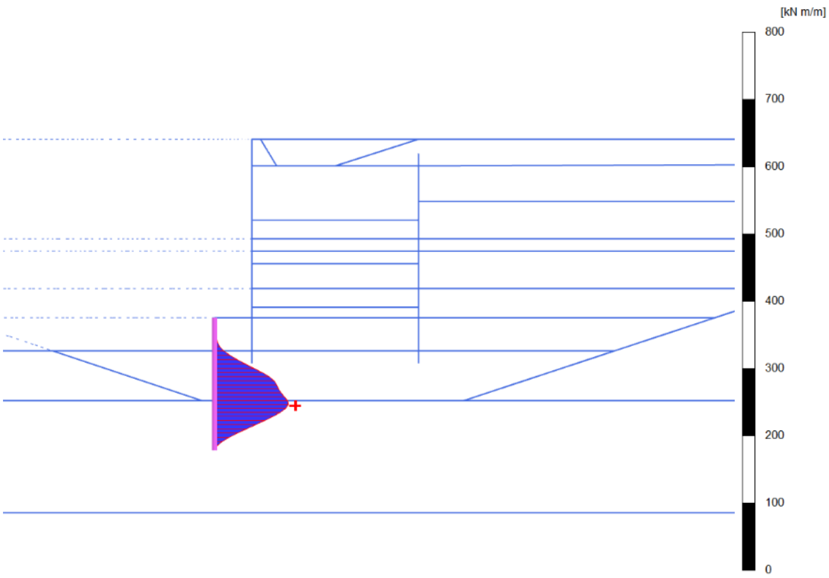

Figure 80: Moment diagram of the underwater sheet pile wall (PLAXIS)

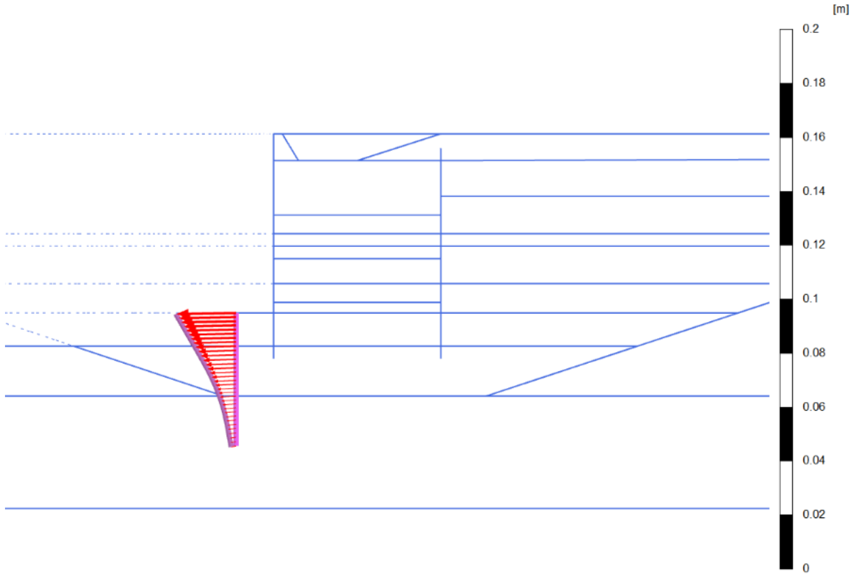

Figure 81: Total deformation of the underwater sheet pile wall (PLAXIS)

According to the above figures the maximum moment and maximum displacement of the sheet pile are equal to 120 kN/m and 2.5 cm respectively. Although the bending moment resistance of the chosen profile for the sheet pile (see Section 7.4.1) is considerably higher than the acting moment the maximum displacement of the sheet pile wall is just within the allowable deformation (see Section 7.4.1). Therefore, it can be concluded that the chosen sheet pile wall profile meet the requirements and consequently the design variant with the underwater sheet pile guarantees the new required nautical depth without compromising the stability of the caisson.

7.4.5 Construction and maintenance

This section describes the main aspects of the constructability, the construction method and maintenance of the design variant with the underwater sheet pile wall.

The underwater sheet pile wall is placed in front of the caisson close to the toe. Therefore, the sheet pile wall should be installed with low-vibration methods or by pressing it without any vibration to avoid erosion of the foundation layer and consequently settlement of the caissons that may lead to instability of the quay wall. The sheet pile wall can be installed with the equipment located on top of the existing quay wall or using floating pontoons as shown in the figure below.

Figure 82: Installation of sheet pile walls using floating pontoons (Deep Excavation website)

After the installation, flame cutting should be performed to cut the upper part of the sheet pile at the required height. The flame cutting operation should be carried out by divers because the retaining wall in located underwater. When this phase has finished, the bed of the berth can be dredged so that the new required nautical depth with the related bed level is reached. Then the scour protection can be placed to prevent erosion that may be caused by the propeller and traverse thrusters jets of the design cruise ships.

Moreover, the design variant includes also berthing facilities such as bollards and fenders. The new required bollards (see Section 6.7) should be placed on top of the structure located above the existing caissons. After the completion of the top of the structure, the big floating fenders necessary to ensure sufficient distance between the keel of the moored design cruise ship and the underwater sheet pile wall (see Section 4.2.4) should be hanged along the full frontage of the berth. Alternatively, to reduce the dimensions of the fenders, the floating fenders may be supported by huge panels that spread the impact load over a bigger surface of the quay wall, like the one adopted at the current cruise terminal.

To summarize, the main steps of the construction method of the design variant with the underwater sheet pile wall are presented below:

1. Driving of the underwater sheet pile wall.
2. Flame cutting of the underwater sheet pile wall carried out by divers.
3. Dredging the berth area to ensure the new required nautical depth.
4. Place the scour protection at the new bottom level in front of the berth area.
5. Place the new required bollards and complete the construction of the top of the structure.
6. Hang the floating fenders along the frontage of the quay wall.

Maintenance and inspection measures are essential to maintain the functionality and safety of a construction and its structural elements. Maintenance strategies of a quay wall depend on the type of construction, the adopted material, the shipping traffic and on the environmental conditions. Therefore, several type of inspections and operations should be planned and carried out during the entire construction stages and lifetime of the structure. Special attention should be given to the inspection and maintenance of the underwater sheet pile wall. Due to the fact that the sheet pile wall is located underwater, divers should be carried out the inspections to ensure the functionality and safety of the structure. In addition, particular maintenance measures should be adopted for the caissons. To do so, sensors can be placed on the top of quay walls. The sensors may provide data of the settlements of the quay wall and on their condition. From, the obtained data the condition of the structure can be established and consequently it is possible to optimize maintenance strategy. Lastly, although the compressive strength of the concrete increases with time (Danad, 2015) special attention should be given to the conditions of the steel reinforcement that plays a crucial role in the strength of the structure.

7.5 Conclusions

From the results of the geotechnical assessment (see Section 7.3) it can be concluded that:

- The soft soil layer was entirely removed and a foundation layer was placed before placing the caissons to avoid instability issues caused by differential settlement of the foundation.
- The foundation layer must be composed of dense granular sand with higher mechanical properties than the backfill sand.
- The water head difference over the caisson is the load that has the most impact on the total displacement of the caisson.
- The friction angle of the backfill soil and of the foundation soil and the Young’s modulus of the foundation soil are the geotechnical input parameters that have the most impact on the total displacement of the caisson.

The detailed design of the design variant with the underwater sheet pile wall (see Section 7.4) proves that a sheet pile profile AZ 50-700, driven in front of the caisson, guarantees the new required nautical depth without compromising the stability of the caisson. Therefore, it is concluded that the design variant with the underwater sheet pile wall can adapt the existing caisson, used as quay wall at the portside of Pier 1 in the Merwehaven for the future cruise terminal of Rotterdam. However, it is important to state that special attention should be given to the construction method and to the maintenance of the underwater sheet pile wall.

8. Conclusions, recommendations and final reflections

This Master thesis report concerns the future cruise terminal in the Port of Rotterdam. The most suitable location for the future cruise terminal is the Pier 1 of the Merwehaven. The Merwehaven is composed of four piers. The piers were constructed between 1923 and 1931 using caissons as quay walls. The objective of this study was to perform a feasibility study focused on the adaptation of the existing quay walls, avoiding the demolition of the existing caissons and consequently the complete construction of new quay walls. This feasibility study was carried out by means of an extensive analysis of the Merwehaven and a brief study of the cruise sector, an assessment of Pier 1, the development and the evaluation of different design variants, a detailed study regarding the mooring loads acting on the design cruise ship and lastly, a detailed design of the best design variant.

8.1 Conclusions

This section presents the conclusions of this report by following the different phases of the adopted approach, which is basically following from the structure of the report.

Assessment of the present situation

After the first Analysis phase (see Chapter 2), which results in the program of requirements, the feasibility study starts with a functional-spatial and structural assessment of the existing quay walls of Pier 1 (see Chapter 3).

The scope of the functional-spatial assessment was to verify whether the quay walls of Pier 1 meet the requirements for the new cruise terminal and identify the main issues that hinder the mooring of the cruise ships. The results of this assessment showed that both quay walls of Pier 1 do not meet the requirements of the new cruise terminal. In more detail, at the portside a technical solution is required to guarantee the new required nautical depth and ensure the stability of the quay wall, while at the riverside an entirely new quay wall and mooring systems are required.

The structural assessment focused on the quay wall at the portside of Pier 1. The berthing area in front of the quay wall has to be deepened to guarantee the new required nautical depth. The assessment aimed to establish the failure mechanisms that may compromise the stability of the caissons, used as a quay wall, in the current situation and due to the deepening of the berth area. The assessment argued that the soil coverage in front of the caissons has a crucial role in the stability of the existing quay wall and consequently that only deepening in front of the caissons is not a feasible design solution. Therefore, a technical solution must be provided to guarantee the new required nautical depth while ensuring the stability of the caissons. Moreover, the assessment proved that the soft soil package was removed and a foundation layer was placed before the installation of the caissons. Lastly, the structural assessment showed that the friction angles of the backfill sand and the foundation layer, the water head difference over the caisson and the bollard force are the variables that have a significant impact on the resulting stability of the caissons.

Design concepts

Different design concepts were developed to solve the issues that obstruct the mooring of the cruise ships, to guarantee the new required nautical depth and to adapt the existing caissons at the portside of Pier 1 (see Chapter 4). The different design concepts were first assessed through a design loop. The scope of the design loop was to identify those design concepts that have a certain level of feasibility and value, which made them design variant and a candidate for the final solution. From the results of the assessment, it turned out that not all the different developed design concepts were suitable to solve the technical problems. Then the remaining design variants were evaluated and rated based on a Multi Criteria Analysis (MCA) and cost estimation. Based on this evaluation, it was concluded that the design variant with the underwater sheet pile wall is the best design variant.

In-depth design

In the design of quay walls, the bollard load plays an important role because it considerably affects the stability of the structure. Therefore, the required bollard capacity has to be defined before performing the detailed design of the best design variant (Chapter 7). The design capacity of bollards is treated differently in different guidelines, leading to different values of the required bollard capacity for the new cruise terminal. According to the different guidelines the minimum bollard capacity that the quay wall of the cruise terminal should have varies between 1100 kN and 1500 kN. According to the guideline of the Port of Rotterdam Authority, the bollards of the cruise terminal should have a capacity of 2340 kN. Because of the significative difference between these values, an extensive study regarding the loads acting on the moored cruise ship and the expected line forces of the design cruise ship was carried out to define the required bollard capacity of the future cruise terminal (see Chapter 6).

Based on the calculation of the forces acting on the moored design cruise ship and the static mooring analysis it was concluded that the existing bollards could not withstand the mooring loads and that the required minimum bollard capacity for future cruise terminal was equal to 1700 kN. Moreover, it turned out that for the design cruise ship the wind load has the most crucial role in the design of the bollard capacity. The effect of passing vessels behind the moored cruise ship is two orders of magnitude lower than the wind loading and is therefore negligible.

The in depth design continues with the detailed design of the design variant with the underwater sheet pile wall. The detailed design mainly focused on geotechnical aspects based on deformation and stability analysis of the design variant. From these analyses, it was first concluded that the soft soil package was entirely removed and a foundation layer was placed before the construction of the caissons. Besides, it was argued that to minimize the settlements of the caisson, the foundation layer must be composed of dense granular soils with higher mechanical properties than the backfill sand. Furthermore, it was concluded that the water head difference over the caisson is the load that has the most impact on the total displacement of the caisson.

Lastly, the detailed design proved that the underwater sheet pile with a profile AZ 50-700, driven in front of the caissons, guarantees the new required nautical depth without compromising the stability of the caissons. Therefore, it was concluded that the design variant with the underwater sheet pile wall can adapt the existing caisson, used as quay wall at the portside of Pier 1 in the Merwehaven, for the future cruise terminal of Rotterdam. However, it was important to state that special attention should be given to the construction method and to the maintenance of the underwater sheet pile wall.

8.2 Recommendation

In each phase, different assumptions and simplifications are made to achieve the objective of these master thesis. The recommendations for future studies are described for each phase.

Assessment of the present situation

The functional-spatial assessment and the program of requirements were based on the dimensions of the design cruise ship. This was based on the fact that cruise ships have continued to grow in all dimensions over the past 40 years. The dimensions of the design cruise ship were the maximum expected during the design lifetime of the structure. However, more research should be done to establish whether the cruise ships will really reach these dimensions or increase even more.

When the design cruise ship is moored along quay wall at the portside, the turning basin area needed by the passing vessels inside the Merwehaven is over crossed. Due to this space reduction, the difficulty of the maneuvers of the vessels that need to reach the other piers of the Merwehaven is increased. This negative impact on the maneuvers for the passing vessels should be investigated in more detail.

The value of the geotechnical parameters adopted structural assessment of the quay wall at the portside of Pier 1 are based on the CPT test located behind the caissons. However, only one CPT is available and this is not sufficient to obtain a reliable estimation of the soil parameters, soil stratigraphy and water levels. Therefore, more field tests should be carried out in front and behind the caissons. Particular consideration should be given to the definition of the friction angle the backfill soil and of the foundation layer.

Moreover, the structural assessment is carried out without the use of partial. If partial factors were to be taken into account, the caisson would not meet current safety standards. Hence, further research is needed to define the safety factors of the caissons. Lastly, more research should be carried out to define the exact value of the design loads of the quay wall surcharge and water head difference over the caisson. Because they play an important role in the stability of the caisson.

Design concepts

Not all proposed options have been used in practice. Other design concepts can be developed to solve the issues that obstruct the mooring of the cruise ships along the quay wall of the portside. The performed design loops of the proposed design concepts consisted of hand calculations based on simplified methods and technical reasoning. Hence, the design loops can be elaborated in more detail.

In the evaluation of the design concepts, the MCA was based on five criteria with different weight factors. However, additional or different criteria can be added to the MCA. Moreover, in the cost estimation, the cost of each design variant include only the cost of the main components and elements that characterize the different design variants. The cost estimation was based on a rough estimation of the amount of the materials used, the price of the materials and the construction costs. Therefore, to obtain a reliable costs estimation of the design variants the estimation should be carried out in more detail and by taking into consideration all the structural components.

In-depth design

The different guidelines for the required bollard capacity of the cruise terminal provide, values which differ significantly. Most of the guidelines are based on the mass of the ship while the *Bolderbelasting Standardisatie Rotterdam* is based on the minimum breaking load of the lines. Thus, more research should be carried out to reduce the significant differences between the provided values.

The wind load acting on the design cruise ship was computed according to the British Standard. This approach and its result should be compared with other guidelines. Furthermore, the British Standard provides graphs for the wind coefficients that are valid for unsheltered vessels in open water. However, there are no wind coefficients graphs available for cruise ships. Therefore, to estimate the value of the wind force coefficients for the design cruise ship, the envelope for container ship was adopted. The effect of this assumption on the results of the wind load should be investigated.

The effect of passing ships was computed according to two methods. In the Wangs's approach, the non-dimensional graphs for the determination of the peak values have a limitation. The peak values are only available till a ratio, between the length of the ships, equal to 0.5. However, the ratio between the length of the passing vessel and the length of the moored design cruise ship was equal to 0.3. For this reason, to define the peak value for ratio this ratio a graphical interpolation was used. The validation of this graphical interpolation was not verified in this report and hence should be investigated.

To model the effect of passing ships with the software ROPES no cruise ship hull was available. For this reason, a container vessel hull form is selected for the design cruise ship. Hence, the effect of this assumption on the output results should be studied.

To define the expected line force of the moored design cruise ship a static mooring analysis was carried out. However, a vessel that is moored along a berth is characterized mainly by dynamic behavior. Thus, the results of this analysis should be compared with the results of a dynamic mooring analysis. Moreover, in the static mooring analysis, the mooring pattern was schematized with the breast lines tied at the middle of the bow and stern of the cruise ship while the spring lines tied at the corners of the cruise ship close to the berth. In practice, however, usually two lines are tied at one bollard and the lines start from different winches placed in different locations of the vessel. Besides, the vertical angle that the lines form with the deck and the elasticity of the mooring lines were not considered in the schematization. Therefore, the effect of these assumptions and simplification of the mooring pattern on the expected line force results should be investigated.

In the detailed design of the design variant with underwater sheet pile wall, the soil layers were assumed to behave according to the Mohr-Coulomb model. The Hardening Soil model should be used for the different soil layer behavior to get more advanced and accurate results for the deformation and stability analysis of the quay wall. However, this model requires many input parameters that should be estimated based on a geotechnical site investigation (SI) report. Therefore, to determine the required input parameters of the different soil layers, fields and laboratory tests should be carried out. Special attention should be given to the definition of the geometry of the foundation layer and on the geotechnical parameters of the backfill soil and the foundation layer and on the definition of the design loads of the quay wall surcharge and water head difference over the caisson. Because all these variables play an important role in the settlements and stability of the caisson.

In the PLAXIS models the dimensions of the concrete element, where the bollard force was applied, were chosen from the technical drawings. In addition, the connection between the concrete element and the caisson was assumed to be fixed. Hence, these assumptions and its effect on the results should be further studied. Moreover, from the output results of the best design variant, high tension stresses were present in the concrete element and at the connection with the caisson. Thus, the spreading of these stresses inside the concrete element should be investigated in more detail.

Moreover, scour protection is strictly required to ensure the overall stability of the quay wall. The erosion that may be generated by the propeller and traverse thruster jets of the design cruise ships and its effect on the stability of the caissons should be studied in detail. Lastly, the underwater sheet pile wall is driven in front of the caisson close to the toe. Therefore, the settlements of the caisson induced by the installation of the sheet pile wall should be investigated in depth.

8.3 Final reflections

Existing quay walls often need to be adapted to new operational requirements. This is may be also the case for the caissons of Pier 1 used as a quay wall in the Merwehaven. Besides, the caissons are already past the end of their technical lifespan (now for civil engineering projects is 50 years). However, environmental and cost optimization often indicates that upgrade of existing quay wall is the preferred option compared to the complete demolition of the existing quay wall and the construction of an entirely new structure (de Gijt & Douairi, 2013). Hence, this last section presents some general reflection and consideration regarding the adaptation and the upgrading of existing quay walls constructed with gravity structures.

The upgrading of a quay wall usually consists of the deepening of the bed level of the berth area or provide mooring for bigger ships. This implies that that the existing quay wall has to retain more soil and withstand increased external forces such as vertical surcharge and bollard forces, in excess of the forces it was actually designed for. Hence, technical adjustments to the quay walls are required, to ensure sufficient strength and stability. To provide the new required depth and upgrade existing structures it is essential to know the loading conditions of the quay wall, the soil conditions and the variation in water levels over the retaining structure. With this information, it is possible to assess the present and future structural integrity by performing computations of the different failure mechanisms of the quay wall. When a simple analysis is not possible, detailed calculations need to be carried out. This complex computation can be performed with finite element analysis methods. The structural assessment of the existing quay wall is crucial to evaluate its ability to withstand the additional dredging or increased loads and to evaluate the risks during execution of the upgrading works. However, it is important to state that the safety of structures has increased considerably in the last decades. As a result, the design of old structures which were valid at the time of construction, may not meet the current safety standards. In this report the stability checks were performed without the use of partial factors and the stability checks of the caissons in the current situation were just meet. Therefore, if partial factors were to be taken into account, the caisson would not meet current safety standards. However, further research with more accurate and detailed data are needed to prove it.

When the structural conditions of the existing quay wall have been assessed to be sufficient, the existing structure may be upgraded by means of technical adjustments. The technical solutions may increase the resisting forces or alternatively decrease the driving forces as shown in the figure below.

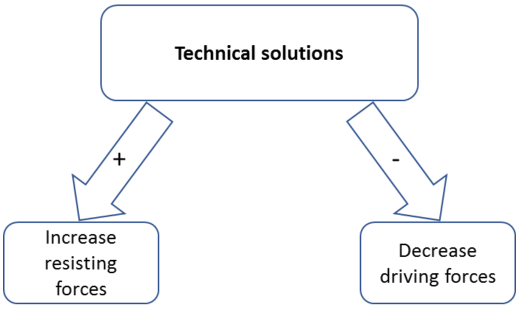

Figure 83: Technical solutions for upgrading quay walls

For gravity structures increasing the resisting forces can be achieved mainly by improving the passive force provided by the bottom material in front of a structure or by improving the mechanical properties of the foundation soil below the structure. The decrease in driving forces can be achieved by reducing the active force acting on the retaining structure. This can be achieved by replacing the soil behind the structure with a soil with a higher friction angle. Sensitivity analysis of the geometrical parameters, acting loads and resistance of structural elements is good design practices to define their impact on the stability of the structure and to determine which technical solutions may be the most efficient. However, the different technical solutions should also be evaluated by a suitable type or level of evaluation such as a Cost-benefit analysis or Multi Criteria Analysis.

Finally, historical events and maintenance registers regarding the quay wall may offer useful information when analyzing the observed behavior of an existing structure. Also in this report maintenance registers and measurements of the settlements could be very useful to describe the behavior of the caissons. To get accurate data regarding the settlement and condition of quay walls sensors can be placed on top and behind the structure. From, the measured data the condition of the structures can be established and consequently it is possible to optimize maintenance strategy. The information provided by the sensors can also be used in the development and improvement of future quay walls.

References

Bezuyen, K., Colenbrander, W., Kuijper, H., Molenaar, W., Spaargaren, C., Vrijling, J., & Baars, S. V. (2009). *General Lectures note Hydraulic structures.* Delft: Department of Hydraulic Engineering.

Brinkgreve, R. (sd). *Lecture notes CIE4361 Behavoir of Soils and Roks.*

Broeken, M., & Gijt, J. d. (2014). *Quay Wall Second edition.* Rotterdam: CRC Press/Balkema.

BS 6349-4 Part 4. (2014). *Maritime works.* The British Standard Instituition.

Danad, M. (2015). *The reuse of caissons from the port of Rotterdam.* Delft: Hydraulic Engineering Faculty of Civil Engineering TU Delft.

Deltares. (2017). *Basisstochasten WBI-2017.* Delft: Deltares.

Eurocode 1. (1990). *Actions on structures - Part 1-4, General actions - Wind actions.* Delft: TGB.

Gijt, J. d. (2004). *Structures in hydraulic engineering Port Infrastructure.* Delft: Hydraulic Engineering Faculty of Civil Engineering.

Gijt, J. d. (2011). *Costs of quay wall.* Rotterdam: Delft University of Technology.

Gijt, J. d., & Douairi, M. (2013). *Upgrading Techniques for Quay Walls.* Delft: Delft University of Technology.

Harper, B., Kepert, J., & Ginger, J. (2008). *GUIDELINES FOR CONVERTING BETWEEN VARIOUS WIND AVERAGING PERIODS IN TROPICAL CYCLONE CONDITIONS.* World Meteorological Organization.

Havenbedrijf Rotterdam NV. (2014). *Ontwerprichtlijnen Havens en Vaarwegen.* Rotterdam: Havenbedrijf Rotterdam.

Havenkrant. (2017, March). *Port of Rotterdam*. Opgehaald van https://www.portofrotterdam.com/nl/havenkrant/havenkrant-editie-30/3-vragen-aan-allard-castelein

HBG, H. B. (1977). *Rapport Caissonbouw.* Rijswijk: hbg.

IsGeschiedenis. (2014). *Geschiedenis haven van Rotterdam*. Opgehaald van www.isgeschiedenis.nl: https://isgeschiedenis.nl/nieuws/geschiedenis-haven-van-rotterdam

Maritiem Nederland. (2017). *Cruise.* Bèta Publishers © 2015.

Molenaar, W., & Voorendt, M. (2017). *Manual Hydraulic Structures.* Delft: Hydraulic Engineering departement .

OCIMF. (2008). *Mooring Equipment Guidelines 3rd Edition.* Livingston: Witherby Seamanship International.

Oil Companies International Marine Forum (OCIMF). (1994). *Prediction of wind and current loads on VLCC's second.* London: Witherby & Co Ltd.

PIANC. (2002). *Guidelines for design of fender systems.* Bruxels: PIANC Secrétariat Général.

PIANC. (2015). *Guidlines for protecting berthing structures from scour caused by ships.* Bruxelles: PIANC Secrétariat Général.

PIANC. (2016). *Guidelines for cruise terminal.* Bruxelles: PIANC Secrétariat Général.

Pinkster Marine Hydrodynamics. (2011). *Ropes User Manual.* PMH BV.

PLAXIS 2D. (2017). *Material Models.* Delft.

PLAXIS 2D. (2017). *Reference Manual.* Delft.

Port of Rotterdam. (2012). *HydroMeteoBundel.* Rotterdam: Havenbedrijf Rotterdam N.V.

Port of Rotterdam. (2015). *Bolderbelasting Standardisatie Rotterdam.* Rotterdam: Havenbedrijf Rotterdam.

Port of Rotterdam. (2016). *Windstatistiek Lekhaven.* Rotterdam: Haven bedrijf Rotterdadm N.V.

Port of Rotterdam Authority. (2015). *Port Infrastructure.* Rotterdam: Port of Rotterdam Authority.

Port of Rotterdam Authority. (2017). *Facts & Figures.* Rotterdam: Port of Rotterdam Authority.

Rijkswaterstaat. (2017). *Vaarwegen in Nederland.* Utrecht : Rijkswaterstaat Centrale Informatievoorziening (CIV).

ROM 0.2-90. (1990). *Actions in the design of Maritime and harbour works.* Madrid: Puerto del Estado.

Roozenburg, N., & Eekels, J. (1995). *Product Design: Foundamentals and Methods.* Delft.

Scherpenzeel, B. V. (2011). *Richtlijnen Afmeervoorzieningen Rotterdam.* Rotterdam: Havenbedrijf Rotterdam N.V.

Toorn, A. V. (2015). *General lecture notes Hydraulic Structures 2.* Delft: Hydraulic Engineering Faculty of Civil Engineering.

Voorendt, M. (2017). *Design priciples of multifunctional flood defences.* Delft: Departement of Hydraulic Engineering.

Voorendt, M., & Molenaar, W. (2017). *Manual Hydraulic Structures.* Delft: Hydraulic Engineering Faculty of Civil Engineering.

Voorendt, M., Molenaar, W., & Bezuyen, K. (2016). *Lecture notes on Caissons.* Delft: Department of Hydraulic Engineering.

Wang, S. (1975). *Dynamic effects of ship passage on moored vessels.* Journal of the waterways harbors and costal engineering division.

Appendices

Appendix A: Geotechnical investigations

Cone penetration test (CPT) results at Pier 1

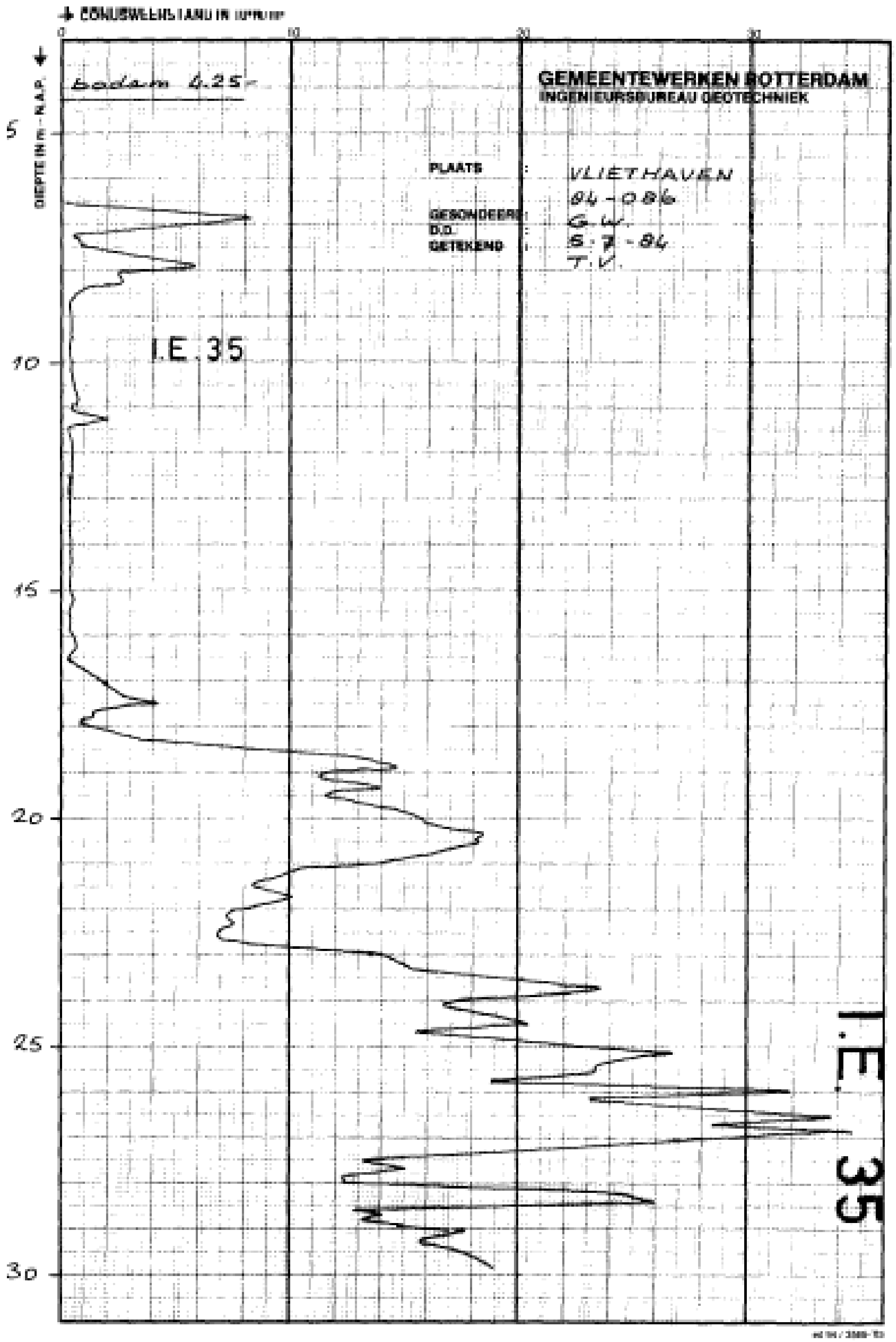

Cone penetration test (CPT) results behind the caissons at Pier 1.

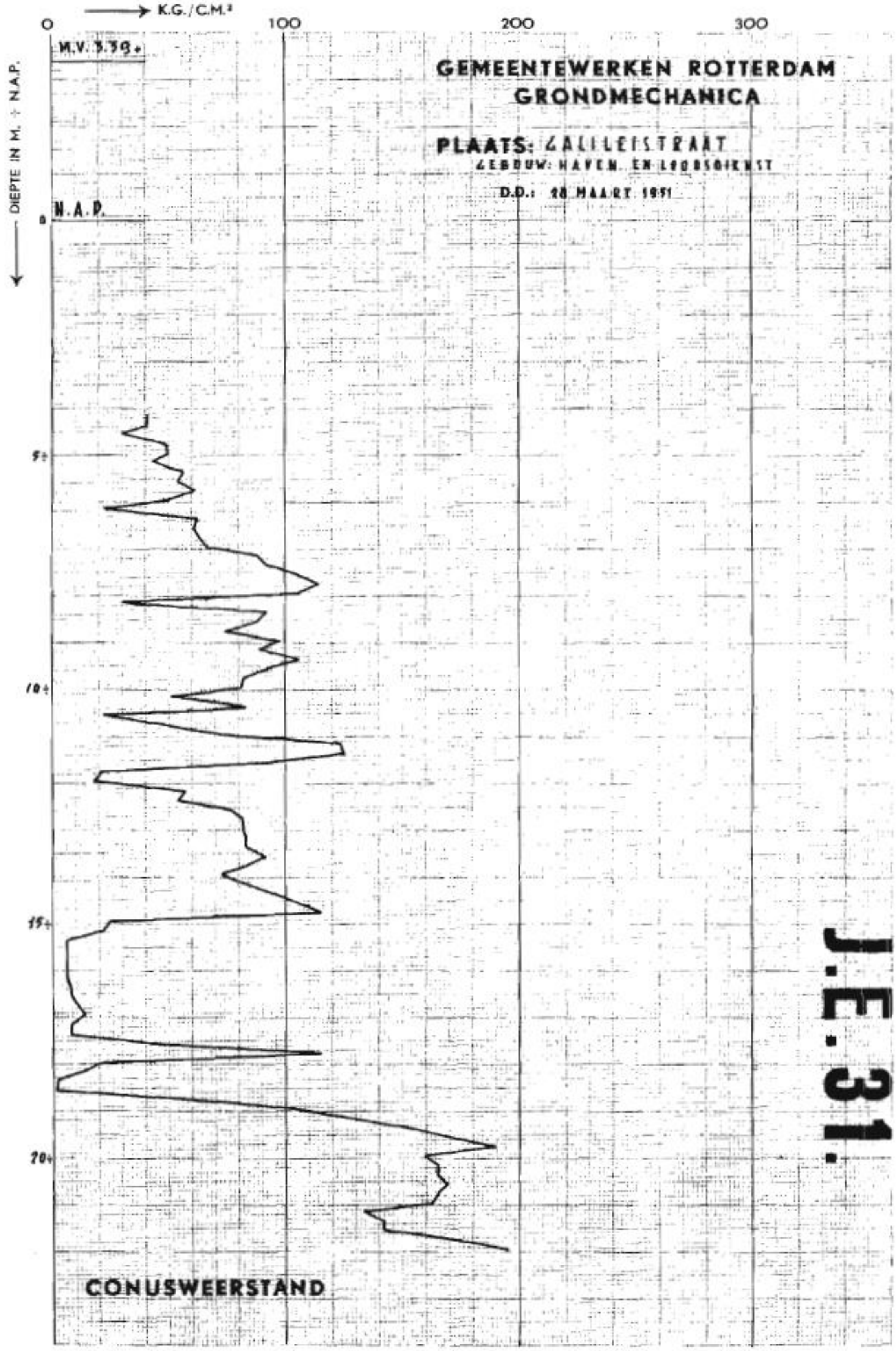

Location of the CPT tests available at Pier 1

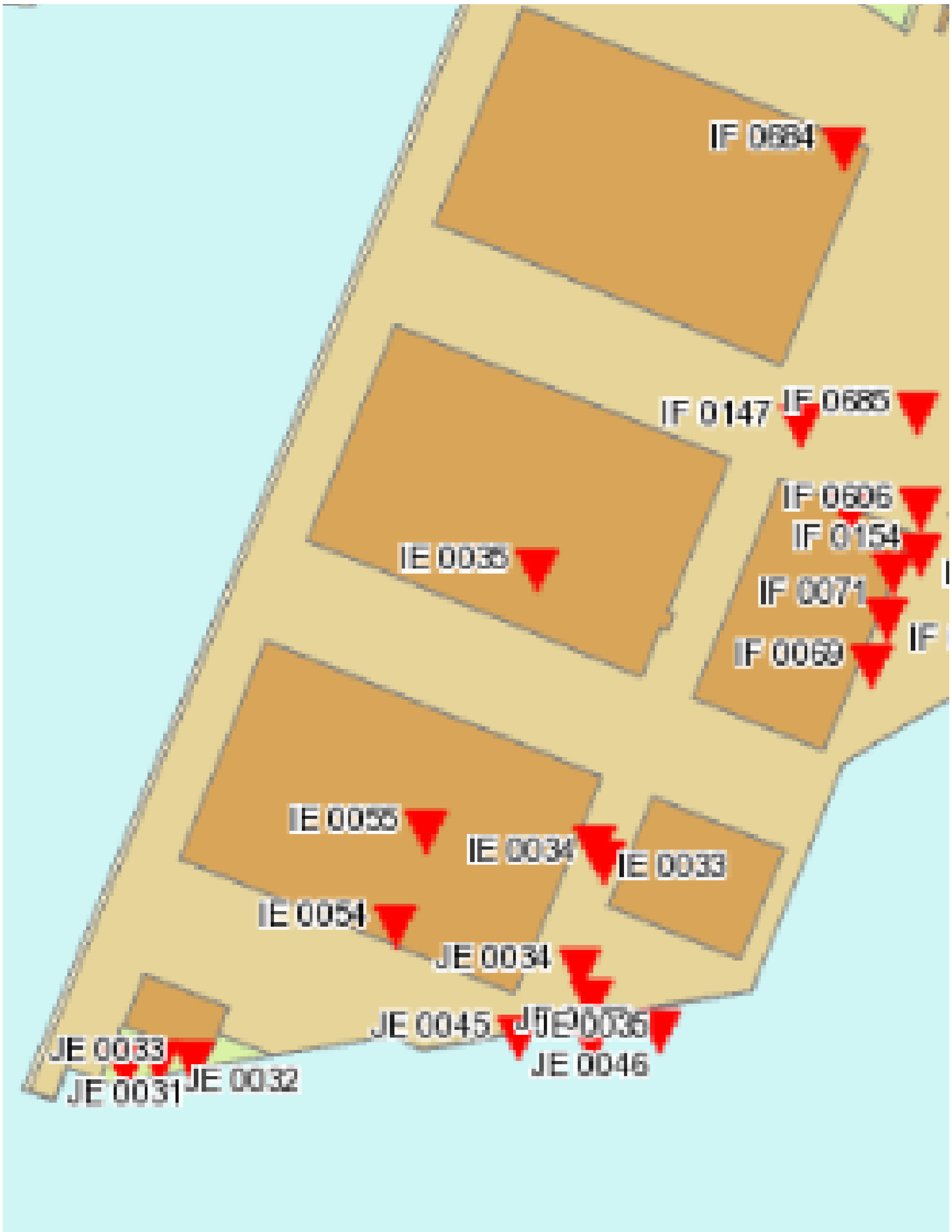

Drill sample profile of the port bottom in the Merwehaven.

Boormonsterprofiel

Identificatie: B37G0712
Coördinaten: 88020, 435435 (RD)
Maaiveld: -5,50 m t.o.v. NAP
Dieptetraject t.o.v. Maaiveld: 0,00 m - 5,75 m

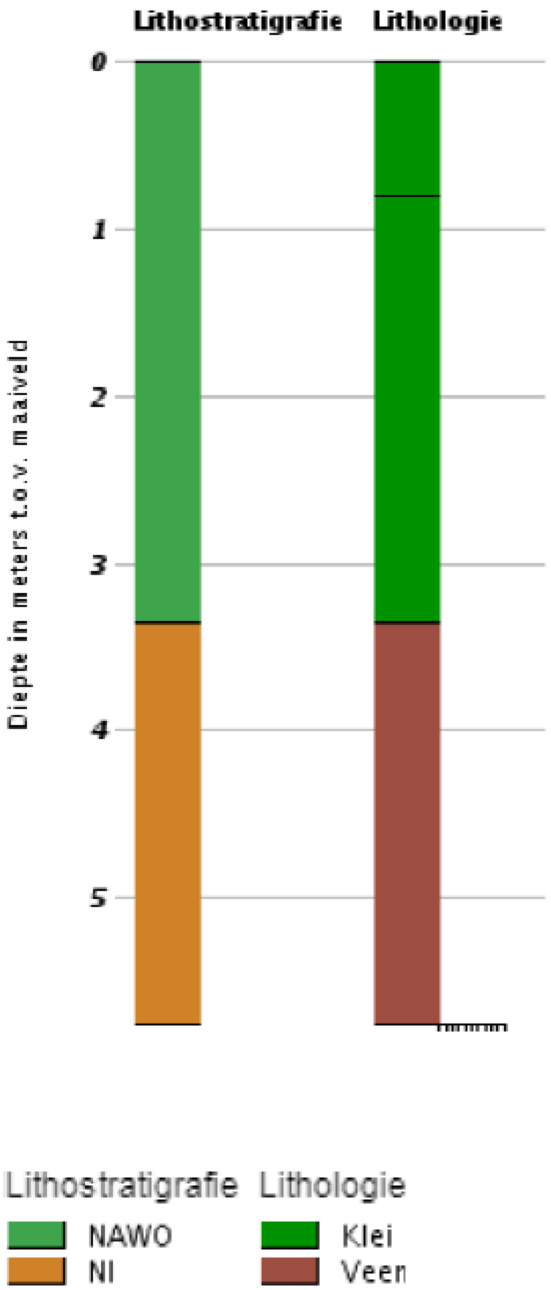

Position of the water pressure sensor at Pier 1.

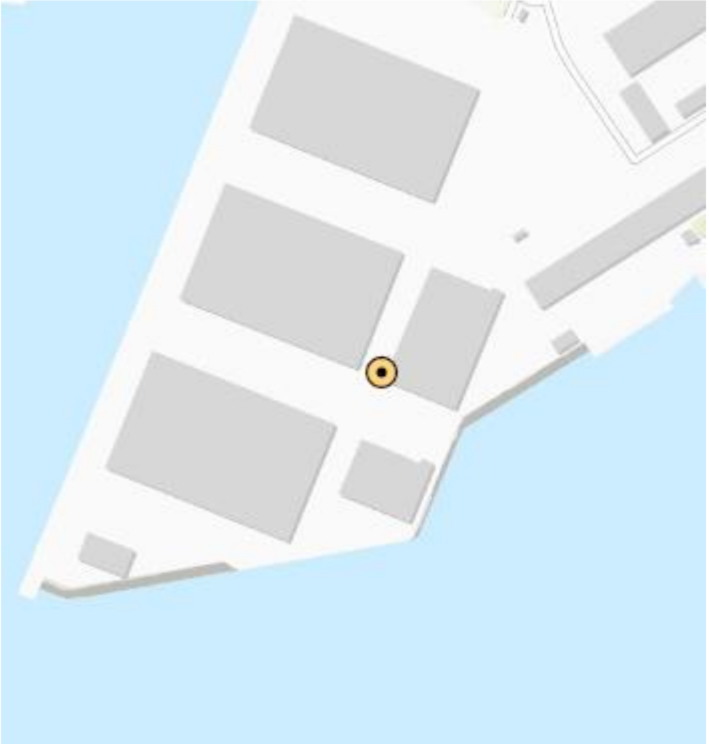

Appendix B: Approach velocity and berthing energy of mooring ships

The approach velocity and the mass of the vessel (water displacement) are the most influential variables in the calculations of the of the berthing energy. The water displacement is the total mass of the vessel in fully loaded conditions. The approach velocity is defined as the vessel speed, perpendicular to the berth, at the moment of initial contact between the ship and the mooring facility. The factors depend on the characteristics of the vessel, fender system and geometry of the berth facility.

To define the berthing speed different tables and graphs are present in literature. The British Standard on Fenders has adopted the design approach velocity presented in the figure below, on which five curves are given corresponding to the following navigation conditions:

a) good berthing, sheltered (i.e. not exposed to waves and/or currents);

b) difficult berthing, sheltered;

c) good berthing, exposed to waves and/or currents;

d) difficult berthing, exposed to waves and/or currents;

e) adverse berthing, exposed to waves and/or currents.

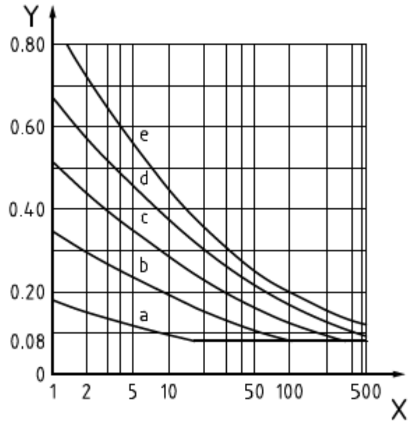

Another aspect that plays a role in the fender design is the berthing angle. This angle is formed at the moment of initial contact between the ship and the mooring facility. However, for vessels larger than 50000 DWT (deadweight tonnage) the berthing angles are generally less than 5 degrees with only occasionally an angle of 6 degrees (PIANC, Guidelines for design of fender systems, 2002).

Appendix C: Geotechnical assessment

The effective vertical stresses are computed before and after the construction of the caissons in the middle of the remaining thickness pf the soft soil layer at a depth of NAP -16.65 m indicated in the figure by the black dot.

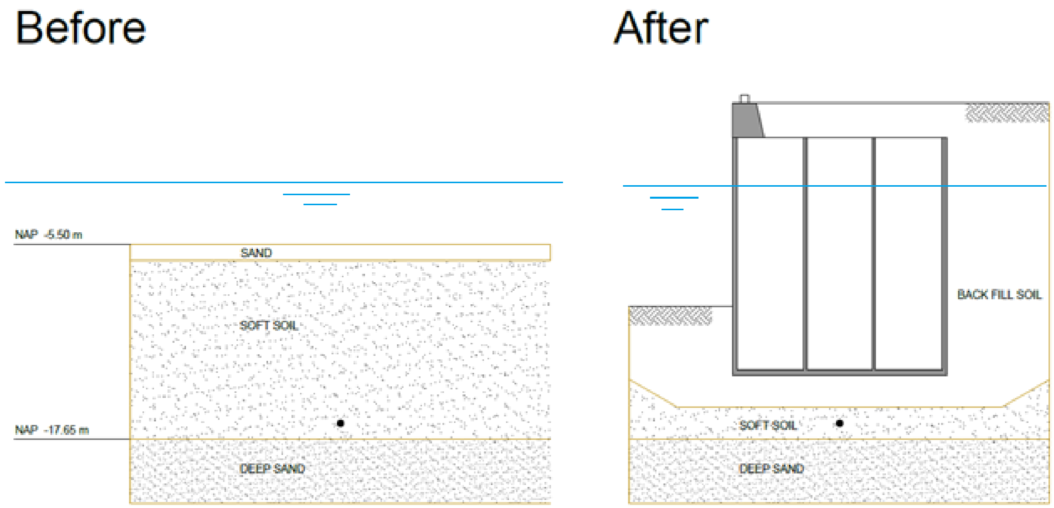

Before

$$\sigma'_{v1} = \left(\gamma_{sand,sat} - \gamma_w\right) * h_{sand} + \left(\gamma_{soft,sat} - \gamma_w\right) * h_{soft} = (20 - 10) * 1 + (18 - 10) * 10 = 90 \, \frac{kN}{m^2}$$

After

$$\sigma'_{v2} = q + \gamma_{sand,dry} * h_{dry} + (\gamma_{caisson} - \gamma_w) * h_{caisson} + \left(\gamma_{sand,sat} - \gamma_w\right) * h_{foundation,sand} +$$

$$+\left(\gamma_{soft,sat} - \gamma_w\right) * h_{soft} = 30 + 18 * 2.15 + (20.33 - 10) * 14.85 + (20 - 10) * 2 + (18 - 10) * 0.5 =$$

$$= 246 \, \frac{kN}{m^2}$$

Where:

$\gamma_{caisson}$ is an equivalent unit weight of the caisson that is obtained as shown below

$$\gamma_{caisson} = \frac{(Q_{concrete} + Q_{ballast}) * L_{caisson}}{V_{caisson}} = \frac{(\gamma_c * A_c + A_b * \gamma_{sat}) * L_{caisson}}{V_{caisson}} =$$

$$= \frac{(25 * 19.19 + 20 * 179.8) * 43.65}{8685.9} = 20.33 \frac{kN}{m^3}$$

Given the above vertical stresses the settlement is computed with the following equation:

$$\Delta H = H_o * \varepsilon = H_o * \left(\frac{C_c}{1 + e_o} * \log\left(\frac{\sigma'_{v2}}{\sigma'_{v1}}\right) + C_{ae} \log\left(\frac{t}{t_{ref}}\right)\right) = 2 * \left(0.23 * \log\left(\frac{246}{90}\right) + 0.009 * \log\left(\frac{80}{1}\right)\right) =$$

$$= 0.24 \text{ m}$$

Appendix D: Stability checks calculations of the caissons

Current situation

For a first stability check calculation, a cross-section in the middle of a caisson (length direction) is considered. The influence of the head walls, toe and heels of the caisson are neglected, which works out as conservative considerations. It is assumed that the caisson is filled with the same soil as the backfill. It is assumed that the soil in front, behind and below the caisson is backfill sand. The the deep sand layer starts at NAP -17.65m.

The water levels behind (land side) and in front (water side) of the caisson are taken so that the maximum unbalanced hydrostatic pressure is developed that is equal to 1.9 m. The current bed level in front of the caisson is equal to NAP -11 m. The soil level behind the caisson is taken equal to the level of the superstructure that is equal to NAP +3.35. The vertical load acting on the on top of the quay wall is equal to 30 kN/m^2. The bollard force (per running meter) is equal to 33.3 kN/m. The mechanical properties of the backfill sand are the following:

Mechanical properties backfill soil	
Dry weight	18 kN/m^3
Submerged weight	20 kN/m^3
Angle of internal friction	30 deg

Given the above mentioned situation the following load configuration is obtained.

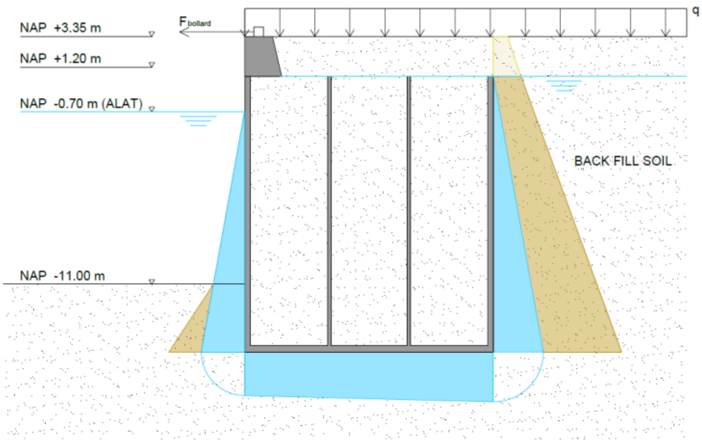

The stability checks are performed per running meter without the use of safety factors. The stability check calculations are performed step by step below.

The loads acting on the caisson are divided in function of the side where they act :

- Loads at the water side

$$Q_{h1,sand} = \sigma'_h * \frac{h_{s1}}{2} = 79.5 * \frac{2.65}{2} = 105.3\ \frac{kN}{m}$$

$$Q_{h1,water} = u_1 * \frac{h_{w1}}{2} = 129.5 * \frac{12.95}{2} = 838.5\frac{kN}{m}$$

$$\sigma'_h = \sigma'_v * K_p = 26.5 * \frac{(1 + \sin(30))}{(1 - \sin(30))} = 79.5\ \frac{kN}{m^2}$$

$$\sigma'_v = (\gamma_{sat} - \gamma_w) * h_{s1_v} = (20 - 10) * 2.65 = 26.5\ \frac{kN}{m^2}$$

$$u_1 = h_{w1} * \gamma_w = 12.95 * 10 = 129.5\ \frac{kN}{m^2}$$

- Loads at the land side

$$Q_{sand,rect} = \sigma'_{h,sand,till\ dry} * h_{caisson} = 22.9 * 14.85 = 340.1 \frac{kN}{m}$$

$$Q_{sand,triang} = (\sigma'_{h,sand,at\ toe} - \sigma'_{h,sand,till\ dry}) * \frac{h_{caisson}}{2} = (72.4 - 22.9) * \frac{14.85}{2} = 367.5\ \frac{kN}{m}$$

$$Q_{h2,water} = u_2 * \frac{h_{w2}}{2} = 148.5 * \frac{14.85}{2} = 1102.6\ \frac{kN}{m}$$

$$\sigma'_{h,sand,till\ dry} = \sigma'_{v,sand,till\ dry} * K_a = 68.7 * \frac{(1 - \sin(30))}{(1 + \sin(30))} = 22.9\ \frac{kN}{m^2}$$

$$\sigma'_{v,sand,till\ dry} = q + \gamma_{dry} * h_{dry} = 30 + 18 * 2.15 = 68.7\ \frac{kN}{m^2}$$

$$\sigma'_{h,sand,at\ toe} = \sigma'_{v,sand,at\ toe} * K_a = 217.2 * \frac{(1 - \sin(30))}{(1 + \sin(30))} = 72.4\ \frac{kN}{m^2}$$

$$\sigma'_{v,sand,at\ toe} = \sigma'_{v,sand,till\ dry} + (\gamma_{sat} - \gamma_w) * h_{caisson} = 68.7 + (20 - 10) * 14.85 = 217.2\ \frac{kN}{m^2}$$

$$u_2 = h_{w2} * \gamma_w = 14.85 * 10 = 148.5\ \frac{kN}{m^2}$$

- Loads due to the uplift force

$$Q_{u,triangle} = (u_2 - u_1) * \frac{b}{2} = (148.5 - 129.5) * \frac{13.4}{2} = 127.3 \frac{kN}{m}$$

$$Q_{u,rectangle} = u_1 * b = 129.5 * 134.4 = 1735.3\ \frac{kN}{m}$$

- The vertical forces that counteract the uplift force are:

$$Q_{concrete} = \gamma_c * A_c = 25 * 19.19 = 479.8 \frac{kN}{m}$$

$$Q_{ballast} = A_b * \gamma_{sat} = 20 * 179.8 = 3596\ \frac{kN}{m}$$

$$Q_{superstructure} = \sigma'_{v,sand,till\ dry} * b = 68.7 * 13.4 = 920.6\ \frac{kN}{m}$$

$$A_c = A_{slab} + V_{frontwallas} + V_{insidewalls} = 19.19\ m^2$$

$$A_b = A_{caisson} - A_c = 179.8\ m^2$$

The caissons are stable if the three stability checks are satisfied.

Horizontal stability check:

$$\sum H \ \leq f \cdot \sum V$$

$$\rightarrow \left(Q_{sand,rect} + Q_{sand,triang} + Q_{bollards} + Q_{h2,water} - Q_{h1,sand} - Q_{h1,water}\right) \leq f * \left(Q_{concrete} + Q_{ballast} + Q_{superstructure} - Q_{u,triangle} - Q_{u,rectangle}\right)$$

$$\rightarrow 899.4 \leq 0.36 * 3133.7 \rightarrow 899.4\ \frac{kN}{m} \leq 1128.1 \frac{kN}{m} \rightarrow \mathbf{ok}!$$

$$f = \frac{2}{3} * \tan(\varphi) = 0.36$$

Rotational stability check:

$$\frac{\sum M}{\sum V} \leq \frac{1}{6} W \;\rightarrow\; \frac{6934.9}{3133.7} \leq \frac{1}{6} \cdot 13.4 \;\rightarrow 2.21\text{ m} \leq 2.33\text{ m} \;\rightarrow \mathbf{ok}!$$

The sum of the moments is taken in the middle of the base slab of the caisson

$$\sum M = -\frac{1}{3} * h_1 * Q_{h1,water} - \frac{1}{3} * h_{s1} * Q_{h1,sand} + \frac{1}{3} * h_{caisson} * \left(Q_{sand,triang} + Q_{h2,water}\right) * + \frac{1}{6} * b * Q_{u,triangle} + h_2 * Q_{bollards} = -\frac{1}{3} * 12.85 * 838.5 - \frac{1}{3} * 2.65 * 105.3 + \frac{1}{3} * 14.85 + (367.5 + 1102.6) + \frac{1}{6} * 13.4 * 127.3 + 17 * 33.3 = 6934.9 \frac{kNm}{m}$$

Vertical stability:

$$\sigma_{k,max} < p'_{max} \;\rightarrow\; 465.6\ \frac{kN}{m^2} < 604.4\ \frac{kN}{m^2} \rightarrow\ \mathbf{ok}!$$

$$\sigma_{k,max} = \frac{\sum V}{b \cdot l} + \frac{\sum M}{\frac{1}{6} l * b^2} = \frac{3133.7}{13.4 * 1} + \frac{6934.9}{\frac{1}{6} 13.4^2 * 1} = 465.6\ \frac{kN}{m^2}$$

$$p'_{max} = 0.5 * \gamma' * B * N_\gamma * i_\gamma * S_\gamma + q' * i_q * N_q * S_q =$$

$$= 0.5 * (20 - 10) * 13.4 * 14.4 * 0.36 * 0.91 + 18.4 * 26.5 * 1.15 * 0.51 = 604.4 \frac{kN}{m^2}$$

$$N_\gamma = \left(N_q - 1\right) \cdot \tan(1.32 \cdot \varphi) = (18.4 - 1) \cdot \tan(1.32 \cdot 30) = 14.4$$

$$N_q = \frac{1 + \sin(\delta)}{1 - \sin(\delta)} \cdot e^{\pi \cdot \tan(\varphi)} = \frac{1 + \sin(30)}{1 - \sin(30)} \cdot e^{\pi \cdot \tan(30)} = 18.4$$

$$i_\gamma = \left(1 - \frac{\sum H}{\sum V}\right)^3 = 0.36$$

$$S_\gamma = 1 - 0.3 * \frac{\sum H}{\sum V} = 0.91$$

$$q' = (\gamma_{sat} - \gamma_w) * h_{s1} = 26.5 \frac{kN}{m^2}$$

$$i_q = \left(1 - 0.7 * \frac{\sum H}{\sum V}\right)^3 = 0.51$$

$$S_q = 1 + \frac{b}{l} * \sin(\varphi) = 1 + \frac{13.4}{45} * \sin(30) = 1.15$$

Deepened situation

To perform the stability checks of the situation with deepening in front of the quay wall the following load configuration is considered.

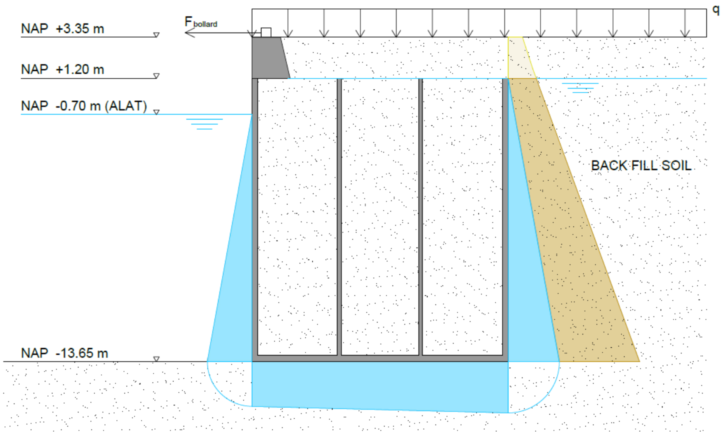

The only difference from the previous scenario is that the soil in front of the quay wall is removed till the new required depth that corresponds to the level of the toe of the caisson. Consequently, the passive soil force is removed. All the other variables are the same. Given the above schematization the stability checks are carried below step by step.

The loads acting on the caisson are divided in function of the side where they act :

- Loads at the water side

$$Q_{h1,water} = u_1 * \frac{h_{w1}}{2} = 129.5 * \frac{12.95}{2} = 838.5 \frac{kN}{m}$$

$$u_1 = h_{w1} * \gamma_w = 12.95 * 10 = 129.5 \frac{kN}{m^2}$$

- Loads at the land side

$$Q_{sand,rect} = \sigma'_{h,sand,till\ dry} * h_{caisson} = 22.9 * 14.85 = 340.1 \frac{kN}{m}$$

$$Q_{sand,triang} = (\sigma'_{h,sand,at\ toe} - \sigma'_{h,sand,till\ dry}) * \frac{h_{caisson}}{2} = (72.4 - 22.9) * \frac{14.85}{2} = 367.5 \frac{kN}{m}$$

$$Q_{h2,water} = u_2 * \frac{h_{w2}}{2} = 148.5 * \frac{14.85}{2} = 1102.6 \frac{kN}{m}$$

$$\sigma'_{h,sand,till\ dry} = \sigma'_{v,sand,till\ dry} * K_a = 68.7 * \frac{(1 - \sin(30))}{(1 + \sin(30))} = 22.9 \frac{kN}{m^2}$$

$$\sigma'_{v,sand,till\ dry} = q + \gamma_{dry} * h_{dry} = 30 + 18 * 2.15 = 68.7 \frac{kN}{m^2}$$

$$\sigma'_{h,sand,at\ toe} = \sigma'_{v,sand,at\ toe} * K_a = 217.2 * \frac{(1 - \sin(30))}{(1 + \sin(30))} = 72.4 \frac{kN}{m^2}$$

$$\sigma'_{v,sand,at\ toe} = \sigma'_{v,sand,till\ dry} + (\gamma_{sat} - \gamma_w) * h_{caisson} = 68.7 + (20 - 10) * 14.85 = 217.2 \frac{kN}{m^2}$$

$$u_2 = h_{w2} * \gamma_w = 14.85 * 10 = 148.5 \frac{kN}{m^2}$$

- Loads due to the uplift force

$$Q_{u,triangle} = (u_2 - u_1) * \frac{b}{2} = (148.5 - 129.5) * \frac{13.4}{2} = 127.3 \frac{kN}{m}$$

$$Q_{u,rectangle} = u_1 * b = 129.5 * 134.4 = 1735.3 \ \frac{kN}{m}$$

- The vertical forces that counteract the uplift force are:

$$Q_{concrete} = \gamma_c * A_c = 25 * 19.19 = 479.8 \frac{kN}{m}$$

$$Q_{ballast} = A_b * \gamma_{sat} = 20 * 179.8 = 3596 \ \frac{kN}{m}$$

$$Q_{superstructure} \ = \sigma'_{v,sand,till\ dry} * b = 68.7 * 13.4 = 920.6 \ \frac{kN}{m}$$

$$A_c = A_{slab} + V_{frontwallas} + V_{insidewalls} = 19.19 \ m^2$$

$$A_b = A_{caisson} - A_c = 179.8 \ m^2$$

The caissons are stable if the three stability checks are satisfied.

Horizontal stability check:

$$\sum H \ \leq f \cdot \sum V$$

$$\rightarrow \left(Q_{sand,rect} + Q_{sand,triang} + Q_{bollards} + Q_{h2,water} - Q_{h1,water}\right) \leq f * \left(Q_{concrete} + Q_{ballast} + Q_{superstructure} \ - Q_{u,triangle} - Q_{u,rectangle}\right)$$

$$\rightarrow 1004.7 \leq 0.36 * 3133.7 \rightarrow 1004.7 \ \frac{kN}{m} \leq 1128.1 \frac{kN}{m} \rightarrow \mathbf{ok}!$$

$$f = \frac{2}{3} * \tan(\varphi) = 0.36$$

Rotational stability check:

$$\frac{\sum M}{\sum V} \leq \frac{1}{6} W \ \rightarrow \ \frac{7027.9}{3133.7} \leq \frac{1}{6} \cdot 13.4 \ \rightarrow 2.24 \ m > 2.23 \ m \ \rightarrow \mathbf{not\ ok}!$$

The sum of the moments is taken in the middle of the base slab of the caisson

$$\sum M = \ -\tfrac{1}{3} * h_1 * Q_{h1,water} + \tfrac{1}{3} * h_{caisson} * \left(Q_{sand,triang} + Q_{h2,water}\right) + \tfrac{1}{6} * b * Q_{u,triangle} + h_2 * Q_{bollards} = -\tfrac{1}{3} * 12.85 * 838.5 - \tfrac{1}{3} * 2.65 * 105.3 + \tfrac{1}{3} * 14.85 + (367.5 + 1102.6) + \tfrac{1}{6} * 13.4 * 127.3 + +17 * 33.3 = 7027.9 \frac{kNm}{m}$$

Vertical stability:

$$\sigma_{k,max} < p'_{max} \ \rightarrow \ 468.7 \ \frac{kN}{m^2} > 274.6 \ \frac{kN}{m^2} \rightarrow \mathbf{not\ ok}!$$

$$\sigma_{k,max} = \frac{\sum V}{b \cdot l} + \frac{\sum M}{\frac{1}{6} lb^2} = \frac{3133.7}{13.4 * 1} + \frac{7027.9}{\frac{1}{6} 13.4^2 * 1} = 468.7 \ \frac{kN}{m^2}$$

$$p'_{max} = 0.5 * \gamma' * B * N_\gamma * i_\gamma * S_\gamma =$$

$$= 0.5 * (20 - 10) * 13.4 * 14.4 * 0.31 * 0.91 = 604.4 \frac{kN}{m^2}$$

$$N_\gamma = \left(N_q - 1\right) \cdot \tan(1.32 \cdot \varphi) = (18.4 - 1) \cdot \tan(1.32 \cdot 30) = 14.4$$

$$N_q = \frac{1 + \sin(\delta)}{1 - \sin(\delta)} \cdot e^{\pi \cdot \tan(\varphi)} = \frac{1 + \sin(30)}{1 - \sin(30)} \cdot e^{\pi \cdot \tan(30)} = 18.4$$

$$i_\gamma = \left(1 - \frac{\sum H}{\sum V}\right)^3 = 0.31$$

$$S_\gamma = 1 - 0.3 * \frac{\sum H}{\sum V} = 0.91$$

Appendix E: Sensitivity analysis of the stability checks

The results of the sensitivity analysis for the stability checks regarding the influence of the different variables are presented below. The horizontal, rotational and vertical safety factors are computed for three different value of each variable.

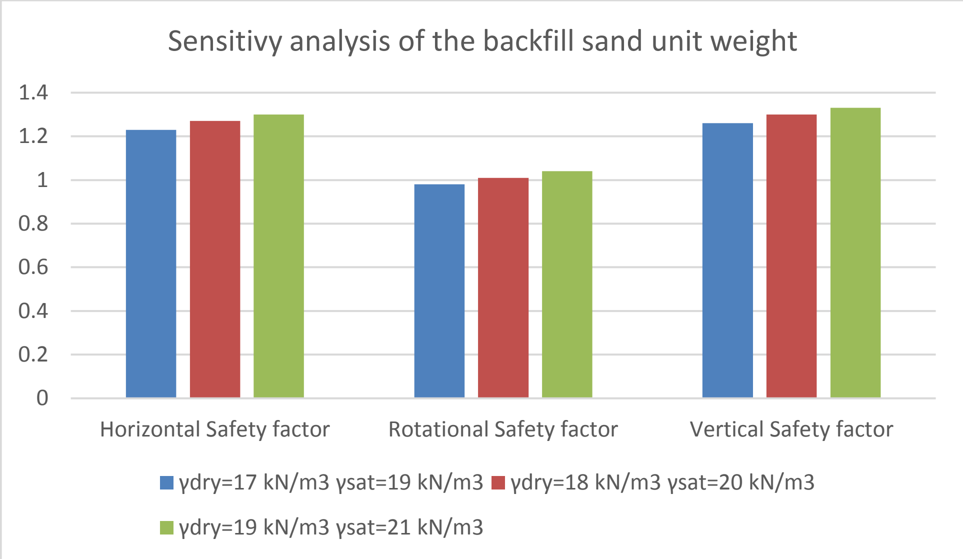

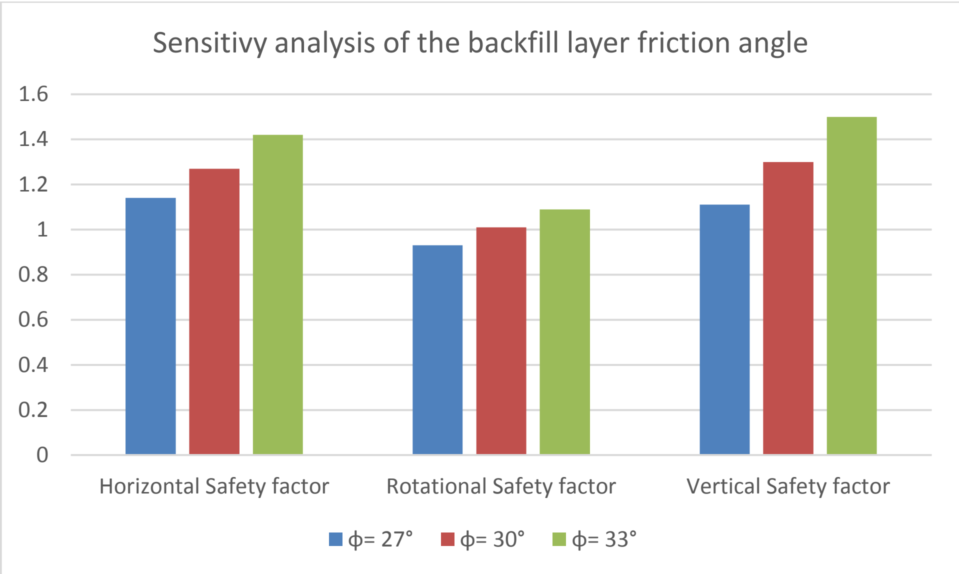

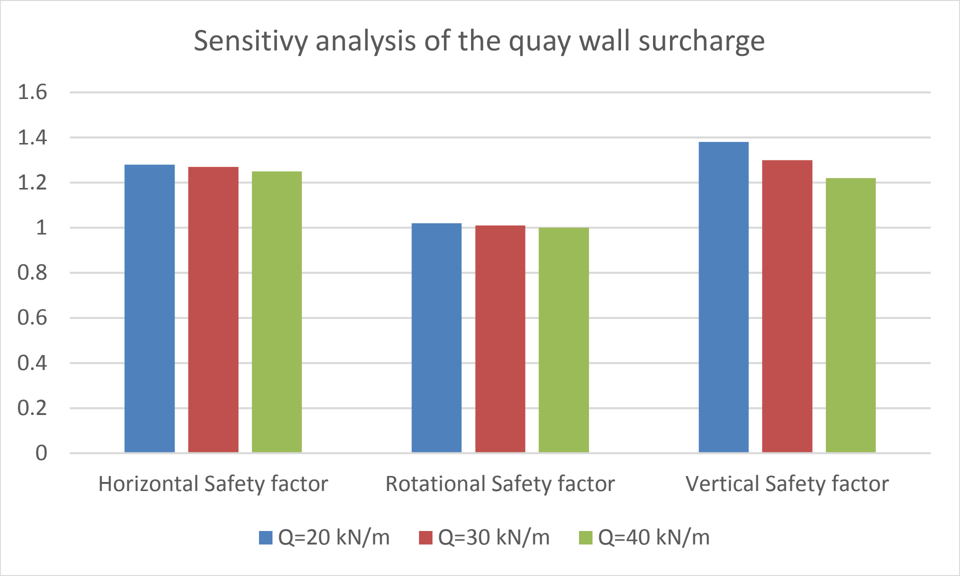
Sensitivy analysis of the quay wall surcharge
1.6
1.4
1.2
1
0.8
0.6
0.4
0.2
0
Horizontal Safety factor
Rotational Safety factor
Vertical Safety factor
Q=20 kN/m
Q=30 kN/m
Q=40 kN/m

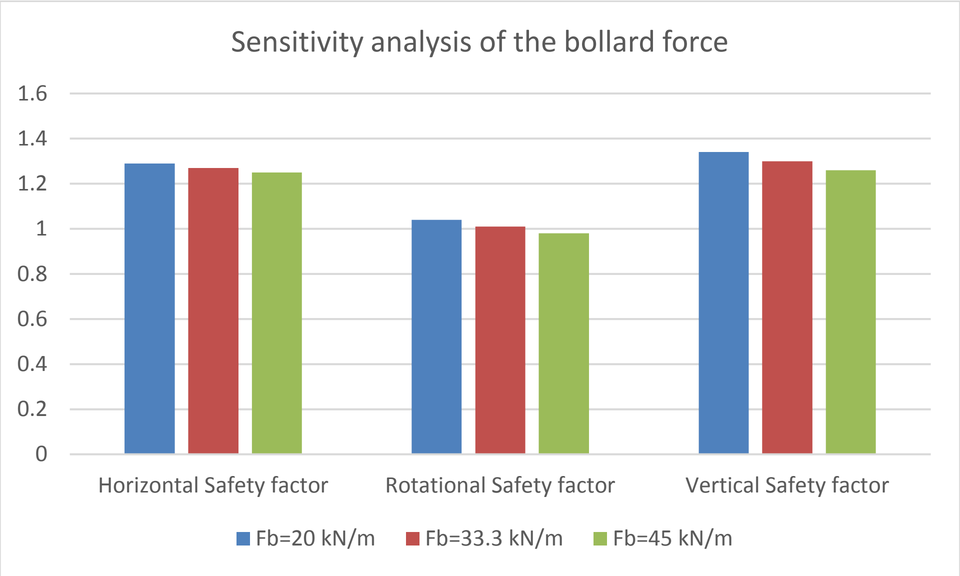
Sensitivity analysis of the bollard force
1.6
1.4
1.2
1
0.8
0.6
0.4
0.2
0
Horizontal Safety factor
Rotational Safety factor
Vertical Safety factor
Fb=20 kN/m
Fb=33.3 kN/m
Fb=45 kN/m

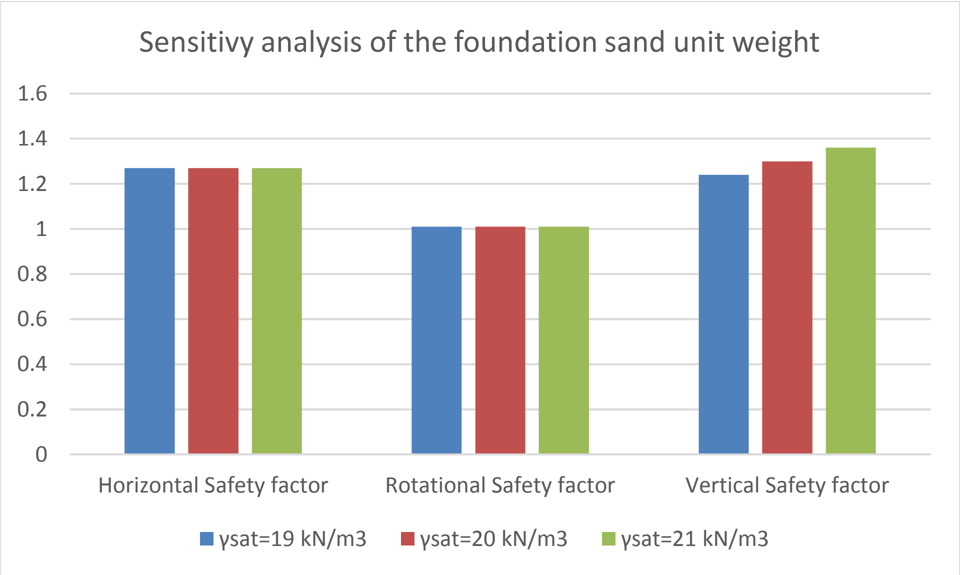
Sensitivy analysis of the foundation sand unit weight
1.6
1.4
1.2
1
0.8
0.6
0.4
0.2
0
Horizontal Safety factor
Rotational Safety factor
Vertical Safety factor
γsat=19 kN/m3
γsat=20 kN/m3
γsat=21 kN/m3

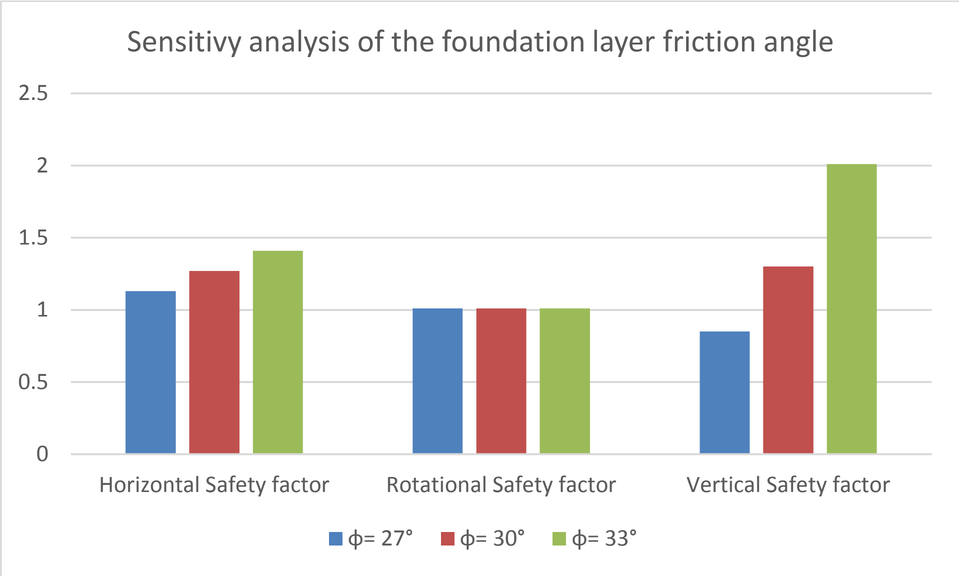
Sensitivy analysis of the foundation layer friction angle
2.5
2
1.5
1
0.5
0
Horizontal Safety factor
Rotational Safety factor
Vertical Safety factor
ϕ= 27°
ϕ= 30°
ϕ= 33°

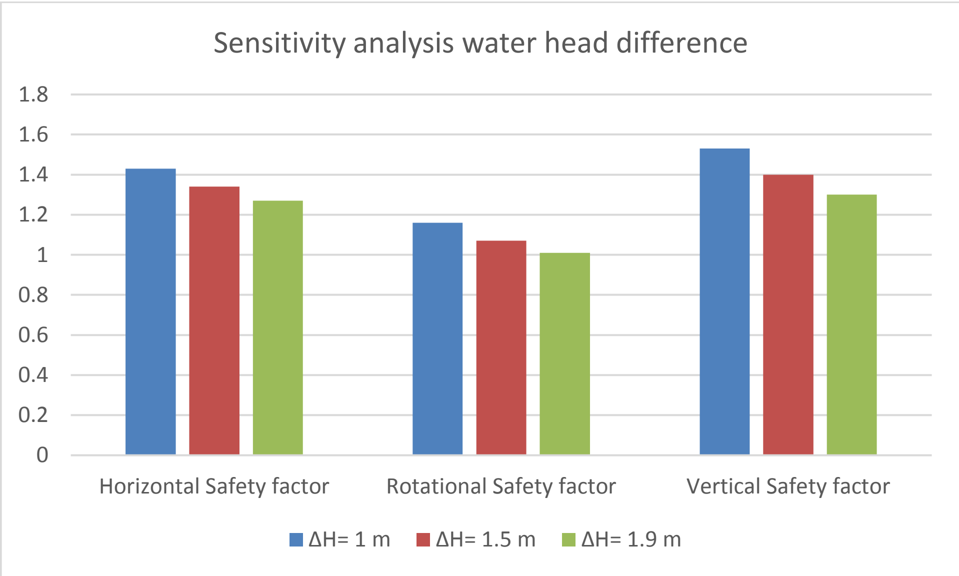
Sensitivity analysis water head difference
1.8
1.6
1.4
1.2
1
0.8
0.6
0.4
0.2
0
Horizontal Safety factor
Rotational Safety factor
Vertical Safety factor
ΔH= 1 m
ΔH= 1.5 m
ΔH= 1.9 m

Appendix F: Berthing energy and Floating fenders

Berthing energy of the design cruise ship

To compute the berthing energy on the design cruise ship, the deterministic method can be used. This method is the oldest and the most commonly used (PIANC, Guidelines for design of fender systems, 2002). It concerns the vessel in the process of berthing and its related energy. The following relation gives the kinetic energy of an approaching ship:

$$E_{kin} = \frac{1}{2} \cdot M \cdot v^2$$

Where:

E_{kin} is the kinetic energy of the approaching vessel

M is the water displacement of the vessel (mass)

V is the velocity perpendicular to the quay wall of the approaching vessel

The characteristic berthing energy that has to be absorbed by the fender system can be computed as shown below.

$$E_c = E_{kin} \cdot C_e \cdot C_m \cdot C_s \cdot C_c$$

Where:

E_c is the characteristic berthing energy

C_e, C_m, C_s, C_c are the eccentricity factor, virtual mass factor, softness factor and berth configuration factor.

The approach velocity and the water displacement of the vessel are the most influential variables in the calculations of the berthing energy. The water displacement is the total mass of the vessel in fully loaded conditions. The approach velocity is defined as the vessel speed, perpendicular to the berth, at the moment of initial contact between the ship and the mooring facility. The factors depend on the characteristics of the vessel, fender system and geometry of the mooring facility.

The different factors need to be defined to obtain the characteristic berthing energy first. The eccentricity factor can be computed using the simplified formula as shown below:

$$C_e = \frac{K^2}{K^2 + R^2} = 0.46$$

Where:

K is the radius of gyration that is equal to $K=(0.19C_b+0.11)\ L_{pp}$ = 84.1 m

C_b is the blocking coefficient of the cruise ship, equal to 0.69

L_{pp} is the length between the two perpendiculars that is equal to 350 m (see Table 6)

R is the distance of the point of contact to the center of mass of the ship

Notice that it assumed that the distance between the impact point with the fender and the bow of the cruise ship is at ¼ of the length between the two perpendiculars (L_{pp}). Hence, the distance of the point of contact (R) is equal to 91.0 m. Moreover, the underwater cross section is usually characterized by a smaller width hence the underwater beam of the design cruise ship is reduced to 50 m.

The virtual mass factor is computed according to the Shigeru Ueda Method (1981) that gives the following expression:

$$C_m = 1 + \frac{\pi \cdot D}{2 \cdot C_b \cdot B} = 1.46$$

Where:

D, B and C_b are the draught, the beam and the blocking coefficient of the design cruise ship.

According to PIANC, Guidelines for design of fender systems, 2002, the berth configuration and softness factor are equal to 1.

Now that all the coefficients are defined the characteristic and design berthing energy can be calculated. The water displacement and the approach velocity of the design cruise ship are given in Section 2.5.

According to the PIANC the design berthing energy (E_d) is obtained by multiplying the characteristic berthing energy (E_c) with a safety factor. The value of the safety factor takes inconsideration abnormal berthing situations. For cruise ships, the safety factor is equal to 2.

The characteristic and the design value of the berthing energy of the design cruise ship are presented in the following table:

Berthing energy	
Characteristic value (E_c)	258 kNm
Design value (E_d)	516 kNm

Floating fenders performance data

Different types of fendering system are available. All these systems absorb the kinetic energy of the berthing ship through elastic deformation. The energy absorbed by fenders is equal to the deflection (d_m) multiplied by the reaction force (R_m) and a certain factor (f) that depends on the fender characteristic (PIANC, Guidelines for design of fender systems, 2002). This relation can be expressed with the following equation.

$$E_f = f \cdot R_m \cdot d_m$$

The ratio R_m / E_f is called Fender Factor and provides information regarding the behavior of the fender system. Fenders with high Fender Factor are called surface protecting factor while fenders with a low Fender Factor are called energy absorbing factors. Usually fenders with a high Fender Factor are used for bigger ships.

The energy that is absorbed by the fender during compression is partially returned to the vessel and partially dissipated in heat. However, also the deflection of the berth facility and the vessel's hull contribute to the absorption of the kinetic energy. The performance data and curves of the selected floating fenders (type "*ISO standard*") are presented below.

Performance data

INITIAL INTERNAL PRESSURE	50kPa			80kPa		
NOMINAL SIZE DIAMETER × LENGTH (mm)	GUARANTEED ENERGY ABSORPTION (GEA)	REACTION FORCE AT GEA DEFLECTION (R)	HULL PRESSURE (INTERNAL PRESSURE) AT GEA DEFLECTION (P)	GUARANTEED ENERGY ABSORPTION (GEA)	REACTION FORCE AT GEA DEFLECTION (R)	HULL PRESSURE (INTERNAL PRESSURE) AT GEA DEFLECTION (P)
	MINIMUM VALUE AT DEFLECTION 60 ±5% kj	TOLERANCE ±10% kN	REFERENCE VALUE kPa	MINIMUM VALUE AT DEFLECTION 60 ±5% kj	TOLERANCE ±10% kN	REFERENCE VALUE kPa
500 x 1000	6	64	132	8	85	174
1000 x 1500	32	182	122	45	239	160
1000 x 2000	45	257	132	63	338	174
1200 x 2000	63	297	126	88	390	166
1350 x 2500	102	427	130	142	561	170
1500 x 3000	153	579	132	214	761	174
2000 x 3500	308	875	128	430	1150	168
2500 x 4000	663	1381	137	925	1815	180
2500 x 5500	943	2019	148	1317	2653	195
3300 x 4500	1175	1884	130	1640	2476	171
3300 x 6500	1814	3015	146	2532	3961	191
3300 x 10600	3067	5257	158	4281	6907	208
4500 x 9000	4752	5747	146	6633	7551	192

Performance Curve

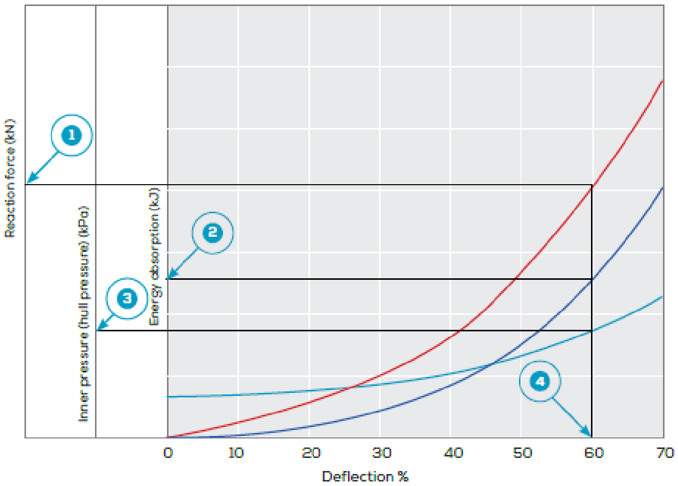

— Reaction force
— Energy absorption
— Inner pressure

1. Reaction force at GEA deflection
2. Guarantee energy absorption (GEA)
3. Hull pressure at GEA deflection
4. GEA deflection

Appendix G: Bolderbelasting Standardisatie Rotterdam

Bollards are posts placed along berth facility where the lines of vessels are tied. Mooring bollards are available in a wide range of sizes, shapes, load ratings, and materials. The most common bollard types found at cruise facilities are single bitt, double bitt and, more occasionally, T-head. The selection of the specific bollards varies somewhat by region and frequently by the preference of the end user (PIANC, Guidelines for cruise terminal, 2016).

The bollards, together with the lines and the winches, form the system that restrain the vessel movements and avoid that the ship turns away. This system is designed is usually designed according to the Minimum Breaking Load (MBL) of the ship lines. The MBL depends on the type of line used by the vessels. However its value is based on the "Equipment number" of the vessel that is established by the IACS (International Association Of Classification Societies).

The bollard should be strongest element of the bollard-line-winch system. Indeed the required failure scenario of the system is the following (Port of Rotterdam, Bolderbelasting Standardisatie Rotterdam, 2015):

1. Winch slips
2. Line fails
3. Bollard deforms
4. Bollard fails

According to the "Bolderbelasting Standardisatie Rotterdam" the design of the bollards is based on a representative load (F_{rep}). This load is based on the maximum load that the lines, adopted on a ship, can withstand and is called minimum breaking load (MBL). The representative load is equal to the maximum load that can occur during normal operational conditions. In the Eurocode this condition is called SLS (Serviceability Limit State). The maximum operational load is equal to the Maximum Holding Force (HMF) of a winch. This force is reached when a winch of a moored vessel fails. Usually, the HMF of a winch is equal to 50-60% of the MBL. Therefore, the representative load of a bollard can be computed according to the following equation:

$$F_{rep} = N \times 0.6 \times MBL$$

Where N is the number of lines tied on the bollard.

The design load (F_d) for the ULS (Ultimate Limit State), the condition where the structure can reach the maximum deformation without reaching failure, is obtained by multiplying the representative load by a safety factor. According to the Eurocode 3 this factor is equal to 1.5. Therefore, the bollard design load is given by the following below.

$$F_d = 1.5 \times N \times 0.6 \times MBL$$

However, in the bollard design another loading condition should also be considered. This condition is a calamity scenario and in the Eurocode, it is called ALS (Accidental Limit State). The ALS takes into consideration the combination of multiple failures. This might happen is case of failure of the mooring system in combination with human failure. And its design load can be obtained according the following equation.

$$F_a = 2 \times MBL + (N-2) \times 0.6 \times MBL$$

In the following table**Error! Reference source not found.** the design load for the three conditions are presented. The "Bolderbelasting standardisatie Rotterdam" advise to design the bollards with a maximum of 3 lines per bollard.

Bolder Design Loads		
Eurocode	2 Lines	3 Lines
SLS	1.2xMBL	1.8xMBL
ULS	1.8xMBL	2.7xMBL
ALS	2xMBL	2.6xMBL

From these results it is clear that the ULS design load for a bollard 3 lines is governing. However, this design load is extremely conservative. Because it assumes that the 3 mooring lines, tied at the bollard, have all the same angle but in practice this is never the case. Therefore, the real acting load is always lower than the design load. It is clear that this lead to an over dimensioning of the bollards system and consequently to an increase of the costs. For this reason, the design can be optimized by proving that the acting loads at the project location are much lower than the MBL required design load.

Typical cross-section of the HbR's standard bollard adopted in the port of Rotterdam

Projectnummer : ntb
Projectnaam : Bolderbelastingen Standaardisatie Rotterdam
Status : Definitief 1.0

Bijlage C de nieuwe standaard HbR bolders

Invoegen tekening met maatvoering bolders en maattabel.

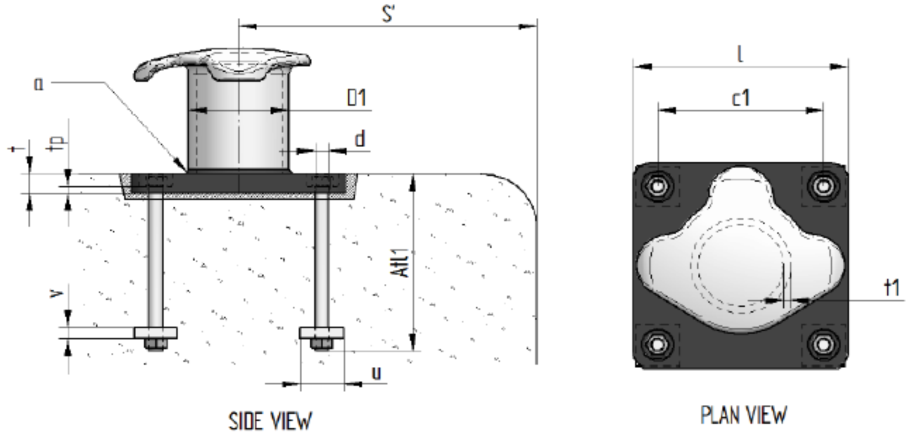

Bolder		**60**	**80**	**100**	**150**	**175**	
D_1	Buiten diameter schacht	350	350	350	350	350	mm
t_1	Wanddikte schacht	20	25	30	50	65	mm
a	Lasdikte	11	15	18	26	30	mm
l	ribbe voetplaat	750	750	750	750	750	mm
t, t_2	dikte voetplaat	70	80	90	100	100	mm
c_1	h.o.h. afstand ankers	580	565	565	550	550	mm
t_p	Dikte voetplaat bij ankers	23	25	35	40	40	mm
n / d	Diameter anker	48	56	56	64	64	mm
u	Ribbe ankerplaat	150	180	210	250	270	mm
v	Dikte ankerplaat	40	50	50	65	70	mm
Atl1	Lengte ankers	650	750	850	1100	1200	mm
ar' / S'	Min. afstand hart bolder vk. beton	500	550	600	700	700	mm

Hoogte van alle bolders van voetplaat tot bovenkant pet is 460 mm. Tot onderkant pet is het 390 mm. Ruim voldoende voor drie tails van 100 mm.

Appendix H: Wind speed

Parameters of the wind speed probability distribution functions for the different location in the Netherlands

Tabel 3.19 Gebruikte drempelwaarden POT series, omni-directioneel en richtingsafhankelijk (bron (Caires, 2009)).

Station \ Sector	omni-directional	345ºN - 15ºN	15ºN - 45ºN	45ºN - 75ºN	75ºN - 105ºN	105ºN - 135ºN	135ºN - 165ºN	165ºN - 195ºN	195ºN - 225ºN	225ºN - 255ºN	255ºN - 285ºN	285ºN - 315ºN	315ºN - 345ºN
Ijmuiden	18.3	12.9	10.6	11.9	10.6	8.3	9.5	14.4	16.3	16.2	17.0	15.7	13.9
Texelhors	18.0	15.3	9.7	11.5	10.4	10.4	10.8	14.8	15.1	14.8	15.3	17.1	14.8
De Kooy	16.9	10.7	10.3	9.5	8.9	9.5	10.9	13.8	17.8	17.5	16.8	14.8	11.7
Schiphol	16.6	8.4	9.7	9.2	8.3	6.9	9.4	11.2	12.9	17.2	14.0	14.0	11.3
De Bilt	11.6	8.6	7.4	7.9	6.8	7.5	8.0	9.0	11.5	11.0	9.4	9.5	7.5
Soesterberg	11.5	7.4	7.4	8.5	8.5	8.1	7.5	9.1	9.9	12.2	10.5	9.6	8.3
Leeuwarden	15.0	9.9	9.0	10.3	9.1	9.0	8.2	11.6	13.5	14.6	14.0	14.6	12.1
Deelen	13.4	8.7	8.3	9.1	8.2	9.0	9.0	10.0	11.2	12.5	10.3	9.8	9.9
Lauwersoog	15.9	11.9	11.8	12.0	12.5	10.8	10.4	12.5	14.1	15.9	15.5	14.8	14.9
Eelde	15.3	7.3	8.3	8.4	8.0	7.8	7.5	10.0	12.6	13.2	12.2	10.6	9.7
Twente	12.1	6.5	6.3	6.7	6.8	5.6	7.2	10.0	10.9	11.0	9.8	9.4	7.4
Cadzand	16.9	13.4	11.6	11.3	10.3	7.0	7.8	11.6	15.3	17.9	15.5	12.8	12.7
Vlissingen	17.0	9.2	10.3	9.2	7.9	8.8	9.7	13.1	14.3	16.9	15.4	13.5	10.4
L.E. Goeree	16.3	11.7	11.8	8.8	9.9	8.9	10.7	14.4	13.5	15.4	14.5	14.6	12.4
Hoek van Holland	17.3	14.4	12.9	11.0	9.1	9.3	10.0	13.8	16.0	17.0	17.0	15.3	16.7
Zestienhoven	14.5	9.2	8.2	9.4	8.1	7.4	8.4	11.1	13.7	13.5	13.1	13.1	10.2
Gilze-Rijen	12.1	7.6	7.9	9.2	7.3	7.1	7.1	9.9	10.7	12.9	11.1	10.9	7.8
Herwijnen	15.0	8.2	7.3	6.9	8.0	7.3	8.4	9.3	13.6	15.1	14.6	11.4	8.1
Eindhoven	13.3	7.4	7.1	8.1	7.1	8.1	7.0	9.2	11.2	12.2	13.4	11.0	8.6
Volkel	13.0	6.6	6.8	9.0	8.0	8.3	6.4	8.3	11.9	11.1	11.5	8.5	6.7
Beek	14.4	6.9	7.2	8.6	7.5	6.6	6.0	10.0	13.1	15.7	10.0	9.1	7.8

Tabel 3.20 Schattingen van de parameter $\hat{\lambda}_u$ van de exponentiële verdeling (bron (Caires, 2009)).

Station \ Sector	omni-directional	345ºN - 15ºN	15ºN - 45ºN	45ºN - 75ºN	75ºN - 105ºN	105ºN - 135ºN	135ºN - 165ºN	165ºN - 195ºN	195ºN - 225ºN	225ºN - 255ºN	255ºN - 285ºN	285ºN - 315ºN	315ºN - 345ºN
Ijmuiden	3.45	3.05	5.15	2.10	3.61	4.77	5.02	2.56	4.83	3.96	2.51	2.86	3.32
Texelhors	4.31	1.84	6.77	3.10	5.81	5.03	4.31	3.88	6.44	7.04	5.39	2.35	4.06
De Kooy	4.04	2.54	2.48	4.80	5.21	2.59	2.05	1.99	1.39	1.45	1.91	2.73	3.76
Schiphol	2.99	6.24	2.65	4.59	3.20	6.80	3.23	3.17	4.30	1.78	2.94	1.89	2.73
De Bilt	6.04	1.67	4.61	3.13	4.93	3.05	2.62	3.68	3.02	4.93	5.75	2.44	4.45
Soesterberg	6.60	5.74	4.58	2.13	2.26	2.32	5.42	2.48	5.66	2.96	6.06	4.63	5.33
Leeuwarden	4.52	3.82	3.77	2.03	3.22	2.60	5.51	2.75	2.52	2.83	3.09	1.71	3.09
Deelen	4.01	2.64	3.80	2.66	3.98	1.18	2.85	3.71	5.11	4.04	7.00	5.46	2.48
Lauwersoog	7.24	4.76	2.92	2.94	1.67	1.95	1.98	3.54	4.68	2.78	3.77	3.38	2.63
Eelde	2.54	7.50	3.88	3.20	3.57	2.69	4.78	4.97	3.33	4.84	4.60	4.49	4.23
Twenty	3.99	6.08	5.81	6.27	4.68	7.15	2.72	2.97	3.82	3.41	5.61	4.60	6.74
Cadzand	5.14	2.13	3.85	2.78	2.16	4.97	6.34	4.91	2.72	2.27	3.48	7.33	4.80
Vlissingen	3.43	4.17	1.39	3.38	5.46	3.14	3.38	3.07	3.38	2.71	2.60	2.06	3.38
L.E. Goeree	5.89	5.34	3.40	8.36	3.11	5.54	3.56	2.20	8.87	5.08	5.25	3.76	5.76
Hoek van Holland	4.09	2.08	2.45	3.25	4.14	3.44	4.50	2.60	2.24	2.16	1.90	3.62	1.09
Zestienhoven	5.72	4.34	5.67	1.86	3.59	4.92	4.60	4.79	3.22	6.20	4.12	2.55	4.95
Gilze-Rijen	6.66	5.32	4.50	2.27	5.08	4.14	5.48	4.37	5.85	2.21	4.98	3.11	6.85
Herwijnen	3.40	3.92	5.46	5.58	4.04	4.15	2.64	5.58	2.09	2.41	1.92	3.81	7.50
Eindhoven	4.43	5.30	6.54	3.74	4.74	1.71	4.74	4.66	5.88	4.32	2.16	2.98	4.85
Volkel	3.88	5.52	5.46	2.43	3.33	1.48	6.99	6.83	3.96	6.72	3.25	4.48	6.23
Beek	3.18	5.66	6.18	1.89	4.63	2.03	6.16	4.10	4.47	1.29	5.76	3.76	3.50

Tabel 3.21 Schattingen van de parameter σ van de exponentiele verdeling, omni-directioneel en richtingsafhankelijk (bron Caires, 2009)

Station \ Sector	omni-directional
IJmuiden	1.65 (1.40, 1.93)
Texelhors	1.95 (1.63, 2.30)
De Kooy	2.03 (1.72, 2.36)
Schiphol	1.86 (1.53, 2.20)
De Bilt	1.80 (1.57, 2.04)
Soesterberg	2.03 (1.78, 2.28)
Leeuwarden	2.13 (1.81, 2.46)
Deelen	1.97 (1.68, 2.29)
Lauwersoog	1.82 (1.61, 2.03)
Eelde	1.90 (1.54, 2.29)
Twenthe	2.09 (1.76, 2.43)
Cadzand	1.90 (1.63, 2.19)
Vlissingen	1.76 (1.47, 2.05)
L.E. Goeree	1.76 (1.55, 2.00)
Hoek van Holland	1.65 (1.43, 1.90)
Zestienhoven	1.96 (1.71, 2.22)
Gilze-Rijen	1.88 (1.66, 2.11)
Herwijnen	2.05 (1.71, 2.44)
Eindhoven	1.65 (1.41, 1.90)
Volkel	1.93 (1.61, 2.26)
Beek	1.77 (1.49, 2.08)

Station \ Sector	345°N -15°N	15°N -45°N	45°N -75°N	75°N -105°N	105°N -135°N	135°N -165°N
IJmuiden	1.56 (1.32, 1.87)	1.44 (1.23, 1.66)	1.22 (0.96, 1.50)	1.40 (1.19, 1.62)	1.17 (1.01, 1.35)	1.57 (1.36, 1.80)
Texelhors	1.59 (1.24, 1.97)	2.01 (1.77, 2.28)	1.53 (1.24, 1.81)	1.78 (1.55, 2.01)	1.58 (1.36, 1.81)	1.95 (1.65, 2.26)
De Kooy	1.90 (1.53, 2.31)	1.92 (1.57, 2.30)	2.00 (1.71, 2.32)	1.71 (1.48, 1.94)	1.18 (0.95, 1.45)	1.36 (1.07, 1.65)
Schiphol	1.70 (1.50, 1.91)	1.23 (1.01, 1.48)	1.38 (1.19, 1.57)	1.30 (1.11, 1.52)	1.08 (0.95, 1.20)	1.09 (0.92, 1.29)
De Bilt	0.97 (0.76, 1.22)	1.19 (1.02, 1.37)	1.28 (1.07, 1.49)	1.26 (1.10, 1.43)	1.04 (0.87, 1.22)	0.94 (0.77, 1.14)
Soesterberg	1.12 (0.99, 1.27)	1.00 (0.86, 1.15)	0.76 (0.60, 0.92)	0.95 (0.78, 1.14)	0.69 (0.57, 0.83)	0.86 (0.76, 0.97)
Leeuwarden	1.72 (1.48, 1.99)	1.40 (1.18, 1.60)	1.85 (1.43, 2.34)	1.45 (1.22, 1.70)	0.98 (0.81, 1.16)	1.37 (1.20, 1.55)
Deelen	1.10 (0.89, 1.29)	1.10 (0.95, 1.27)	1.17 (0.96, 1.39)	1.14 (0.98, 1.33)	0.96 (0.70, 1.24)	1.05 (0.87, 1.24)
Lauwersoog	1.80 (1.56, 2.02)	1.39 (1.15, 1.65)	1.42 (1.18, 1.67)	1.26 (1.00, 1.54)	0.99 (0.78, 1.22)	1.26 (1.00, 1.55)
Eelde	1.35 (1.21, 1.49)	1.03 (0.87, 1.19)	1.26 (1.06, 1.48)	1.09 (0.93, 1.27)	0.96 (0.77, 1.15)	1.32 (1.14, 1.51)
Twenthe	1.08 (0.95, 1.22)	1.13 (0.98, 1.31)	0.99 (0.88, 1.12)	0.91 (0.79, 1.04)	0.93 (0.83, 1.03)	1.13 (0.93, 1.34)
Cadzand	1.93 (1.53, 2.36)	1.23 (1.03, 1.43)	1.41 (1.15, 1.67)	1.42 (1.13, 1.76)	1.21 (1.04, 1.39)	1.58 (1.38, 1.78)
Vlissingen	1.30 (1.11, 1.50)	0.95 (0.74, 1.17)	1.23 (1.05, 1.43)	1.32 (1.16, 1.49)	1.35 (1.14, 1.55)	1.40 (1.20, 1.62)
L.E. Goeree	1.74 (1.50, 1.98)	1.45 (1.18, 1.72)	1.78 (1.58, 1.98)	1.53 (1.19, 1.94)	1.47 (1.28, 1.68)	1.28 (1.07, 1.48)
Hoek van Holland	1.44 (1.14, 1.74)	1.54 (1.25, 1.87)	1.35 (1.13, 1.59)	1.26 (1.09, 1.44)	1.22 (1.03, 1.42)	1.34 (1.15, 1.53)
Zestienhoven	1.59 (1.36, 1.80)	1.45 (1.27, 1.64)	0.89 (0.71, 1.08)	1.10 (0.93, 1.29)	1.02 (0.87, 1.19)	1.22 (1.06, 1.40)
Gilze-Rijen	1.31 (1.15, 1.49)	1.19 (1.01, 1.36)	1.09 (0.89, 1.31)	1.30 (1.14, 1.47)	1.02 (0.87, 1.16)	1.03 (0.90, 1.17)
Herwijnen	1.28 (1.08, 1.47)	1.35 (1.18, 1.53)	1.46 (1.27, 1.66)	1.31 (1.09, 1.55)	1.21 (1.03, 1.42)	1.11 (0.90, 1.32)
Eindhoven	1.26 (1.11, 1.43)	1.11 (0.99, 1.24)	1.16 (1.00, 1.33)	1.06 (0.93, 1.20)	0.94 (0.72, 1.16)	1.00 (0.86, 1.13)
Volkel	0.99 (0.86, 1.12)	1.02 (0.90, 1.15)	1.00 (0.82, 1.22)	1.11 (0.92, 1.29)	0.81 (0.62, 1.03)	1.13 (1.00, 1.26)
Beek	1.20 (1.06, 1.35)	1.15 (1.02, 1.28)	0.86 (0.68, 1.07)	1.19 (1.03, 1.36)	1.21 (0.95, 1.51)	1.38 (1.22, 1.55)

Station \ Sector	165°N -195°N	195°N -225°N	225°N -255°N	255°N -285°N	285°N -315°N	315°N -345°N
IJmuiden	1.52 (1.23, 1.82)	1.74 (1.51, 1.97)	1.99 (1.72, 2.31)	1.83 (1.51, 2.20)	1.74 (1.43, 2.06)	1.83 (1.56, 2.12)
Texelhors	1.63 (1.36, 1.92)	1.82 (1.60, 2.06)	2.17 (1.91, 2.45)	2.11 (1.80, 2.44)	1.98 (1.55, 2.48)	1.81 (1.49, 2.16)
De Kooy	1.65 (1.31, 2.01)	1.34 (0.99, 1.74)	1.58 (1.21, 1.97)	2.06 (1.65, 2.55)	1.88 (1.54, 2.27)	2.21 (1.86, 2.58)
Schiphol	1.39 (1.16, 1.64)	1.89 (1.62, 2.19)	1.78 (1.37, 2.24)	2.08 (1.72, 2.45)	1.95 (1.56, 2.37)	1.89 (1.54, 2.26)
De Bilt	1.21 (1.02, 1.40)	1.50 (1.27, 1.77)	2.00 (1.71, 2.26)	2.08 (1.83, 2.34)	1.70 (1.36, 2.07)	1.52 (1.30, 1.77)
Soesterberg	1.09 (0.90, 1.30)	1.46 (1.29, 1.66)	2.03 (1.68, 2.41)	2.02 (1.76, 2.30)	1.75 (1.50, 2.00)	1.43 (1.23, 1.64)
Leeuwarden	1.45 (1.21, 1.71)	2.04 (1.67, 2.45)	1.98 (1.64, 2.33)	2.12 (1.78, 2.51)	1.84 (1.41, 2.37)	2.01 (1.67, 2.39)
Deelen	1.21 (1.02, 1.40)	1.41 (1.24, 1.59)	2.02 (1.74, 2.33)	2.10 (1.84, 2.37)	1.89 (1.64, 2.17)	1.30 (1.07, 1.56)
Lauwersoog	1.58 (1.35, 1.81)	1.94 (1.68, 2.21)	1.89 (1.59, 2.24)	1.89 (1.59, 2.20)	1.90 (1.60, 2.21)	1.66 (1.36, 1.99)
Eelde	1.35 (1.17, 1.54)	1.70 (1.42, 1.98)	1.93 (1.66, 2.19)	1.92 (1.65, 2.21)	1.85 (1.59, 2.13)	1.44 (1.23, 1.68)
Twenthe	1.17 (0.96, 1.39)	1.27 (1.08, 1.48)	2.02 (1.66, 2.37)	2.06 (1.79, 2.36)	1.96 (1.68, 2.25)	1.30 (1.14, 1.47)
Cadzand	1.62 (1.43, 1.84)	1.63 (1.32, 1.94)	1.70 (1.35, 2.09)	2.04 (1.74, 2.39)	2.13 (1.89, 2.37)	1.89 (1.63, 2.16)
Vlissingen	1.48 (1.23, 1.75)	1.50 (1.27, 1.76)	1.83 (1.49, 2.19)	1.93 (1.58, 2.30)	1.71 (1.37, 2.07)	1.57 (1.31, 1.83)
L.E. Goeree	1.13 (0.88, 1.38)	1.72 (1.51, 1.92)	1.81 (1.53, 2.10)	1.96 (1.68, 2.24)	1.90 (1.61, 2.20)	2.06 (1.78, 2.34)
Hoek van Holland	1.39 (1.15, 1.65)	1.24 (1.01, 1.48)	1.69 (1.38, 2.04)	1.80 (1.43, 2.21)	1.84 (1.56, 2.14)	1.42 (1.03, 1.86)
Zestienhoven	1.30 (1.14, 1.48)	1.39 (1.16, 1.63)	1.96 (1.72, 2.20)	2.14 (1.83, 2.47)	2.15 (1.70, 2.63)	2.00 (1.73, 2.28)
Gilze-Rijen	1.45 (1.23, 1.69)	1.61 (1.42, 1.80)	2.02 (1.64, 2.46)	2.02 (1.76, 2.29)	1.94 (1.63, 2.27)	1.32 (1.17, 1.49)
Herwijnen	1.42 (1.25, 1.62)	1.34 (1.04, 1.64)	1.96 (1.56, 2.36)	2.19 (1.71, 2.67)	2.14 (1.77, 2.52)	1.69 (1.51, 1.89)
Eindhoven	1.17 (1.01, 1.35)	1.52 (1.34, 1.68)	1.74 (1.50, 1.99)	1.68 (1.35, 2.04)	1.79 (1.47, 2.15)	1.40 (1.21, 1.59)
Volkel	1.36 (1.21, 1.53)	1.49 (1.26, 1.74)	1.96 (1.73, 2.20)	2.08 (1.70, 2.48)	1.93 (1.65, 2.24)	1.24 (1.07, 1.40)
Beek	1.43 (1.22, 1.64)	1.34 (1.17, 1.52)	1.56 (1.18, 1.94)	2.10 (1.84, 2.38)	1.70 (1.43, 1.98)	1.28 (1.09, 1.50)

Wind speeds with different return periods for each wind direction of the Zestienhoven

Wind direction	0°N	30°N	60°N	90°N	120°N	150°N	180°N	210°N	240°N	270°N	300°N	330°N
Wind speed with a return period of 1 year	11.5 m/s	10.7 m/s	10.0 m/s	9.5 m/s	9.0 m/s	10.3 m/s	13.1 m/s	15.3 m/s	17.1 m/s	16.1 m/s	15.1 m/s	13.4 m/s
Wind speed with a return period of 10 years	15.2 m/s	14.1 m/s	12.0 m/s	12.0 m/s	11.4 m/s	13.1 m/s	16.1 m/s	18.5 m/s	21.6 m/s	21.1 m/s	20.1 m/s	18.0 m/s
Wind speed with a return period of 25 years	16.7 m/s	15.4 m/s	12.8 m/s	13.0 m/s	12.3 m/s	14.2 m/s	17.3 m/s	19.8 m/s	23.4 m/s	23.0 m/s	22.0 m/s	19.8 m/s
Wind speed with a return period of 50 years	17.8 m/s	16.4 m/s	13.4 m/s	13.8 m/s	13.0 m/s	15.0 m/s	18.2 m/s	20.8 m/s	24.7 m/s	24.5 m/s	23.5 m/s	21.2 m/s
Wind speed with a return period of 100 years	18.9 m/s	17.4 m/s	14.1 m/s	14.6 m/s	13.7 m/s	15.9 m/s	19.1 m/s	21.7 m/s	26.1 m/s	26.0 m/s	25.0 m/s	22.6 m/s

Appendix I: Static mooring analysis in MatrixFrame

Wind loading direction 150°N:

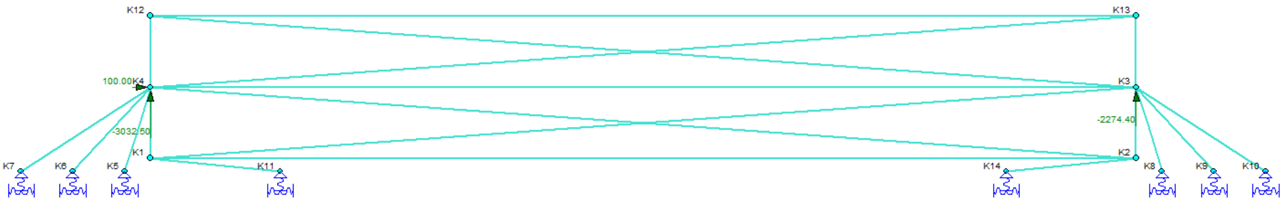

Wind loading direction 180°N:

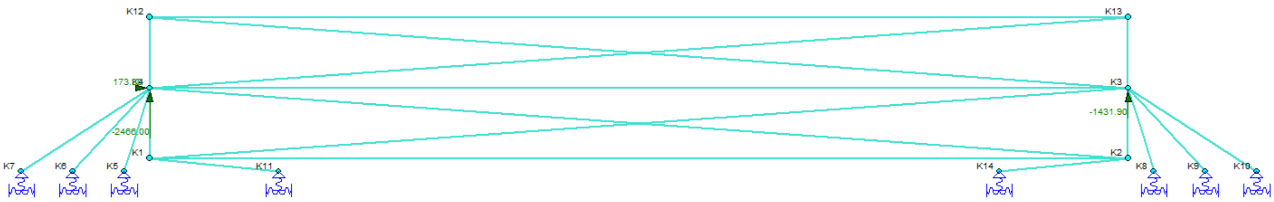

Spring support reactions with wind loading direction 150°N:

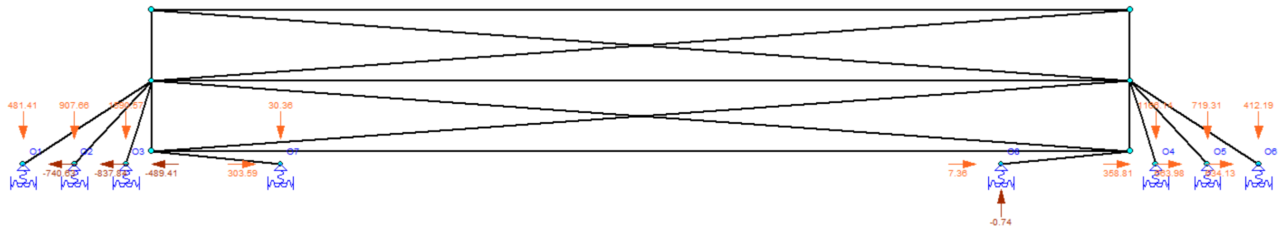

Spring support reactions with wind loading direction 180°N:

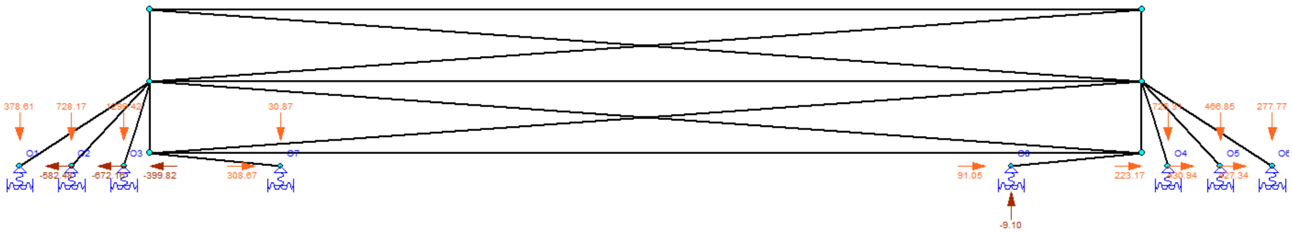

Wind loading direction 150°N without spring line at the stern:

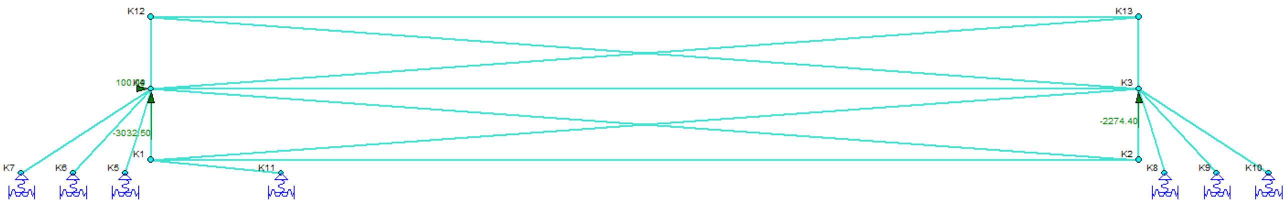

Wind loading direction 180°N without spring line at the stern:

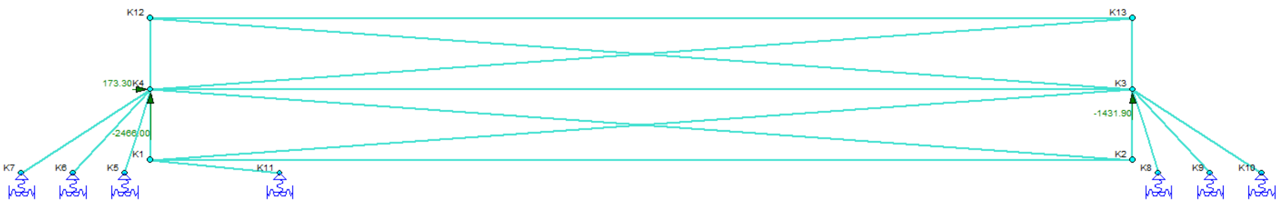

Spring support reactions with wind loading direction 150°N without spring line at the stern:

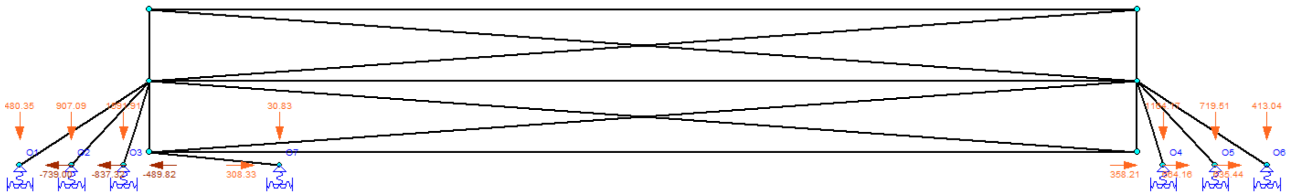

Spring support reactions with wind loading direction 150°N without spring line at the stern:

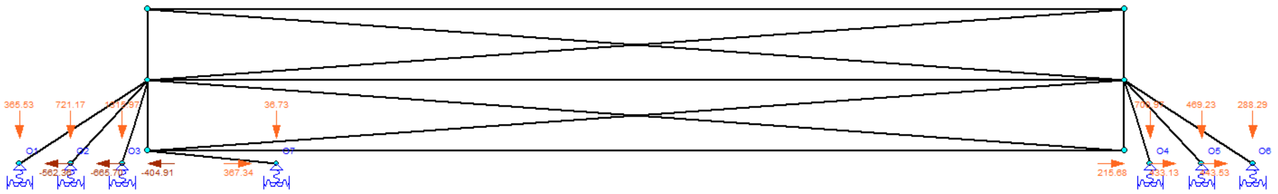

Appendix J: Geotechnical input parameters

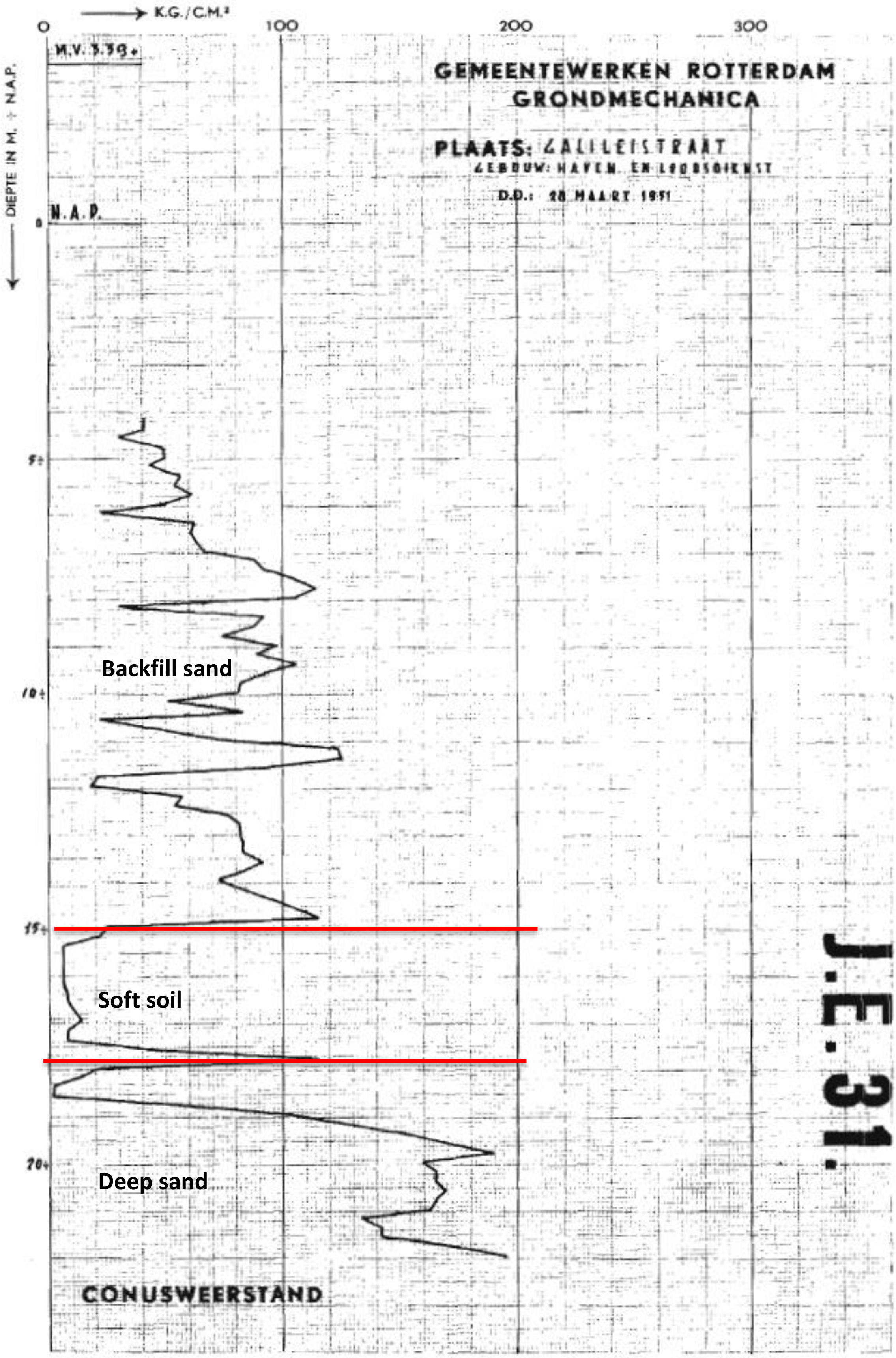

Stiffness parameters according to Manual Hydraulic Structures for sand material

The Young's modulus *E* results from:

$$E_{oed} = \frac{(1-\nu)}{(1+\nu)(1-2\nu)}E$$

with:

E_{oed} = constrained modulus (*modulus bij zijdelingse opsluiting*):

$$E_{oed} = 4q_c \qquad 0 < q_c < 10 \text{ MPa}$$
$$= 2q_c + 20 \text{ MPa} \qquad \text{for:} \qquad 10 < q_c < 50 \text{ MPa}$$
$$= 120 \text{ MPa} \qquad 50 \text{ MPa} < q_c$$

ν [-] = Poisson's ratio (*dwarscontractiecoëfficiënt*): ν = 0,3

From the above CPT the cone resistances (q_c) of the sand layers are obtained:

$$q_{c,backfillsand} = 10 \text{ MPa}$$
$$q_{c,deepsand} = 20 \text{ MPa}$$

Consequently, rewriting the above equations the Young's modulus of the sand layers are equal:

$$E_{backfill} = E_{eod,backfill}\frac{(1+\nu)(1-2\nu)}{(1-\nu)} = 40 \cdot 0.74 = 29.6 \text{ MPa}$$

$$E_{deepsand} = E_{eod,deepsand}\frac{(1+\nu)(1-2\nu)}{(1-\nu)} = 60 \cdot 0.74 = 44.4 \text{ MPa}$$

Stiffness parameters according to CUR2003-7 for sand material

- richtwaarde uit sondering voor zand (OCR=1) : $E_{oed} \approx 3\ q_c$ waarbij $E_{50} \approx 2/3\ E_{oed}$;
- richtwaarde uit sondering voor zand (OCR>1): $E_{oed} \approx 5\ q_c$ waarbij $E_{50} \approx 2/3\ E_{oed}$;
- bij belasten geldt $E \approx E_{50}$;
- bij ontlasten geldt $E > E_{50}$;

Assuming for both sand layers an OCR equal to one (conservative assumption) the Young's modulus of the sand layers are approximately:

$$E_{backfill} = \frac{2}{3}E_{eod,backfill} = \frac{2}{3}\cdot 3 \cdot q_{c,backfillsand} = 20 \text{ MPa}$$

$$E_{deepsand} = \frac{2}{3}E_{eod,deepsand} = \frac{2}{3}\cdot 3 \cdot q_{c,deepsand} = 40 \text{ MPa}$$

The two methods provides different values for the Young's modulus of the sand layers therefore, an average between the two values is chosen, which works out as conservative considerations. The average values are computed as shown below:

$$E_{backfill} = (29.6 + 20)/2 \approx 25 \text{ MPa}$$
$$E_{deepsand} = (44.4 + 40)/2 \approx 42 \text{ MPa}$$

Stiffness parameters according to Manual Hydraulic Structures for soft soil materials

$$c_u = f_{undr} = \frac{q_c}{20} \qquad \text{(clay/loam)}$$

$$c_u = f_{undr} = \frac{q_c}{30} \qquad \text{(peat, humous clay)}$$

$$E_u \approx E = 100 \cdot f_{undr} \qquad \text{(clay/peat)}$$

$$E_u \approx E = 40 \cdot f_{undr} \qquad \text{(loam)}$$

$$\nu = 0{,}4$$

The cone resistance (q_c) of the soft soil layer is approximately 0.7 MPa consequently Young's modulus of the soft soil layer is equal to:

$$E_{softsoil} = 100 \frac{q_{c,softsoil}}{20} = 3.5 \text{ MPa}$$

Stiffness parameters according to CUR2003-7 for soft soil materials

– $E_{undr;50} \approx 15000\ C_u / I_p$ met I_p [%], er dient nog wel een omrekening plaats te vinden naar een effectieve E_{50}.

The above formula depends on the Plasticity Index of the soft soil layer. However, this parameter is not available and consequently the stiffness parameter cannot be computed. Hence, the Young's modulus of the soft soil layer according to the Manual Hydraulic Structures is chosen.

Friction and dilatancy angles for sand materials

The friction and the dilatancy angles for sand can be estimated by the using the following formulas:

$$\phi' = 29^\circ + \frac{q_c}{4\ \text{MPa}/^\circ}$$

$$\psi = \varphi' - 30^\circ$$

The friction and the dilatancy angles of the backfill soil and deep sand are equal to:

$$\varphi_{backfill} = 31.5^o$$

$$\psi_{backfill} = 1.5^o$$

$$\varphi_{deepsand} = 34^o$$

$$\psi_{deepsand} = 4^o$$

These values are at the high side, leading to a favorable condition. In order to make a more conservative design these values are lowered to the following values:

$$\varphi_{backfill} = 30^o$$

$$\psi_{backfill} = 0^o$$

$$\varphi_{deepsand} = 32^o$$

$$\psi_{deepsand} = 2^o$$

Appendix K: PLAXIS results

Effect of the acting loads on the quay wall displacement

Total deformation of the caisson without soft soil layer with the application of the quay wall surcharge equal to 30 kN/m

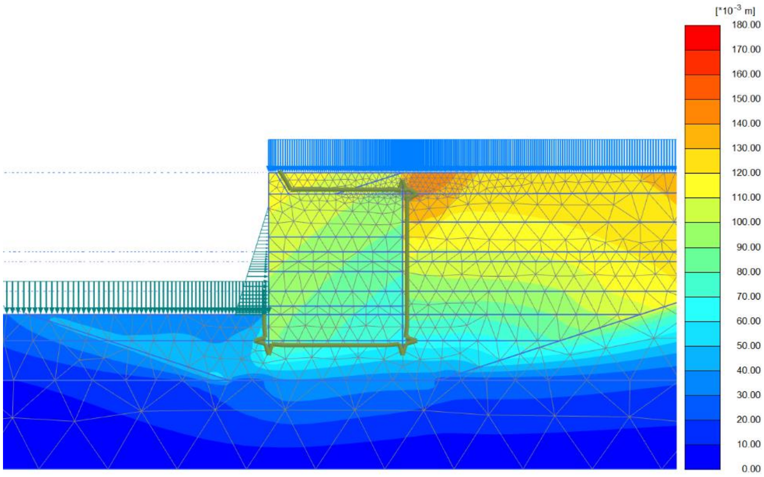

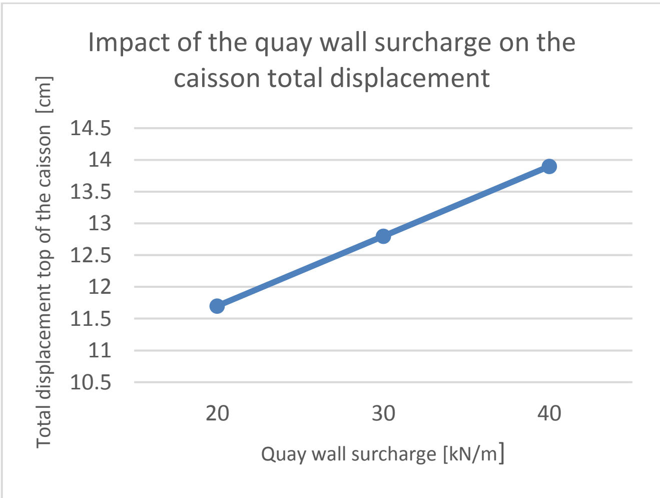

Total deformation of the caisson without the soft soil layer with the application of the bollard force equal to 33.3 kN/m

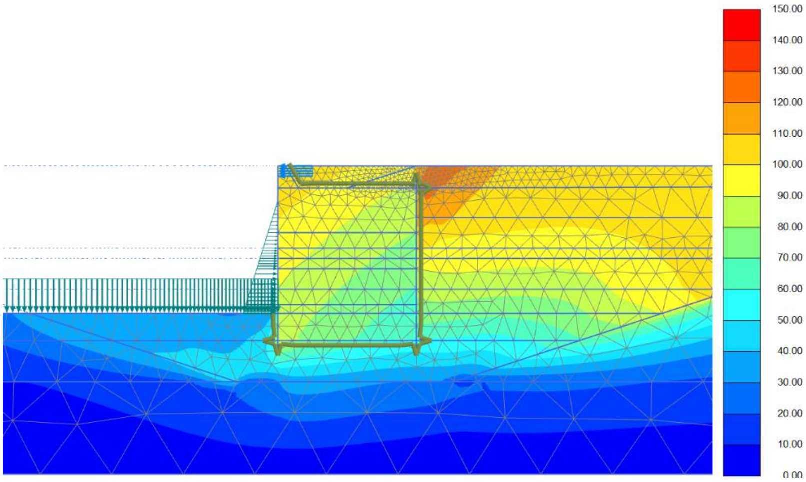

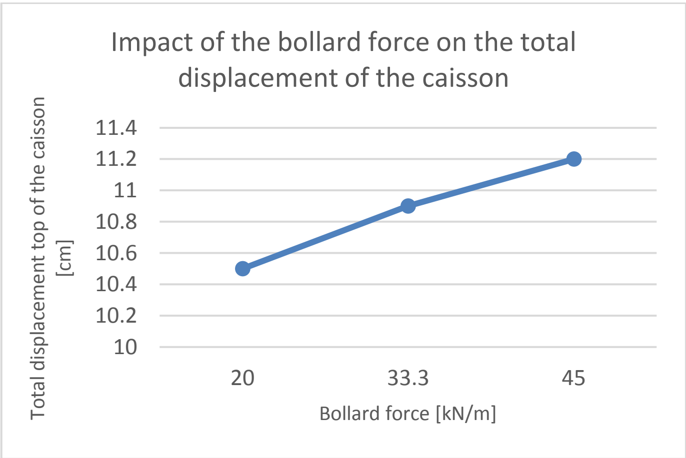

Total deformation of the caisson without the soft soil layer with the application of the water head difference equal to 1.2 m

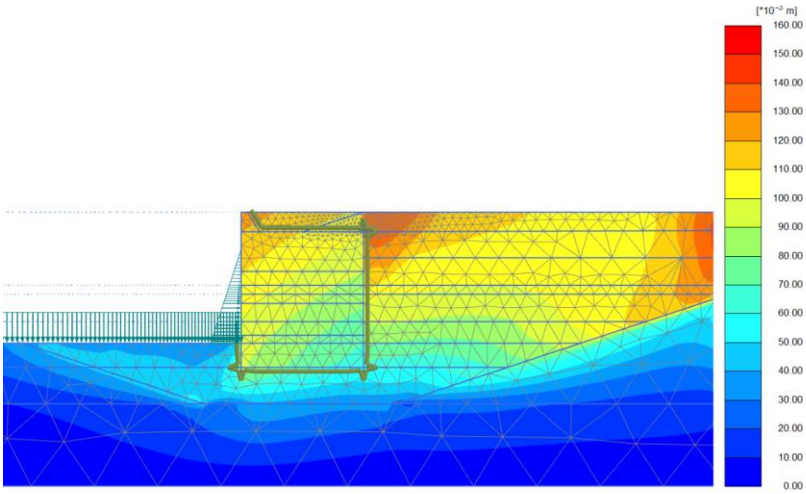

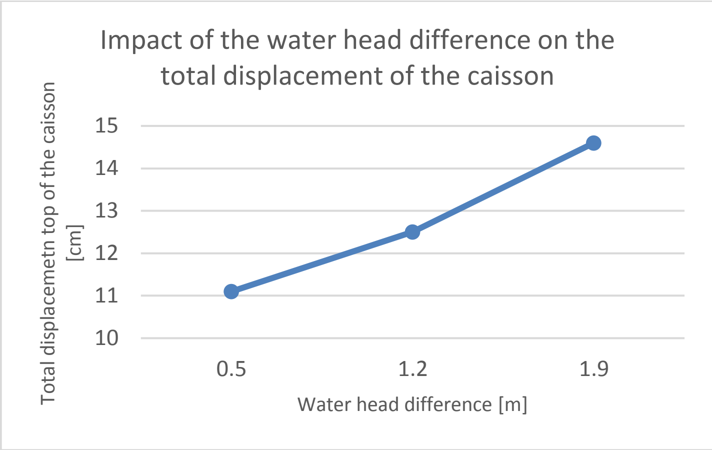

Effective principal stresses at foundation level of the caisson in the current situation

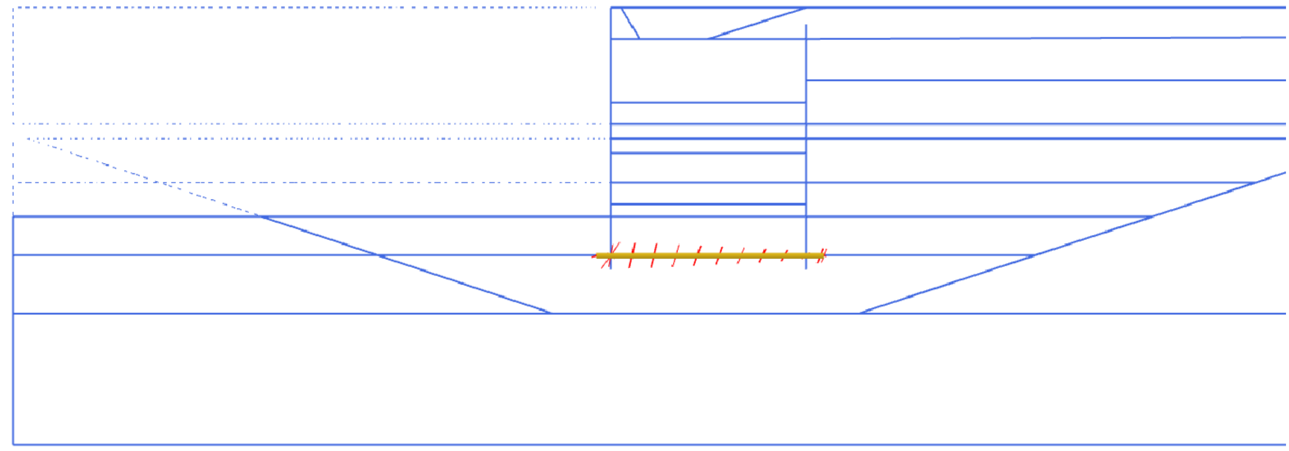

Effective principal stresses (scaled up $5.00*10^{-3}$ times)

Maximum value = -9.742 kN/m² (Element 1647 at Stress point 19755)

Minimum value = -403.2 kN/m² (Element 1621 at Stress point 19442)

Effect of the geotechnical parameters on the quay wall displacement

Geotechnical input parameter	Value	Displacement top of the quay wall (cm)	Variation in the Displacement (%)
Caisson in the current situation	-	19	-
Dry and saturated volumetric weight of the backfill soil	17 and 19 kN/m^3	19	0
	19 and 21 kN/m^3	19	0
Friction angle of the backfill soil	27°	22	+15.8
	33°	15	-21.1
Young's modulus of the backfill soil	32.5 MPa	19	0
	40 MPa	19	0
Saturated volumetric weight of the foundation soil	19 kN/m^3	19	0
	21 kN/m^3	18	-5.3
Friction angle of the foundation soil	27°	21	+10.5
	33°	16	-15.8
Young's modulus of the foundation soil	32.5 MPa	16	-15.8
	40 MPa	15	-21.1
Saturated volumetric weight of the deep sand	19 kN/m^3	19	0
	21 kN/m^3	18	0
Friction angle of the deep sand	30°	20	+5.3
	34°	18	-5.3
Young's modulus of the deep sand the caisson	48 MPa	18	-5.3
	55 MPa	17	-10.5
Saturated volumetric weight of the soft soil layer	16 kN/m^3	19	0
	20 kN/m^3	19	0
Friction angle of the soft soil layer	20°	18	-5.3
	25°	19	0
Cohesion of the soft soil layer	2 kN/m^2	18	+5.3
	8 kN/m^2	19	0
Young's modulus of the soft soil layer	2 MPa	20	+5.3
	5 MPa	18	-5.3

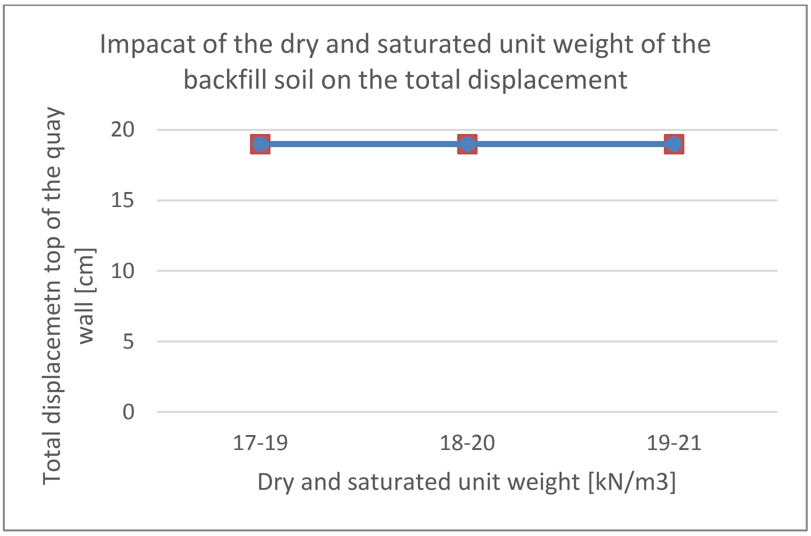
Impacat of the dry and saturated unit weight of the backfill soil on the total displacement
Total displacemetn top of the quay wall [cm]
20
15
10
5
0
17-19
18-20
19-21
Dry and saturated unit weight [kN/m3]

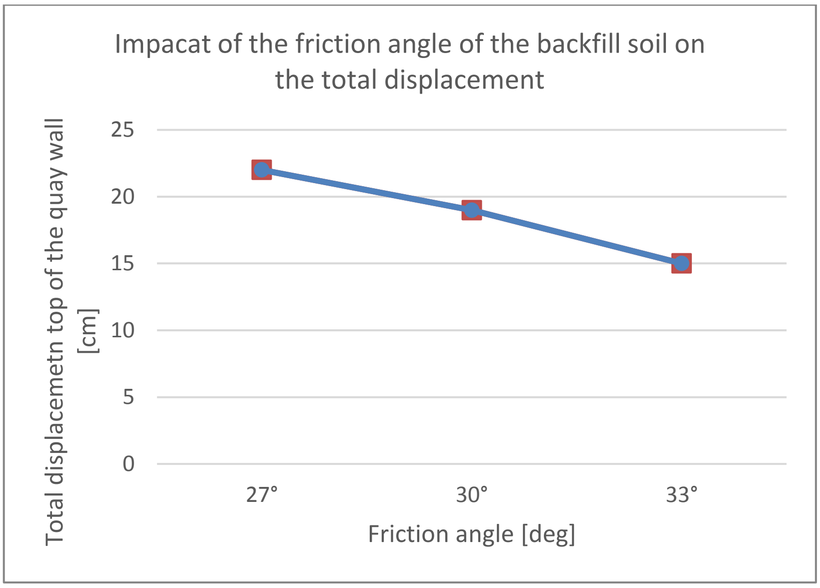
Impacat of the friction angle of the backfill soil on the total displacement
Total displacemetn top of the quay wall [cm]
25
20
15
10
5
0
27°
30°
33°
Friction angle [deg]

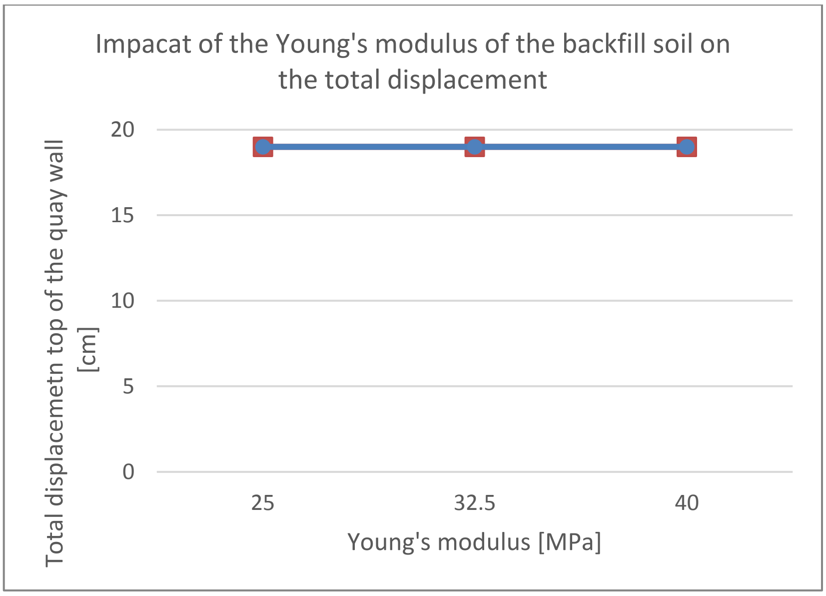
Impacat of the Young's modulus of the backfill soil on the total displacement
Total displacemetn top of the quay wall [cm]
20
15
10
5
0
25
32.5
40
Young's modulus [MPa]

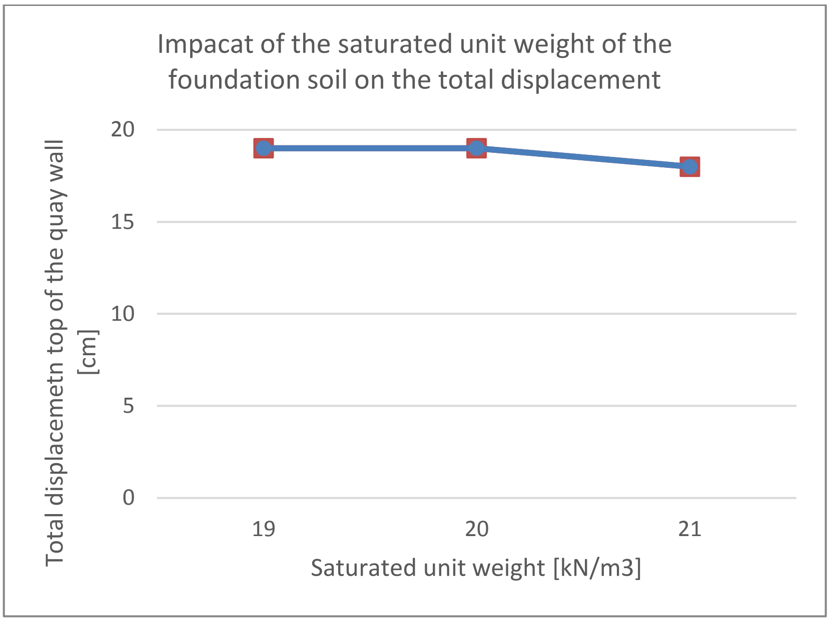
Impacat of the saturated unit weight of the foundation soil on the total displacement
Total displacemetn top of the quay wall [cm]
20
15
10
5
0
19
20
21
Saturated unit weight [kN/m3]

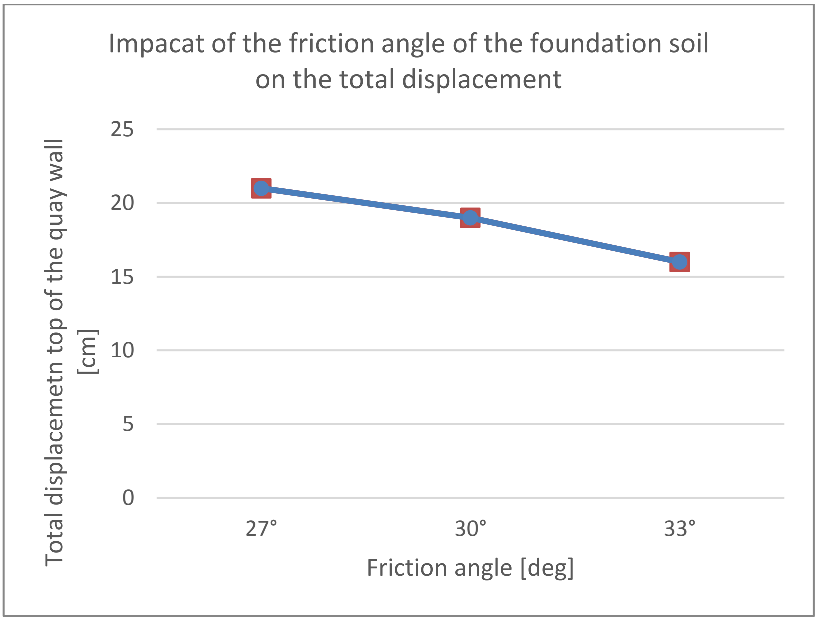
Impacat of the friction angle of the foundation soil on the total displacement
Total displacemetn top of the quay wall [cm]
25
20
15
10
5
0
27°
30°
33°
Friction angle [deg]

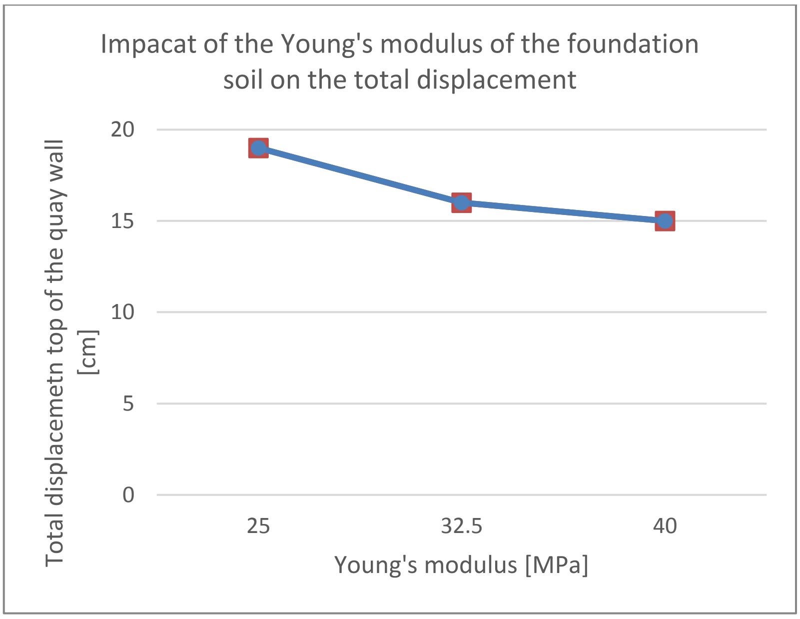
Impacat of the Young's modulus of the foundation soil on the total displacement
Total displacemetn top of the quay wall [cm]
20
15
10
5
0
25
32.5
40
Young's modulus [MPa]

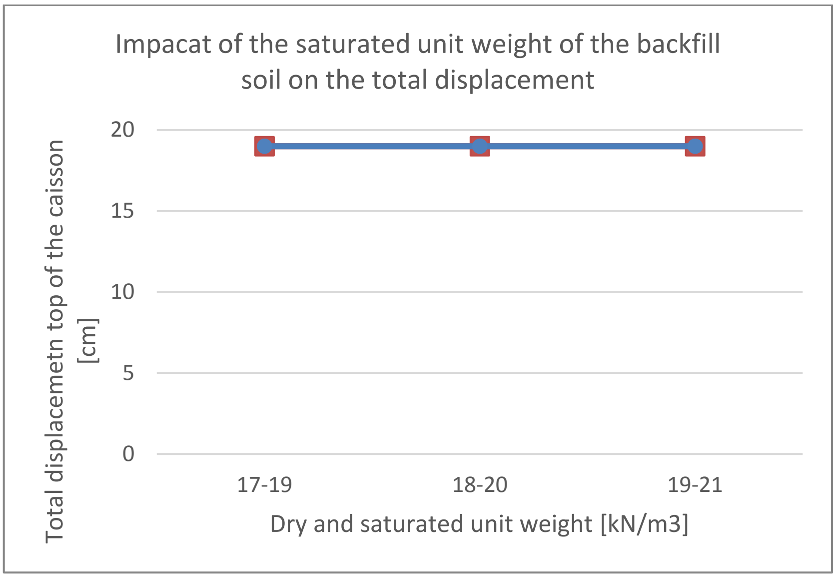

Impacat of the saturated unit weight of the backfill soil on the total displacement
Total displacemetn top of the caisson [cm]
20
15
10
5
0
17-19
18-20
19-21
Dry and saturated unit weight [kN/m3]

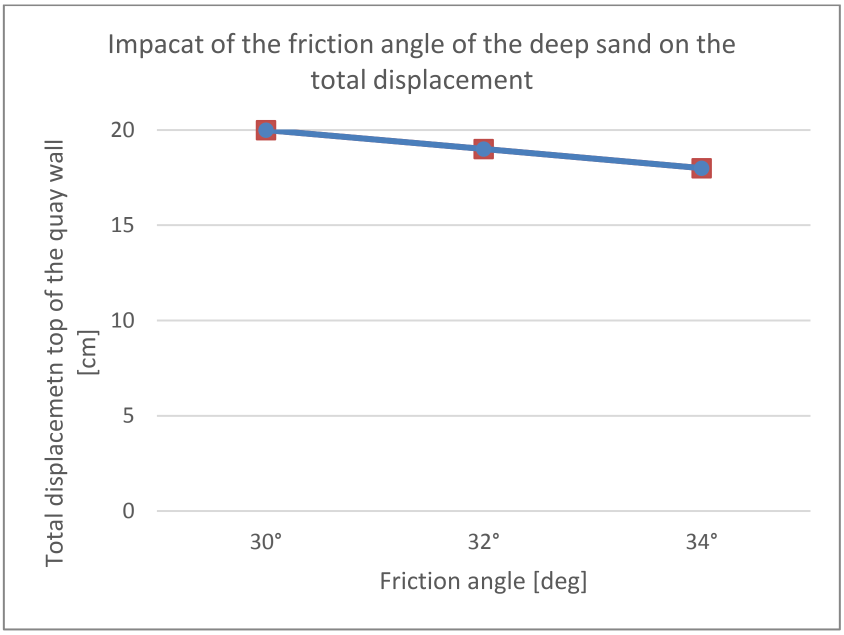

Impacat of the friction angle of the deep sand on the total displacement
Total displacemetn top of the quay wall [cm]
20
15
10
5
0
30°
32°
34°
Friction angle [deg]

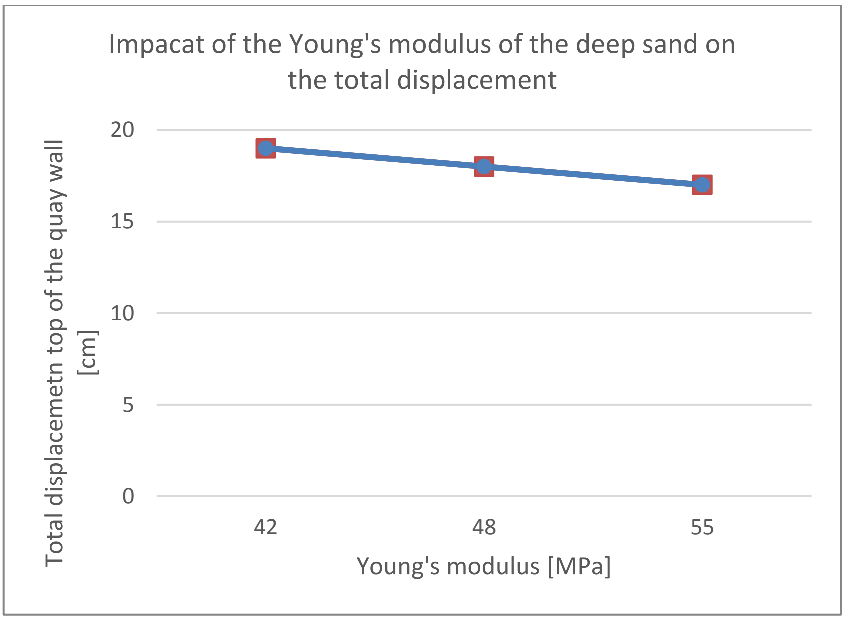

Impacat of the Young's modulus of the deep sand on the total displacement
Total displacemetn top of the quay wall [cm]
20
15
10
5
0
42
48
55
Young's modulus [MPa]

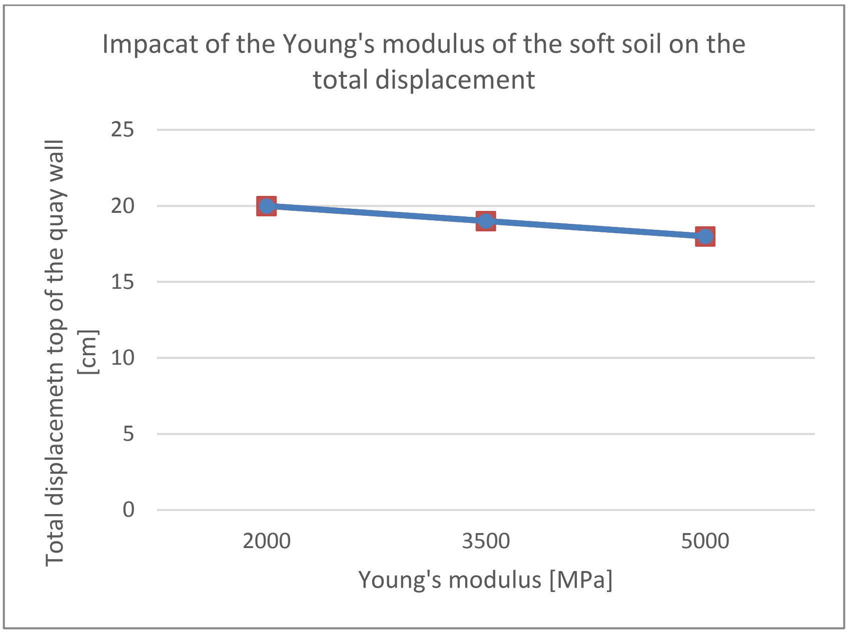

Overall scaled 50 times displacement of the design option with underwater sheet pile wall

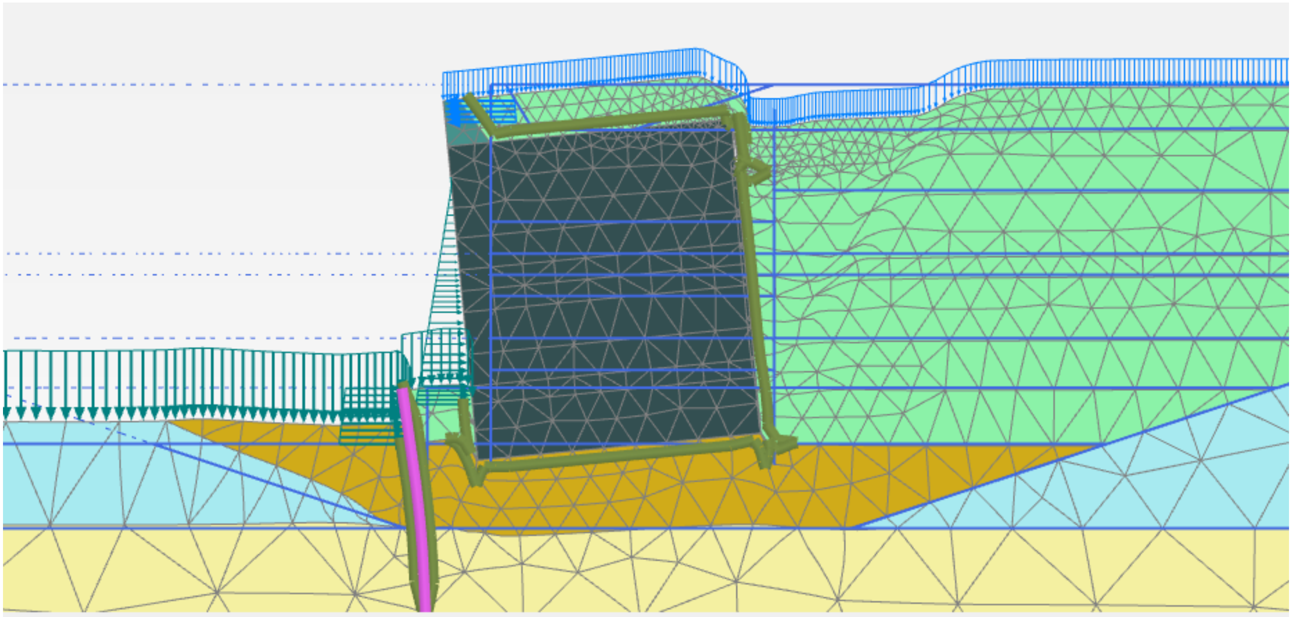

Deformed mesh |u| (scaled up 50.0 times)

Maximum value = 0.05422 m (Element 489 at Node 1166)